

University of Southampton Research Repository ePrints Soton

Copyright © and Moral Rights for this thesis are retained by the author and/or other copyright owners. A copy can be downloaded for personal non-commercial research or study, without prior permission or charge. This thesis cannot be reproduced or quoted extensively from without first obtaining permission in writing from the copyright holder/s. The content must not be changed in any way or sold commercially in any format or medium without the formal permission of the copyright holders.

When referring to this work, full bibliographic details including the author, title, awarding institution and date of the thesis must be given e.g.

AUTHOR (year of submission) "Full thesis title", University of Southampton, name of the University School or Department, PhD Thesis, pagination

UNIVERSITY OF SOUTHAMPTON

FACULTY OF NATURAL AND ENVIRONMENTAL SCIENCES

School of Chemistry



Impact of oligonucleotide chemistry and silencing mechanism on applications in gene silencing and genome editing

by

Hannah Michelle Pendergraff

Thesis for the degree of Doctor of Philosophy

October 2015

UNIVERSITY OF SOUTHAMPTON

ABSTRACT

FACULTY OF NATURAL AND ENVIRONMENTAL SCIENCES

SCHOOL OF CHEMISTRY

Doctor of Philosophy

Impact of oligonucleotide chemistry and silencing mechanism on applications in gene silencing and genome editing

Hannah Michelle Pendergraff

Endogenous gene regulation is an essential tool for the survival of all organisms. In recent years, scientists have gained valuable mechanistic insight into these endogenous gene regulation pathways. Using synthetic oligonucleotides (chemically modified DNA or RNA), we have been able to tap into these pathways and manipulate gene expression.

The development of techniques such as solid phase synthesis have enabled researchers to make custom-made oligonucleotides quickly and efficiently. Although solid phase synthesis is a routine method of obtaining oligonucleotides, more complicated oligonucleotides, e.g. chemically modified or longer RNAs, require optimization of the synthesis cycle and deprotection methodology. In order to synthesize complex oligonucleotides in high yield and purity, we tested several synthesis reagents, cycles, deprotection conditions, and purification methods. Using these optimized conditions, we have successfully synthesized a variety of oligonucleotides for gene silencing and genome editing applications. For synthesis of locked nucleic acid (LNA)-containing phosphorothioate oligonucleotides, tetraethylthiuram disulphide (TETD) is insufficiently reactive but 3-Ethoyx-1,2,4-dithiazoline-5-one (EDITH) gives excellent results.

ADAM33 is a susceptibility gene for asthma and bronchial hyperresponsiveness and is implicated in airway remodeling, but its function is only partially understood. Oligonucleotide-mediated gene silencing of ADAM33 could provide valuable insight to its biology and allow us to observe airway development under low ADAM33 expression levels. We show potent silencing of ADAM33 in MRC-5 lung fibroblasts using four different classes of oligonucleotides: siRNAs, single-stranded siRNAs, LNA gapmers, and novel conjugates of antisense oligonucleotides. We observed that several LNA gapmers showed subnanomolar potency when transfected with a cationic lipid, and low micromolar potency when delivered gymnotically. Also, we observed that RNase H-dependent antisense oligonucleotides greatly outperformed RISC-dependent oligonucleotides for

i

silencing *ADAM33*. As *ADAM33* mRNA is 95% retained in the nucleus, this work is consistent with recent findings that antisense oligonucleotides are often more potent against nuclear-localised transcripts.

single-stranded siRNAs (ss-siRNAs) are chemically modified single stranded oligonucleotides that engage the RISC complex, they have the potential to combine the advantages of both duplex siRNAs and antisense oligonucleotides. One disadvantage of the published single-stranded siRNA chemical modification scheme is the use of 2'-O-methoxyethyl-RNA at the 3' terminus. This modification is not available to most researchers so the use of the ss-siRNA technology has been limited up to the present. During our ADAM33 work, we observed that making small changes to the 3' terminus of our single-stranded siRNAs could greatly improve the potency of the oligonucleotide. We found that replacing the 3' terminal 2'-O-methoxyethyl residues with the commercially available 2'-O-methyl or LNA modifications actually improved the potency of the single-stranded siRNA against ADAM33. We developed and optimized single-standed siRNAs based on four additional active siRNA duplex sequences targeting different genes within mammalian cells. In one additional gene, PR, we were able to support our ADAM33 findings that single-stranded siRNAs show improved potency with 2'-O-methyl or LNA modification at the 3' terminus. However, the single-stranded siRNAs against three target genes in two HEK-293 cell lines failed to show any gene silencing activity with any 3' terminus modification. The failure of the oligonucleotides could be related to the specific cell lines used for the experiments as we also observed increased toxicity with our single-stranded siRNAs in these cells compared to their parent siRNA duplex.

Additionally, as chemically modified oligonucleotides can be used to provide greater affinity and specificity to their target sequence, we wanted to explore whether chemical modifications can improve DNA cleavage activity and specificity for genome editing applications. For this work, we used the clustered regularly interspaced short palindromic repeats/crispr associated (CRISPR/Cas9) type II system, which is commonly used in genome editing applications as it requires only two guide RNAs (crRNA, tracrRNA) and a single protein (Cas9 nuclease) for cleavage of a target dsDNA. We wanted to explore whether the use of chemically modified crRNA could improve the specificity or efficiency of cleavage of target DNA when compared to an unmodified crRNA. However, as no work has been published on chemically modified crRNAs, it was unknown whether the CRISPR/Cas system could tolerate chemical modifications and retain cleavage ability. Using a variety of chemically modified crRNAs, we were successfully able to obtain cleavage of our target DNA sequence, although none of our chemically modified crRNAs were able to match the cleavage efficiency of our unmodified crRNA.

Table of Contents

Table	of Conten	ts	iii
List of	Tables		ix
List of	Figures		xi
DECLA	RATION C	OF AUTHORSHIP	xix
Ackno	wledgem	ents	xx i
Definit	tions and	Abbreviations	xxiii
Chapte	er 1:	Introduction	1
1.1	Overvie	ew of nucleic acids	1
1.2	DNA to	protein	2
1.3	Oligonu	ucleotide-mediated gene regulation	4
	1.3.1	Rationale for oligonucleotide therapeutics	4
	1.3.2	Antisense oligonucleotides	5
	1.3.3	siRNA and the RISC complex	8
1.4	Current	t chemical modifications	11
1.5	Oligonu	ucleotide delivery	13
	1.5.1	Endocytosis	13
	1.5.2	Gymnotic delivery of oligonucleotides	15
	1.5.3	Oligonucleotide conjugates	16
	1.5.4	Lung delivery of oligonucleotides	17
1.6	Asthma	1	17
	1.6.1	ADAM33	18
1.7	Solid ph	nase oligonucleotide synthesis	18
1.8	•	tative real-time polymerase chain reaction	
1.9		e editing	
	1.9.1	Zinc finger nucleases	2 3
	1.9.2	Transcription activator-like effectors	
	1.9.3	Clustered regularly interspaced short palindromic repeats	
1 11		Objectives	
1.1(
	1 10 1	Ontimizing aliganucleatide solid phase synthesis	20

	1.10.2	Gene silencing of ADAM33	29
	1.10.3	Development of ss-siRNA chemistry	30
	1.10.4	Genome editing with CRISPR/Cas9	30
Chapt	ter 2:	Solid phase oligonucleotide synthesis	31
2.1	Introdu	ction	31
	2.1.1	Detritylation	31
	2.1.2	Activation and coupling	32
	2.1.3	Capping	33
	2.1.4	Oxidation or sulfurization	34
	2.1.5	Cleavage from support	35
	2.1.6	Nucleobase protection and deprotection	36
	2.1.7	RNA 2'-hydroxyl protection and desilylation	38
	2.1.8	Oligonucleotide purification	38
2.2	LNA gap	omer synthesis and purification	39
	2.2.1	LNA gapmer synthesis using TETD as a sulfurizing reagent	39
	2.2.2	Troubleshooting LNA gapmer synthesis	41
	2.2.3	LNA gapmer synthesis using TETD and BTT	43
	2.2.4	LNA gapmer synthesis using EDITH	45
2.3	S Single-s	stranded siRNA synthesis and purification	46
	2.3.1	ss-siRNA synthesis using TETD	46
	2.3.2	ss-siRNA synthesis using EDITH	48
2.4	EDITH s	tudies	49
2.5	Unmod	ified RNA oligonucleotide synthesis	52
	2.5.1	Synthesis cycle	52
	2.5.2	Unmodified RNA purification	55
2.6	5 Conclus	sions	56
Chapt	ter 3:	Oligonucleotide-mediated silencing of ADAM33	59
3.1	Introdu	ction	
3.2		cation of active siRNA duplexes	
٥.2		·	
	マノ1	Choosing siRNA sequences	59

	3.2.2	Duplex siRNA results	
3.3	ss-siRNA	design64	
3.4	Locked r	nucleic acid gapmers show increased potency for silencing ADAM33 68	
	3.4.1	LNA gapmer design69	
	3.4.2	LNA gapmer results70	
3.5	Oligonu	cleotide conjugates for cellular uptake73	
	3.5.1	Hexadecyloxypropyl conjugates73	
	3.5.2	Bio cleavable hexadecyloxypropyl conjugates76	
	3.5.3	Dynamic light scattering	
3.6	Discussion	on and Conclusions80	
Chapto	er 4:	Single stranded siRNAs81	
4.1	Introduc	tion81	
	4.1.1	Previous ss-siRNA work81	
	4.1.2	Potent ss-siRNAs with chemical modifications81	
	4.1.3	Additional ss-siRNA publications83	
	4.1.4	Current ss-siRNA work	
4.2	ADAM3	3 inhibition by ss-siRNAs84	
4.3	ss-siRNA	s targeting progesterone receptor86	
4.4	Oligonu	cleotides targeting SIN3A90	
4.5	EGFP-ta	rgeting oligonucleotides91	
4.6	Conclusi	ons96	
Chapte	er 5:	Genome editing using the CRISPR/Cas type II system with chemical	ly
	modifi	ed crRNAs97	
5.1	Introduc	tion97	
5.2	Gene sil	encing using the type II CRISPR/Cas system97	
	5.2.1	Experimental Design	
	5.2.2	Results	
	5.2.3	Chemically modified crRNA106	
5.3	Conclusi	ons and Future Work108	
Chante	er 6:	Concluding remarks	

Chapte	er 7:	Experimental	. 113
7.1	Oligonu	cleotide synthesis	. 113
	7.1.1	RNA	. 113
	7.1.2	ss-siRNA synthesis	. 113
	7.1.3	LNA gapmers	. 114
	7.1.4	1-O-hexadecylpropanediol	. 114
	7.1.5	Bio cleavable hexadecyloxypropyl conjugates	. 115
7.2	Oligonu	cleotide quantitation and validation	. 116
7.3	Oligonu	cleotide purification and electrophoresis	. 116
7.4	Mamma	alian cell culture and transfection	. 116
	7.4.1	MRC-5 fibroblast cells	. 116
	7.4.2	MCF-7 cells	. 117
	7.4.3	HEK293 and eGFP-HEK293 cells	. 117
	7.4.4	RNA harvest and quantitative real-time PCR (qRT-PCR)	. 118
	7.4.5	Thermal denaturation by UV Melt analysis	. 119
	7.4.6	Fluorescence microscopy for detection of GFP	. 119
7.5	Cloning	experiments	. 119
	7.5.1	Luria broth media	. 119
	7.5.2	LB Agar plates	. 119
	7.5.3	SOC media	. 119
	7.5.4	Plasmid purification	. 119
	7.5.5	Transformation	. 120
	7.5.6	Colony PCR	. 120
	7.5.7	Agarose gel	. 120
	7.5.8	DNA sequencing	. 120
7.6	CRISPR/	Cas experiments	. 120
	7.6.1	DNA amplification	. 120
	7.6.2	PCR cleanup	. 121
	7.6.3	DNA cleavage assay	. 121
Refere	nces		. 123
Annen	div A	Solid phase synthesis cycle for 1µM RNA	145

Appendix B	Solid phase synthesis cycle for 1µM Sulfr+	149
Appendix C	Solid phase synthesis cycle for modified 1µM Sulfr+	153
Appendix D	Mass spectrometry values	157
Appendix E	Mass Spectra	161

List of Tables

Table 1. Six diff	erent solid phase synthesis conditions for our EDITH delivery study50)
Table 2. siRNA s	sequences designed to target ADAM33 mRNA63	L
Table 3. siRNA s	sequences designed to target ADAM33 mRNA63	3
Table 4. ss-siRN	A sequences and their parent ds siRNAs designed for ADAM33 inhibition. For	
	duplex sequences, sense strand is listed on top. Modification code: RNA, dna,	2′
	OMe, 2'-F, 2'-MOE, '+': LNA, 'S': phosphorothioate, P: 5' phosphate. ND, T_m no	ot
	determined60	5
Table 5. LNA ga	pmer sequences: LNA: -'S': phosphorothioate; lower case: DNA70)
Table 6. Oligoni	ucleotide sequences for ADAM33 inhibition. For duplex sequences, sense stranc	si k
	listed on top. Modification code: RNA, dna, 2'-OMe, 2'-F, 2'-MOE, '+': LNA, 'S'	:
	phosphorothioate, P: 5' phosphate. ND, Tm not determined85	5
Table 7. Oligoni	ucleotide sequences for <i>PR</i> inhibition. For duplex sequences, sense strand is list	ed
	on top. Modification code: RNA, dna, 2'-OMe, 2'-F, 2'- MOE, '+': LNA, 'S':	
	phosphorothioate, P: 5' phosphate88	3
Table 8. Oligoni	ucleotide sequences for SIN3A inhibition. For duplex sequences, sense strand is	
	listed on top. Modification code: RNA, dna, 2'-OMe, 2'-F, 2'-MOE, '+': LNA, 'S'	:
	phosphorothioate, P: 5' phosphate90)
Table 9. Oligoni	ucleotide sequences for SIN3A inhibition. For duplex sequences, sense strand is	
	listed on top. Modification code: RNA, dna, 2'-OMe, 2'-F, 2'- MOE, '+': LNA, 'S	' :
	phosphorothioate, P: 5' phosphate92	2
Table 10. Insert	sequences for ligation into a plasmid that would express crRNAs used to target	:
	eGFP in mammalian HEK293 cells. P represents 5'-phosphate required for	
	ligation100)
Table 11. crRNA	A sequences used to target eGFP in plasmid-free CRISPR/Cas system. DNA bindi	ng
	domains (DBD) are shown in red, while tracrRNA binding domains (tracrBD,	
	constant 3'-half) are shown in black104	1

Table 12. Chemically modified crRNAs used in this study. Modification code: RNA, dna, 2'-OMe,	
2'-F, '+': LNA, 's': phosphorothioate107	

List of Figures

Figure 1. The five	e nucleobases of DNA and RNA2	2
Figure 2. DNA ba	bonding2	_
Figure 3. 5′ m ⁷ G	cap of pre-mRNA transcripts	3
Figure 4. mRNA	schematic A) pre-mRNA following 5' capping B) mature mRNA sequence follow	_
	5' capping, splicing, and polyadenylation	3
Figure 5. Steric b	olocking antisense oligonucleotide mechanisms A) pre-mRNA targeting ASO for	
	alternative splicing mechanisms B) steric blocking of ribosomal machinery by	
	ASO C) anti-miRNA ASO	7
Figure 6. Schema	atic diagram of the RNase H catalytic mechanism(61)	3
Figure 7. Schema	atic representing the gene silencing mechanism of siRNAs and miRNAs that	
	function through the RISC complex. Adapted from (46)	€
Figure 8. Structu	res of some common current chemical modifications used for oligonucleotide	
	therapeutics11	1
Figure 9. Schema	atic of a 3-9-3 gapmer design sequence. Red colored circles represent a high	
	affinity, nuclease resistant chemically modified nucleotide and the white circl	es
	represent unmodified or PS DNA nucleotides13	3
Figure 10. Endoc	cytic pathway schematic. Oligonucleotides enter into the early endosome of ce	lls
	via endocytosis and must escape to the cell cytosol before degradation in the	1
	lysosome15	5
Figure 11. Additi	onal chemically modified oligonucleotides used in gymnotic delivery studies.16	6
Figure 12. Solid p	ohase oligonucleotide synthesis cycle20)
Figure 13. Schem	natic of the fluorescent detection methods of qRT-PCR21	1
Figure 14. Image	e representing that a Ct value is the value of the number of PCR amplification	
	cycles for the fluorescent signal to reach above the background threshold22	,

Figure 15. Representative quantification of gene expression of an oligonucleotide treated sample
to a negative control sample using the $\Delta\Delta Ct$ method. This is not actual data.23
Figure 16. Representative qRT-PCR results graph. The relative gene expression level is graphed
normalized to the negative control sample set at a value of 123
Figure 17. Schematic of zinc finger nuclease dimer bound to target DNA24
Figure 18. Schematic of TALEN dimer bound to target DNA
Figure 19. Schematic representing spacer acquisition and target DNA cleavage. Invading foreign
DNA is processed into small DNA fragments by Cas nucleases. The invading
foreign DNA (spacers) are incorporated into the host genome, becoming pre-
CRISPR RNA. The pre-CRISPR RNA is transcribed into mature CRISPR RNA.
Mature CRISPR RNA complexes with Cas nucleases to target incoming foreign
DNA for cleavage26
Figure 20. Schematic representing the crRNA, tracrRNA, and Cas9 complex targeting a double
stranded DNA. The three components combine creating the CRISP\Cas complex.
The crRNA guides the complex to the complementary invading DNA strand. The
CRISPR\Cas complex binds and cleaves the foreign DNA directly adjacent to the
PAM sequence causing a double strand break
Figure 21. Mechanism of the detritylation step of solid phase synthesis where the DMT protecting
group is removed by a 3% TCA solution32
Figure 22. Activation and coupling solid phase synthesis cycle step
Figure 23. Capping mechanism of solid phase oligonucleotide synthesis
Figure 24. Mechanism of iodine/water/pyridine-mediated oxidation commonly used in solid phase
oligonucleotide synthesis35
Figure 25. Mechanism of sulfurization by EDITH in solid phase oligonucleotide synthesis35
Figure 26. Cleavage of an oligonucleotide from a standard solid support36
Figure 27. Cleavage of an oligonucleotide from a Unylinker support
Figure 28. Protection of DNA or RNA nucleobases used in solid phase synthesis
Figure 29. Mechanism of the displacement of <i>N</i> -benzoyl Cytosine by the methylamine
denrotection 38

Figure 30. Mechanism of re	emoval of TBS protecting group from RNA by fluorine
Figure 31. Structure of TET	D sulfurizing reagent39
Figure 32. Representative r	mass spectrometry analysis on and LNA gapmer synthesized using TETE
as a sulfu	rizing reagent. This shows LNA 33-G which should have a mass peak
4798.1 g/	mol. This analysis was performed using a Time of Flight mass
spectrom	neter41
Figure 33. Results of a 20%	analytical polyacrylamide gel showing the failure of the LNA gapmer
solid pha	se synthesis with TETD sulfurization. LNA gapmer sequences are
described	d in detail in Chapter 3. The control oligonucleotide was a purchased
16-mer Ll	NA gapmer. The dye was bromophenol blue. The gel was stained
using Stai	ins-all41
Figure 34. Mass spectrome	etry results on the dT oligonucleotides that were synthesized to
troublesh	noot the failed LNA gapmer synthesis. A) List of dT oligonucleotides
used for t	this troubleshooting experiment B) PS dT oligonucleotide with
purchase	d dT column C) PS dT oligonucleotide with Unylinker solid support D)
PO dT oliį	gonucleotide with Unylinker solid support43
Figure 35. Mass spectrome	etry results on LNA gapmers 33-G, H, I, and Q A) Oligonucleotide
expected	and predicted mass. B) Mass spectrometry results. The red boxes
indicate t	the correct mass peak44
Figure 36. Results of a 20%	analytical polyacrylamide gel showing the failure of the LNA gapmer
solid pha	se synthesis with TETD sulfurization. LNA gapmer sequences are
described	d in detail in Chapter 3. The control oligonucleotide was a purchased
16-mer Ll	NA gapmer. The dye was bromophenol blue. The gel was stained
using Stai	ins-all45
Figure 37. Mass spectrome	etry analysis of the two initial LNA gapmers made using the EDITH
method.	A) The expected and obtained mass spectrometry values of LNAs 33-M
and 33-P.	B) Mass spectrometry spectra for LNAs 33-M and 33-P46
Figure 38. 5' – 3' ss-siRNA s	sequence representing the 5 different synthesis steps required for solic
phase syr	nthesis of the ss-siRNAs. $'s'$: phosphorothioate; 2'-F; 2'-OMe; MOE; P: 5
phosphat	re47
Figure 39. Mass spectrome	etry analysis of a synthesized ss-siRNA verifying the synthesis product
to he cor	roct 19

synthesis product to be the correct mass49
Figure 41. Results of EDITH studies A) phosphorothioated LNA sequence used in the EDITH studies
with the expected and calculated mass LNA; $'_{\text{S}}$: phosphorothioate B)
representative mass spectrometry analysis of LNAs synthesized in the EDITH
study. The red box indicated the correct molecular weight product 51
Figure 42. LNA dimer formation. LNA; 's' phosphorothioate
Figure 43. Results of a 20% polyacrylamide gel showing the six LNAs used for the EDITH study
compared against a known molecular weight LNA. The control is an LNA gapmer
of known weight, 4800 g/mol. The LNAs 1-6 are ~5500 g\mol which would
correspond to the LNA running as a dimer51
Figure 44. Mass spectrometry analysis of synthesized RNA showing the correct mass peak and a
+261 peak53
Figure 45. Unylinker adduct with exact mass calculated
Figure 46. Mass spectrometry analysis of synthesized RNA showing the correct mass peak using a
180 minute heated cleavage step54
Figure 47. CPG with 3' RNA nucleobase attached
Figure 48. 16% polyacrylamide analytical gel showing the failure RNA sequences, with the highest
molecular weight correct RNA sequence on the top. These oligonucleotides are
unmodified 40-mer RNAs of mixed sequences. The gel was stained using Stains-
all56
Figure 49. qRT-PCR results of relative <i>ADAM33</i> mRNA levels when HMH-1 is co-transfected with
various transfection agents. The siRNA was transfected at 50nM concentration
and normalized to a no-lipid control. Error bars are standard deviation of the
average result from independent experiments
Figure 50. qRT-PCR results of relative <i>ADAM33</i> mRNA levels when treated with duplex siRNAs. All
siRNAs were transfected at 50nM concentration and normalized to a scrambled
siRNA control. Error bars are standard deviation of technical replicates 63
Figure 51. qRT-PCR results of relative <i>ADAM33</i> mRNA levels when treated with duplex siRNAs. All
siRNAs were transfected at 50nM concentration and normalized to a non-

Figure 40. Mass spectrometry analysis of a synthesized ss-siRNA ss-A33-MOE-2, verifying the

	treated (NT) control. Error bars are standard deviation of two independent
	biological replicates64
Figure 52. A) Ur	nmodified 5'-terminal phosphate chemically synthesized to the ss-siRNAs B) 5'
	terminal (E)-vinylphosphonate modification necessary for in vivo ss-siRNA
	studies66
Figure 53. qRT-F	PCR results comparing relative potencies of duplexes siRNA and ss-siRNA. All
	results are normalized to a scrambled siRNA duplex control. Error bars are
	standard deviation of biological replicated. All oligonucleotides were
	transfected at 50nM67
Figure 54. qRT-F	PCR results comparing relative potencies of different chemical modification
	schemes on ss-siRNA activity. All results are normalized to a scrambled siRNA
	duplex control. All oligonucleotides were transfected at 50nM. Error bars are
	standard deviation of biological replicates68
Figure 55. Scher	matic showing LNA gapmers folding to form stable hairpins. These make
	unsuitable antisense oligonucleotides, particularly in the cases when LNA-LNA
	base pairs can form, since they are unlikely to unfold even in the presence of a
	fully complementary RNA target69
Figure 56. qRT-F	PCR results showing relative <i>ADAM33</i> inhibition by LNA gapmers. All results are
	normalized to a scrambled siRNA duplex control. Error bars are standard
	deviation of biological replicates. All oligonucleotides were transfected at 50nM
Figure 57 qRT-P	CR results showing dose response analysis of LNAs 33-O and 33-R. All results are
	normalized to a scrambled LNA gapmer control. Error bars are standard
	deviation of technical replicates71
Figure 58. qRT-F	PCR dose response results. Oligonucleotides are delivered at 1μM dose and
	normalized to a non-treated control. Error bars are standard deviation of
	technical replicates72
Figure 59. Gymi	notically delivered gapmers are effective inhibitors of ADAM33. qRT-PCR gymnotic
	transfection results. Oligonucleotides are delivered at $3\mu\text{M}$ dose and
	normalized to a non-treated control (NT). Error bars are standard deviation of
	two biological replicates73
Figure 60 Chem	nical structure of hexadecyloxypropyl LNA conjugate 74

Figure 61. qRT-P	PCR gymnotic transfection results. Oligonucleotides are delivered at $3\mu\text{M}$	dose
	and normalized to a non-treated control. Error bars are standard deviate	tion of
	technical replicates	75
Figure 62 aRT-F	PCR results showing dose response analysis of ADAM33-O, R, and P and th	eir linid-
riguic oz. qivi i		·
	conjugates. All results are normalized to non-treated (NT) sample. Error	
	standard deviation of biological replicates	/6
Figure 63. Chem	nical structure of disulfide hexadecyloxypropyl LNA conjugate	77
Figure 64. Sche	matic describing the synthesis of disulphide hexadecyloxypropyl LNA conj	ugate.
		77
Figure 65. qRT-F	PCR results showing dose response analysis of 33-O and conjugates. All re	sults are
	normalized to NT sample. Graph based on one biological replicate	78
Figure 66. Resul	ts of DLS measurement on 33-O, 33-O conjugate, and bio cleavable 33-O	
	conjugate. Note that the scale of the y axis varies widely; these data inc	dicate no
	significant aggregation for the free oligonucleotide but a well defined	
	association of both types of conjugates	79
Figure 67. Mod	ified nucleotides that have been included in ss-siRNAs in this study	84
Figure 68. qRT-F	PCR results comparing potencies of different chemical modification schem	es on ss-
	siRNA activity. All results are normalized to a scrambled siRNA duplex co	ontrol. All
	oligonucleotides were transfected at 50nM. Error bars are standard dev	iation of
	two biological replicates	86
Figure 69. A) Du	plex siRNA and control for inhibition of progesterone receptor. Sense stra	ınd is
	listed on top. Modification code: RNA, dna. (B) qRT-PCR results of PR mi	RNA
	levels when MCF 7 cells are treated with siRNAs at 50 nM concentration	ı. Error
	bars represent standard deviation of three biological replicates	87
Figure 70. qRT-F	PCR results of PR mRNA levels when MCF 7 cells are treated with ss-siRNA	s. Error
	bars represent standard deviation of six biological replicates. * = p<0.05	88
Figure 71. Dose	response data of MCF 7 cells treated with PR targeting ss-siRNA oligonuc	leotides
	at various concentrations. Data is normalized to the 0 oligonucleotide	
	concentration points. N=9 for the 50 nM dose and n=3 for the other	
	concentrations	80

Figure 72. A) qRT-PCR results of <i>SIN3A</i> mRNA levels when treated with duplex siRNAs. HEK293
cells were reverse transfected with siRNAs. All siRNAs were transfected at 50nM
concentration and normalized to a scrambled siRNA control. B) qRT-PCR results
of SIN3A mRNA levels when HEK293 cells are treated with ss-siRNAs. Samples
are normalized to a NT control and transfected at 50nM concentrations. In all
cases, error bars are standard deviation of N=491
Figure 73. qRT-PCR results of EGFP mRNA levels when treated with duplex siRNAs. All siRNAs were
transfected at 50nM concentration and normalized to a NT control. Error bars
are standard deviation of n=4. (C)94
Figure 74. qRT-PCR results of EGFP mRNA levels when treated with duplex siRNAs. All siRNAs were
transfected at 50nM concentration and normalized to a NT control. Error bars
are standard deviation of n=4. (C) Fluorescent image of EGFP-expressing cells
treated with duplex siRNAs showing potent knockdown of EGFP at the protein
level relative to control oligomers or untreated controls95
Figure 75. Simple schematic of the CRISPR plasmid developed by Cong et al.(281). The plasmid is
transcribed starting at the U6 promoter. The plasmid is digested by BbsI
restriction enzymes causing a double strand break where a new CRISPR insert
can be ligated into the plasmid99
Figure 76. Schematic of a gel image following a Ndel restriction digest. The successfully ligated
product will be ~390 base pair fragment and an unsuccessfully ligated product
will be ~366 base pairs. Unfortunately the gel image was too faint for an image.
Figure 77 Results of optimization experiment using crRNA Fu 2 targeting eGFP DNA. Either 50
nM Cas9 and tracrRNA:crRNA complex (Lane 1) or 100 nM Cas9 and
tracrRNA:crRNA complex (Lane 2) was used in the presence of 0.1 μg (Lane 1) or
$0.2~\mu g$ (Lane 2) target DNA. 1000 bp ladder was used as reference. 1% agarose
gel stained with Nancy-520105
Figure 78. Results of 1% agarose gel showing the egfp cleavage by the Cas9: tracrRNA: CRISPR
RNA complex with various CRISPR RNAs105
Figure 79. Results of 1% agarose gel showing the same sample, HP egfp, with and without SDS
treatment

Figure 80.	Results of 1% agarose gel showing the egfp cleavage by the Cas9: tracrRNA: CR	SPR
	RNA complex with various chemically modified CRISPR RNAs. Gel is	
	representative of three independent experiments	108

DECLARATION OF AUTHORSHIP

l,	[please print name]
	lare that this thesis and the work presented in it are my own and has been generated by me as result of my own original research.
[title	e of thesis]
••••	
I co	nfirm that:
1.	This work was done wholly or mainly while in candidature for a research degree at this University;
2.	Where any part of this thesis has previously been submitted for a degree or any other qualification at this University or any other institution, this has been clearly stated;
3.	Where I have consulted the published work of others, this is always clearly attributed;
4.	Where I have quoted from the work of others, the source is always given. With the exception of such quotations, this thesis is entirely my own work;
5.	I have acknowledged all main sources of help;
6.	Where the thesis is based on work done by myself jointly with others, I have made clear exactly what was done by others and what I have contributed myself;
	[Delete as appropriate] None of this work has been published before submission [or] Parts of this work have been published as: [please list references below]:
Sign	ned:

Acknowledgements

First and foremost, I would like to thank my parents for their constant support, love, and guidance. None of this would be possible without you.

Jon Watts: thanks for taking a chance on me. You've been a great mentor and friend, and I can never thank you enough. Although this experience hasn't always been fun, it has been a chance of a lifetime. I will always be grateful.

I would like to thank my former supervisor, David Corey, for his support throughout my scientific journey. You've been a great role model.

I would like to thank my lab mates and friends. You've made this experience amazing. Thanks for the laughs, drinks, and memories.

And I would like to acknowledge the enormous support we received from Dorcus Brown of ATD Bio and Ali Tavassoli, without their generosity, I would not have had a completed project.

Definitions and Abbreviations

ADAM A disintegrin and metalloproteinase domain AGO2 Argonaute 2 **ASO** Antisense oligonucleotide **BLAST** Basic local alignment tool BTT 5-benzylthio-1-*H*-tetrazole cET Constrained ethyl **CRISPR** associated Cas CRISPR Clustered regularly interspaced short palindromic repeats crRNA CRISPR RNA disiRNA Dicer-substrate siRNA **DLS** Dynamic light scattering **DMT** dimethoxytrityl DNA Deoxyribonucleic acid **Double stranded RNA** dsRNA **EDITH** 3-Ethoyx-1,2,4-dithiazoline-5-one **GalNAc** N-acetylgalactosamine HD Huntingtin's Disease **HPLC** High-performance liquid chromatography Half maximal inhibitory concentration IC₅₀

Liter

L

LNA Locked nucleic acid

miRNA micro RNA

MOE methoxyethyl

mol mole

MP metalloproteinase

mRNA Messenger RNA

m⁷G 7-methyl-guanosine cap

PAM Protospacer adjacent motif

PO phosphodiester

PR Progesterone receptor

pre-mRNA Precursor messenger RNA

PS phosphorothioate

RACE Rapid amplification of cDNA ends

RNP ribonucleoprotein

RIP RNA- immunoprecipitation

RISC RNA-induced silencing complex

RNA Ribonucleic acid

RNAi RNA interference

RSV Respiratory syncytial virus

siRNA Small interfering RNA

ss-siRNA Single stranded siRNA

TALENs Transcription activator-like effector nucleases

TBS Tert-butyldimethylsilyl

TCA Trichloroacetic acid

TETD Tetraethylthiuram disulphide

T_m Melting temperature

tracrRNA Transactivating CRISPR RNA

tRNA Transfer RNA

V:I Vector: insert

ZFN Zinc finger nucleases

ZNA Zipped nucleic acid

2' F 2'-fluoro RNA

2'F-ANA 2'-deoxy-2'-fluoroarabino nucleic acid

3' UTR 3' untranslated region

5' UTR 5' untranslated region

Chapter 1: Introduction

1.1 Overview of nucleic acids

The term nucleic acid was coined by Swiss scientist Friedrich Mieschner in 1869 because it was discovered within the nucleus of lymphocytes and it contained acidic phosphate groups (1). Deoxyribonucleic acid (DNA) and ribonucleic acid (RNA) contain the same building blocks: a phosphate group, a nitrogenous base, and a 5-carbon sugar, either deoxyribose for DNA or ribose for RNA.

The only distinction between the native structure of DNA and RNA is the 2'OH group on the ribose of RNA. The additional hydroxyl group impacts the structure and conformation of RNA, giving it very different properties from DNA.

There are five DNA and RNA nucleobases: adenine, guanine, cytosine, thymine (DNA), and uracil (RNA) (Figure 1). Each base is attached to a sugar ring at the 1' position, and the sugars are linked together with a phosphate backbone. DNA and RNA bind to their compliment nucleobase using Watson and Crick base pairing (Figure 2)(2). Watson-Crick base pairing proved that with the DNA double helix, a pyrimidine base (thymine or cytosine) will always bond with a purine base (guanine or adenine). The G:C base pair contains three hydrogen bonds while the A:T base pairs only contain two. The GC-content of a nucleic acid sequence helps to estimate the thermal stability of a DNA sequence of interest due to the base stacking interactions of GC base pairs (3, 4).

Chapter 1

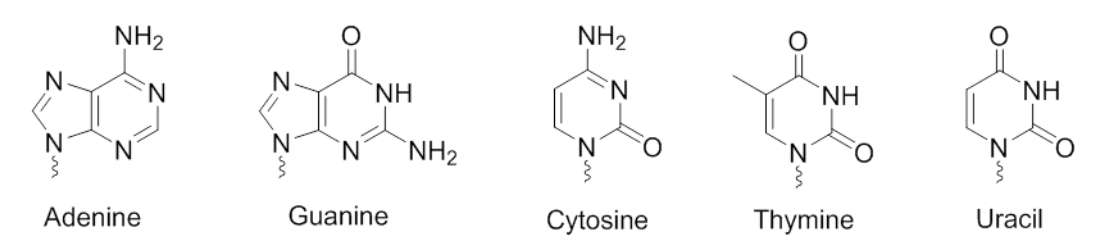


Figure 1. The five nucleobases of DNA and RNA.

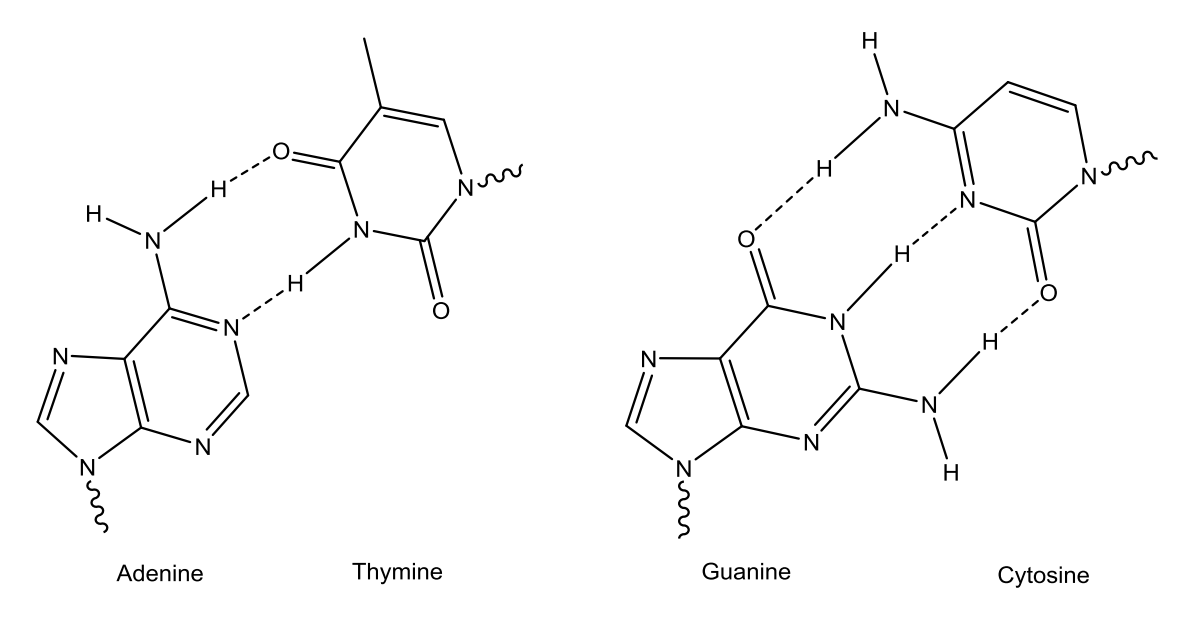


Figure 2. DNA base pair interactions showing the adenine:thymine and guanine:cytosine hydrogen bonding.

1.2 DNA to protein

Transcription is the first step in gene expression where the enzyme RNA polymerase creates a complementary RNA transcript from a segment of DNA (5, 6). RNA polymerase II catalyzes the transcription of precursor messenger RNAs (pre-mRNA), small interfering RNA (siRNA), and micro RNAs (miRNA) in the nucleus (7-11), and RNA polymerase III is responsible for the transcription of small non-coding RNAs, such as transfer RNA (tRNA)(12).

In both prokaryotic and eukaryotic cells, pre-mRNA needs further processing to become mature mRNA (13). Pre-mRNA must undergo three main processing events to become a stable mRNA transcript and be exported to the cell cytoplasm. The first processing event consists of attaching a methylated guanosine by a 5' to 5' triphosphate linkage to the transcribed pre-mRNA (Figure 3). The step in the pre-mRNA maturation is called 5' capping by adding the 7-methyl-guanosine cap (m^7G) (14-17).

$$H_2N$$
 N
 H_2N
 N
 H_2N
 N
 H_2N
 N
 H_2N
 N
 H_2N
 N
 H_2N
 H_2N

Figure 3. 5' m⁷G cap of pre-mRNA transcripts.

The second post-transcriptional pre-mRNA modification is the addition of ~250 adenosine ribonucleotides at the 3' end of the pre-mRNA transcript, forming a poly(A) tail (18) (Figure 4). This polyadenylation process takes place in both prokaryotic and eukaryotic cells (19). In eukaryotic cells, poly(A) tail has many useful roles, including mRNA protection against nucleases, aiding with the export of messenger RNA (mRNA) to the cytoplasm from the nucleus, and helping to stimulate and regulate translation (20, 21).

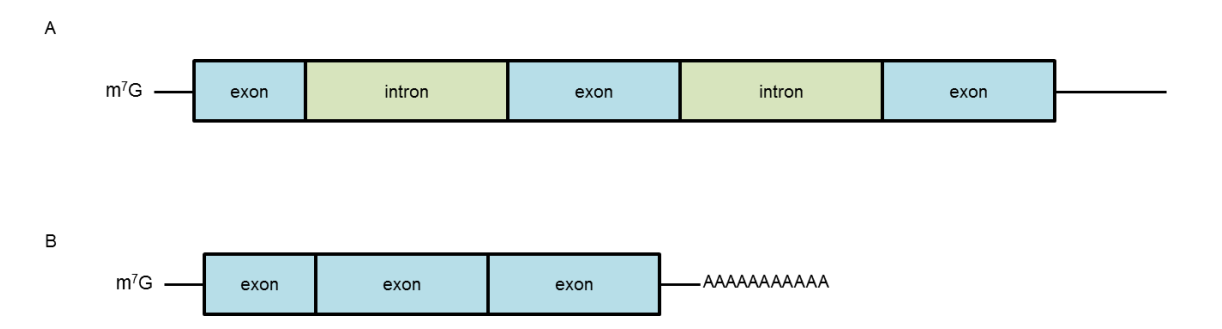


Figure 4. mRNA schematic A) pre-mRNA following 5' capping B) mature mRNA sequence following 5' capping, splicing, and polyadenylation.

During the process of transcription, the pre-mRNA is also undergoing splicing, in which the transcribed introns are removed and the exons are joined (22-24). Importantly, most pre-mRNA transcripts have several splice variants or alternatively spliced products (25, 26). Through the alternatively spliced variants of a transcript, up to hundreds of different proteins can result from a single mRNA transcript (27-30). Unfortunately, not all splice variants are beneficial to an organism. Many abnormally spliced mRNA transcripts are responsible for diseases such as cancer and some hereditary diseases (31-34).

Chapter 1

After transcription and processing, the mRNA may be exported to the cytoplasm to undergo translation, in which proteins are synthesized by cellular ribosomes with the aid of tRNAs using mRNA as a template. Once the mRNA is translated, the completed polypeptide chain folds into an active protein, and often undergoes additional post-translational modification.

1.3 Oligonucleotide-mediated gene regulation

1.3.1 Rationale for oligonucleotide therapeutics

Gene regulation is an essential tool for the survival of all organisms. Endogenous gene regulation mechanisms allow a cell to control the expression of RNAs and proteins, and every step from transcription to post-translational modification is regulated (35, 36). Synthetic agents that would allow us to control gene expression would provide a powerful platform for treating disease.

1.3.1.1 Small molecule drug development

The average cost of discovery and development of a new therapeutic is estimated at over \$800 million (37) due to the time and resources invested by researchers in the discovery and trials process as well as to the high failure rate of drug candidates (38).

Historically the pharmaceutical industry has focused attention on small molecule therapeutics which typically target proteins. One limitation of the small molecule therapeutic approach is the tremendous amount of resources that must be invested into the discovery of every drug candidate.

There are several steps in the drug discovery process of small molecule therapeutics, starting with target identification and validation. Following validation of a biological drug target, a screening assay needs to be developed and a high throughput screen is typically carried out with up to millions of compounds. Leads undergo a long optimization process in order to improve potency, make the drug more stable *in vivo*, and reduce off-target effects. After all of the aforementioned steps are completed, the drug candidate can be progressed to preclinical and clinical trials.

1.3.1.2 Oligonucleotides as therapeutics

Oligonucleotides are short sequences of DNA or RNA used to either activate or inhibit the expression of a gene of interest (39-41). Using oligonucleotides for therapeutic gene silencing is not a recent approach. Zamecnik and Stephenson (42) first reported the inhibition of viral replication and cell transformation in Rous sarcoma virus by a specific complementary antisense oligonucleotide in 1978. Over the past 40 years, the manipulation of gene expression by

oligonucleotides has led to the development of over 100 potential drugs currently in clinical trials for the treatment of various diseases, including genetic diseases, cancers, and viruses (43-45).

The discovery of oligonucleotides as therapeutics has allowed the early stages of drug discovery to be streamlined (37). Unlike small molecule therapeutics which typically target proteins, oligonucleotides target a specific DNA or RNA sequence which allows for a rapid, sequence-based design of lead compounds. Since the therapeutic efficacy of oligonucleotides can be quickly established, several hundred potential sequences can be evaluated within a short time frame. There are already a number of well-established oligonucleotide chemistries offering high specificity to the target RNA or DNA sequence, these modification patterns can be applied broadly between drug targets.

Although there are advantages of oligonucleotide therapeutics over small molecule drugs, many challenges still need to be overcome. The main challenges include toxicity, off-target effects, and inefficient cellular uptake.

Before we can explore how chemistry can help overcome these obstacles, however, we need to look at the principal mechanisms by which oligonucleotide therapeutics can achieve gene silencing. In all cases, this depends on the oligonucleotide binding a specific region of target RNA, through Watson-Crick base pairing. However, depending on the chemistry of the oligonucleotide and the biological partners involved, the mechanism can vary widely.

1.3.2 Antisense oligonucleotides

The conceptually simplest approach to oligonucleotide-mediated gene silencing is to introduce a single stranded oligonucleotide that is complementary ("antisense") to its target. This so-called antisense oligonucleotide (ASO) must find its target mRNA unassisted since there is no endogenous cellular machinery to protect and guide it once inside the cell (46).

The use of antisense oligonucleotides as therapeutics was not a well-developed strategy, even after the initial paper by Zamecnik and Stephenson (42). Several reasons contributed to the lack of antisense oligonucleotide developments. Firstly, the concept of antisense oligonucleotides being able to enter eukaryotic cells was not widely accepted. It was assumed that the negatively charged oligonucleotide would not be able to pass the outer cell membrane (47). Secondly, oligonucleotide synthesis methods had not yet been optimized, resulting in a challenging process to synthesize an oligonucleotide of sufficient length for ASO applications (47). Thirdly, there were not many RNA and DNA target sequences available, as the breakthrough Human Genome Project was still decades away (47, 48).

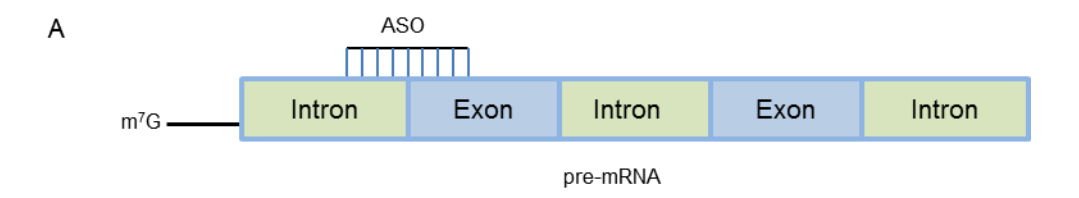
Chapter 1

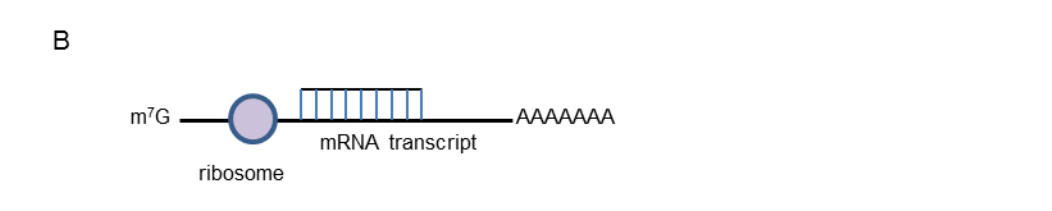
Once those obstacles were overcome, the use of ASOs as therapeutic agents became a widely-used practice. There are two distinct mechanisms by which an ASO can inhibit gene expression, either an RNase H-dependent mechanism or steric blockage mechanisms (49).

One therapeutic steric blocking technique involves the use of 'anti-miR' ASOs. As miRNAs bind to complementary mRNA strands, anti-miR ASOs bind to complementary miRNAs (Figure 5C). This ASO:miRNA binding causes a steric blockage of the miRNA to the target mRNA sequence leading to upregulation of gene expression. This technique has been used for numerous *in vivo* mRNA targets and it a promising therapeutic tool (*50-54*).

Another clinically relevant steric blockage approach used by ASOs involves alternative splicing mechanisms (Figure 5A). For instance, using ASOs to target the pre-mRNA of the liver protein, *APOB*, can lead to exon skipping and a lowering of LDL levels (*55*). Alternatively, Peacey *et al.* used an ASO to target the pre-mRNA of the *TAU* protein to inhibit exon splicing (*56*).

ASOs can also bind to mature mRNA and cause steric blocking of the ribosome during translation (Figure 5B). However this approach is typically only efficient when the ASO binds either to the AUG start or the 3'UTR of the mRNA(49). One main reason that the target mRNA site must not be in a coding region is that the ribosomal machinery can readily unwind the ASO from its target mRNA (49).





miRNA

Figure 5. Steric blocking antisense oligonucleotide mechanisms A) pre-mRNA targeting ASO for alternative splicing mechanisms B) steric blocking of ribosomal machinery by ASO C) anti-miRNA ASO

AAAAAA

1.3.2.1 RNase H

С

RNase H is a non-sequence specific endonuclease that cleaves the RNA strand in an RNA/DNA duplex (57, 58) (a proposed mechanism for the hydrolysis is shown in Figure 6). RNase H is capable of cleaving the target mRNA strand in both the cell cytoplasm and the nucleus (59). However, recent work indicated that RNase H dependent mechanisms tend to be more potent for nuclear targets than cytoplasmic targets (60).

Figure 6. Schematic diagram of the RNase H catalytic mechanism(61)

1.3.3 siRNA and the RISC complex

1.3.3.1 Duplex siRNAs

The second principal gene silencing pathway in therapeutic development makes use of double-stranded RNA. This is perhaps surprising since the 'antisense strand' of this duplex is not immediately available for binding to a target RNA, being tied up in a duplex. Indeed, the observation of potent gene silencing by double-stranded RNA was sufficiently surprising and important to earn a Nobel prize for its discoverers, Andrew Fire and Craig Mello (62). This type of silencing was named RNA interference (RNAi), and occurs when the dsRNA is taken up by the RNA-induced silencing complex (RISC), an endogenous gene silencing protein complex within cells (62, 63) (Figure 7).

microRNAs (miRNAs) are small non-coding RNAs which play roles in RNA silencing and post-transcriptional gene regulation. miRNA are RNAs that fold back on themselves forming a stable hairpin structure called a pre-miRNA. Before being incorporated into RISC, pre-miRNAs are processed by the protein Dicer to remove the stem-loop structure and become mature miRNAs. miRNA use Watson-Crick base pairing to bind complementary mRNA targets and cause gene silencing by three mechanisms. Firstly, they may guide the RISC complex to a target mRNA causing cleavage of the mRNA strand. Secondly, miRNAs may also cause mRNA destabilization by binding and shortening the polyA tail. And thirdly, they may bind a target mRNA and cause translational blockage.

To make use of the RNAi pathway for therapeutic use, researchers have traditionally administered a duplex small interfering RNA (siRNA) or miRNA (64). siRNAs and miRNAs are double-stranded RNAs, having a guide strand (antisense strand) that is complementary to the target RNA sequence and a passenger strand (sense strand) that is complementary to the guide strand (65). Once in the cytoplasm, the duplex RNA associates with Argonaute 2, the main catalytic component of the RISC complex (66). Once loaded into RISC, the passenger strand of the duplex is removed, and the guide strand guides the RISC complex to the target RNA. If the duplex siRNA is perfectly complimentary to the target mRNA strand, the mRNA will be cleaved by Argonaute 2. However, if the siRNA contains mismatches in relation to the target mRNA, translation is repressed by a complex mechanism involving both translational blockage mechanism and mRNA degradation by a cleavage-independent mechanism (67, 68) (Figure 7).

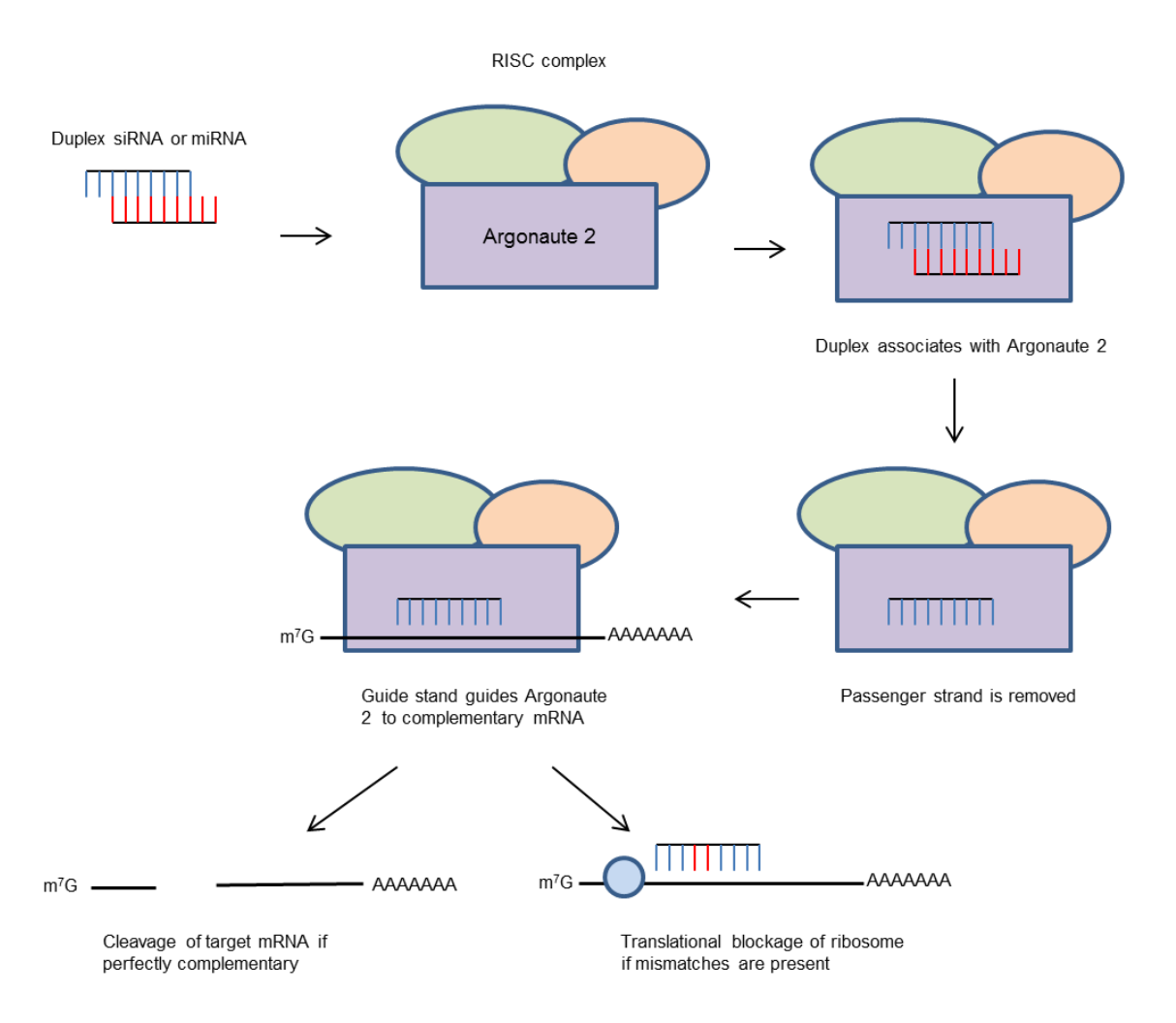


Figure 7. Schematic representing the gene silencing mechanism of siRNAs and miRNAs that function through the RISC complex. Adapted from (46)

The oligonucleotide target is of crucial importance for the optimal chemistry to be used for gene silencing (69). As Behlke presented, RISC-engaging oligonucleotides are generally more potent silencers of cytoplasmic non-coding RNA targets (60).

1.3.3.2 Single-stranded siRNAs

The RNAi pathway normally responds to double-stranded RNA. However, it has been previously reported that single stranded RNAs were able to inhibit gene expression via the RNAi pathway by associating with RISC components Argonaute 2 and Dicer (70) but were much less potent than duplex siRNAs at inhibition gene expression (71, 72).

A milestone was reached in 2012 when it was published that a chemically modified single-stranded siRNA (ss-siRNA) was able to inhibit the mutant Huntingtin gene and PTEN in potencies comparable to duplex siRNAs (73, 74) using a chemical modification motif based primarily on a pattern of alternating 2'-fluoro and 2'-O-methyl modifications. This alternating pattern has been previously identified as highly potent in the context of duplex siRNAs (75, 76). Since duplex RNA is harder to deliver *in vivo* than single stranded oligomers, ss-siRNAs could combine the best of both previous gene silencing classes: a single-stranded oligonucleotide that can effectively be delivered *in vivo* while also achieving the potency of a duplex siRNA by engaging the RISC complex. More detail about previous and current work on the chemistry of ss-siRNAs is given in chapter 4.

1.4 Current chemical modifications

Unmodified DNA and RNA is inherently unstable in biological systems due to nuclease digestion. Chemical modifications are incorporated into DNA or RNA oligonucleotide strands to improve affinity of the oligonucleotide for the desired target, improve biodistribution *in vivo*, increase stability in biological systems, increase potency, and have a longer duration of silencing. For our work, we will only concern ourselves with the phosphate backbone and sugar modifications for our oligonucleotides (Figure 8).

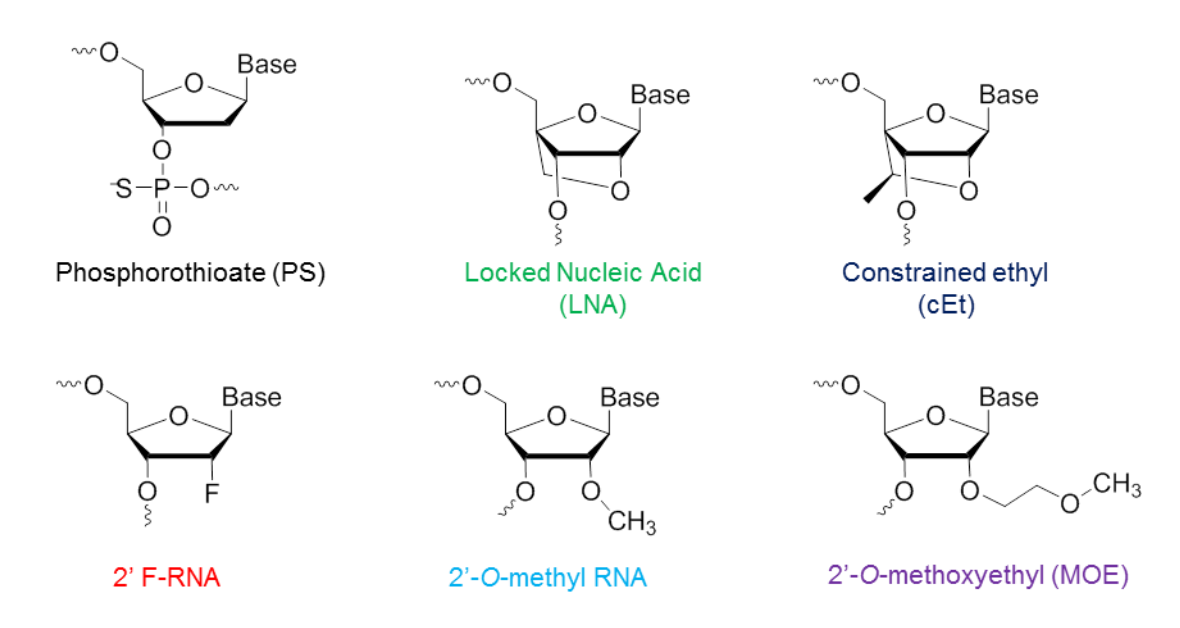


Figure 8. Structures of some common current chemical modifications used for oligonucleotide therapeutics.

The most widely used therapeutic modification is phosphorothioate (PS), in which a non-bridging phosphate oxygen is replaced by a sulfur atom (77). PS was first synthesized in 1966 by Fritz Eckstein (78) and evidence of the stability of PS linkages to nuclease digestion was soon published (79).

The PS modification greatly increases oligonucleotide stability in biological systems, increasing the half-life of the modified DNA or RNA to 1-3 days which is more stable to nucleases than unmodified DNA or RNA (80). Oligonucleotides that contain the PS modification are capable of recruiting RNase H to cleave the desired target, leading both to a decrease in RNA level and reduced protein expression (81). Even though the PS modification is a powerful tool for oligonucleotide therapeutics, it has two main limitations: a tendency to bind proteins nonspecifically, leading to undesirable off target effects when introduced into biological systems, and a reduced affinity for the target complementary RNA (82).

The rings of oligonucleotide sugars are the other most common site of modification, maintaining a similar structure and conformation to RNA. Typical 2' modifications preorganize the nucleoside

into a C3'-endo conformation that mimics the structure of RNA. RNA/RNA duplexes typically show higher affinity than hybrids, and these 2'-modified RNA analogues often show even higher binding affinity than RNA itself (83).

The 2'fluoro-RNA (2'F) modification has a fluorine atom in the place of the 2'OH group on the ribose. This modification has the highest binding affinity of the 2' RNA modifications due to the electronegativity of fluorine (84). A large family of modifications replace the hydroxyl group with an alkoxy substitutent. Notable examples include methyl and methoxyethyl substituents, both of which feature in FDA-approved oligonucleotide drugs. The 2'-O-methyl analogues, for example, shows increased binding, improved resistance to nucleases (85) and reduced stimulation of the innate immune system (86). The 2'-O-methoxyethyl (MOE) modification shows even higher nuclease stability and higher binding affinity: by replacing the 2'OH hydrogen of the RNA ribose with a methoxyethyl group, the melting temperature ($T_{\rm m}$) is increased by 2°C per modified nucleotide (87).

Locked nucleic acids (LNA) contain bicyclic sugars in which a methylene bridge links the 2'-oxygen and 4'-carbon of RNA. This rigidifies the LNA into a RNA-like N-type conformation (88, 89). LNAs are extremely thermally stable when bound to a complementary RNA (90) increasing the $T_{\rm m}$ by approximately 5°C per substitution (91). Constrained ethyl (cET), a derivative of LNA, is a cyclic version of the MOE modification and has shown a 5 fold potency over MOE modifications (92).

All of the aforementioned 2' chemical modifications are insufficient recruiters of RNase H when the oligonucleotide is uniformly modified (93, 94). Fully modified oligomers can be used to work through a translational blockage mechanism, but this approach is ineffective for applications where cleavage is needed to repress expression of the gene of interest, such as when non-coding transcripts are the target. Translational blockage also tends to be a lower potency approach for gene silencing. Thus another approach was needed, that brings together high affinity with RNase H activity.

In 1993, Monia *et al.* reported optimizing RNase H activity in mammalian cells by using an oligonucleotide containing 2'-modified RNA near the termini and a central region or 'gap' of DNA (95). These 'gapmers' have become the dominant class of RNase H dependent ASOs. Today's gapmers include two to five nucleotides per "wing" of high affinity, RNA-like modified nucleotides, flanking eight to ten central DNA nucleotides (46) (Figure 9). The central section provides the DNA/RNA hybrid needed for the recruitment of RNase H within a cell, while the wings provide the oligonucleotide with the higher target affinity and increased nuclease resistance. The backbone of gapmers is typically made with PS linkages throughout both sections.



Figure 9. Schematic of a 3-9-3 gapmer design sequence. Red colored circles represent a high affinity, nuclease resistant chemically modified nucleotide and the white circles represent unmodified or PS DNA nucleotides.

1.5 Oligonucleotide delivery

An oligonucleotide cannot be effective unless it is able to enter the cell, avoid nuclease digestion, and base pair with the target sequence. There are several factors that affect the degree of cellular uptake of oligonucleotides, including the cell type, temperature, and the structure and concentration of the oligonucleotides (96). The use of a cationic lipid transfection agent (eg. Lipofectin) is often used to aid in cellular uptake of the oligonucleotides *in vitro* (97). However, these transfection reagents can be toxic to cultured cells, and this kind of delivery vehicle is usually not used *in vivo*. It would be beneficial to have oligonucleotides that efficiently enter cells and reach their target sequence without any assistance.

The methods used for the delivery of oligonucleotides vary greatly depending on the types of oligonucleotides used. siRNAs cannot enter the cell without the aid of conjugation or a transfection agent of some sort. This is due to the negatively charged hydrophilic phosphate backbone being exposed to the negatively charged cell membrane. Without the aid of a cationic agent, cellular uptake of siRNAs is extremely limited. Single-stranded oligonucleotides are more flexible than duplex oligonucleotides. They are amphiphilic and are more easily able to bind to cell surface receptors. Single-stranded oligonucleotides, therefore may be taken up by the cell without the aid of conjugations or formulations.

1.5.1 Endocytosis

Nakai *et al.* proposed that there are five distinct mechanisms by which an oligonucleotide can enter a cell: 1) passive diffusion, 2) carrier-mediated uptake, 3) receptor mediated endocytosis, 4) absorbance mediated endocytosis, and 5) fluid phase endocytosis (*98*). Passive diffusion is a method of entry into cells that requires no input of chemical energy and is dependent on the permeability of the cell membrane (*99*). Carrier-mediated uptake requires a specific carrier recognizing a ligand in order to enter cells. With both passive diffusion and carrier-mediated uptake, the oligonucleotide will enter the cytoplasm directly upon entry into cells (*100*). Both receptor mediated and absorbance mediated endocytosis describe a process in which cells take up molecules by the plasma membrane budding inward and forming an endosome (*101*). Similarly, fluid phase endocytosis also results in the formation of an endosome, but the initiation

of endosomal formation and uptake is not dependent on receptor binding. This process is routinely used by cells to 'clean up and test' their surrounding environment (102).

siRNAs and antisense oligonucleotides enter cells through an endocytic pathway via an endosome (103). At high oligonucleotide concentrations, ASOs enter cells in a fluid-phase endocytosis mechanism, but this process can lead to non-specific effects due to the high levels of oligonucleotide (104). The most efficient mode of entry for oligonucleotides into cells is by receptor-mediated endocytosis (105). Cell plasma membrane proteins bind to the oligonucleotide and become internalized. Once the oligonucleotide is internalized but entrapped in an endosome, it must escape into the cytoplasm to be therapeutically beneficial (Figure 10).

The first compartment in the endocytic pathway is an early endosome. Early endosomes are classified by the initial enclosing of the cell membrane into compartments. The early endosome is used to recycle materials back into the cell via tubules, mainly through a slightly acidic pH causing the material to disassociate from its receptor. An effective oligonucleotide would ideally escape the endosome at this phase in order to avoid an increasingly acidic pH in the later stages of the endocytic pathway. As the endosome matures, it becomes a late endosome, where additional material sorting takes place. Late endosomes are lacking the tubules of early endosomes and have a more acidic pH of 5.5. The last compartment of the endocytic pathway is the lysosome. The function of the lysosome is to break down cellular waste which is then returned to the cytoplasm as raw materials for cell building. The lysosome accomplishes the breakdown of materials with a pH of 4.8 and active lysosomal hydrolases.

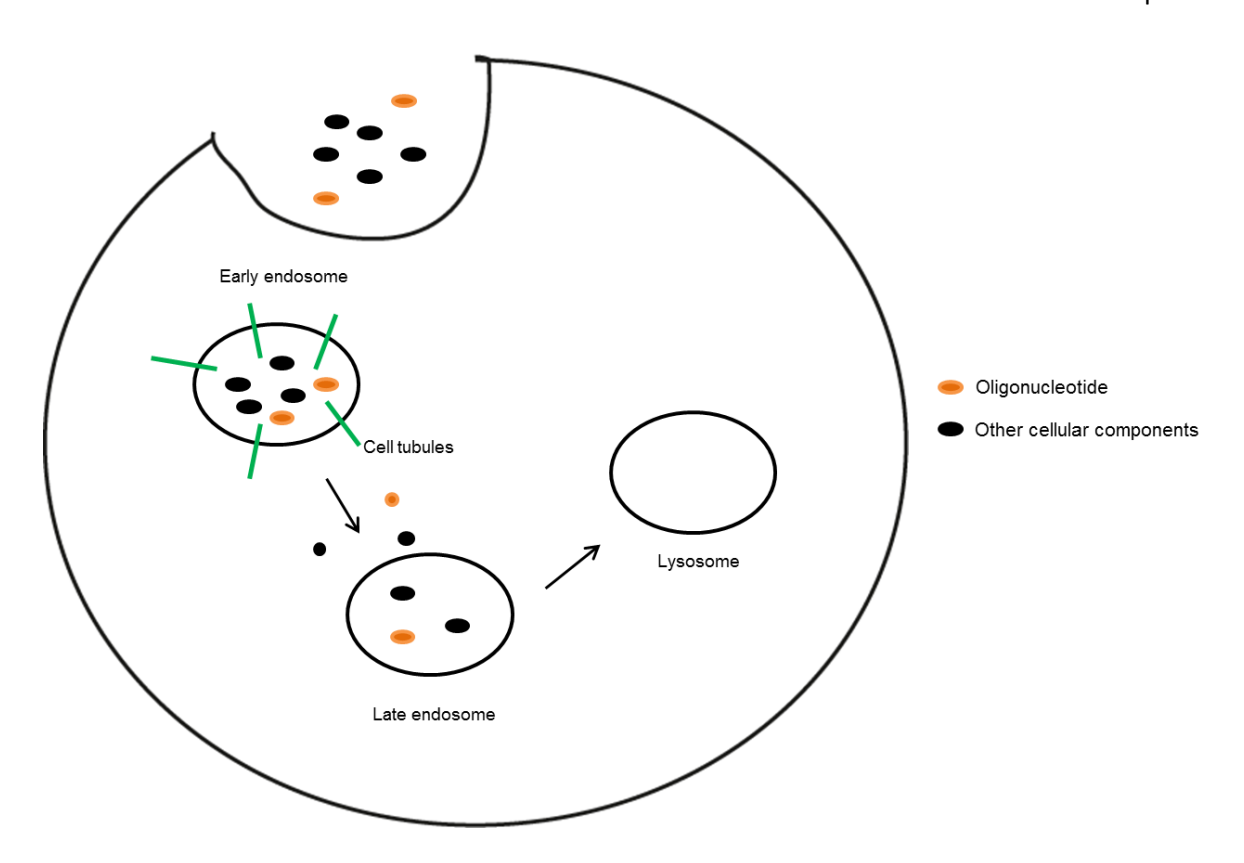


Figure 10. Endocytic pathway schematic. Oligonucleotides enter into the early endosome of cells via endocytosis and must escape to the cell cytosol before degradation in the lysosome.

1.5.2 Gymnotic delivery of oligonucleotides

Transfection methods including electroporation and lipofection (formulation with cationic lipids) provide useful tools for aiding the uptake of oligonucleotides into cultured cells. However, these methods are often too toxic for in vivo use, and the correlation between *in vitro* and *in vivo* activity if often limited. Stein *et al.* developed a process called "gymnosis" that does not require any type of serum additives or transfection reagent in order to have sequence specific gene silencing when working with cultured cells (106). As oligonucleotides are polyanions they cannot enter into cells through passive diffusion (107). Gymnotically delivered oligonucleotides instead enter into the endosomes of cells through a fluid phase endocytosis mechanism (108).

This method shows a better correlation with *in vivo* activity. In gymnosis, short (12-15 mer) PS-modified gapmer oligonucleotides containing LNA or '-deoxy-2'fluoroarabino nucleic acid (2'F-ANA) showed optimal uptake into cells (106). Since the initial report of gymnotic delivery, many labs have gymotically delivered several types of oligonucleotides in order to silence a target gene including PS-modified LNA gapmers (109-111), zipped nucleic acid (ZNA) conjugated LNAs (112), or 2'F-ANA (113) (Figure 11).

Several differences are present between lipofection and gymnotic delivery of oligonucleotides to cells. Firstly, while for a lipofection the oligonucleotides are taken up by cells within 4-24 hours,

gymnotically delivered oligonucleotides must remain on the cultured cells for the duration of the experiment due to much slower cellular uptake of oligonucleotides. Gymnosis also depends on the cells being in an actively dividing growth phase. Also, gymnotic transfections require a much higher concentration of oligonucleotide than lipofection (nM concentrations with lipofection to μ M concentrations with gymnotic delivery). However, gymnotic delivery has very low toxicity since it does not use any toxic transfection reagents or supplements, and shows a much higher correlation between *in vitro* work and *in vivo* activity due to the absence of serum additives.

Figure 11. Additional chemically modified oligonucleotides used in gymnotic delivery studies.

1.5.3 Oligonucleotide conjugates

One promising technique for improving oligonucleotide uptake into cells is to covalently attach a small molecule that is recognized by cell-surface receptors (114-116). In order for this strategy to be effective, two conditions must be met: the covalent linkage chosen must be stable to the conditions of oligonucleotide synthesis or suitable for post-synthesis conjugation, and the modification must not interfere with the oligonucleotide's specificity to the target mRNA (117).

There has been a great focus on conjugates to siRNAs in particular, given the challenge of siRNA delivery in vivo and their very high hydrophobicity (118). Several strategies have been developed to aid siRNAs in cellular uptake, especially with the attachment of lipophilic molecules. Soutschek et al. (119) and Wolfrum et al. (114) are two of multiple groups that demonstrated that covalent conjugation of cholesterol to siRNAs triggered uptake of siRNAs into liver cells in vivo.

However, like many chemical modifications, useful conjugates can often be applied to both siRNA or ASO approaches. For instance, in 2010, Akinc *et al.* published work from Alnylam Pharmaceuticals on their use of an *N*-acetylgalactosamine (GalNAc)-cluster conjugated to an siRNA to target ApoE in the liver (*120*). And in 2014, Prakash *et al.* demonstrated that the same GalNAc conjugate could provide a 5-10 fold increase in the potency of MOE or cEt gapmer ASOs with targets in the liver (*116*). Naked oligonucleotides already tend to accumulate in the liver

(121), so it is significant that the GalNAc conjugates that were targeted to a liver-cell-surface receptor showed such dramatically increased potency.

1.5.4 Lung delivery of oligonucleotides

Oligonucleotide delivery into the lungs is a very challenging process due to many endogenous biological lung protection barriers, such as an overlying mucus layer, cilia, and phagocytes in the lungs to destroy foreign particles. Delivery of oligonucleotides by inhalation would be transformational for treating lung diseases since the lungs are the entry point for many pathogens (viruses and bacteria), one of the primary sites for tumor development, and of primary relevance in the pathology of many genetic diseases (122).

Several studies have been published reporting the successful treatment of lung diseases with oligonucleotides. In 2005, Bitco *et al.* reported successful treatment of respiratory syncytial virus (RSV) with intranasally delivered duplex siRNAs with and without the aid of transfection agents (123). Their study reported that treatment of mice 4 hours prior to viral exposure showed a 99% reduction in RSV relative to the untreated mice. Additionally, they showed that siRNA treatment post-viral exposure also had a therapeutically relevant knockdown of RSV. In 2010, DeVincenzo *et al.* reported an RSV study on eighty-eight human male volunteers testing siRNA efficacy against RSV upon delivery via nasal spray (124). The patient's RSV levels were collected by nasal washes and measured at 2-3 days post treatment. In all of the treated patients, statistically significant knockdown of RSV was observed.

1.6 Asthma

Asthma is a common chronic inflammatory lung disease involving structural changes in the airways leading to airway obstruction, remodelling, hyperresponsiveness, and bronchospasms (125, 126). An estimated 300 million people worldwide suffer from asthma, and over 250,000 deaths annually are caused by the disease (127). Although many treatment options are available for the treatment of asthma symptoms, the disease remains a worldwide health problem.

Both environmental factors, such as smoking, air pollution, or dust, and genetic factors impact the severity of asthma symptoms (128). Studies have shown a correlation between early allergen exposure and asthma, spawning the idea that limiting allergen exposure could affect asthma development (129). Asthma has been shown to have between 35% and 95% genetic contributions, but identifying the asthma-causing genes was challenging until genome wide sequencing made linkage analysis of asthma associated genes possible (130).

1.6.1 ADAM33

ADAM (a disintegrin and metalloproteinase domain) 33 is the first asthma susceptibility gene to be identified by positional cloning (131). It encodes a membrane anchored protein belonging to the zinc metalloprotease superfamily, located on chromosome 20p13 (132). The ADAM33 protein has 7 functional domains which have been linked to diverse cellular processes including proteolysis (133), cell adhesion (134), intracellular signaling (135), and membrane fusion (136). Although many studies have been conducted on ADAM33, the exact physiological functions of gene and its role in the pathophysiology of asthma are still unknown (137). ADAM33 is expressed solely in mesenchymal cells especially smooth muscle cells and fibroblasts (138, 139).

A number of single nucleotide polymorphisms (SNPs) of *ADAM33* have been used to predict lung function of children ages 3-5, although no one particular SNP has been common to all populations (140). These mutations have been linked to airway remodeling, which in the past has been considered to be the result of long-standing inflammation (141). However, airway biopsies taken from young children have shown tissue restructuring before the onset of asthma symptoms (142). The inhibition of *ADAM33* gene expression in early stages of life could potentially prevent or correct the airway remodeling that leads to asthma and could be a novel treatment option. Moreover, recent results by our collaborators E. Davies and H.M. Haitchi show that inhibition of *ADAM33* in a mouse model can reverse pathological airway remodeling (unpublished). Thus oligonucleotide-mediated silencing of *ADAM33* has the potential to be a clinically useful approach in treating the root causes of asthma.

1.7 Solid phase oligonucleotide synthesis

Solid phase oligonucleotide synthesis is a routine method for obtaining a sequence specific, custom-made, unmodified or chemically modified oligonucleotide. Four pivotal contributions led to the development of the current phosphoramidite method used almost universally today, including for this project.

In 1955, Sir Alexander Todd's group at Cambridge University published the first account of the chemical synthesis of a dithymidinyl nucleotide, creating the phosphate linkage using either H-phosphonate or phosphoryl chloride reagents (143, 144). This method was novel, but did have limitations such as the phosphoryl chloride intermediate was very sensitive to hydrolysis.

By the late 1950s, the synthesis of oligonucleotides longer than a few bases became possible when H. Gobind Khorana (then at the University of Chicago) developed the phosphodiester method of oligonucleotide synthesis, which consists of a phosphorylated nucleoside that can be

activated and coupled to a desired nucleotide (145). In addition, Khorana developed most of the nucleoside protecting groups we still use today.

In the late 1960s, the phosphotriester method of oligonucleotide synthesis was published by Robert Letsinger (Northwestern University). Letsinger observed that protecting the nonbridging oxygen of the phosphate prevented the formation of branched structures that had previously been a major class of impurities. (146) Letsinger also developed the phosphite triester approach (using P(III) rather than P(IV) species as reagents). The idea that P(III) would be more reactive than P(V) to nucleophilic attack was non-intuitive, but this change dramatically reduced reaction times. This change required the inclusion of an additional oxidation step in each synthesis cycle (147). Finally, Letsinger was also the first to apply a solid phase approach to oligonucleotide synthesis (148).

In the early 1980s, Marvin Caruthers (University of Colorado) made a very small but highly significant modification to Letsinger's synthesis. He replaced the chloride leaving group with an amine (149, 150). This substitution changed the field because the resulting phosphoramidite could be synthesized in advance, stably stored, and used when needed with only a mild acid-activation step before coupling.

Today's phosphoramidite-based synthesis, used almost universally, makes use of 3'-O-(N,N-diisopropyl phosphoramidite) building blocks (149) and adds one nucleotide per synthesis cycle in the 3'-5' direction. The phosphoramidite synthesis cycle is summarized in Figure 12; each step will be described in more detail in Chapter 2.

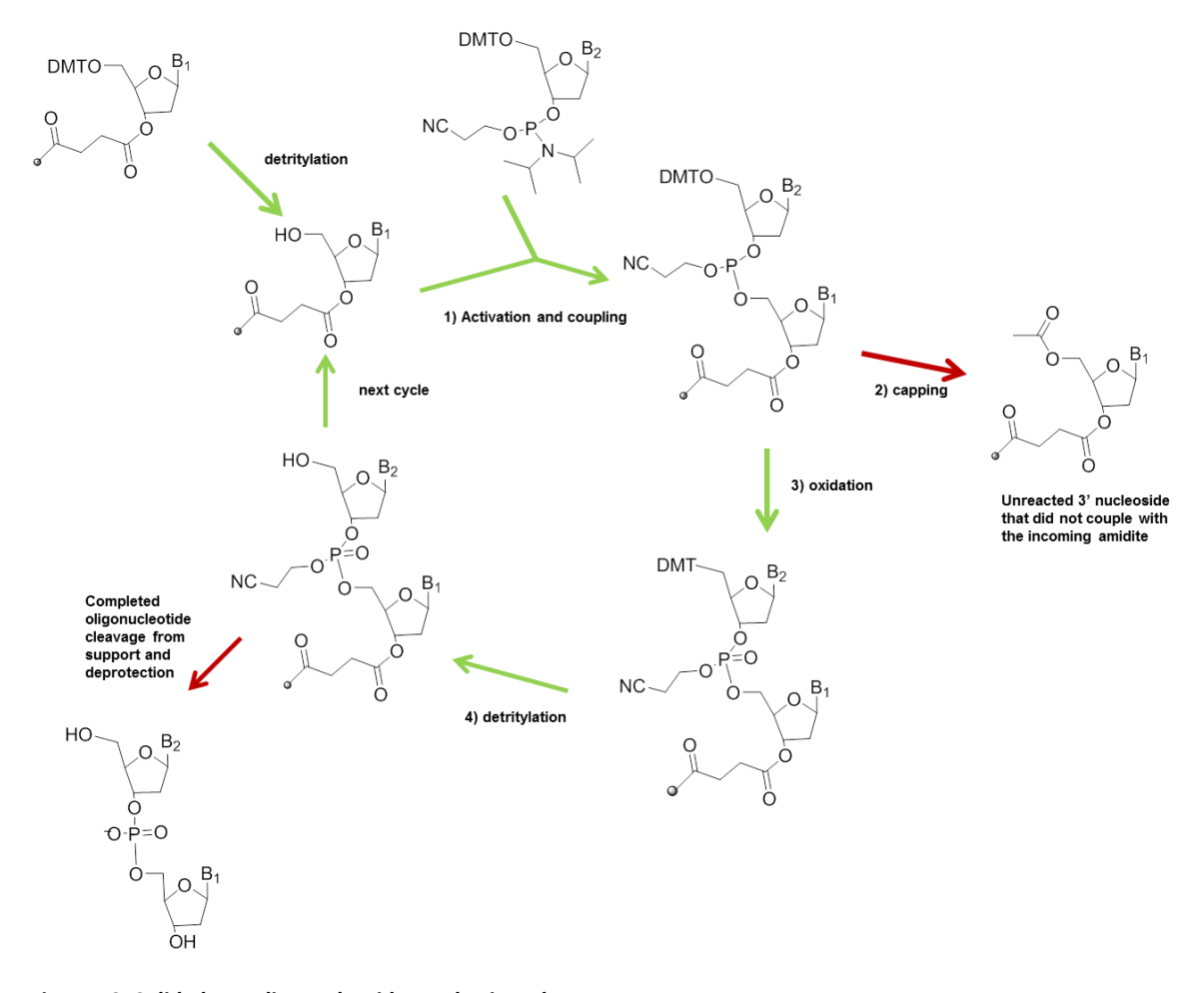


Figure 12. Solid phase oligonucleotide synthesis cycle.

1.8 Quantitative real-time polymerase chain reaction

For this thesis work, quantitative real-time polymerase chain reaction (qRT-PCR) was used to quantitate levels of gene transcription upon treatment with our gene-specific oligonucleotides. qRT-PCR monitors the amplification of a specific DNA target sequence in real-time as it is being PCR amplified (151-154). The real-time PCR system is a thermal cycler with the ability to detect a fluorescence signal emitted by an excited flurophore at a specific wavelength (151, 154, 155).

qRT-PCR reactions use the same reagents as conventional PCR but qRT-PCR reactions also contain a fluorescent label that can be monitored. There are two main detection methods used for qRT-PCR experiments: Taqman probes (155-157) which emit a fluorescent signal upon DNA amplification and SYBR dyes (158-160) which emits a fluorescent signal when bound to double stranded DNA (Figure 13).

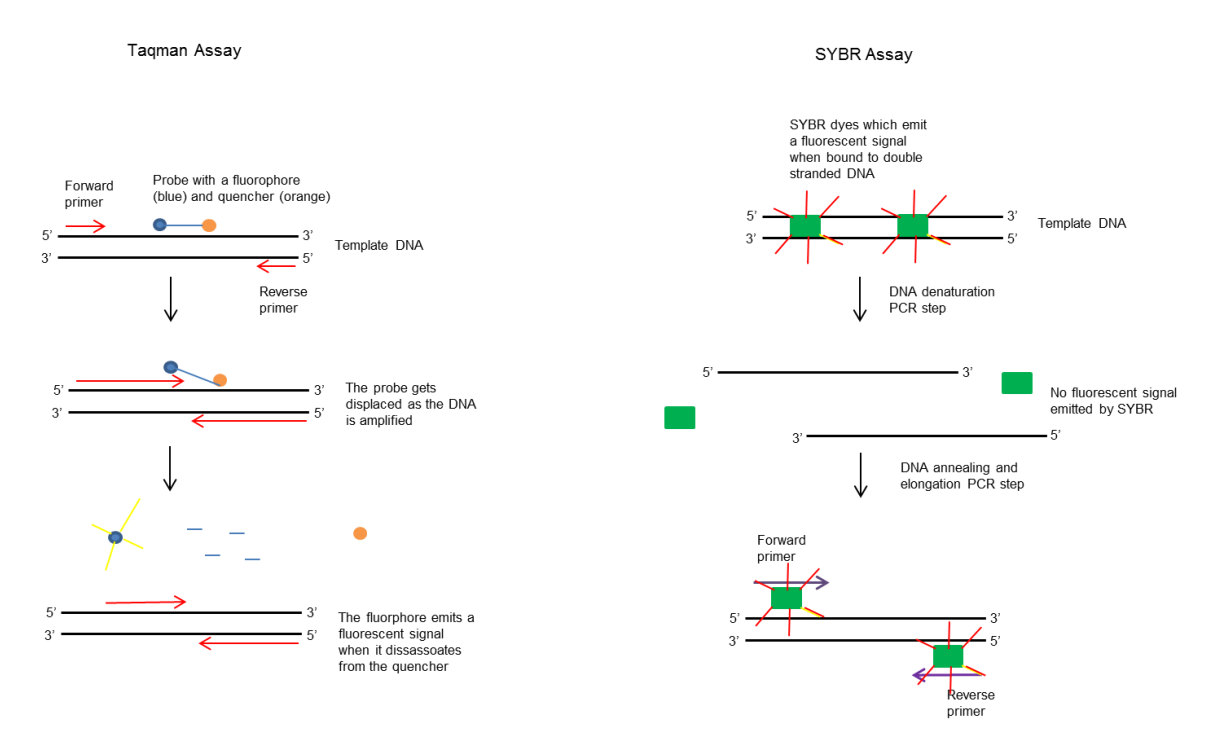


Figure 13. Schematic of the fluorescent detection methods of qRT-PCR.

The quantification of the fluorescent signal associated with the amplification of a target gene is normalized to an internal reference gene (e.g. GapDH or 18-S RNA) (154, 161-165). The data from a qRT-PCR experiment is presented as a Ct value initially, which is the number of amplification cycles for the fluorescent signal to cross the threshold of detection (154, 156, 164, 166)(Figure 14). The lower Ct values indicate a higher amount of gene transcription.

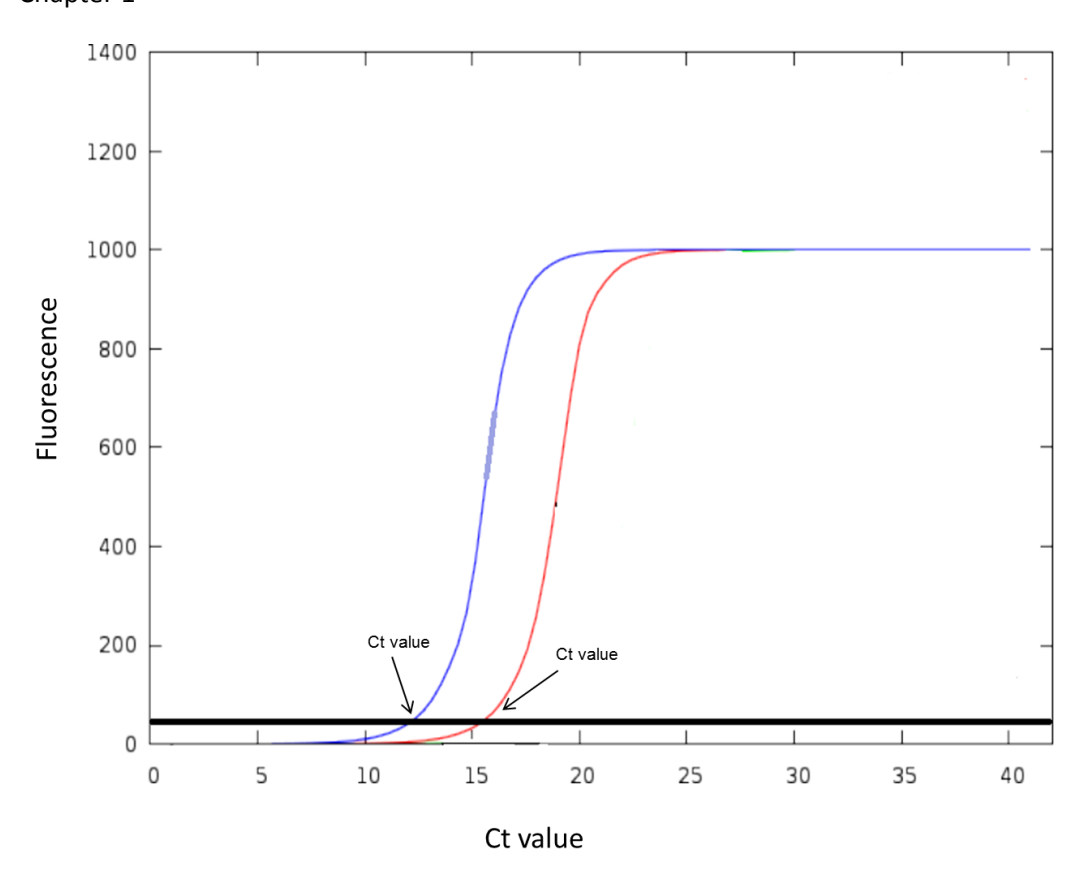


Figure 14. Image representing that a Ct value is the value of the number of PCR amplification cycles for the fluorescent signal to reach above the background threshold.

The Ct values from the gene of interest are normalized to both the reference gene and a scrambled or non-treated (NT) sample (154, 162-164, 167). This method is referred to as the ' $\Delta\Delta$ Ct' method (162-164, 167). The quantitation equation is as follows: $\Delta\Delta$ Ct= Δ Ct (oligonucleotide treated gene of interest - oligonucleotide treated control gene) - Δ ct (negative control sample from gene of interest- negative control sample from control gene) (162-164, 167). The fold change in the gene of interest sample is then calculated using the equation: The fold change= 2-($^{\Delta\Delta$ Ct}) (162-164, 167) (Figure 15). The qRT-PCR data from this thesis work is presented in graph form as the relative 'gene of interest expression' on the y-axis versus the oligonucleotide concentration on the x-axis. The negative control value is set to 1.0 and the oligonucleotide expression levels are normalized to that value.

		Oligonucleotide treated sample Ct	Negative control sample Ct
Row			
1	Oligonucletide treated sample Ct	24	20
2	GAPDH control gene Ct of the oligonucleotide treated sample	18	18
3	Oligonucleotide treated sample Ct –GAPDH Ct of the oligonucleotide treated sample	6	2
4	Value from row 3 - Value from row 3 of negative control sample Ct	4	0
5	Fold change of sample	0.06	1

The level of gene expression for the oligonucleotide gene of interest relative to the negative control sample is 0.06%. This means that the oligonucleotide inhibits 99.94% of the expression of this gene.

Figure 15. Representative quantification of gene expression of an oligonucleotide treated sample to a negative control sample using the ΔΔCt method. This is not actual data.

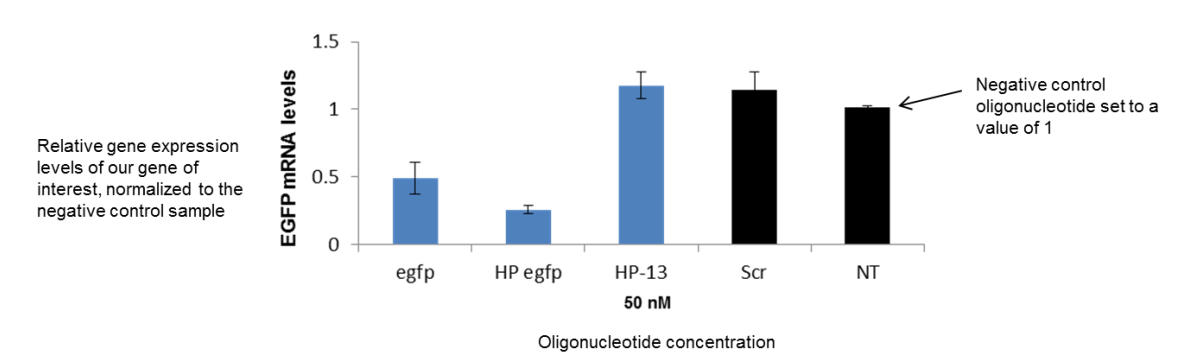


Figure 16. Representative qRT-PCR results graph. The relative gene expression level is graphed normalized to the negative control sample set at a value of 1.

1.9 Genome editing

Genome editing allows DNA within a genome to be replaced, inserted, or removed using artificial nucleases that create double strand breaks in the target DNA sequence. Genome engineering has a diverse range of applications including the exploration of gene function as well as therapeutic purposes such as correction of genetic mutations, elimination of viral sequences and exploration of genetic functions. Due to recent advances in genome engineering, researchers are now able to rapidly and reproducibly modify a specific sequence of DNA.

1.9.1 Zinc finger nucleases

Zinc finger nucleases are site-specific nucleases containing two protein domains, one which binds DNA and contains the zinc finger (a small protein structural motif stabilized by one or more zinc

ions) and the other domain is the nuclease domain which uses Fokl restriction enzyme to catalytically cleave target DNA.

Zinc finger proteins are highly abundant proteins in eukaryotic genomes, with various functions including DNA recognition (168). The zinc finger proteins are capable of recognizing and binding three base pairs of DNA (169). Approximately 3-6 zinc finger proteins can be combined together and tethered to a nuclease, to produce a zinc finger nuclease that can site-specifically target DNA (169). However, the process of developing a multi-zinc-finger protein that targets a DNA sequence is non-intuitive and requires significant empirical optimization. Moreover, zinc finger nucleases must be constructed as dimers, based on two independent binding events, since the catalytic component, the Fokl restriction enzyme, must dimerize in order to cleave DNA (Figure 17).

The zinc finger nuclease creates a double strand break in the target DNA strand. Genome editing is enabled at this stage, as the endogenous DNA repair pathways are utilized to either insert a new fragment of DNA into the genome or remove the cleaved section entirely. Zinc finger nucleases have been used for gene disruption in model organisms (170-173) or gene correction in human cells and plants (169, 174, 175). And recently, a zinc finger nuclease was approved by the United States Food and Drug Administration as a cancer immunotherapy (176).

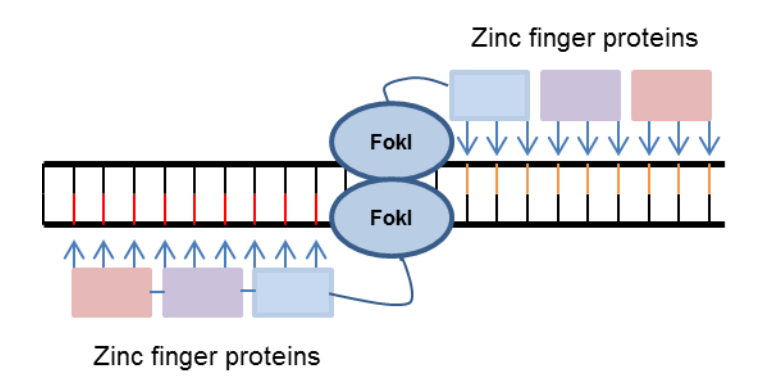


Figure 17. Schematic of zinc finger nuclease dimer bound to target DNA.

1.9.2 Transcription activator-like effectors

Another popular genome engineering technique uses transcription activator-like effector nucleases (TALENs) which cleave target DNA sequences by fusing the DNA binding domain of TAL effectors (proteins secreted by *Xanthomonas* bacteria) with a DNA cleavage domain of a Fokl restriction enzyme. To date, TALENs have been used for genome engineering in several organisms including cattle (177), mouse (178), and human (179-181).

Transcription activator-like effectors (TALEs) are proteins which are transcriptional activators that bind specifically to gene promotors in plants to regulate gene expression (182). TALEs contain a central repeat domain which mediates target DNA recognition. Natural TALEs contain nuclear localization signals which aid the protein into plant nuclei where it binds and activates gene expression.

However, for genome engineering purposes, TALEs may be fused with FokI (constituting the TALEN) in order to bind and cleave target DNA sequences. TALENs may be constructed to target almost any DNA sequence by altering the central repeat domain of the TALES (183) (Figure 18). As with zinc finger nucleases, the TALENs must create a dimer in order for DNA cleavage by FokI.

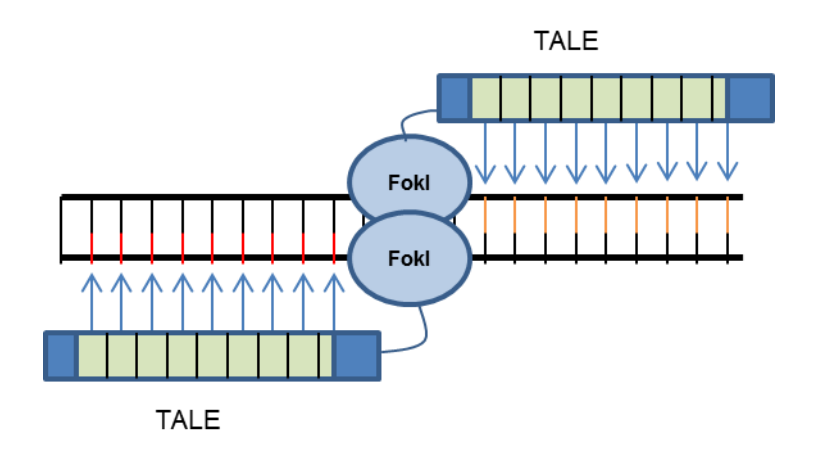


Figure 18. Schematic of TALEN dimer bound to target DNA.

1.9.3 Clustered regularly interspaced short palindromic repeats

Comparable to the RNAi gene silencing pathway in eukaryotes, bacteria and archea have evolved defensive systems for protection against foreign invading threats, such as viruses (184, 185). The clustered regularly interspaced short palindromic repeats (CRISPR)/CRISPR-associated (Cas) system is an adaptive immunity against invading threats and is present in 50% of bacteria and 90% of archea (186).

The first report of bacterial genome repeat sequences was published by Ishino *et al.* in 1987 for *Escherichia coli (187)*, and additional clustered repeat sequences were identified in the genome of other bacteria and archaea species in 2000 (*188*). CRISPR repeats range from 23 – 50 nucleotides long with an average length of 31 nucleotides. The CRISPR repeats are separated by spacer regions ranging from 17 to 84 nucleotides, with an average of 36 nucleotides. In 2005, it was suggested that CRISPR/Cas genes could actually be an adaptive immunity defense in bacteria (*189-191*) when the spacer regions were identified as nucleotide sequences from invading phage or viral genomes. This observation was further validated in 2007 when Barrangou *et al.* altered

the resistance of phage attacks in *Streptococcus thermophiles* by altering the spacer DNA sequences (192).

The CRISPR spacers are a heritable memory of past bacterial cellular intrusions. Invading foreign DNA is processed into small DNA fragments by Cas nucleases. The spacers are transcriptional templates for the production of crRNAs. The mature crRNA guides the appropriate Cas protein to the target DNA strand where it is cleaved (Figure 19).

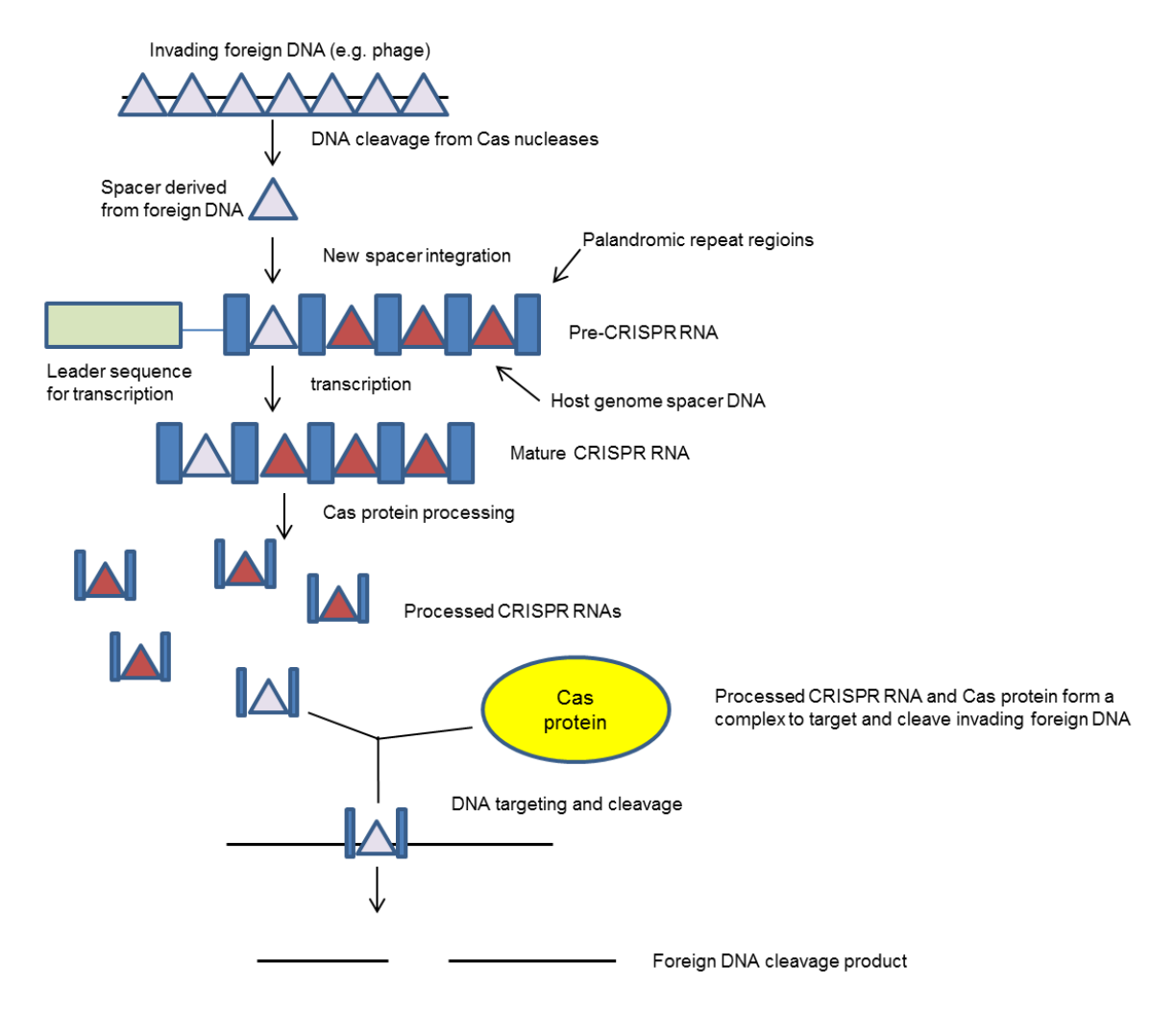


Figure 19. Schematic representing spacer acquisition and target DNA cleavage. Invading foreign DNA is processed into small DNA fragments by Cas nucleases. The invading foreign DNA (spacers) are incorporated into the host genome, becoming pre-CRISPR RNA. The pre-CRISPR RNA is transcribed into mature CRISPR RNA. Mature CRISPR RNA complexes with Cas nucleases to target incoming foreign DNA for cleavage.

1.9.3.1 CRISPR types I, II, and III

CRISPR-Cas systems are classified into three distinct categories by their mechanism of cleavage due to the various Cas genes associated with the CRISPR complex (193). However, all three categories operate through three main stages: adaptation of novel spacer sequences; expression and processing of crRNAs from pre-crRNA precursors; and interference where the foreign DNA or RNA is targeted and cleaved by the CRISPR-Cas complex.

All three CRISPR-Cas systems have Cas1 and Cas2 proteins, which play a critical role in the adaptation of spacer sequence integration (194).

1.9.3.2 CRISPR-Cas type II

Of the three types of CRISPR-Cas systems, type II is the most used in genome editing applications and will be the system used in this thesis work. One of the greatest advantages of the type II system over the others is the use of a single nuclease for cleavage, Cas9.

The CRISPR-Cas type II system most commonly used for genome editing originates from *S. pyogenes* and is adaptable for many genome editing applications (195). Cleavage using this system only requires a mature CRISPR RNA (crRNA), a helper RNA called transactiving CRISPR RNA (tracrRNA), and a Cas 9 protein (196).

As mentioned previously, an invading foreign DNA is processed by Cas nucleases, and the 'spacer' foreign DNA fragments are incorporated into the host cell's genome (197). The spacer DNA sequences are incorporated into the host cell genome in between segments of CRISPR DNA which contain short palindromic repeats. Following transcription, a mature crRNA sequence is present, with the incorporated foreign sequence inserted (197, 198).

The crRNA contains the DNA targeting sequence (from the foreign DNA spacer sequence) and a second domain that is complementary to tracrRNA (185). The tracrRNA is a trans-encoded RNA that is endogenous to the cell and specific for *S.pyogens* (199, 200). The crRNA and tracrRNA hybridize and form a ternary complex with Cas9 (201) (Figure 20).

Cas9 protein has three distinct domains: HNH, RuvC-like, and Pi (202). The HNH and Ruv-C domains are the nuclease domains which are responsible for target DNA cleavage (202). The Ruv-C domain cleaves the non-target DNA strand while the HNH domain cleaves the complementary DNA strand, creating a double strand break in the target DNA sequence (203). The Pi domain is responsible for recognizing the Protospacer adjacent motif (PAM) sequence in the target DNA (202).

PAM is a DNA sequence that immediately follows the DNA sequence targeted by the CRISPR RNA (204). Therefore, PAM is not a component of the CRISPR\Cas complex, but it is a component of the invading virus, phage, or plasmid (205). The CRISPR\Cas complex will not cleave or bind a target DNA sequence that is not immediately followed by a PAM sequence (206) and the PAM sequence determines 'self' from 'not self' bacterial sequences (207). Each CRISPR\Cas type has a specific PAM sequence (208).

The simplicity of the type II system over ZFN and TALENs makes it ideal for genome editing applications. Almost any DNA sequence may be targeted by merely changing the crRNA sequence. The only caveat is the targeted DNA sequence must be adjacent to a PAM sequence. In 2012, Jinek *et al.* reported that the CRISPR-Cas type II system can be exploited for use in RNA-programmable genome editing (185). Since that breakthrough, CRISPR/Cas9 technology has been used in many organisms, including human (209-211), monkeys (212), rats (213), mice (214), and pigs (215) to name a few.

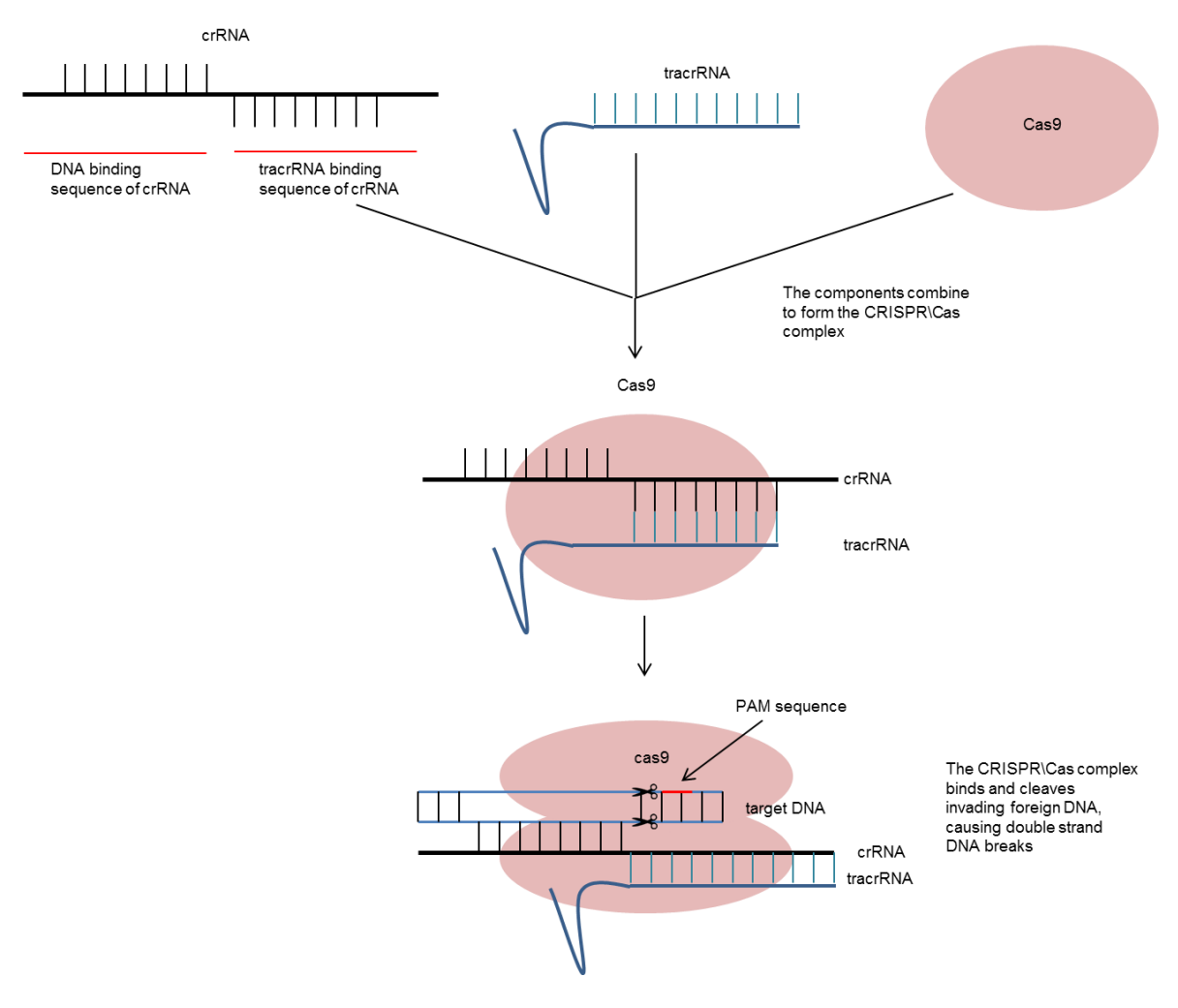


Figure 20. Schematic representing the crRNA, tracrRNA, and Cas9 complex targeting a double stranded DNA. The three components combine creating the CRISP\Cas complex. The crRNA guides the complex to the complementary invading DNA strand. The CRISPR\Cas complex binds and cleaves the foreign DNA directly adjacent to the PAM sequence causing a double strand break.

1.10 Thesis Objectives

1.10.1 Optimizing oligonucleotide solid phase synthesis

The first objective for this thesis work involved optimizing the solid phase synthesis of our oligonucleotides. As all of this thesis work was centered on gene silencing or editing with oligonucleotides, we needed an efficient way to synthesize our oligonucleotides

1.10.2 Gene silencing of ADAM33

Our collaborator, Hans Michael Haitchi, had previously designed siRNA oligonucleotides to inhibit *ADAM33* gene expression. However, using unmodified duplex siRNAs, he achieved only moderate success (70% inhibition) in cultured cells. Moreover, duplex siRNAs can be challenging to deliver *in vivo*. The objective of this thesis chapter was to design single stranded oligonucleotides which were more potent than the initial siRNA duplex.

1.10.3 Development of ss-siRNA chemistry

In the course of our research into the silencing of *ADAM33*, we observed that minor modifications to the 3' terminus of the ss-siRNA oligonucleotides greatly reduced or enhanced the potency. We tested whether this observation was specific to *ADAM33* gene silencing in MRC-5 lung fibroblast cells, or if the discovery was applicable across several cell lines and genetic targets. We also sought to develop a chemistry for ss-siRNAs based only on modifications that are widely available, which would help make the technique much more widely accessible than the currently used modifications which are proprietary and not widely available.

1.10.4 Genome editing with CRISPR/Cas9

The CRISPR/Cas9 type II system has quickly become a very popular technology for genome editing. The requirement for only three key components, tracrRNA, crRNA, and Cas9 nuclease, allows this system to be very versatile. However, currently all of the published work uses expressed or unmodified RNA for the crRNA and tracrRNA. The objective of this project was to test whether chemically modified crRNA and tracrRNA could improve the properties of CRISPR guide RNAs relative to unmodified RNA.

Chapter 2: Solid phase oligonucleotide synthesis

2.1 Introduction

As mentioned in section 1.7, solid phase oligonucleotide synthesis is a routine method for obtaining sequence specific, custom-made, unmodified or chemically modified oligonucleotides. Although the method of phosphoramidite oligonucleotide synthesis is straightforward, each type of chemically modified oligonucleotides required a thorough optimization in order to achieve higher yields and purer products. The optimization conditions used for the oligonucleotides in this thesis work as well as a detailed outline of the solid phase synthesis steps are presented in this chapter.

2.1.1 Detritylation

The nucleotide building blocks used in solid phase synthesis are protected at the 5' end by a dimethoxytrityl (DMT) group, which was first published by Schaller *et al.* in 1963 (216). The DMT group is removed with a solution of 3% trichloroacetic acid (TCA) in dichloromethane (DCM) (Figure 21). Detritylation must occur before the oligonucleotide synthesis can begin, and it is also the final synthesis step before the addition of a new amidite.

When the DMT group is removed, the resulting carbocation emits an orange color with a λ_{max} of 503 nm. As a stable ion, this species also affects the conductance of the deprotection solution in a measurable way. Either of these approaches allow oligonucleotide synthesizers to measure the trityl yield for each synthesis cycle to monitor the synthesis efficiency during synthesis. A high stepwise percentage yield has a great impact on the overall synthesis yield and efficiency.

Although detritylation is a necessary step for solid phase synthesis, there need to be precautions when programming the synthesis cycle. An oligonucleotide should not be exposed to acid for an extended period of time due to possible depurination. Depurination is a chemical reaction where a purine (adenosine or guanosine) base is hydrolytically cleaved from the sugar.

Figure 21. Mechanism of the detritylation step of solid phase synthesis where the DMT protecting group is removed by a 3% TCA solution.

2.1.2 Activation and coupling

Following the detritylation step of the bound 3' nucleotide, the diisopropylamino group of the incoming phosphoramidite is activated, typically using either 0.5M tetrazole or 0.3M 5-benzylthio-1-*H*-tetrazole (BTT) in acetonitrile. Approximately 10-20 equivalents of activated phosphoramidite relative to the bound oligonucleotide are added per coupling step.

For activation and coupling, the disopropylamino group of the incoming phosphoramidite is protonated by the tetrazole, making it a good leaving group. The protonated disopropylamino group is rapidly displaced due to a nucleophilic attack on the phosphorus by the 5'-hydroxyl group of the bound nucleoside creating a new phosphorus-oxygen bond (Figure 22).

Figure 22. Activation and coupling solid phase synthesis cycle step.

2.1.3 Capping

The capping step in the solid phase synthesis cycle functions as a 'damage control' step. Since no synthesis produces 100% yield, there will be unreacted 5'-OH groups that could couple with the next phosphoramidite, causing a single nucleotide deletion in the final oligonucleotide. As this can occur at each step, this produces a large number of n-1 deletion products that are very difficult to remove. Therefore, capping is done by adding a mixture of acetic anhydride and *N*-methylimidazole, dissolved in THF and pyridine, to the synthesis column. These conditions acetylate the 5'-OH, forming an acetate ester which is unreactive to further synthetic cycles, and in turn making the sequence with the nucleotide deletion easier to separate from the full-length product (Figure 23).

Figure 23. Capping mechanism of solid phase oligonucleotide synthesis.

2.1.4 Oxidation or sulfurization

The newly formed linkage is a phosphite triester at the end of the coupling step and it is very unstable in acidic conditions. Before the synthesis cycle can continue the backbone must therefore be oxidized or sulfurized to form a stable 2-cyanoethyl protected phosphate triester. A solution of 0.02M to 0.1M iodine in the presence of water and pyridine is used for the oxidation (Figure 24) and 3-Ethoxy-1,2,4-dithiazoline-5-one (EDITH) is one of a number of sulfurizing reagents (Figure 25) (217).

Figure 24. Mechanism of iodine/water/pyridine-mediated oxidation commonly used in solid phase oligonucleotide synthesis.

Figure 25. Mechanism of sulfurization by EDITH in solid phase oligonucleotide synthesis.

2.1.5 Cleavage from support

Prior to being cleaved from the solid support, a final detritylation step is performed. Once the oligonucleotide is synthesized, it must be cleaved from the support column. Cleavage is completed in either a one or two step process. If a standard support column with the first 3' nucleoside already attached is used, cleavage can occur quickly through a simple ester aminolysis mechanism using ammonia or methylamine (Figure 26). If Unyliker is used as a support column, it

must go through a dephosphorylation step after the ester hydrolysis, achieved with base and heating (Figure 27).

Figure 26. Cleavage of an oligonucleotide from a standard solid support.

Figure 27. Cleavage of an oligonucleotide from a Unylinker support.

2.1.6 Nucleobase protection and deprotection

Due to the nucleophilic nature of the exocyclic primary amino groups on the nucleobases, protecting groups are used during oligonucleotide synthesis to avoid side reactions. Thymine and uracil have no exocyclic amino group so they do not need to be protected (Figure 28).

N-benzoyl deoxy Adenosine

$$\begin{array}{c|c} & & & \\ & & & \\ & & & \\ & & & \\ & & & \\ & & & \\ & & \\ & & \\ & & \\ & & \\ & & \\ & & \\ & & \\ & & \\ & & \\ & & \\ &$$

N-isobutyryl deoxy Guanosine

N-acetyl deoxy Cytosine

Figure 28. Protection of DNA or RNA nucleobases used in solid phase synthesis.

2.1.6.1 DNA and 2' modified RNA deprotection

A common way to remove the base protecting groups is by heating the oligonucleotide at 55°C overnight in ammonium hydroxide. This step is completed in conjunction with the oligonucleotide being cleaved from the support column. However, deprotection in ammonium hydroxide is only applicable to DNA nucleobases or 2'modified RNA nucleobases.

The aforementioned ammonium hydroxide deprotection method will degrade unmodified RNA so an alternative deprotection method must be used. The oligonucleotide can be heated for 10 minutes in a 33% aqueous ethanolic methylamine / ammonium hydroxide solution to deprotect

the nucleobases and cleave the oligonucleotide from the solid support. This deprotection method may be used on any oligonucleotide, DNA or RNA, as long as the cytosine nucleobase is protected with an N-acetyl group as opposed to an N-benzoyl group. *N*-benzoylcytosine is not suitable since benzamide can be displaced by the methylamine under these conditions (Figure 29). In the case of the N-acetyl protection, the removal of the acetyl group is sufficiently fast as to avoid a parallel side reaction. Alternatively, a 3:1 solution of ammonium / ethanol may be used for base protection of any DNA or RNA oligonucleotides. For this method, the oligonucleotide is deprotected for 48 hours at room temperature.

Figure 29. Mechanism of the displacement of N-benzoyl Cytosine by the methylamine deprotection.

2.1.7 RNA 2'-hydroxyl protection and desilylation

The main difference between DNA and RNA is the presence of a 2'OH group on the ribose ring of RNA. Thus, during solid phase synthesis, the RNA amidites must be protected both at the nucleobases and the 2'OH. The tert-butyldimethylsilyl (TBS) method of RNA protection is the method used for this project. Following synthesis and base deprotection, the desilylation step occurs with fluoride – in our case generally a 4:1 DMSO / TEA·3HF solution (Figure 30).

Figure 30. Mechanism of removal of TBS protecting group from RNA by fluorine.

2.1.8 Oligonucleotide purification

Once an oligonucleotide has been synthesized, cleaved from the solid support, and deprotected, a purification step is typically required in order to remove any truncated products or impurities.

High-performance liquid chromatography (HPLC) and gel electrophoresis are two common ways in which an oligonucleotide is purified. In this project, oligonucleotides were purified by polyacrylamide denaturing gel electrophoresis. Gel electrophoresis is a technique that separates products based on both hydrodynamic properties and electrical charge. The gel purification method is typically used for oligonucleotides with hydrophobic components (e.g. lipid tail) or oligonucleotides >100 bases due to the greater loss in yield as compared to alternative purification methods.

2.2 LNA gapmer synthesis and purification

The LNA gapmers synthesized for this thesis work are single stranded, 15-mer antisense oligonucleotides that are fully phosphorothioated. As mentioned in section 1.4, our LNA gapmers consist of 3 LNA modifications at both the 5' and 3' end of the oligonucleotide with 9 central unmodified DNA nucleotides. LNA gapmer sequence design follows several sets of parameters that will be outlined in Chapter 3. The solid phase synthesis parameters of synthesizing the LNA gapmers used required several troubleshooting steps in order to achieve high yields of the correct full length oligonucleotide.

2.2.1 LNA gapmer synthesis using TETD as a sulfurizing reagent

For our initial LNA gapmer solid phase synthesis (Appendix B), all amidites were dissolved in anhydrous acetonitrile at a 0.15 mol/L concentration, with the exception of LNA ^{Me}C which was dissolved in 3:1 anhydrous acetonitrile: THF. For sulfurization, tetraethylthiuram disulphide in acetonitrile (TETD) (Figure 31) was used as it has been previously reported to achieve high synthesis yields (*218*). The sulfurization step for this reaction was 900 seconds following an 8 second TETD addition to the column.

Figure 31. Structure of TETD sulfurizing reagent.

Following the solid phase synthesis, the oligonucleotides were deprotected and cleaved from the Unylinker solid support using a 3:1 ammonium hydroxide: ethanol solution for 48 hours at room

temperature. A deprotection in ammonium hydroxide at 55°C for 16 hours would have also been acceptable for this type of modified oligonucleotide.

A Time of Flight mass spectrometry analysis did not show the correct molecular weight peak for the LNA gapmers. The mass spectrometry analysis for LNA-G (sequence and more details on this gapmer in Chapter 3) is shown as a representative figure for the data obtained for all of the synthesized gapmers (Figure 32). Following the mass spectrometry, a 20% polyacrylamide analytical gel was run on all of the LNA gapmers (sequences in Chapter 3) in order to check the efficiency of the synthesis. The analytical gel results confirmed that the synthesis of the LNA gapmers was not successful (Figure 33). A successful synthesis gel would have showed a cleaner band the same molecular weight as the LNA control and faint lower molecular weight bands to indicate the size of the 'failure' sequences.

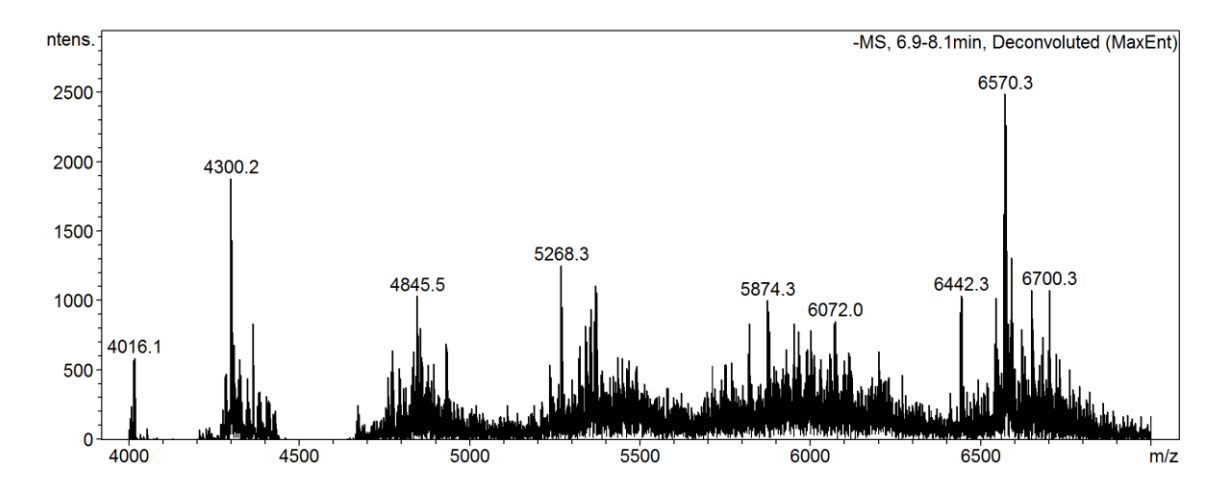


Figure 32. Representative mass spectrometry analysis on and LNA gapmer synthesized using TETD as a sulfurizing reagent. This shows LNA 33-G which should have a mass peak 4798.1 g/ mol. This analysis was performed using a Time of Flight mass spectrometer.

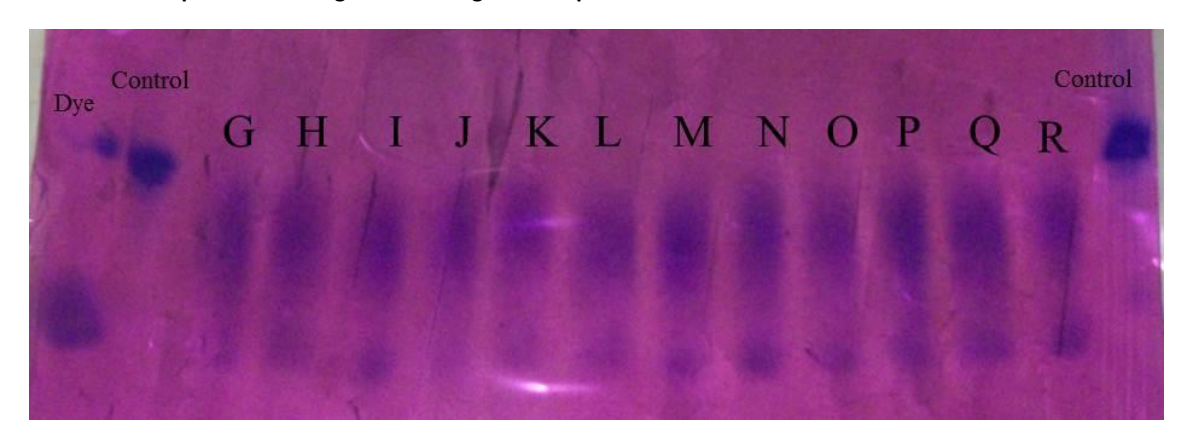


Figure 33. Results of a 20% analytical polyacrylamide gel showing the failure of the LNA gapmer solid phase synthesis with TETD sulfurization. LNA gapmer sequences are described in detail in Chapter 3. The control oligonucleotide was a purchased 16-mer LNA gapmer. The dye was bromophenol blue. The gel was stained using Stains-all.

2.2.2 Troubleshooting LNA gapmer synthesis

We began to investigate the failed LNA gapmer syntheses by first testing whether our Unylinker solid phase support column was compatible with a 3' phosphorothioate addition. Three oligonucleotides were synthesized, each addressing a different potential support column problem. The dT oligonucleotides were synthesized using TETD as before with a 900 second sulfurizing time.

- A fully phosphorothioated 8-mer DNA-thymine oligonucleotide was synthesized using a purchased support column that already had the first 3' DMT protected attached. This oligonucleotide tested whether the failed LNA syntheses were from the first coupling of the amidite to the Unylinker support column.
- 2. A fully phorphorothicated 8-mer DNA-thymine with a universal Unylinker support column was synthesized. This experiment tested the coupling efficiency with a sulfurizing reagent is used to couple the first amidite to the column.

3. An 8-mer DNA-thymine was synthesized and every linkage was phosphorothioated with the exception of a 3' terminal phosphodiester linkage which connected the nucleoside to the Unylinker support column. This experiment tested if the coupling efficiency was improved in the 3' nucleoside was linked with a phosphodiester backbone.

The oligonucleotides were deprotected, concentrated to dryness, and quantitated. The mass spectrometry results show that all three 8-mer DNA-thymine sequences were the correct product so it was concluded that the Unylinker support was not responsible for the failed LNA gapmer syntheses (Figure 34).

 Support column
 Expected mass (g/mol)
 Mass spec results (g/mol)

 8-mer dT column
 2484.0
 2482.0

 8-mer dT with PS unylinker
 2484.0
 2483.1

 8-mer dT with PO unylinker
 2484.0
 2483.1

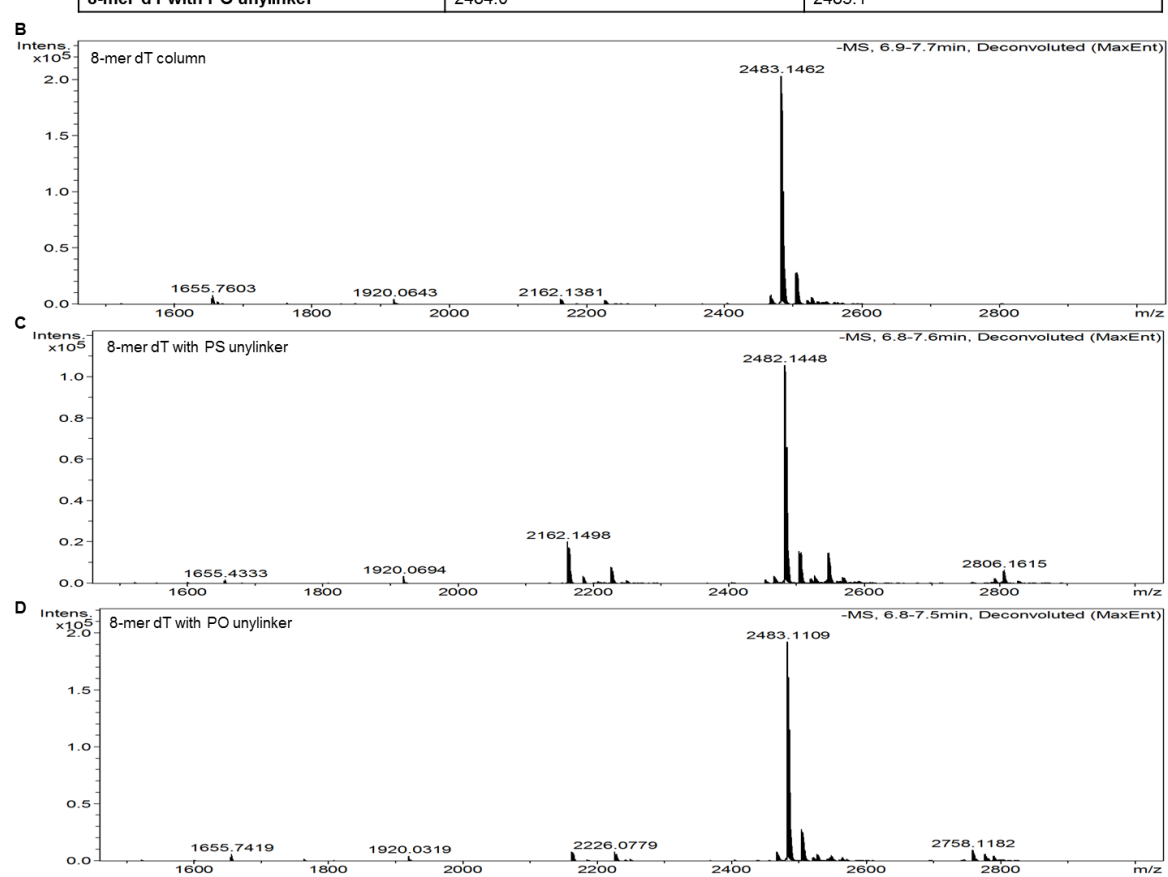


Figure 34. Mass spectrometry results on the dT oligonucleotides that were synthesized to troubleshoot the failed LNA gapmer synthesis. A) List of dT oligonucleotides used for this troubleshooting experiment B) PS dT oligonucleotide with purchased dT column C) PS dT oligonucleotide with Unylinker solid support D) PO dT oligonucleotide with Unylinker solid support.

2.2.3 LNA gapmer synthesis using TETD and BTT

Α

Four of the previously attempted LNA gapmer sequences were resynthesized with changes made to the synthesis reagents and the solid phase synthesis cycle. As previously, TETD was used as a sulfurizing agent, but the sulfurization time was extended to add an additional 900 seconds following an 8 second TETD addition to the column. We also used BTT instead of tetrazole as activator with a coupling time of 100 seconds for the DNA additions and 600 seconds for the LNA additions. Following synthesis, the oligonucleotides were deprotected and cleaved from the Unylinker solid support using ammonium hydroxide for 16 hours at 55°C.

The UV spectroscopy, mass spectrometry (Figure 35) and analytical gel results showed that the correct LNA gapmer product was obtained but in a very low yield and purity.

Α

<u>Oligonucleotide</u>	Expected Mass (g/mol)	Actual Mass (g/mol)	
33-G	5023.0	5021.3	
33-Н	5007.0	5006.2	
33-1	5016.0	5015.2	
33-Q	5006.0	5004.1	

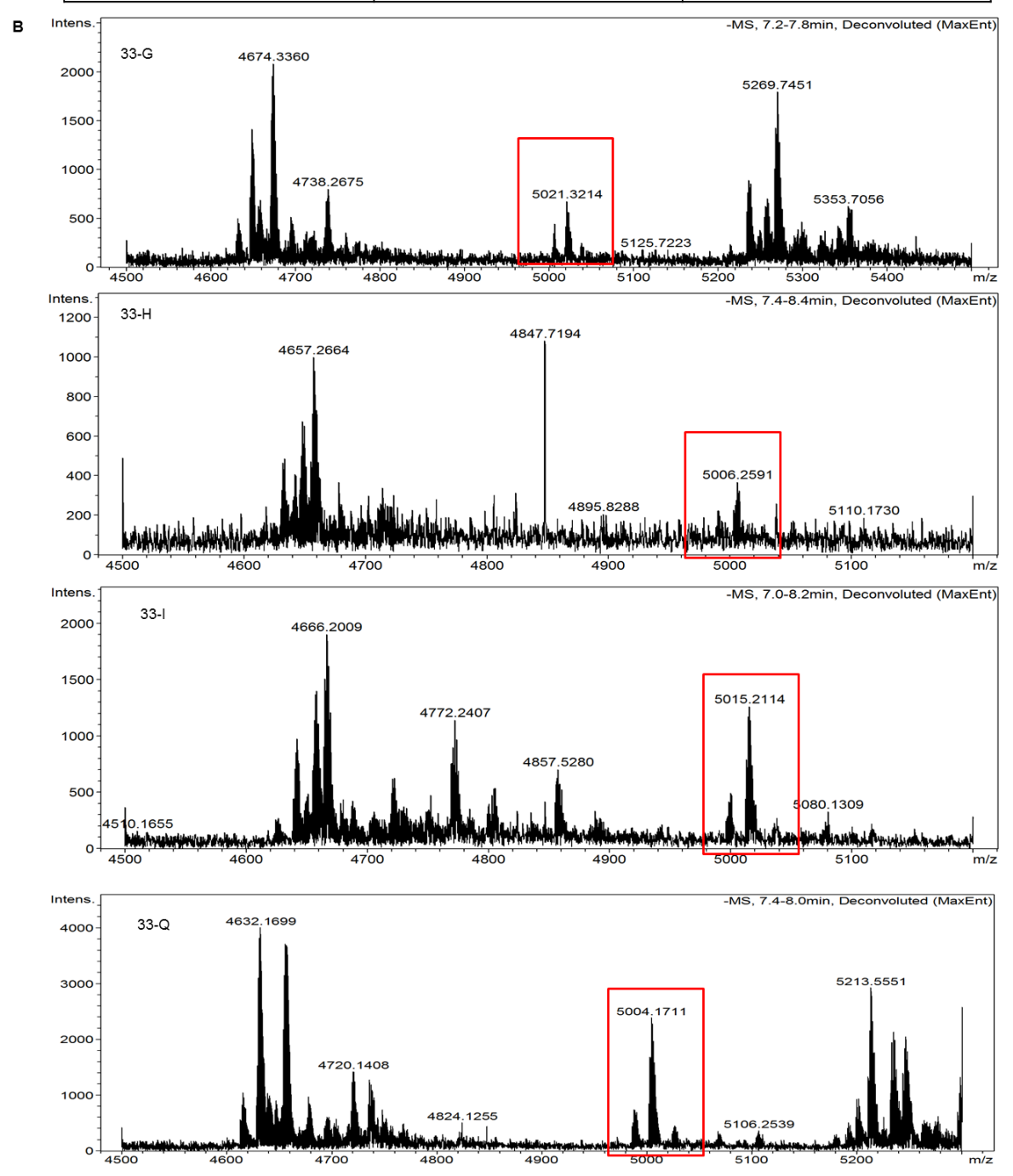


Figure 35. Mass spectrometry results on LNA gapmers 33-G, H, I, and Q A) Oligonucleotide expected and predicted mass. B) Mass spectrometry results. The red boxes indicate the correct mass peak.

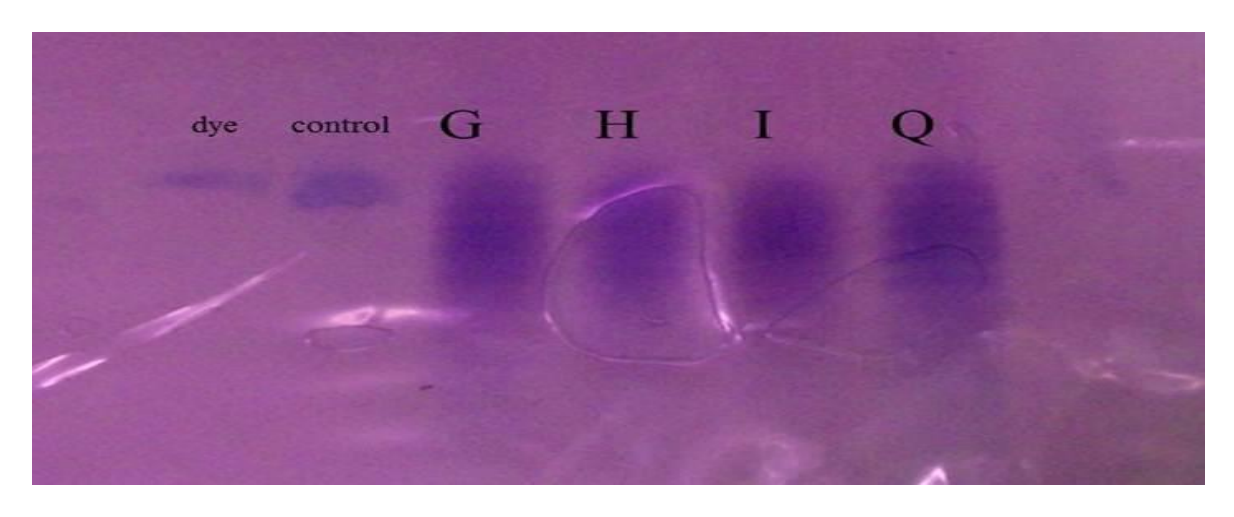


Figure 36. Results of a 20% analytical polyacrylamide gel showing the failure of the LNA gapmer solid phase synthesis with TETD sulfurization. LNA gapmer sequences are described in detail in Chapter 3. The control oligonucleotide was a purchased 16-mer LNA gapmer. The dye was bromophenol blue. The gel was stained using Stains-all.

2.2.4 LNA gapmer synthesis using EDITH

Based on the failure of the previous two LNA gapmer syntheses, two LNA gapmers were synthesized using a 0.05M solution of 3-Ethoxy-1,2,4-dithiazoline-5-one (EDITH) in acetonitrile (Appendix C). EDITH is an alternative sulfurizing reagent to TETD. As used previously, BTT was used instead of tetrazole as a coupling reagent with the coupling times remaining at 600 seconds. The sulfurization cycle was altered to an 8 second addition of EDITH to the column followed by a 60 second wait time. Then an additional 6 second EDITH addition to the column followed by a 60 second wait.

The mass spectrometry (Figure 37) results show that the two randomly selected LNA gapmers, 33-M and 33-P, synthesized using the EDITH method were the correct product. The additional ten LNA gapmers were synthesized using the EDITH method and were characterized by mass spectrometry.

Α

Oligonucleotide	Expected Mass (g/mol)	Actual Mass (g/mol)	
33-M	5012.0	5011.1	
33-P	4994.0	4993.1	

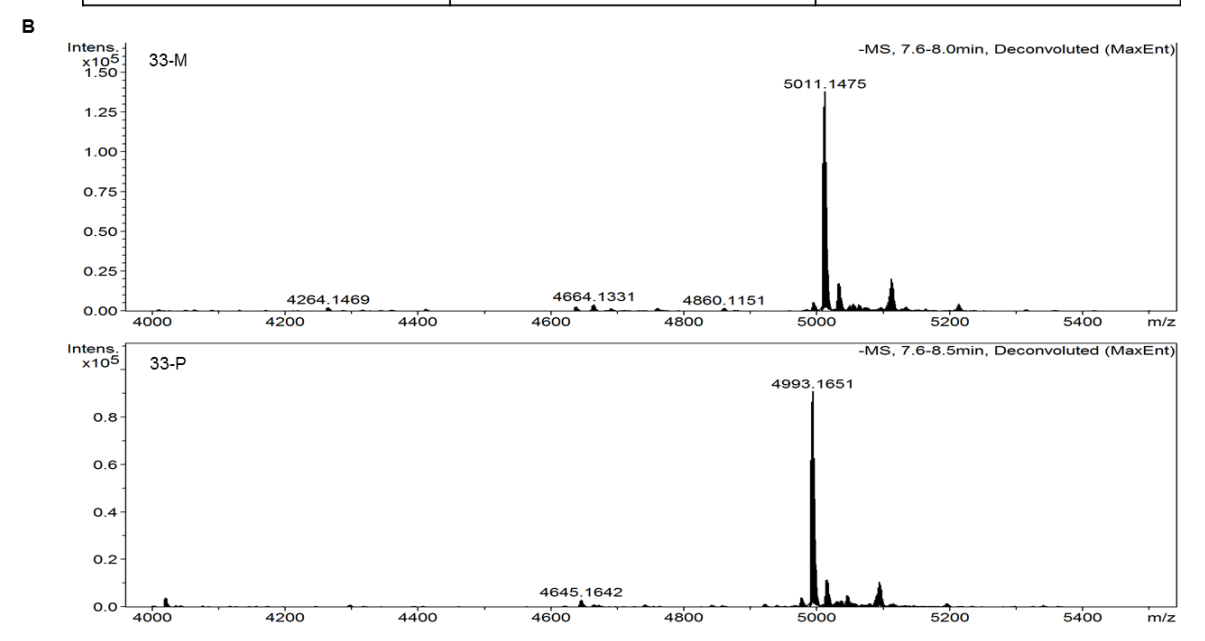


Figure 37. Mass spectrometry analysis of the two initial LNA gapmers made using the EDITH method. A) The expected and obtained mass spectrometry values of LNAs 33-M and 33-P. B) Mass spectrometry spectra for LNAs 33-M and 33-P.

2.3 Single-stranded siRNA synthesis and purification

For the projects outlined in the following chapters, several ss-siRNA oligonucleotides with alternating phosphodiester and phosphorotihioate linkages had to be synthesized via solid phase synthesis. The oligonucleotide sequence design and rationale will be discussed at a later time, with this section focusing on the synthesis and purification methods of the ss-siRNA oligonucleotides used.

2.3.1 ss-siRNA synthesis using TETD

The initial ss-siRNA solid phase synthesis experiments were performed in conjunction with the initial LNA gapmer solid phase synthesis experiments so we initially used TETD as a sulfurizing reagent for the ss-siRNA synthesis as well. Initially, tetrazole was used as a coupling agent in the ss-siRNA synthesis with a 600 second wait time per coupling addition. TETD was used as a sulfurizing agent with a 900 second wait time. All of the phosphoramidites were dissolved in anhydrous acetonitrile at a 0.15 mol/L concentration.

The Applied Biosystems 394 DNA/RNA synthesizer used for the ss-siRNA synthesis is equipped with auxiliary lines present in order to add up to 8 modified amidites to the synthesizer.

Unfortunately, our initial ss-siRNAs needed 10 modified amidites (Figure 38). For that reason, our initial ss-siRNAs had to be synthesized in five different steps with alternating synthesis cycles which are detailed in Chapter 6.

- 1. The ss-siRNA 3' end must be attached to the Unylinker solid support. A MOE modification was attached using TETD for the sulfurization steps.
- 2. Following the MOE addtions at the 3' end of the ss-siRNA, a stretch of 8 nucleotides were added, alternating between 2'-OMe and 2'-F RNA modifications, all with phosphorothioate linkages.
- 3. The next 10 nucleotide additions were also alternating 2'-O-methyl and 2'-F RNA modifications but had phosphodiester linkages. TETD was replaced with 0.2M lodine in pyrimide for the oxidation cycle.
- 4. The 5' terminal 2'-OMe nucleoside is attached via a phosphorothioate linkage so TETD was used as a sulfurizing agent with a sulfurizing synthesis cycle.
- 5. The 5' phosphate group was added to the ss-siRNA last and was oxidized with 0.2M Iodine in pyridine.

$$\underline{P-U_S}_{5} \underbrace{ACAGUUCCAG}_{3} \underbrace{G_SU_SA_SC_SU_SU_SC_SC_S}_{2} \underbrace{A_SA}_{1}$$

Figure 38. 5′ – 3′ ss-siRNA sequence representing the 5 different synthesis steps required for solid phase synthesis of the ss-siRNAs. 's': phosphorothioate; 2′-F; 2′-OMe; MOE; P: 5′ phosphate.

Following the ss-siRNA synthesis, the oligonucleotides were deprotected and cleaved from the Unylinker support using ammonium hydroxide at 55°C for 16 hours. The correct ss-siRNA sequence was synthesized and verified by mass spectrometry analysis (

Figure 39). Details of the ss-siRNA layout and sequence design will be discussed in detail in Chapters 3 and 4.

Α	

Support column	Expected mass (g/mol)	Mass spec results (g/mol)
ss-A33-MOE-1	7131.0	7131.6
ss-HP-A33-2	7407.0	7106.6
ss-HP-A33-3	7091.0	7090.6

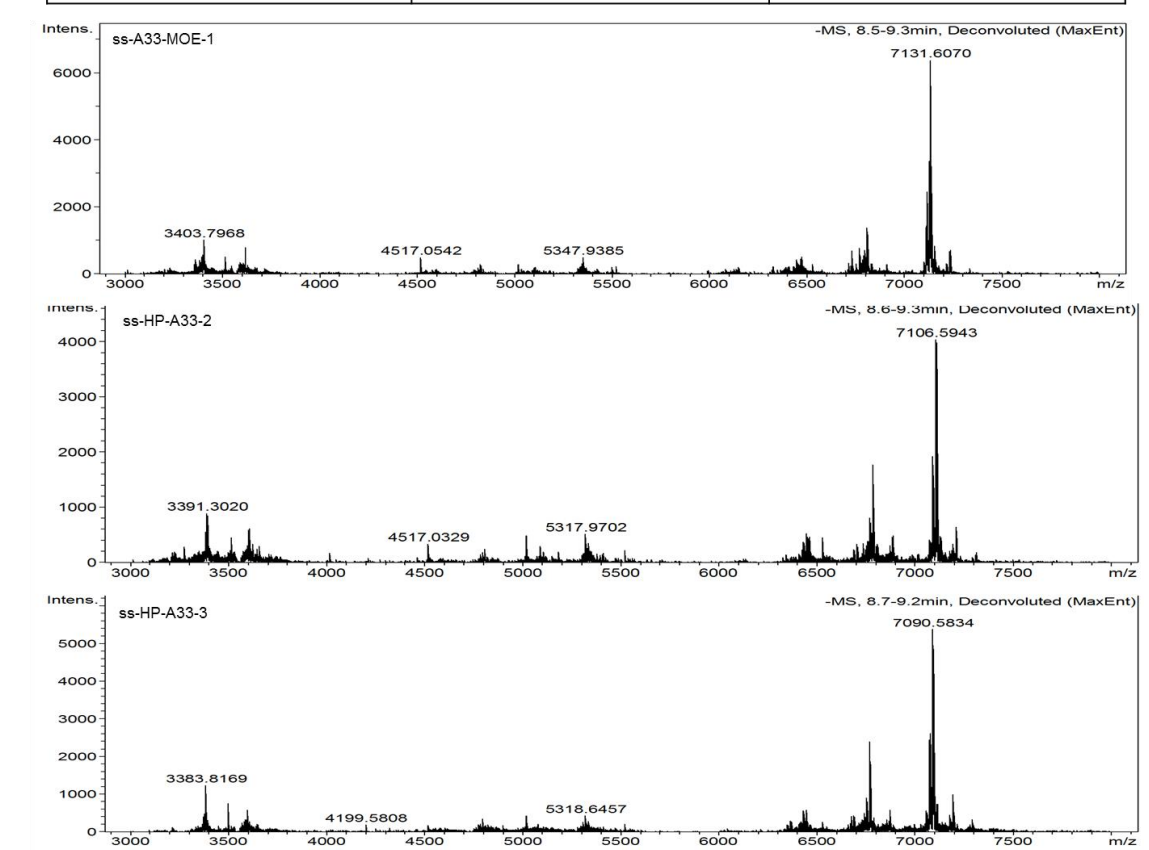


Figure 39. Mass spectrometry analysis of a synthesized ss-siRNA verifying the synthesis product to be correct.

2.3.2 ss-siRNA synthesis using EDITH

Following the LNA gapmer solid phase synthesis success using EDITH as a sulfurizing reagent, we decided to synthesize our additional ss-siRNAs using EDITH for the phosphorothioate linkages. As previously carried out for the LNA gapmer synthesis, 0.05M EDITH was dissolved in anhydrous acetonitrile. For the sulfurization step, an 8 second addition of EDITH to the column with a 60 second wait time was followed by 6 second addition of EDITH to the column with a 60 second wait time. Also, in the subsequent ss-siRNA syntheses, BTT also replaced tetrazole as a coupling reagent, keeping the coupling time at 600 seconds per addition.

As described above, the ss-siRNAs were synthesized in several different steps due to the limited number of auxiliary lines for modifications on the solid phase synthesizer, and the need to manually change cycles between PS and PO backbone chemistry. The five synthesis steps changed slightly due to the chemical modification scheme of the ss-siRNAs being slightly different, mainly with the alternation of PO and PS linkages following every nucleotide. The ss-siRNA sequence design and layout will be discussed in further detail in Chapter 4.

Following the ss-siRNA synthesis, the oligonucleotides were deprotected and cleaved from the Unylinker support using ammonium hydroxide at 55°C for 16 hours. The correct ss-siRNA sequence was synthesized and verified by mass spectrometry analysis. A representative oligonucleotide, ss-A33-MOE-2, is show to indicate the correct products were obtained from mass spectrometry (Figure 40). Although we were able to achieve the correct ss-siRNA product using either TETD and EDITH as sulfurizing reagent, we chose to continue using EDITH for our sulfurization steps due in part to the dramatic decrease in sulfurizing time which cause a decrease of ~13 minutes per PS linkage in the synthesis time.

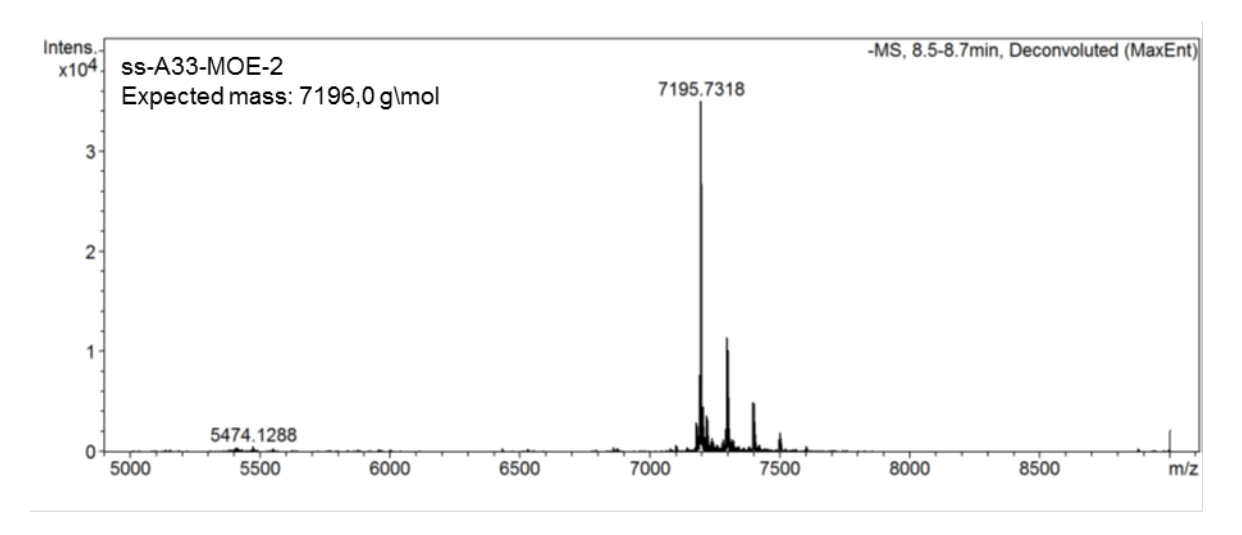


Figure 40. Mass spectrometry analysis of a synthesized ss-siRNA ss-A33-MOE-2, verifying the synthesis product to be the correct mass.

2.4 EDITH studies

With the solid phase synthesis success we achieved using EDITH as a sulfurizing reagent, we decided to try to optimize the protocol used for EDITH-based synthesis. The end goal for this experiment was to determine if we could use less EDITH per synthesis cycle. Since our previous syntheses used two additions of EDITH per PS linkage (an 8 second addition followed by a 6 second addition). A mixed 8mer sequence of LNA (Figure 41A) was chosen for this synthesis and was made fully phosphorothioated. BTT was used as coupling reagent and the sequences were built on Unylinker support. We chose six different solid phase synthesis conditions for our EDITH delivery (Table 1).

Table 1. Six different solid phase synthesis conditions for our EDITH delivery study.

Experiment	EDITH Delivery 1 (seconds)	Wait 1 (seconds)	EDITH Delivery 2 (seconds)	Wait 2 (seconds)
1	8	60	6	60
2	8	120	NA	NA
3	8	60	NA	NA
4	6	60	2	60
5	8	30	6	30
6	6	30	2	30

The six oligonucleotides were deprotected and cleaved from the Unylinker support using a fast deprotection method of 33% ethanolic methylamine: ammonium hydroxide at 65°C for 90 minutes.

A mass spectrometry analysis was run on the oligomers showing that all six synthesis methods produced an almost identical (within 0.3 g/mol) mass. However the mass peak is showing 1841 g/mol instead of the correct 2763 g/mol. This weight corresponds to 2/3 of the correct mass, and may be explained if the LNA is flying in MS as a dimer (Figure 42), and if the mass spectrometry deconvolution software is recognizing one fewer charge on our LNA dimer (Figure 41B). A 20% polyacrylamide analytical gel was also run in order to verify the mass spectrometry results (Figure 43). The control LNA used in gel for comparison has a molecular weight of 4800 g/mol. The EDITH LNAs are running at a higher molecular weight of ~5500 g/mol which would correspond to the LNA sequences running as duplexes. The LNA-LNA homoduplex formed between the two strands is highly favorable (Figure 42).

Α	Oligonucleotide sequence	Expected Mass g\mol	Actual Mass g\mol
	$A_sC_sT_sG_sG_sC_sC_sC$	2763.0	1841.6 with small 2762.8 peak

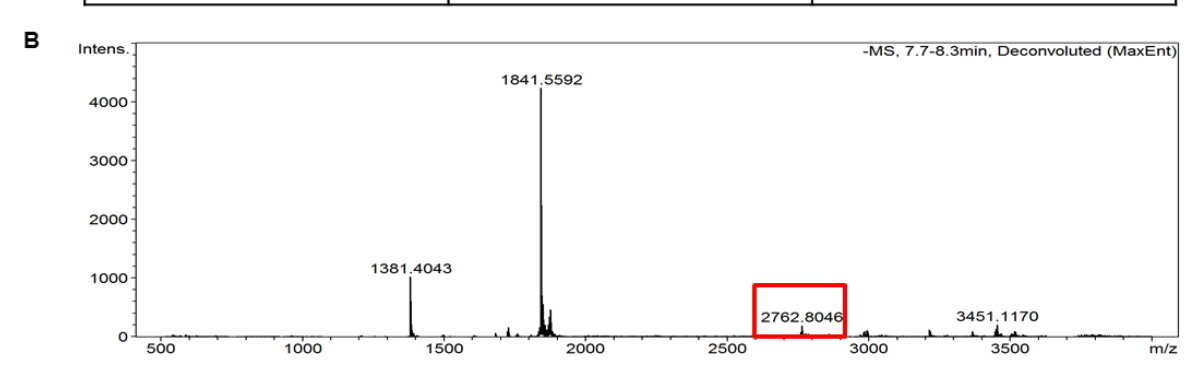


Figure 41. Results of EDITH studies A) phosphorothioated LNA sequence used in the EDITH studies with the expected and calculated mass LNA; 's': phosphorothioate B) representative mass spectrometry analysis of LNAs synthesized in the EDITH study. The red box indicated the correct molecular weight product.

$$A_sC_sT_sG_sG_sC_sC$$
 $| | | | | |$
 $C_sC_sC_sG_sG_sT_sC_sA$

Figure 42. LNA dimer formation. LNA; 's' phosphorothioate.

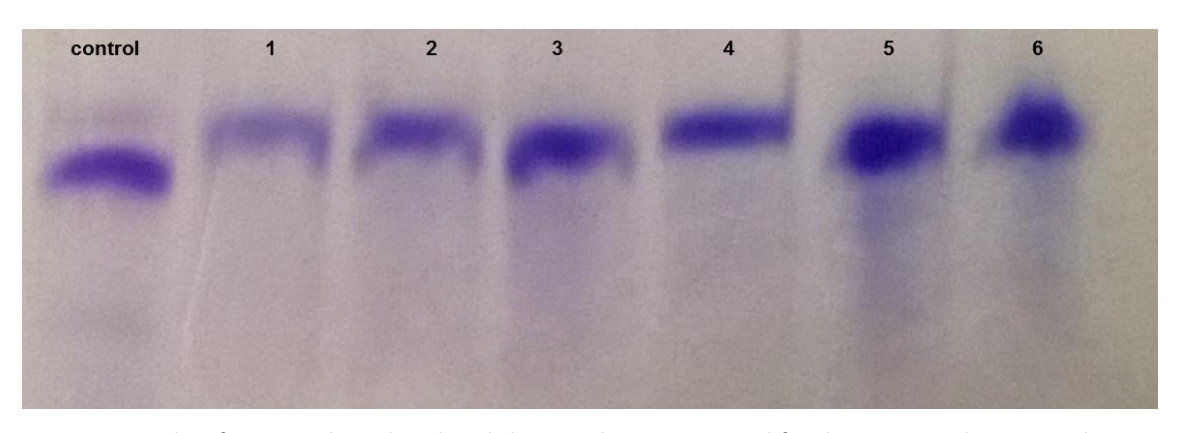


Figure 43. Results of a 20% polyacrylamide gel showing the six LNAs used for the EDITH study compared against a known molecular weight LNA. The control is an LNA gapmer of known weight, 4800 g/mol. The LNAs 1-6 are ~5500 g\mol which would correspond to the LNA running as a dimer.

From the EDITH studies, we can conclude that all of the EDITH conditions resulted in synthesis products of equal mass. Although the solid phase synthesis products cannot be isolated at this time due to the dimerization of the sequences, it can be concluded that no one synthesis condition produces better oligonucleotides than the other. For the purposes of our lab's future

syntheses, any of the EDITH conditions would be appropriate for synthesis. Thus this project was successful in identifying conditions with reduced consumption of EDITH but result in high efficiency sulfurization.

2.5 Unmodified RNA oligonucleotide synthesis

For the projects outlined in the following chapters, several oligonucleotides containing native or 'unmodified' ribonucleotides (i.e. RNA containing a 2'-OH group) had to be synthesized via solid phase synthesis (Appendix A). These were typically made with phosphodiester linkages, but some sequences contained phosphorothioates. The oligonucleotide sequence design and rationale will be discussed at a later time, with this section focusing on the synthesis and purification methods of the unmodified RNA oligonucleotides used.

2.5.1 Synthesis cycle

For the RNA synthesis described in this thesis, we purchased 2-O-TBS-protected RNA phosphoramidites for the solid phase oligonucleotide synthesis. The amidites were dissolved in anhydrous acetonitrile to a 0.15 mol/L concentration. BTT was used instead of tetrazole as a coupling agent. The coupling time for the RNA additions was 10 minutes per base. The oligonucleotides were manually cleaved from the solid support due to the ammonium hydroxide used in the solid phase synthesizers end cycle. The detailed synthesis cycle is listed in Appendix 1. Unylinker solid support was used on all RNAs synthesized unless otherwise stated.

2.5.1.1 Deprotection and cleavage from the solid support

Unfortunately, several troubleshooting conditions were required in order to improve the RNA deprotection efficiency. For the RNAs used in this thesis, a "fast deprotection solution" consisting of 1:1 33% methylamine / concentrated ammonium hydroxide was added to the oligonucleotide to cleave both the base protecting groups and the solid support. However, the end product was not of consistently high quality if changes were made to the time the sample was heated during deprotection.

When a Unylinker solid support is used for synthesis, the deprotection conditions must be harsher than if an alternative solid support is used. In our experience, the deprotection must involve a heating step in order to fully cleave the RNA from the Unylinker, but the RNA will degrade if left too long (>90 minutes) in the 33% methylamine / ammonium hydroxide with heat.

2.5.1.1.1 Deprotection at room temperature for 90 minutes

We allowed one set of synthesized RNAs to incubate in 33% methylamine/ ammonium hydroxide for 90 minutes at room temperature in order to cleave the oligonucleotide from the Unylinker solid support and deprotect the nucleobases. Upon mass spectrometry analysis, it was found that in several of the RNAs, the correct mass peak was indicated, but a $^{\sim}$ +274 peak was also present (Figure 44). We reasoned that this peak could be due to inefficient cleavage from the Unylinker (Figure 45).

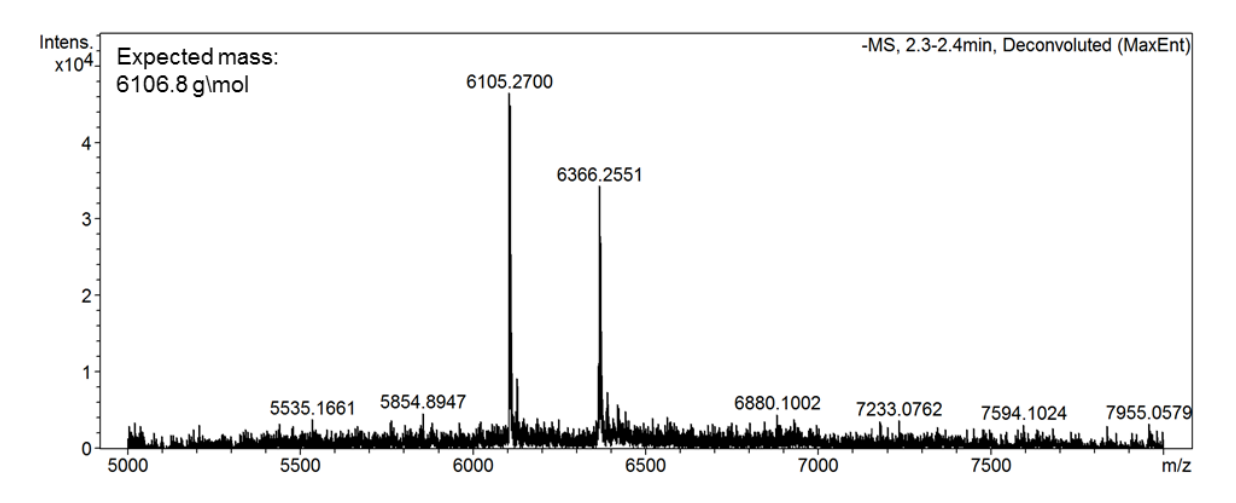
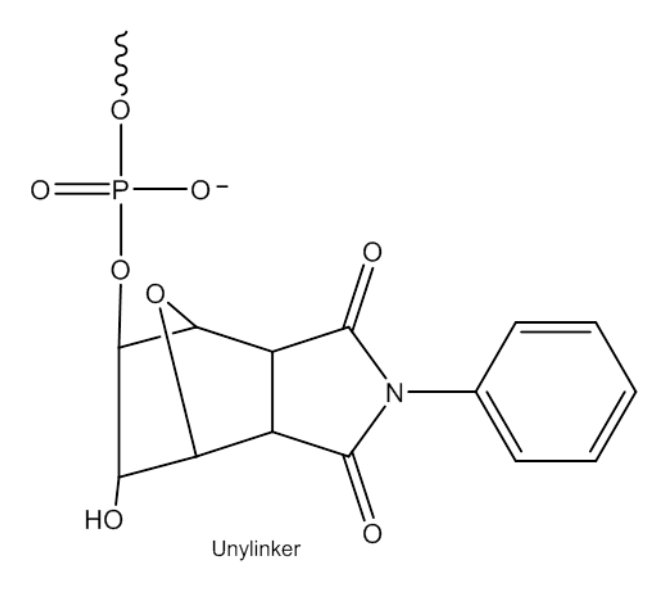


Figure 44. Mass spectrometry analysis of synthesized RNA showing the correct mass peak and a +261 peak.



Exact mass: 368.05

Figure 45. Unylinker adduct with exact mass calculated.

2.5.1.1.2 Deprotection at 65°C for 180 minutes

The above set of RNAs were resynthesized and deprotected using harsher deprotection conditions. We heated the samples at 65°C for three hours in 1:1 33% methylamine /

concentrated ammonium hydroxide solution in order to fully cleave the oligonucleotide from the Unylinker support (Figure 46). Although this deprotection method worked well for cleaving the oligonucleotide from the Unylinker support, it did cause degradation of the RNA causing a lower yield than with the previous deprotection conditions. The yield was calculated by measuring the UV absorbance values and calculating the Beer-Lamberbert Law value (Absorbance=molar extinction coefficient*concentration*length path).

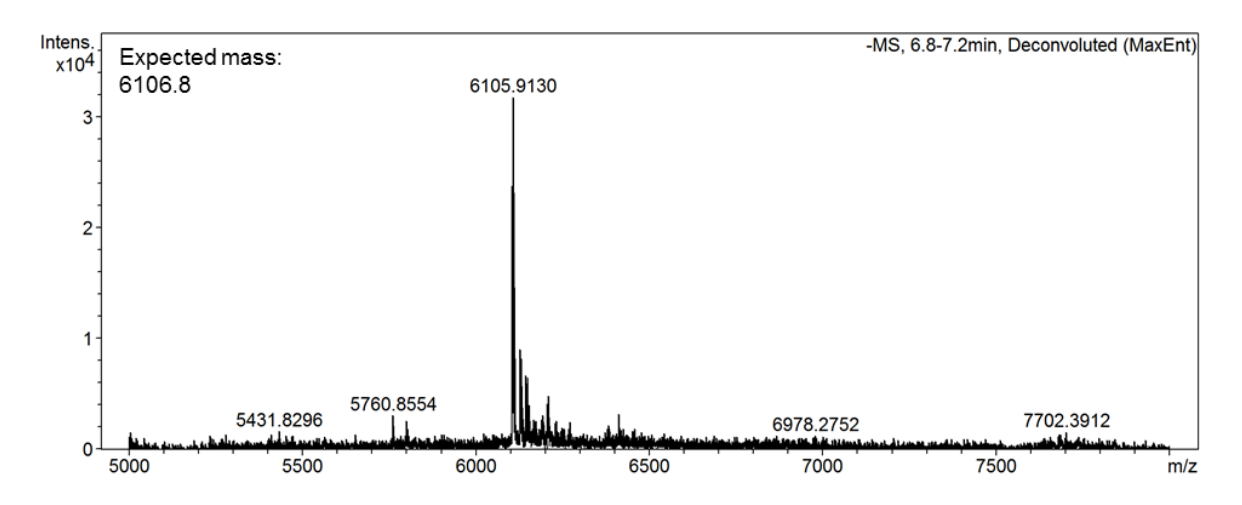


Figure 46. Mass spectrometry analysis of synthesized RNA showing the correct mass peak using a 180 minute heated cleavage step.

2.5.1.1.3 Deprotection at 65°C for 10 minutes

For the project outlined in Chapter 5, we needed to synthesize some 40-mer RNAs. Longer unmodified RNAs are more challenging to make synthetically due, in part, to the 2' TBS protecting group not being fully stable to the basic deprotection conditions used. If the RNA loses the 2' TBS protecting group, it can lead to phosphodiester chain cleavage or 3' to 2'-phosphate migration. For this reason, and from our experiences with the aforementioned cleavage conditions, we chose to use an alternative solid support for the longer RNA synthesis. Thus CPG was purchased with the 3' nucleoside already attached (Figure 47), which allowed the oligonucleotide to be cleaved from the solid support by heating for 10 minutes at 65°C in33% methylamine / concentrated ammonium hydroxide.

Figure 47. CPG with 3' RNA nucleobase attached.

2.5.2 Unmodified RNA purification

In our experience, unmodified RNA is rarely clean enough for experimental use without purification. The synthesis tends to contain a large number of failure sequences which need to be discarded before the RNA is ready for use. This is due to the less efficient coupling of RNA due to the bulky 2'-OH protecting group causing steric hindrance. Either a 16% or 20% polyacrylamide denaturing gel (depending on oligonucleotide length) was run for each RNA sequence in order to isolate the full length product from the truncated sequences. The detailed gel electrophoresis protocol is provided in Chapter 6.

For our longer oligonucleotides, we did not have a suitable standard molecular weight control oligonucleotide or marker to use on the gels. For these gels, we loaded our oligonucleotides onto the gels in the absence of a molecular weight marker. Upon Stains-all staining, the highest molecular weight band is isolated for further analysis. We initially assume that the highest molecular weight band is the full length oligonucleotide product. Each lower molecular weight band indicates a truncated oligonucleotide sequence.

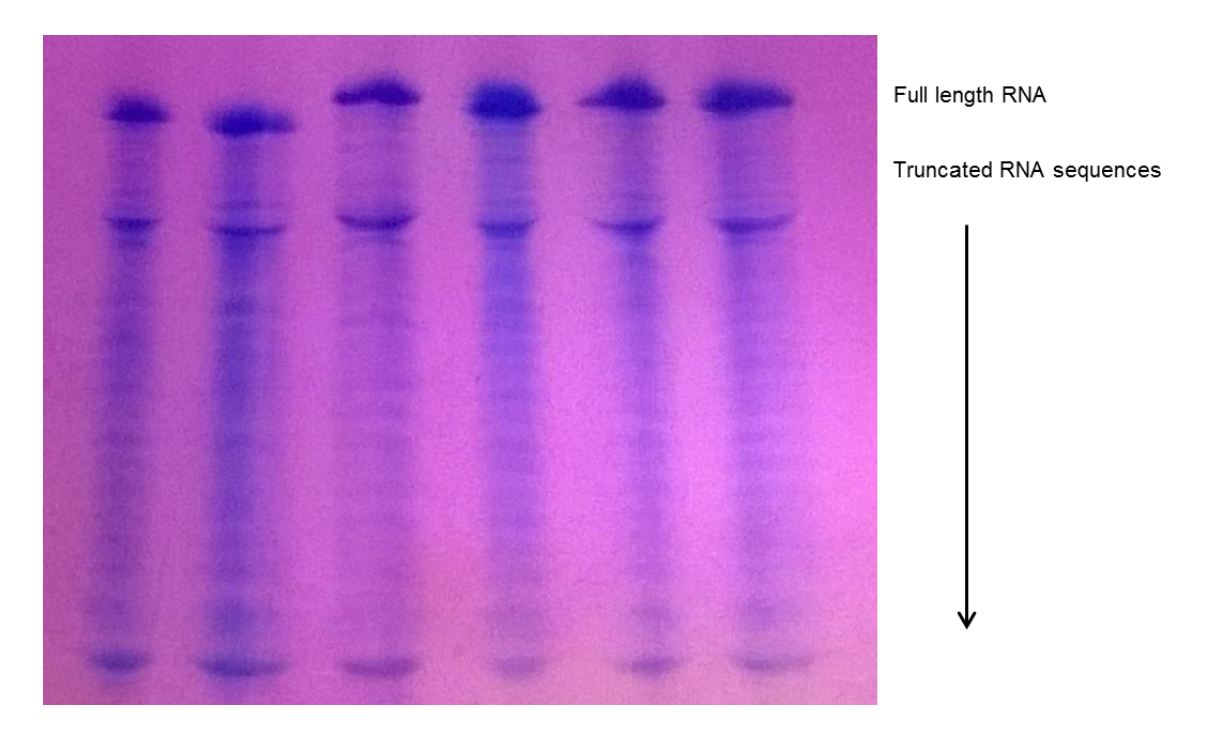


Figure 48. 16% polyacrylamide analytical gel showing the failure RNA sequences, with the highest molecular weight correct RNA sequence on the top. These oligonucleotides are unmodified 40-mer RNAs of mixed sequences. The gel was stained using Stains-all.

2.6 Conclusions

Several different classes of oligonucleotides were utilized in the experiments described in this thesis. We needed to optimize the solid phase synthesis of each different class of oligonucleotides. In all cases, the yield needed to be high enough for multiple experiments, and the purity needed to be adequate for cellular and biophysical assays.

We examined the poor yield and purity of our phosphorothioated LNA gapmers and determined that using a 0.05M EDITH sulfurization solution with a decreased sulfurization time as compared to TETD was the key to a correctly synthesized oligonucleotide with a high yield. For the LNA gapmers synthesized with EDITH as sulfurizing agent, the oligonucleotides were clean enough to avoid HPLC or gel purification. However, a Nap-10 column was used to remove any small molecule impurities left from the deprotection stage.

Once the EDITH experiments had been optimized, we were able to more successfully synthesize our ss-siRNAs. It is true that the synthesis for this type of oligonucleotides is very time consuming due to the need to make the sequence in several stages with oxidation vs sulfurization. However, the ss-siRNAs contain a 2'-modification on every ribose thus they do not require a desilylation step and are less sensitive to degradation than oligomers containing normal ribonucleotides. In addition, because of the absence of a TBS protecting group and 2'-OH group, these oligomers are compatible with deprotection and cleavage from Unylinker support.

For optimal synthesis of unmodified RNA oligonucleotides, Unylinker solid support should be avoided. Although we were eventually able to cleave the oligonucleotide from the Unylinker successfully and to achieve adequate yields during synthesis, the results were not always consistent and always required significant purification. In order for the Unylinker to be fully cleaved from the oligonucleotide, it requires heating in basic solution at 65° for several hours, during which time some of the TBS groups fall off leading to 2'-oxygen attack on phosphate and degradation of the RNA. For unmodified RNA synthesis, it is better to use a succinyl-lcaa-cpg solid support with the 3' nucleoside attached. This allows for less harsh deprotection conditions, thus greater purity and higher yield of oligonucleotide.

Chapter 3: Oligonucleotide-mediated silencing of ADAM33

3.1 Introduction

As mentioned in section 1.6, asthma is a common chronic inflammatory lung disease involving structural changes in the airways leading to airway obstruction, remodelling, hyperresponsiveness, and bronchospasms (125, 126). ADAM33 is the first asthma susceptibility gene to be identified by positional cloning (131). Several single point mutations (SNPs) within ADAM33 have been linked to asthma and bronchial hyperresponsiveness, but no single mutation is common to all disease populations.

To improve our understanding of the biology of *ADAM33* function, our collaborator, Dr. Hans Michael Haitchi (Faculty of Medicine, University of Southampton), has developed models including *ex vivo* human embryonic lung explant culture and *in vivo* mouse models (*219*). Oligonucleotide-mediated gene silencing of *ADAM33* in a human embryonic lung explant model would allow the study of airway branching and development under conditions of low *ADAM33* expression.

The ultimate goal of this work is the development of a therapeutic approach that can prevent or correct the pathological airway remodeling that seems to underlie asthma in a majority of cases. Our compounds could be used to explore therapeutic *ADAM33* inhibition in murine *in vivo* models to prevent or correct inappropriate airway remodeling and thus treat asthma at its origin rather than simply treating symptoms with Broncho-dilator and anti-inflammatory drugs.

In this chapter, we describe the development of three classes of oligonucleotides that inhibit the expression of *ADAM33* with varying effectiveness. We also describe novel conjugates that show improved uptake in lung fibroblasts.

3.2 Identification of active siRNA duplexes

3.2.1 Choosing siRNA sequences

Our collaborator, Dr. Hans Michael Haitchi, previously identified two siRNA duplexes, **HMH-1** and **HMH-2**, that were able to achieve up to 70% *ADAM33* inhibition in MRC-5 fibroblast cells (*220*). It was our aim to design and synthesize additional siRNA duplexes to try to achieve greater *ADAM33*

inhibition and to have additional sequences to use in for our comparison studies between duplex siRNAs and ss-siRNA oligonucleotides.

Our first step was to design and synthesize additional siRNA duplexes that target various regions of *ADAM33* mRNA. When designing siRNA sequences, there are published guidelines to consider (221, 222):

- 1) The 5' terminus of the antisense strand should be an A/U as opposed to a G/C; this is because the RISC complex tends to incorporate the strand of the siRNA duplex with lowest binding affinity at its 5' end. Moreover, the 5' end of the antisense strand should be A/U rich, especially in the first third of the sequence
- 2) The 5'-terminus of the sense strand should be a G/C as opposed to an A/U for the same reason
- 3) The duplex should contain fewer than 9 consecutive GC base pairs as this has been experimentally shown to be a possible suppressor of RISC activity

The siRNA sequences were selected by using the following three steps:

- The University of California, Santa Cruz (UCSC) genome browser¹ was used to find the mRNA sequence of the ADAM33 isoform that will be the oligonucleotide target for this project.
- 2. ADAM33 mRNA was folded computationally using the mFOLD program² (223). The results of the mFOLD program show several of the most stable secondary structures of the folded RNA. From those predicted secondary structures, a conclusion can be made as to which regions on the mRNA sequence are the most predicted to be single stranded and not a self-forming hairpin. Single stranded regions of RNA are the best target since they are more accessible to binding by oligonucleotides. Short sequences of 25-30 nucleotides are chosen for further analysis. Oligonucleotides are designed to be the complement of the target mRNA sequence.
- 3. The chosen potential oligonucleotide design sequences are aligned with nucleotide sequences for the entire human transcriptome³ using the Basic Local Alignment Tool (BLAST) (224). This program allows potential oligonucleotide off-target effects to be identified.

-

¹ http://genome.ucsc.edu/

² http://mfold.rna.albany.edu/?q=mfold

³ all human RefSeq (http://www.ncbi.nlm.nih.gov/refseq/) data)

Using as positive controls the previously designed siRNAs **HMH-1** and **HMH-2**, which target the region coding for the metalloproteinase (MP) domain and the 3'UTR of *ADAM33* mRNA respectively (225), eleven additional duplex siRNAs were designed and synthesized, targeting various regions of *ADAM33* mRNA (Table 2) (Appendix D and E). siRNA duplexes **HMH-1**, **HMH-2**, and **HP-1** thru **HP-4** have a 3'-overhang on the antisense strand only (this is to help promote preferential loading into the RISC complex) (226). This 3'-overhang consisted of two dT residues as is common in the design of duplex siRNAs (75) (Appendix D and E).

Although some siRNA duplexes do not follow all of the published design guidelines, they were selected in order to span various target sites along the mRNA.

Table 2. siRNA sequences designed to target ADAM33 mRNA.

siRNA			nce- s is on					о, а	ntis	ense	T _m (°C)
HMH-1	5 '	tt	GGA CCU			 AAC UUG				5 '	71
HMH-2	5 '	tt	GGU CCA	-		 CUC GAG				5 ′	77
HP-1	5 '		AGA UCU	_		 UGG ACC				5 ′	64-65
HP-2	5 '		GGG CCC	_		UGG ACC				5 ′	72-73
HP-3	5 '	tt	UGC ACG			 AGA UCU	_			5 ′	72
HP-4	5 '		UGG ACC			 CGG GCC				5 ′	77
HP-5	5 ′		CCC GGG			 GAU CUA			tt	5 ′	71
HP-6	5 '	tt	UGG ACC			 GGC CCG			tt	5 ′	76-78
HP-7	5 ′		AGU UCA		-	 AAG UUC			tt	5 ′	72-73
HP-8	5 '	tt	CCA GGU			CUA GAU		-	tt	5 ′	68
HP-9	5 ′		AGG UCC			UGG ACC			tt	5 ′	ND
HP-10	5 '	tt	GAU CUA			AUG UAC			tt	5 ′	65-68
HP-11	5 '		UAG AUC			CUG GAC			tt	5 ′	69
Scr	5 ′		AGU UCA			 CUG GAC			tt	5 ′	82-83

3.2.2 Duplex siRNA results

In order to ensure the most accurate data showing the inhibition of *ADAM33* mRNA by our siRNA duplexes, we initially screened the previously tested positive control siRNA, **HMH-1**, into MRC-5, a human lung non-diseased fibroblast cell line previously used for *ADAM33* experiments (227). Three different classes of transfection agents were used for transfection optimization of siRNA delivery into MRC-5 cells (Figure 49):

- 1) Viromer Blue and Green are polymers that were designed to exploit viral mechanisms for endosomal escape.
- 2) Lipofectamine RNAimax is a cationic lipid transfection agent (228). Cationic lipids have a positively charged headgroup which interacts with the negatively charged phosphate on the nucleic acid (229).
- 3) Polyplus INTERFERin is a non liposomal cationic amphiphile which, like a cationic lipid, binds to oligonucleotides and interacts with the anionic cell surface (230).

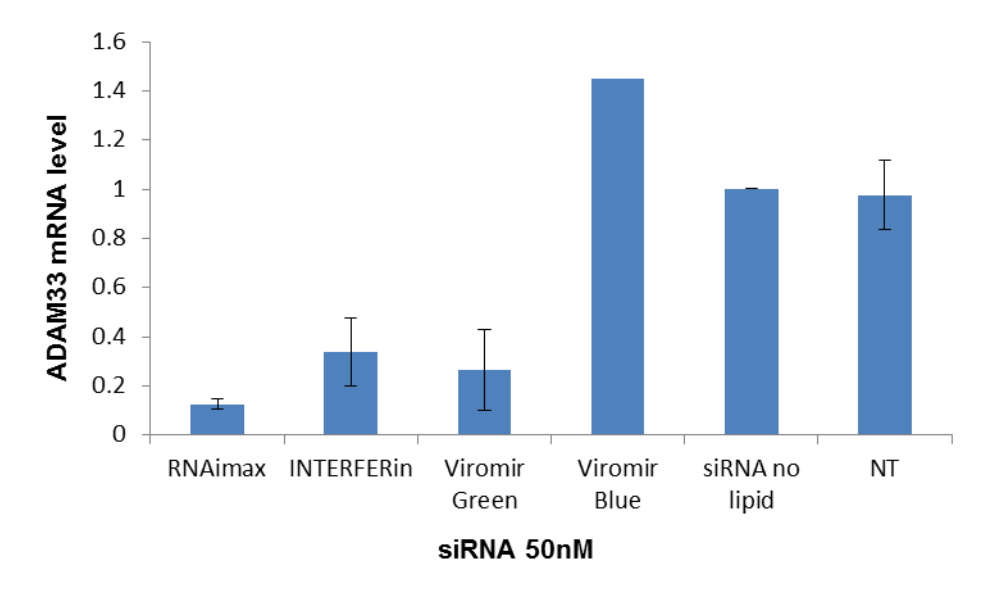


Figure 49. qRT-PCR results of relative ADAM33 mRNA levels when HMH-1 is co-transfected with various transfection agents. The siRNA was transfected at 50nM concentration and normalized to a no-lipid control. Error bars are standard deviation of the average result from independent experiments.

The transfection results showed that Viromir Blue was consistently inactive (indeed, it appeared to slightly activate *ADAM33* expression relative to the controls). Viromir Green achieved an average of 74% knockdown. The Polyplus INTERFERin showed an average knockdown of about 67%. Lipofectamine RNAiMAX showed not only the highest degree of knockdown but also the most consistent results between multiple transfections (average of 88% knockdown). Based on the results, we decided to move forward using the RNAiMAX cationic lipid since it showed the most consistent, potent gene silencing.

After the optimization of transfection conditions, we tested the two positive control siRNAs as well as the eleven newly designed siRNA duplexes in MRC-5 fibroblast cells, measuring the RNA levels by qRT-PCR (Table 2, Figure 50). The results showed that from the newly designed siRNAs, the most potent sequences, **HP-1** and **HP-2**, were only able to achieve 40% *ADAM33* inhibition as opposed to the 70-80% inhibition from the positive control siRNA **HMH-1**.

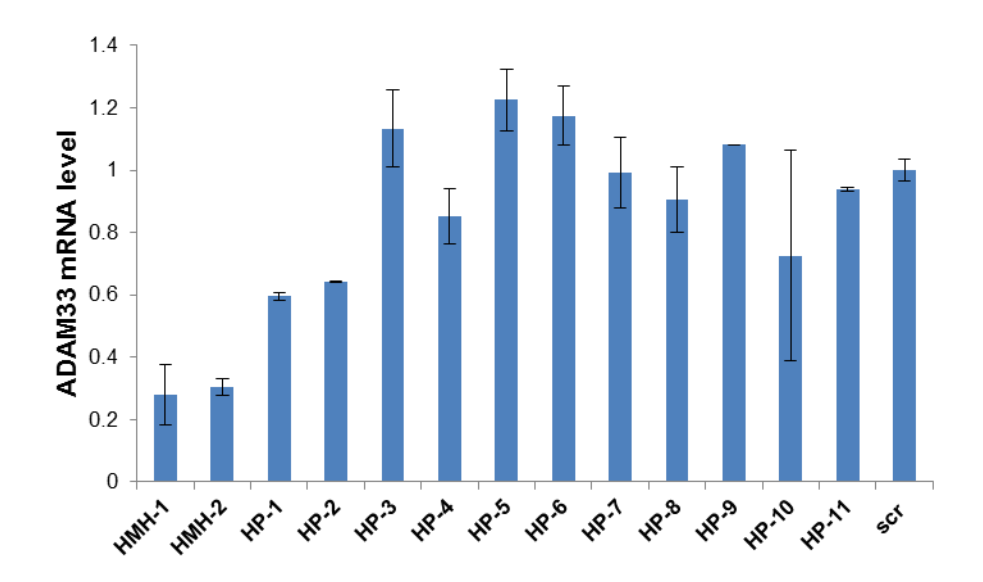


Figure 50. qRT-PCR results of relative ADAM33 mRNA levels when treated with duplex siRNAs. All siRNAs were transfected at 50nM concentration and normalized to a scrambled siRNA control. Error bars are standard deviation of technical replicates.

These first eleven siRNAs failed to match the potency of the control siRNA, **HMH-1**, so in an attempt to develop potent siRNAs, four additional siRNAs were designed and synthesized targeting various regions of *ADAM33* mRNA (Table 3) (Appendix D and E).

Table 3. siRNA sequences designed to target ADAM33 mRNA.

siRNA	Sequence- sense strand is on the top, antisense strand is on the bottom; RNA; dna	T _m (°C)
HP-12	5' UAG CUC CUA AAA UGA ACA G tt tt AUG GAG GAU UUU ACU UGU C 5'	60-61
HP-13	5' CAU GCA AUU UCC ACG GAC C tt tt GUA CGU UAA AGG UGC CUG G 5'	69-70
HP-14	5' CUG AAA ACC AUG ACA CCU U tt tt GAC UUU UGG UAC UGU GGA A 5'	64
HP-15	5' GAC AUU CAG GUG GCG CUG A tt tt CUG UAA GUC CAC CGC GAC U 5'	73-74

qRT-PCR analysis showed that these additional siRNAs, like the first batch we designed, failed to surpass the controls in activity. (Figure 51). This hit rate is significantly lower than most mRNA targets, and the overall silencing is only moderate (with the most active duplex, **HMH-1**, giving a silencing of 60-80%).

However, with this panel of siRNAs ranging from moderately effective to ineffective, we decided to move on to the next part of our study: designing single stranded analogues of a subset of these sequences.

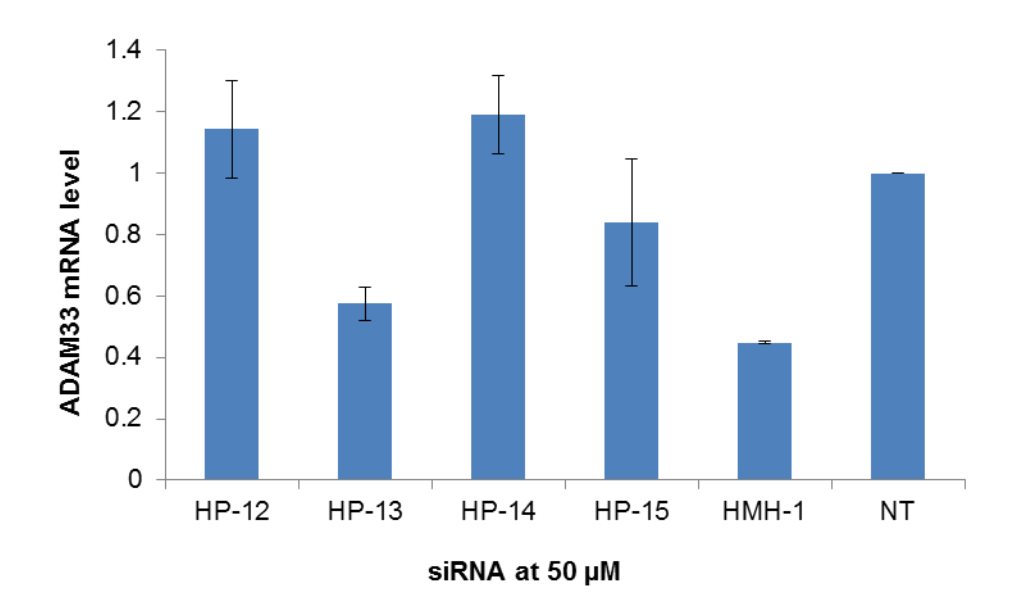


Figure 51. qRT-PCR results of relative ADAM33 mRNA levels when treated with duplex siRNAs. All siRNAs were transfected at 50nM concentration and normalized to a non-treated (NT) control. Error bars are standard deviation of two independent biological replicates.

3.3 ss-siRNA design

Due to systematic delivery problems associated with duplex siRNAs *in* vivo (231), a single stranded oligonucleotide would be beneficial for future *in vivo* and *ex vivo ADAM33* studies. We decided to compare the potencies of duplex siRNAs and ss-siRNAs on *ADAM33* inhibition due to some recent ss-siRNAs being as potent both *in vitro* and *in vivo* as their duplex complement (73, 74) when using an alternating 2'-OMe and 2'F RNA chemical modification scheme. Since both the duplex siRNAs and the ss-siRNAs take advantage of RISC mediated gene silencing, ss-siRNAs could be a potent inhibitor of *ADAM33* that can be delivered without the aid of transfection agents.

In 2002, it was discovered that only one strand of the duplex siRNA serves to guide Argonaute2 (and associated RISC factors) to its target (72). This finding opened the doors for researchers to attempt to achieve potent gene silencing through single stranded RNAs (71, 73, 74, 232-237). Through these studies, it was shown that the single stranded RNA needed to be both chemically modified and chemically phosphorylated in order to be efficacious.

Our ss-siRNAs were designed using a chemical modification motif adapted from *Lima et al. (74)* which uses a pattern of alternating 2'F and 2'-OMe modifications which have been shown to improve potency when incorporated into duplex siRNAs (75, 76).

For our studies, we began by comparing the gene silencing ability of ss-siRNAs with their parent siRNA duplexes. Each ss-siRNA sequence is identical to the antisense strand of the parent duplex siRNA, with the exception that the sequence derived from the 'overhangs' of the parent sequence were set to be adenosine rather than thymine.

We initially synthesized three ss-siRNAs (**ss-A33-MOE-1**, **ss-HP-2**, and **ss-HP-3**) with sequences based on the antisense strands of siRNAs HMH-1, HP-2, and HP-3, respectively (Table 4). These represent three siRNA duplexes with potent, moderate and negligible silencing activity, respectively. The three ss-siRNAs were synthesized containing a mixed backbone modification scheme with one 5'-phosphorothioate linkage, nine phosphodiester linkages followed by ten PS linkages. The 3'-end of the sequences contained two PS-linked MOE adenosines, while the remaining sequence was an alternating pattern of 2'F and 2'OMe (Table 4) (Appendix D and E). The ss-siRNAs were chemically phosphorylated at the 5'-end which is a requirement for oligonucleotide uptake by RISC. (5'-phosphates have been shown to be sufficient for experiments in cultured cells (73, 74, 236, 237), but a metabolically stable phosphate analogue such as (E)-vinylphosphonate is required for *in vivo* studies (74, 238) (Figure 52).

Table 4. ss-siRNA sequences and their parent ds siRNAs designed for ADAM33 inhibition. For duplex sequences, sense strand is listed on top. Modification code: RNA, dna, 2'-OMe, 2'-F, 2'-MOE, '+': LNA, 'S': phosphorothioate, P: 5' phosphate. ND, T_m not determined.

siRNA duplex	Sequence	T _M (°C)
HMH-1	5' GGA AGU ACC UGG AAC UGU A TT CCU UCA UGG ACC UUG ACA U 5'	71
HP-A33-2	5' GGG AGA UGC UCA UGG AAA C TT CCC UCU ACG AGU ACC UUU G 5'	72-73
HP-A33-3	5' UGC UUG AGC UGG AGA AGA A TT ACG AAC UCG ACC UCU UCU U 5'	72
Scr	5' AGU GGA GGG CGC CUG CCA C TT TT UCA CCU CCC GCG GAC GGU G 5'	82-83
ss-siRNA	Sequence (5' – 3')	
ss-A33- MOE-1	$\mathtt{P-}\underline{\mathtt{U}_{s}}\mathbf{\underline{A}}\underline{\mathtt{C}}\mathbf{\underline{A}}\underline{\mathtt{G}}\mathbf{\underline{U}}\underline{\mathtt{U}}\underline{\mathtt{C}}\underline{\mathtt{C}}\mathbf{\underline{A}}\underline{\mathtt{G}}\mathbf{\underline{G}}_{s}\underline{\mathtt{U}_{s}}\mathbf{\underline{A}}_{s}\underline{\mathtt{C}}_{s}\mathbf{\underline{U}_{s}}\underline{\mathtt{U}_{s}}\underline{\mathtt{C}}_{s}\underline{\mathtt{C}}_{s}\underline{\mathtt{A}}_{s}\underline{\mathtt{A}}$	ND
ss-HP- A33-2	$\mathbf{P} - \underline{\mathbf{G}}_{\mathbf{S}} \underline{\mathbf{U}} \underline{\mathbf{U}} \underline{\mathbf{C}} \underline{\mathbf{C}} \underline{\mathbf{M}} \underline{\mathbf{G}} \underline{\mathbf{G}} \underline{\mathbf{G}} \underline{\mathbf{C}}_{\mathbf{S}} \underline{\mathbf{U}}_{\mathbf{S}} \underline{\mathbf{C}}_{\mathbf{S}} \underline{\mathbf{C}}_{\mathbf{S}} \underline{\mathbf{C}}_{\mathbf{S}} \underline{\mathbf{C}}_{\mathbf{S}} \underline{\mathbf{A}}_{\mathbf{S}} \underline{\mathbf{A}}$	78
ss-HP- A33-3	$\mathtt{P-}\underline{\mathtt{U}_{\mathrm{S}}}\underline{\mathtt{U}}\underline{\mathtt{C}}\underline{\mathtt{U}}\underline{\mathtt{C}}\underline{\mathtt{U}}\underline{\mathtt{C}}\underline{\mathtt{C}}\underline{\mathtt{C}}\underline{\mathtt{G}}\underline{\mathtt{C}}_{\mathrm{S}}\underline{\mathtt{U}_{\mathrm{S}}}\underline{\mathtt{C}}_{\mathrm{S}}\underline{\mathtt{A}}_{\mathrm{S}}\underline{\mathtt{A}}_{\mathrm{S}}\underline{\mathtt{G}}_{\mathrm{S}}\underline{\mathtt{C}}_{\mathrm{S}}\underline{\mathtt{A}}_{\mathrm{S}}\underline{\mathtt{A}}_{\mathrm{S}}\underline{\mathtt{A}}$	79
ss-A33- MOE-2	$\mathtt{P-}\underline{\mathtt{U}}_{\mathtt{S}} \underline{\mathtt{A}}_{\mathtt{S}} \underline{\mathtt{C}} \underline{\mathtt{A}}_{\mathtt{S}} \underline{\mathtt{G}} \underline{\mathtt{U}}_{\mathtt{S}} \underline{\mathtt{U}} \underline{\mathtt{C}}_{\mathtt{S}} \underline{\mathtt{C}}_{\mathtt{S}} \underline{\mathtt{U}} \underline{\mathtt{A}}_{\mathtt{S}} \underline{\mathtt{C}}_{\mathtt{S}} \underline{\mathtt{U}}_{\mathtt{S}} \underline{\mathtt{U}}_{\mathtt{S}} \underline{\mathtt{C}}_{\mathtt{S}} \underline{\mathtt{C}}_{\mathtt{S}} \underline{\mathtt{A}}_{\mathtt{S}} \underline{\mathtt{A}}$	76-77
ss-A33- OMe	$P - \underline{U}_S \underline{A}_S \underline{C} \underline{A}_S \underline{G} \underline{U}_S \underline{U} \underline{C}_S \underline{C} \underline{A}_S \underline{G} \underline{G}_S \underline{U} \underline{A}_S \underline{C}_S \underline{U}_S \underline{U}_S \underline{C}_S \underline{C}_S \underline{A}_S \underline{A}$	78
ss-A33- LNA	$\mathbf{P} - \underline{\mathbf{U}}_{\mathbf{S}} \mathbf{A}_{\mathbf{S}} \underline{\mathbf{C}} \mathbf{A}_{\mathbf{S}} \underline{\mathbf{G}} \mathbf{\mathbf{U}}_{\mathbf{S}} \underline{\mathbf{C}}_{\mathbf{S}} \underline{\mathbf{C}}_{\mathbf{S}} \underline{\mathbf{G}} \mathbf{\mathbf{G}}_{\mathbf{S}} \underline{\mathbf{U}} \mathbf{A}_{\mathbf{S}} \underline{\mathbf{C}}_{\mathbf{S}} \underline{\mathbf{U}}_{\mathbf{S}} \underline{\mathbf{C}}_{\mathbf{S}} \underline{\mathbf{C}}_{\mathbf{S}} \underline{\mathbf{C}}_{\mathbf{S}} + \mathbf{A}_{\mathbf{S}} + \mathbf{A}_{\mathbf{S}}$	79

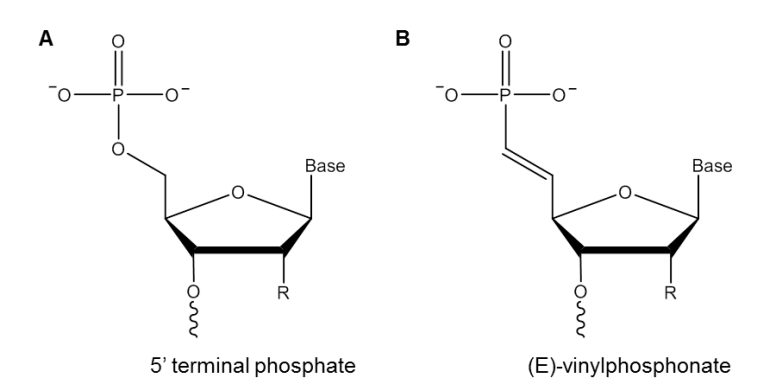


Figure 52. A) Unmodified 5'-terminal phosphate chemically synthesized to the ss-siRNAs B) 5' terminal (E)-vinylphosphonate modification necessary for *in vivo* ss-siRNA studies.

The ss-siRNAs were transfected into MRC-5 fibroblasts cells with the aid of RNAiMAX cationic lipid transfection agent. The ss-siRNAs **ss-A33-MOE-1**, **ss-HP-2**, and **ss-HP-3** based on this modification scheme described above showed negligible silencing activity (Figure 53).

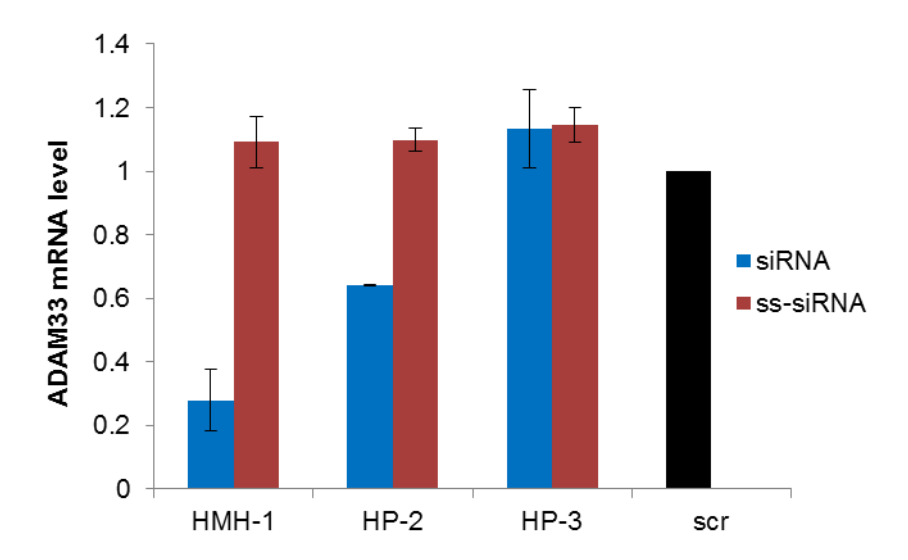


Figure 53. qRT-PCR results comparing relative potencies of duplexes siRNA and ss-siRNA. All results are normalized to a scrambled siRNA duplex control. Error bars are standard deviation of biological replicated. All oligonucleotides were transfected at 50nM.

We decided to vary the chemical modification scheme of our ss-siRNAs to see if an alternative PS arrangement or 3' terminus modification would improve the oligonucleotide potency. Three additional ss-siRNAs were synthesized with altered chemical modification schemes (Table 4, bottom three entries). Only the most potent duplex siRNA, HMH-1, served at a template sequence strand for this set of ss-siRNA oligonucleotides. All three of the new ss-siRNAs (ss-A33-MOE-2, ss-A33-OMe, and ss-A33-LNA) were designed with a different pattern of phosphate modification from the first set of strands. Namely, this new set was designed to contain an alternating PS and PO linkage pattern throughout the entire 5' side of the sequence, followed by seven 3' terminal PS linkages (Table 4). The sugar chemistry of the two 3' terminal adenosines was also altered, either maintaining MOE modification (ss-HMH-MOE-2) or changing this to 2'-OMe (ss-HMH-OMe), or LNA modifications (ss-HMH-LNA).

In the recent literature, all the ss-siRNAs described contain 3'-terminal MOE modifications, in spite of the fact that MOE is not commercially available (73, 74, 235-237). This reflects the fact that all of the recent literature has been done by teams involving ISIS pharmaceuticals, who hold the patent rights to MOE. Surprisingly, our results showed that only the ss-siRNA containing 2'-O-methyl RNA (ss-A33-OMe) at the 3' end was able to approach the potency of the duplex siRNA (Figure 54).

Surprisingly, some of the inactive ss-siRNAs appeared to cause a small but reproducible activation of *ADAM33* expression relative to a scrambled control.

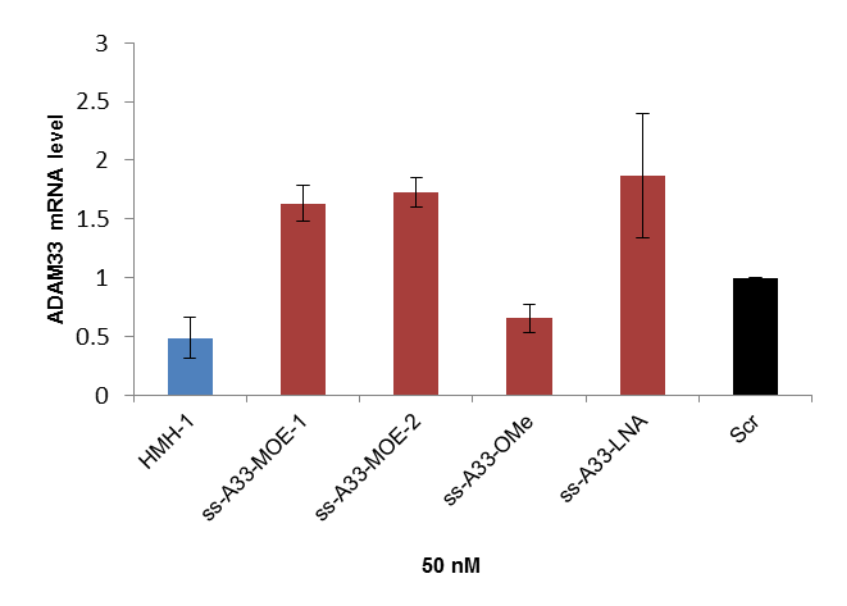


Figure 54. qRT-PCR results comparing relative potencies of different chemical modification schemes on ss-siRNA activity. All results are normalized to a scrambled siRNA duplex control. All oligonucleotides were transfected at 50nM. Error bars are standard deviation of biological replicates.

Our findings show that the potency of ss-siRNAs can be increased dramatically by making small changes to the chemical modification scheme. These results can prove valuable to researchers who would like to use the ss-siRNA approach to gene silencing since our most potent design uses only commercially available monomers. We followed up on these observations using additional sequences, genes and cell lines in chapter 4.

For many gene silencing applications, RISC recruitment and activation could be the key to potent results. However, for our goal of simply silencing *ADAM33*, RISC-based mechanisms might not be necessary. We therefore decided to test silencing by gapmer antisense oligonucleotides as well.

3.4 Locked nucleic acid gapmers show increased potency for silencing ADAM33

Since locked nucleic acid (LNA) was first reported in 1998 (239), the use of LNAs in antisense gene silencing has become a serious therapeutic option. The high binding affinity of LNA and its analogues allows the design of short ASOs that inhibit their targets with high potency (92, 240, 241). Moreover, these short ASOs can often be delivered *in vitro* and *in vivo* without the aid of transfection agent (92, 106).

3.4.1 LNA gapmer design

Since the LNA modification increases the binding affinity of the oligonucleotide to its target but also potentially to itself, special care must be taken when designing a LNA gapmer sequence. The sequence selection was done using the guidelines listed in section 3.2.1 as well as an additional guideline: shortlisted LNA gapmer sequences were computationally folded using Integrated DNA Technologies OligoAnalyzer software⁴ as a final step in sequence selection. This software can be used to predict possible hairpins or self-structure that the sequences are likely to form. The avoidance of LNA-LNA base pairs in particular is important; given the very high stability of LNA-LNA base pairs, such a hairpin would be unlikely to unfold even in the presence of a fully complementary RNA target (Figure 55).

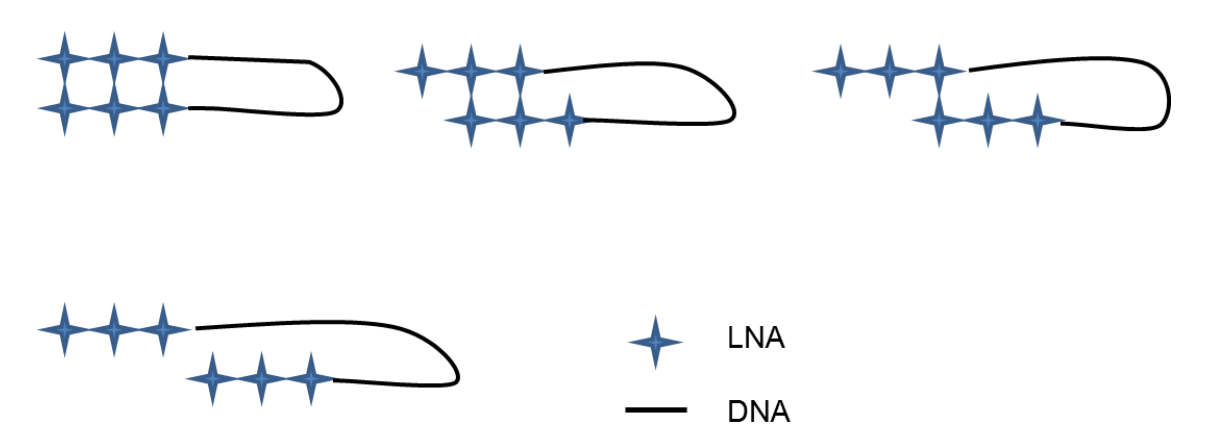


Figure 55. Schematic showing LNA gapmers folding to form stable hairpins. These make unsuitable antisense oligonucleotides, particularly in the cases when LNA-LNA base pairs can form, since they are unlikely to unfold even in the presence of a fully complementary RNA target.

Twelve LNA 3-9-3 gapmers were designed and synthesized to target ADAM33 mRNA (Table 5) (Appendix D and E). All were synthesized with fully phosphorothioate backbone.

⁴ https://www.idtdna.com/analyzer/Applications/OligoAnalyzer/

Table 5. LNA gapmer sequences: LNA: -'S': phosphorothioate; lower case: DNA.

LNA	<u>Sequence</u>
33-G	$T_sG_sA_st_sc_sc_sg_st_sg_st_sg_sg_sT_sT_sG$
33-Н	$A_sT_sG_sa_st_sc_sc_sg_st_sg_st_sg_sG_sT_sT$
33-I	$A_sA_sT_sg_sa_st_sc_sc_sg_st_sg_st_sG_sG_sT$
33-J	$C_sA_sA_s$ $t_sg_sa_st_sc_sc_sg_st_sg_sT_sG_sG$
33-K	$C_sC_sG_sg_sg_sg_sc_sa_st_sg_sg_sA_sG_sA$
33-L	$T_sG_sT_sc_sa_st_sg_sg_st_st_st_st_sC_sA_sG$
33-M	$G_sG_sT_sg_st_sc_sa_st_sg_sg_st_st_sT_sT_sC$
33-N	$A_sG_sG_st_sg_st_sc_sa_sg_sg_st_sT_sT_sT$
33-O	$T_sC_sA_st_st_st_st_sa_sg_sg_sa_sg_sC_sT_sA$
33-P	$T_sT_sC_sa_st_st_st_st_sa_sg_sg_sa_sG_sC_sT$
33-Q	$T_sG_sT_st_sc_sa_st_st_st_st_sa_sg_sG_sA_sG$
33-R	$T_sC_sC_sg_st_sg_sg_sa_sa_st_st_sG_sC_sA$
lna ctrl	A _s T _s T _s t _s t _s a _s t _s t _s c _s g _s g _s a _s G _s C _s T

3.4.2 LNA gapmer results

3.4.2.1 LNA gapmer delivery using cationic lipid transfection reagent

Initially, the twelve PS LNA gapmers were transfected at a 50nM concentration into MRC-5 fibroblast cells using RNAiMAX cationic lipid as a transfection agent. LNAs **33-G**, **33-N**, **33-O**, **33-P**, **33-Q**, and **33-R** all achieved >80% inhibition of *ADAM33* RNA when normalized to a scrambled control (Figure 56). A dose response analysis was performed in order to determine the half maximal inhibitory concentration (IC_{50}) values for inhibition by LNAs **33-O** and **33-R** (Figure 57). The IC_{50} value is a quantitative measure of how effective an oligonucleotide or substance is at inhibiting a biological target (242). The dose response data shows potent and dose-dependent *ADAM33* inhibition.

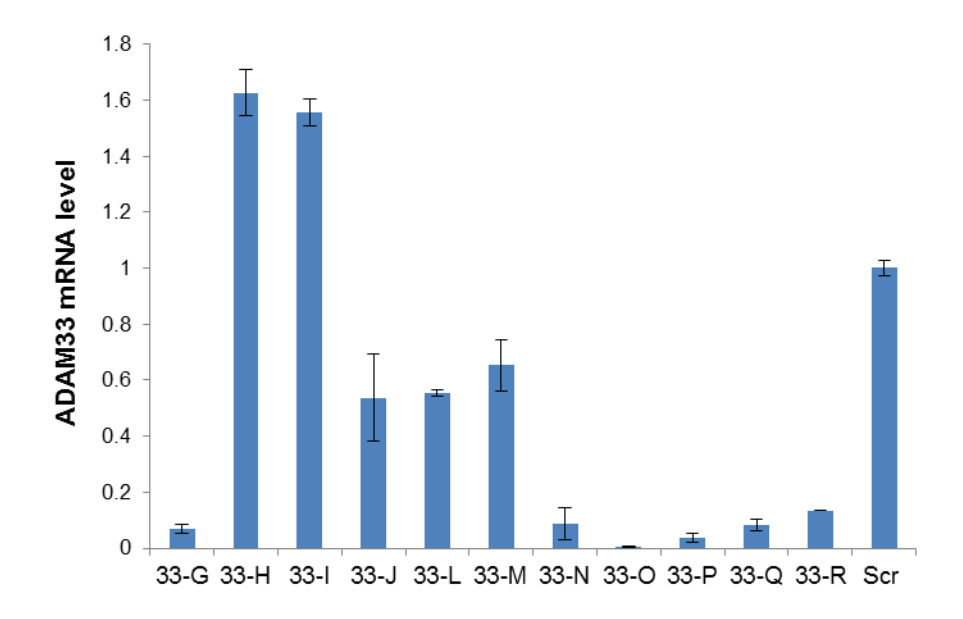


Figure 56. qRT-PCR results showing relative ADAM33 inhibition by LNA gapmers. All results are normalized to a scrambled siRNA duplex control. Error bars are standard deviation of biological replicates. All oligonucleotides were transfected at 50nM.

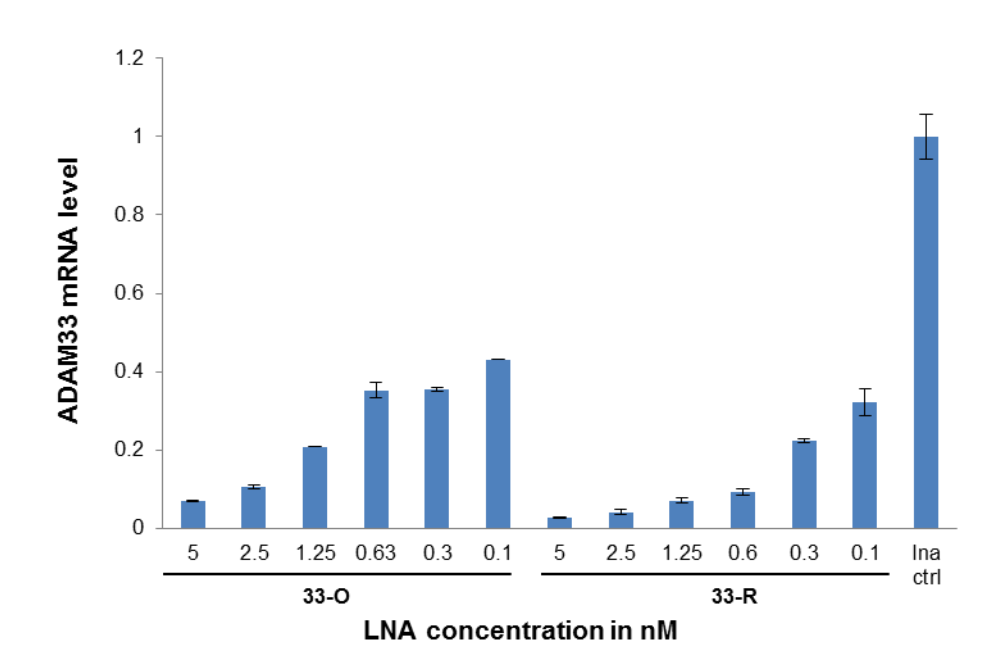


Figure 57 qRT-PCR results showing dose response analysis of LNAs 33-O and 33-R. All results are normalized to a scrambled LNA gapmer control. Error bars are standard deviation of technical replicates.

3.4.2.2 Gymnotic delivery of LNA gapmers

Although the LNA gapmers were highly potent in cultured cells, the efficiency of lipid-mediated transfection *in vitro* does not always correlate to *in vivo* studies. For our future *ex vivo* lung tissue and *in vivo* lung experiments, we will need an oligonucleotide that has the ability to achieve potent *ADAM33* inhibition without the aid of a transfection agent. We used the gymnotic delivery

approach reported by Stein *et al.* (106) in order to test a) if the LNA gapmers could enter the MRC-5 cells without the use of transfection agents, b) how the potency of the LNA gapmers delivered via gymnotic delivery would compare with the transfections using cationic lipid, and c) whether the gymnotically delivered LNA gapmers were toxic to cultured cells.

A time course experiment was performed by gymnotically delivering **33-O** into MRC-5 cells at a $1\mu M$ dose to determine the optimal day to harvest the cells after treatment, between day 4 and day 9. Our results suggested that the optimal day to harvest might be day 7 post-treatment (Figure 58), but the time course experiment also indicated that a $1\mu M$ oligonucleotide concentration was not high enough to achieve significant *ADAM33* inhibition.

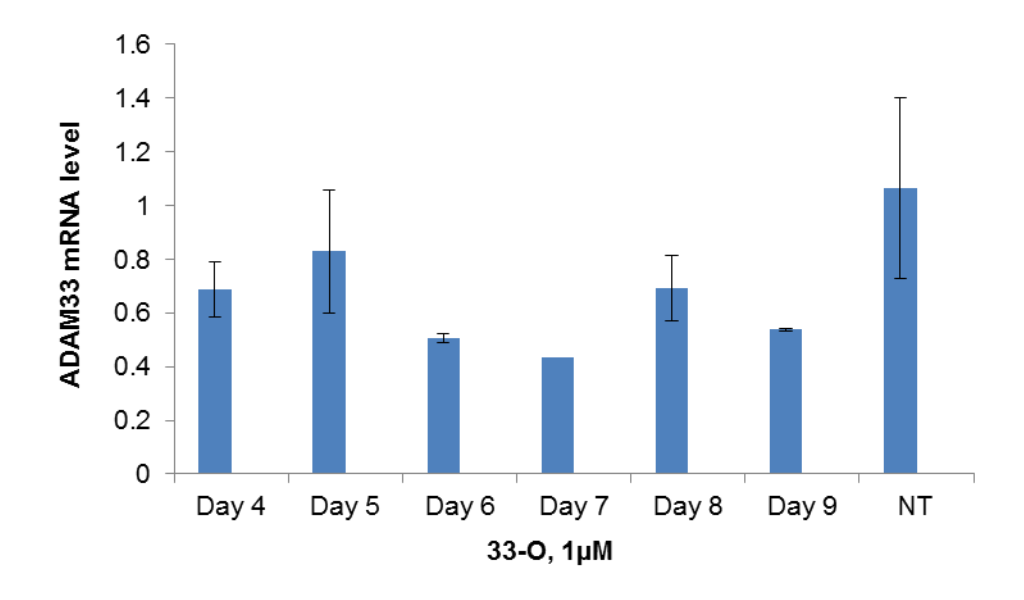


Figure 58. qRT-PCR dose response results. Oligonucleotides are delivered at 1µM dose and normalized to a nontreated control. Error bars are standard deviation of technical replicates.

We then selected LNA gapmers **33-G**, **N**, **O**, **P**, and **R** for further testing. Our data show that **33-N**, **O**, and **P** inhibited *ADAM33* expression >80% and **33-R** showed 60% inhibition at a 3μ M dose, harvesting day 7 post-treatment (Figure 59).

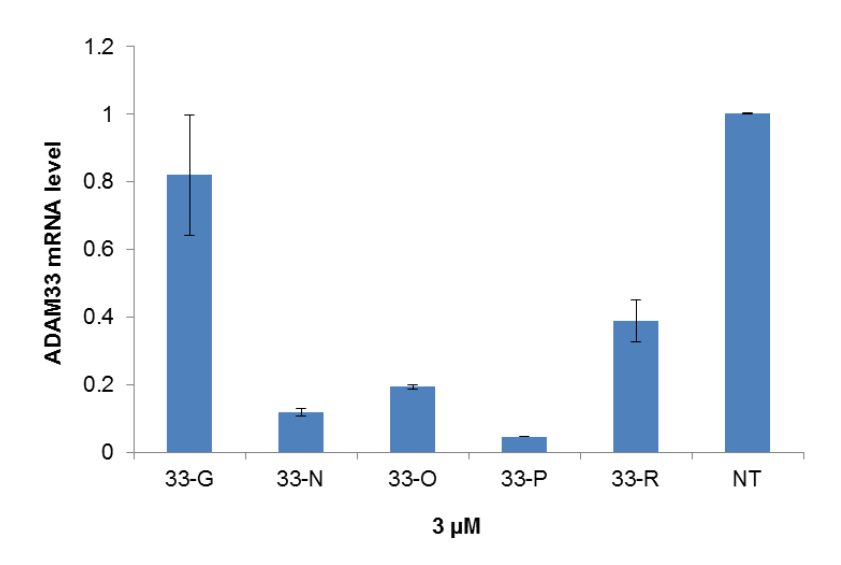


Figure 59. Gymnotically delivered gapmers are effective inhibitors of *ADAM33*. qRT-PCR gymnotic transfection results. Oligonucleotides are delivered at 3μM dose and normalized to a non-treated control (NT). Error bars are standard deviation of two biological replicates.

From these series of experiments we were able to determine that the gymnotically delivered LNA gapmers achieved up to 90% knockdown of *ADAM33*. The potency of the gymnotically delivered oligonucleotides was not as high as the cationic lipid mediated LNA delivery, but there were advantages to gymnotic delivery. For instance, the gymnotically delivered LNAs showed no observable toxicity to cultured cells for any of our tested sequences.

3.5 Oligonucleotide conjugates for cellular uptake

3.5.1 Hexadecyloxypropyl conjugates

As mentioned previously, one therapeutic hurdle for oligonucleotides is their limited uptake into cells (121). One promising technique has been to attach a small molecule covalently such that it is recognized by cell-surface receptors (114-116). In order for this strategy to be effective, several conditions must be met: the covalent linkage chosen must be stable to the conditions of oligonucleotide synthesis or suitable for post-synthetic conjugation, and the modification must not interfere with the oligonucleotide's specificity to the target mRNA (117). We chose to synthesize, covalently attach and test a lipid conjugate based on 1-O-hexadecyloxy-1,3-propanediol, which has been previously shown to increase small molecule uptake by MRC-5 fibroblast cells (243) and improve the oral bioavailability of nucleoside drugs (244) (Figure 60).

LNA conjugated 1-O-hexadecylpropanediol

Figure 60. Chemical structure of hexadecyloxypropyl LNA conjugate.

A 1-O-hexadecylpropanediol phosphoramidite was synthesized in two steps by lab member Alexandre Debacker and former member Liisa Niitso. Treatment of propanediol in DMF with NaH followed by addition of hexadecyl bromide and catalytic potassium iodide gave 1-O-hexadecyl-1,3,-propanediol in a single step as previously observed (245); recrystallisation with hexane yielded white crystals of excellent purity. The phosphoramidite was synthesized under standard conditions (231) using 2-cyanoethyloxy(N,N-diisopropylamino)phosphonamidic chloride. The phosphoramidite was then conjugated to the 5' end of LNA gapmers 33-O, P, and R via solid phase synthesis.

In order to assess the efficacy of the lipid conjugated LNA gapmers, we gymnotically delivered LNA gapmers **33-O**, **P**, and **R** and the corresponding lipid-conjugated LNA gapmers at a 3μ M dose into MRC-5 fibroblast cells (Figure 61). Our results indicate that after a seven-day treatment, the LNA-conjugated **33-O** and **R** showed slightly improved potency against *ADAM33* compared with the unconjugated LNA gapmers.

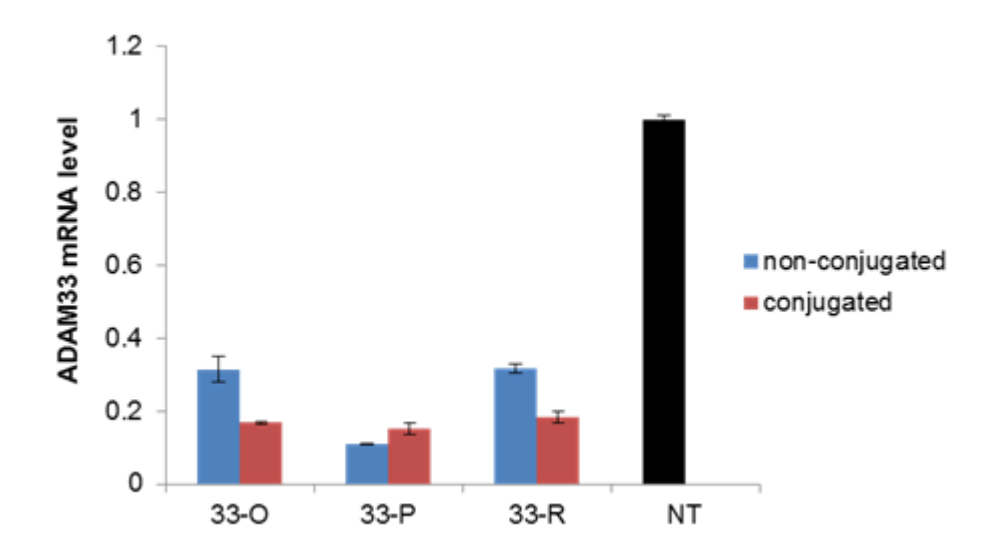


Figure 61. qRT-PCR gymnotic transfection results. Oligonucleotides are delivered at 3μM dose and normalized to a non-treated control. Error bars are standard deviation of technical replicates.

In order to determine if the lipid conjugation improved potency against *ADAM33* at a lower dose range, a dose response analysis was performed comparing ADAM33 RNA levels upon treatment with the LNA gapmers and their lipid-conjugated counterparts when delivered gymnotically (Figure 62). These results show that the lipid-conjugated **33-O** and **R** are more potent than the unconjugated oligonucleotides, especially at lower concentrations.

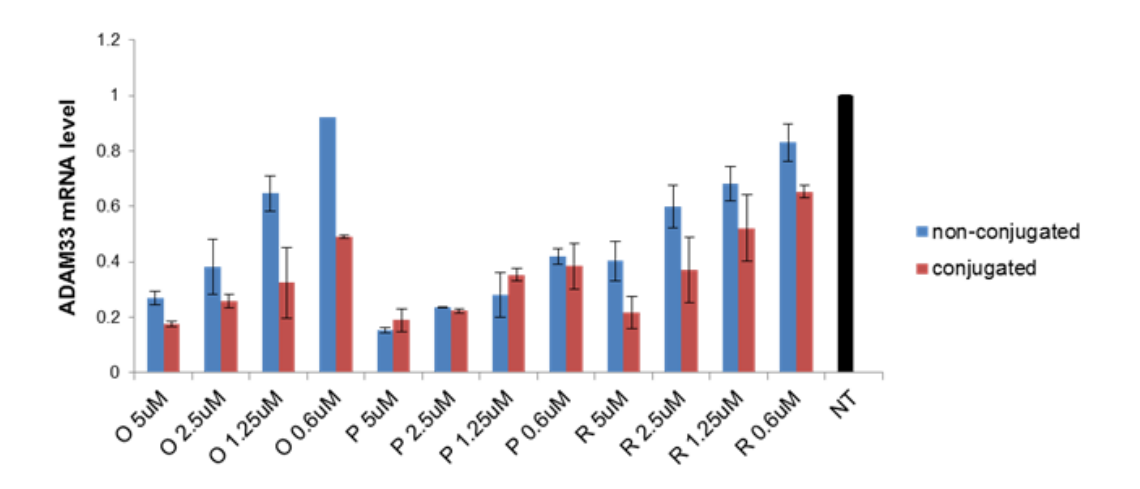


Figure 62. qRT-PCR results showing dose response analysis of ADAM33-O, R, and P and their lipid-conjugates. All results are normalized to non-treated (NT) sample. Error bars are standard deviation of biological replicates.

3.5.2 Bio cleavable hexadecyloxypropyl conjugates

While we were encouraged by the small improvement in potency we observed, we wondered if we could further improve on this potency. It is possible that the hydrophobic conjugate might improve the initial recognition and binding to cell membrane, but might trap the oligomer at the cell membrane rather than releasing it into the cell. To address this risk, we made a biocleavable analogue of our 1-*O*-hexa-decyloxy-1,3-propanediol conjugated LNA gapmers.

We chose to synthesize a bio cleavable version of the 1-*O*-hexa-decyloxy-1,3-propanediol conjugated LNA gapmer, using a disulphide bond to join the LNA gapmer with the conjugate (Figure 63). This synthesis was done by Mike Moazami. This synthesis was completed in stages Mike Moazami as follows (Figure 64).

6-chlorohexanol was refluxed with potassium iodide and thiourea in EtOH overnight, the following morning a solution of NaOH was added and all left to stir at room temperature overnight. The mix was bought to reflux for 3 hours, then cooled to room temperature and acidified with 1M HCl(aq) to pH= 3. The mixture was extracted with Et2O and the organics removed in vacuo to give 6-mercaptohexanol as a clear oil in a quantitative yield.

To a solution of 6-mercaptohexanol in MeOH was added Et3N and iodine. The reaction was exposed to atmospheric oxygen and allowed to stir at room temperature before being concentrated *in vacuo*. The residue was taken into water and extracted (DCM), the organic phase dried and concentrated in vacuo to give a residue that was purified by column chromatography to provide 6,6'-Disulfanediylbis(hexan-1-ol) as an off white solid in 79% yield.

6,6'-Disulfanediylbis(hexan-1-ol) was dissolved in pyridine and DMT-Cl added. The reaction was stirred overnight, then concentrated in vacuo and purified by column chromatography to give 6-((6-(Bis(4- methoxyphenyl)(phenyl)methoxy)hexyl) disulfanyl)hexan-1-ol as a clear yellow oil in a 79% yield. This compound was phosphitylated using 2-cyanoethyl N,N-diisopropylchlorophosphoramidite in THF to give the final linker phosphoramidite as a clear yellow oil in 92 % yield.

Figure 63. Chemical structure of disulfide hexadecyloxypropyl LNA conjugate.

Figure 64. Schematic describing the synthesis of disulphide hexadecyloxypropyl LNA conjugate.

Disulfide conjugates have been used previously for therapeutic applications, with one disulfide linked antibody drug, Mylortarg®, approved by the FDA for the treatment of acute myeloid leukemia (246-250). The main advantage of using a disulfide linker is that it is relatively stable in serum but readily cleaved in the reducing environment of the cell (251-253).

We chose to compare only the LNA gapmer **33-O** with its conjugated counterparts. The oligonucleotides were gymnotically delivered into MRC-5 lung fibroblast cells and incubated for 8 days post transfection, with a media change and additional oligonucleotide added day 5 post transfection.

The data shows extremely potent *ADAM33* knockdown with the conjugated and unconjugated LNA gapmers (Figure 65). From these results, it does not appear that the biocleavable LNA gapmer showed any significant improvement in potency over the conjugated LNA gapmer. However, this experiment will need to be repeated in order to clarify the results.

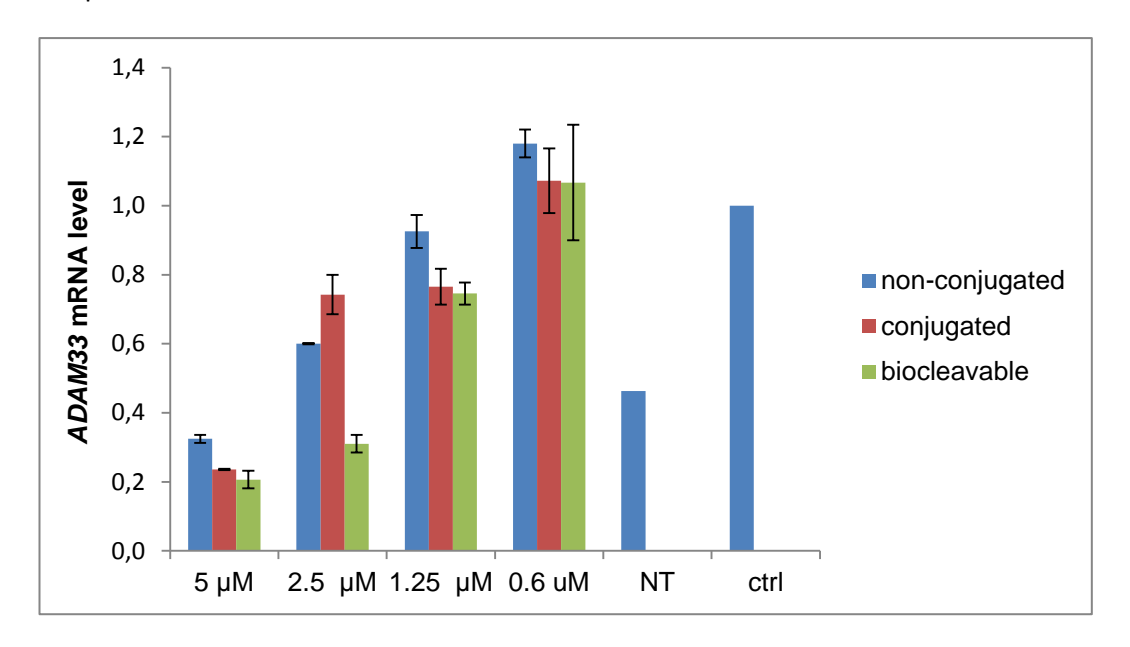


Figure 65. qRT-PCR results showing dose response analysis of 33-O and conjugates. All results are normalized to NT sample. Graph based on one biological replicate.

3.5.3 Dynamic light scattering

We wanted to explore why our conjugate showed improved activity relative to its free counterpart. One hypothesis is that the hydrophobic tail interacts directly with cell surfaces. However, another recently suggested hypothesis is that the hydrophobic tail changes the biophysical properties of the conjugate to favor association into clusters. These clusters in turn could show improved recognition behaviour by scavenger receptors on cell surfaces (254).

Dynamic light scattering (DLS) is a technique used to determine the size distribution profile of small particles in solution and can be used to study particle aggregation or complex formation. We chose to run this assay in order to gain some mechanistic insight as to why our conjugated LNA gapmers were more potent than their unconjugated versions. It was hypothesized that our 1-*O*-hexa-decyloxy-1,3-propanediol-conjugated LNA gapmers were forming micelles which aided in cell penetration.

Our collaborator, Dr. Yong Yu (A*STAR Singapore), performed DLS experiments comparing the effective size in solution of our unconjugated LNA gapmer (33-O), our 1-O-hexa-decyloxy-1,3-propanediol conjugated LNA gapmer (33-O conjugated), and our disulphide linked 1-O-hexa-decyloxy-1,3-propanediol conjugated LNA gapmer (bio cleavable 33-O conjugate). The data indicated that, as expected, the unconjugated LNA gapmer was not forming well-defined complexes in suspension, but both of the 1-O-hexa-decyloxy-1,3-propanediol conjugated LNA gapmers did show complex formation (Figure 66).

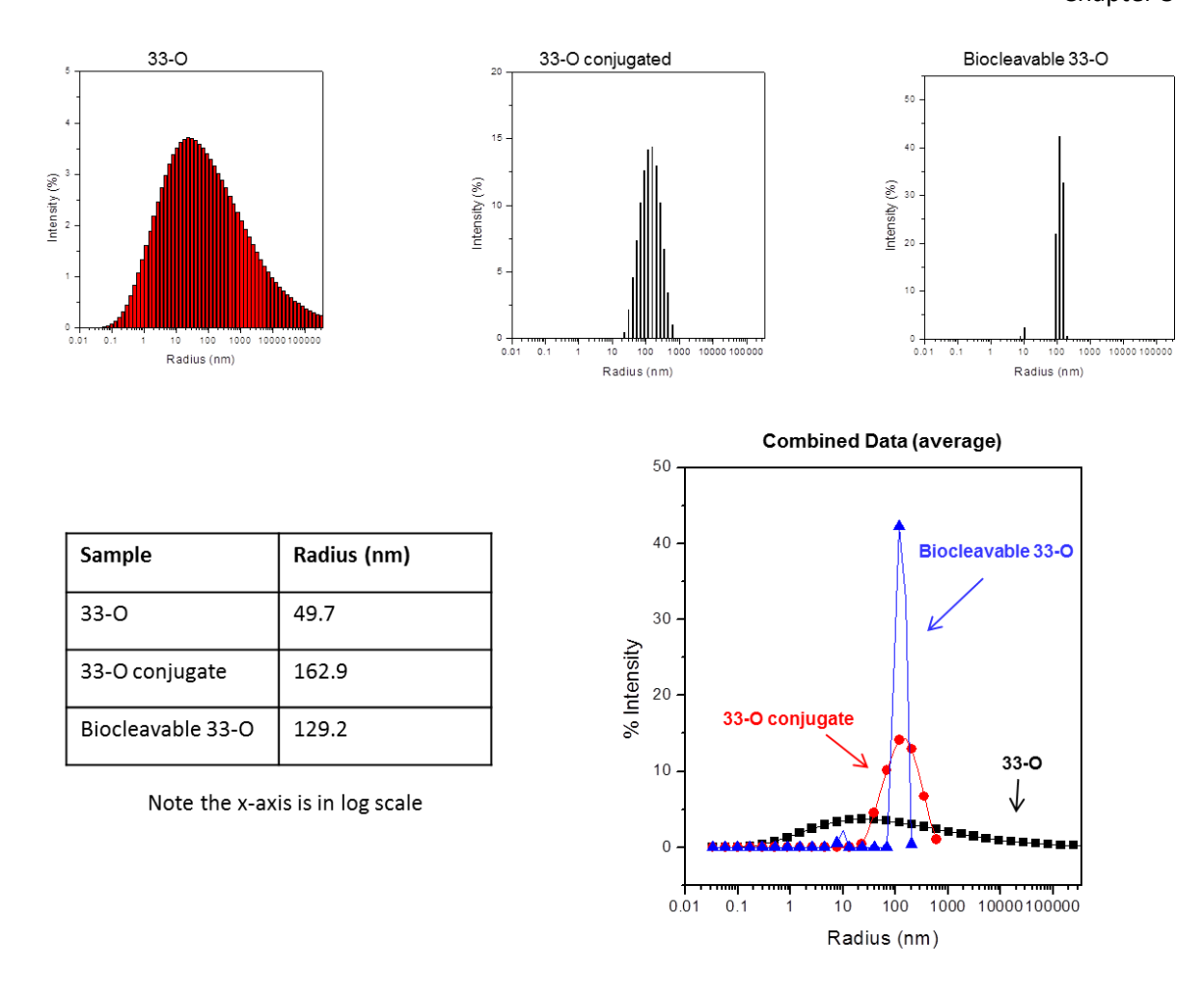


Figure 66. Results of DLS measurement on 33-O, 33-O conjugate, and bio cleavable 33-O conjugate. Note that the scale of the y axis varies widely; these data indicate no significant aggregation for the free oligonucleotide but a well defined association of both types of conjugates.

The idea that uptake may be favored by self-assembly of oligomers into micelles or clusters was recently studied thoroughly by Wood *et al.* (254). They demonstrated that different chemically modified oligonucleotides can inherently have varying self-assembly behavior and that self-assembling oligomers showed improved uptake behavior in vivo. Our results support the idea that conjugation may be an important route to developing oligonucleotides that efficiently self-assemble into clusters or micelles. Previous work has described very long polymer conjugates that induce self-assembly of oligonucleotides into clusters (255). Other work showed that oligonucleotides with hydrophobic conjugates could be made to assemble around a liposomal core (256). However, our work demonstrates the idea that even a simple hydrophobic conjugate may be sufficient to induce efficient self-assembly into clusters/micelles. The current paradigm for uptake of oligonucleotide conjugates has been dominated by the idea that the ligand moiety interacts with cell-surface receptors. However, it may be that the hydrophobic ligands are on the inside of a cluster and it is the oligonucleotides themselves that interact with scavenger receptors. In this case, further work should focus on optimizing the length, shape and chemistry

requirements of the hydrophobic moiety for the purpose of optimizing self-assembly as a means to improved uptake.

3.6 Discussion and Conclusions

Cellular delivery is one of the biggest obstacles facing oligonucleotides as therapeutic agents. For future *ADAM33* lung delivery experiments, a single-stranded oligonucleotide will be beneficial due to the possibility of delivery without the aid of transfection agents. Oligonucleotide conjugates such as the ones we described may further improve the therapeutic potential of oligonucleotide drugs.

In our work, we compared the potency of several classes of oligonucleotides; duplex siRNAs, ss-siRNAs, PS LNA gapmers, and lipid conjugated LNA gapmers. We showed that our antisense oligonucleotides are several fold more potent for *ADAM33* inhibition than any RISC-based oligonucleotides tested in this study.

Surprisingly for a mRNA, approximately 90% of *ADAM33* mRNA remains in the nucleus (257). As mentioned previously in Chapter 1, it has been recently shown in the context of noncoding RNA that RISC-engaging oligonucleotides (siRNAs) typically show more gene silencing efficacy against cytoplasmic RNA targets while RNase H based antisense oligonucleotides are more potent against nuclear targets (258). This recent finding could explain why our LNA gapmers outperformed the RISC engaging oligonucleotides for this predominantly nuclear mRNA target. Our results suggest that the relationship between subcellular localisation and silencing efficacay might not be limited to noncoding RNAs, but might apply to mRNA targets as well.

We not only identified several LNA gapmers that are highly potent at inhibiting *ADAM33*, but also developed a novel hexadecyloxypropyl conjugate that is straightforward to synthesize and improves the potency of gapmers when delivered gymnotically. Through DLS we were able to determine that the normal and biocleavable conjugates formed a complex structure which could aid in cellular uptake. Our data indicate that a conjugated single stranded LNA gapmer oligonucleotide is an excellent candidate for future experiments both in mice and embryonic lung explant models, and should be considered as a therapeutic candidate for treating the root causes of asthma.

Chapter 4: Single stranded siRNAs

4.1 Introduction

In 2012, it was reported that chemically modified single-stranded siRNAs (ss-siRNAs) were capable of engaging the RISC complex (74, 259) which is a method of gene silencing typically reserved for duplex RNAs. As single stranded oligonucleotides are more flexible than duplexes and are amphiphilic rather than entirely hydrophilic, they can more easily bind to cell surface proteins and more easily be taken up by cells without depending on delivery strategies such as conjugation or formulation. For this reason, ss-siRNAs might present a 'best of both worlds' scenario as they have been reported to be as potent as duplex siRNAs in gene silencing but have the advantages of a single stranded oligonucleotide for delivery purposes.

4.1.1 Previous ss-siRNA work

In 2002, Martinez *et al.* identified that only one strand of an siRNA duplex, the antisense or guide strand, is incorporated into the RISC complex (72). Using cell extracts, it was observed that a single stranded RNA was as potent as a duplex siRNA at gene silencing (72). However, when single stranded siRNAs were introduced into living cells, several groups have observed potency that is much lower for single strands than for their duplex siRNA congeners (71, 232).

4.1.2 Potent ss-siRNAs with chemical modifications

The ss-siRNA technology used in this thesis work was first developed by ISIS Pharmaceuticals. In 2012, Lima *et al.* (74) and his team achieved potent knockdown of *PTEN* mRNA both *in vitro* and *in vivo* using a novel chemical design for ss-siRNAs. For their work, several chemical modification strategies were tested, including fully 2'F modified, fully PS modified, and alternative 3' terminus nucleotides of various chemistries, in order to see which chemical modification scheme produced the most significant *PTEN* knockdown (74). From this data, it was determined that the most potent inhibition of *PTEN* was achieved when an alternating pattern of 2'F and 2'-OMe in the body of the oligomer was used as opposed to a uniformly modified chemical modification scheme. Lima also designed an alternating PS and PO modified linkages with up to nine 3' PS modifications consecutively. This modification scheme outperformed a fully PS modified ss-siRNA. The 3' terminus of the ss-siRNA (corresponding to the overhang of a traditional siRNA) was modified using two 2'-MOE adenosines.

Lima *et al.* claimed that this ss-siRNA technology genuinely engaged the RISC complex rather than simply acting through some antisense-type effect. To justify this claim, they performed a series of well-designed experiments: First, they provided evidence that only 5'-phosphorylated ss-siRNAs were functional (this demonstrates the engagement of RISC since it is well known that RISC uptake requires a phosphate (*74, 235, 259, 260*) while antisense oligonucleotides have no such requirement). Second, a 5' rapid amplification of cDNA ends (RACE) experiment (*261*) was performed which showed that upon treatment with ss-siRNAs, the complementary mRNA target was consistently cleaved leaving a single cleavage product. Argonaute 2 (AGO 2) is known to cleave singly at the PO bond lying across from nucleotides 10 and 11 of the guide strand (*262-264*). Due to the RACE results, it can be concluded that the ss-siRNA cleavage is consistent with AGO2 cleavage products and not other forms of mRNA cleavage such as RNase H. RNase H for example would have multiple products as RNase H is a non-sequence specific endonuclease.

Using the ss-siRNA technology, Yu et al. demonstrated on the effects of ss-siRNA treatment against the causative agent of Huntingtin's Disease (HD) (259). Huntingtin's Disease is a neurological disorder caused by an expanded CAG repeat in Exon 1 of the HTT gene (265). Although genetically the Huntingtin's Disease is quite simple, treatment for the disease has been problematic. HTT is a crucial gene for many cellular processes (266) so completely inhibiting the gene may not be an appropriate therapeutic option. However, selectively inhibiting the mutant CAG expansion which causes HD while leaving the wild-type allele intact would be a viable treatment for the disease and symptoms.

Using the ss-siRNAs, Yu et al. published that not only could the ss-siRNAs selectively inhibit mutant HTT while leaving the wild-type allele intact, but also achieved the allele-selectivity of previously published duplex siRNAs that also had potent allele-selectivity in vitro (259, 267). Yu et al. performed several experiments supporting the claim that the ss-siRNAs do engage the RISC complex for silencing the mutant HTT gene:

- 1) A double transfection was performed where a duplex siRNA which targets Argonaute proteins was transfected into cultured cells. After 24 hours, the ss-siRNAs were transfected onto the same cultured cells. This experiment showed that after depletion of AGO2 inside the cells, the ss-siRNAs were not active, indicating that AGO2 is crucial for the mechanism of silencing.
- 2) An RNA-immunoprecipitation (RIP) assay was carried out to determine AGO2 protein interactions with mRNA transcripts. Upon treatment with the ss-siRNAs, AGO2 was shown to be recruited to the HTT mRNA transcript. However, when the cells were treated with an LNA gapmer which operates through and AGO2-independent mechanism, there was no association of AGO2 with the HTT mRNA.

Importantly, the anti-HTT ss-siRNAs described by Yu *et al.* were able to selectively inhibit mutant HTT *in vivo*. It has been reported previously that duplex siRNAs can inhibit HTT (267-269), but HD is a neurological disorder and delivery of duplex siRNAs to the brain is quite challenging. In the absence of a delivery vehicle, they do not penetrate brain cells, but when formulated, they were only taken up by cells proximal to the site of infusion (270). The ss-siRNAs were able to distribute throughout the central nervous system after introduction into the cerebrospinal fluid, and allele-selectively inhibit mutant HTT in a statistically significant way (259).

4.1.3 Additional ss-siRNA publications

Following the initial ss-siRNA reports in 2012, other studies have been conducted using ss-siRNA technology. In 2013, Liu *et al.* showed that ss-siRNAs can selectively inhibit ataxin-3. Like *HTT*, ataxin-3 is a gene in which an expanded CAG repeat causes Machado-Joseph disease and an allele-selective gene silencing approach is a very valuable therapeutic option (*236*). Liu went further in 2014 when she published on the how the sequence length and ss-siRNA composition effected the allele-selectivity and potency of ss-siRNAs when targeting HTT (*237*). ss-siRNAs have also been used against additional CAG repeat expansion genes, such as atrophin-1 which causes Dentatorubral-pallidoluysian atrophy (*260*). Additionally, ss-siRNA technology has been used for alternative purposes than gene silencing. Liu *et al.* used ss-siRNA technology to target nuclear splice sites to increase dystrophin protein isoforms which is a potential therapeutically beneficial treatment for Duchenne muscular dystrophy (*271*) ss-siRNAs have also been used to target gene promoters, regulating gene expression at the transcriptional level. Matsui *et al.* demonstrated that an ss-siRNA was capable of targeting the nuclear progesterone receptor (PR) gene promotor and inhibiting PR expression (*235*).

4.1.4 Current ss-siRNA work

As mentioned in Chapter 1, the published designs for potent ss-siRNAs contain either a 5'-phosphate or phosphonate (272), an alternating pattern of 2'F and 2'-OMe in the body of the oligomer, and an 3'-terminus of 2'-MOE (74). One limitation of existing ss-siRNA technology is that the published work is carried out using proprietary modifications that are not available to most researchers (273). For in vivo use the 5'-phosphonate analogue is required and is difficult to access, but for in vitro experiments a simple 5'-phosphate is sufficient (274). The 3'-terminus is generally modified with MOE, which is not commercially available.

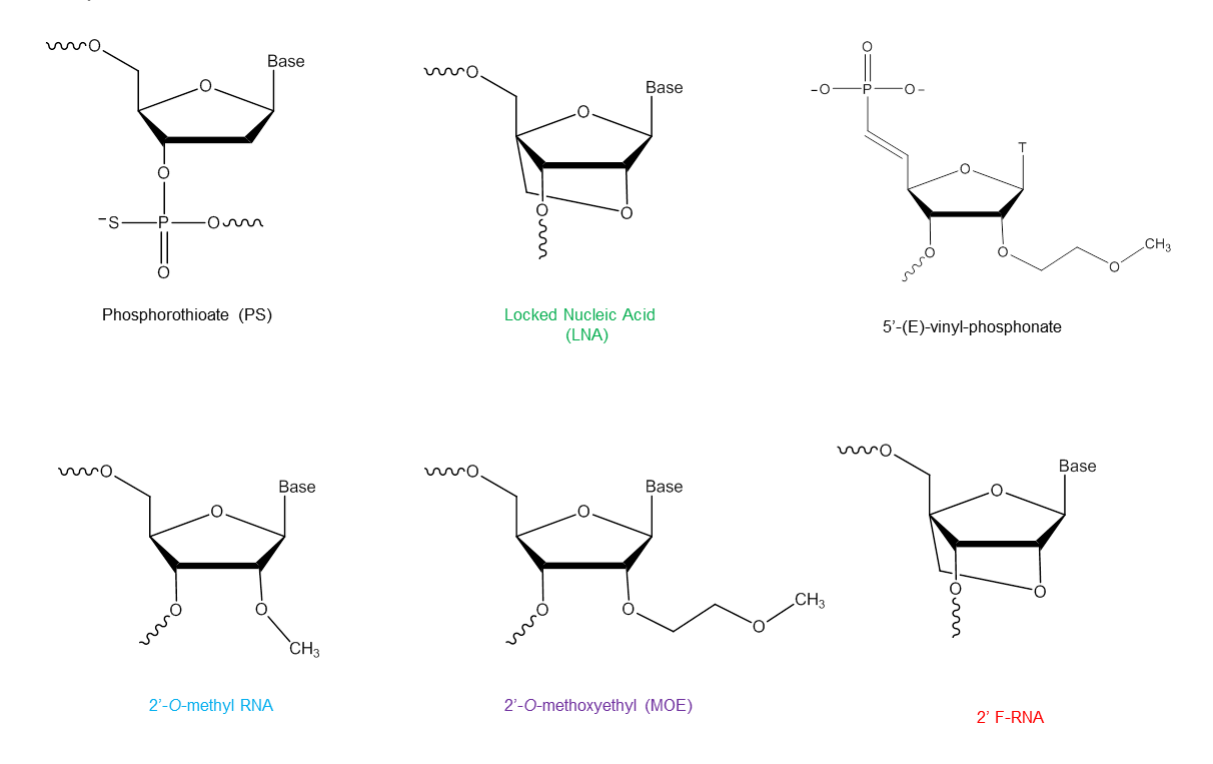


Figure 67. Modified nucleotides that have been included in ss-siRNAs in this study.

4.2 ADAM33 inhibition by ss-siRNAs

As mentioned in Chapter 3, we previously observed knockdown of *ADAM33* using a duplex siRNA, **HMH-1**, in MRC-5 lung fibroblast cells. We designed and tested several duplex siRNAs to inhibit *ADAM33*, but none of the additional siRNAs were able to match the potency of the initial siRNA, **HMH-1**. Three duplex siRNAs were chosen as 'parent' strands for our ss-siRNA design, using the antisense strand as the template sequence. However, not only did none of our initial ss-siRNAs match the potency of their duplex siRNA partner, but they showed no activity against *ADAM33*.

As both the duplex siRNAs and the ss-siRNAs are RISC-engaging compounds, we were curious as to why the duplex siRNAs outperformed the ss-siRNAs. We began to investigate if altering the chemical modification scheme of ss-siRNA could enhance the potency of the oligonucleotides on *ADAM33* inhibition. All of our ss-siRNAs were designed using a chemical modification motif adapted from Lima *et al.* (74) based on a pattern of alternating 2'F and 2'-OMe modifications. As mentioned in Chapter 3, Our initial ss-siRNA, **ss-A33-MOE-1**, contained a mixed backbone modification scheme consisting of one 5'PS linkage, ten PO linkages followed by nine PS linkages, and two PS-linked MOE adenosines at the 3' end (Table 6)(Appendix D and E).

Table 6. Oligonucleotide sequences for ADAM33 inhibition. For duplex sequences, sense strand is listed on top. Modification code: RNA, dna, 2'-OMe, 2'-F, 2'-MOE, '+': LNA, 'S': phosphorothioate, P: 5' phosphate. ND, Tm not determined.

siRNA	sequence	T _m (°C)
HMH-1	5' GGA AGU ACC UGG AAC UGU A tt CCU UCA UGG ACC UUG ACA U 5'	71
Scr	5' AGU GGA GGG CGC CUG CCA C tt tt UCA CCU CCC GCG GAC GGU G \'5	82-83
ss- siRNA	Sequence (5' – 3')	
ss-A33- MOE-1	$P-\underline{U}_{S}\underline{A}\underline{C}\underline{A}\underline{G}\underline{U}\underline{U}\underline{C}\underline{C}\underline{A}\underline{G}\underline{G}_{S}\underline{U}_{S}\underline{A}_{S}\underline{C}_{S}\underline{U}_{S}\underline{U}_{S}\underline{C}_{S}\underline{C}_{S}\underline{A}_{S}\underline{A}$	ND
ss-A33- MOE-2	P-U-A-CA-GU-UC-CA-GG-UA-C-U-U-C-C-A-A	76-77
ss-A33- OMe	P-U_A_CA_GU_UC_CA_GG_UA_C_U_U_C_C_A_A	78
ss-A33- LNA	P-U_A_CA_GU_UC_CA_GG_UA_C_U_U_C_C_+A_S+A	79

We next altered the chemical modification scheme of the ss-siRNAs to try to achieve greater inhibition when targeting ADAM33 mRNA (Figure 68). Besides the original sequence of **ss-A33-MOE-1**, we synthesized three additional ss-siRNAs using a 5' phosphate followed by alternating PS and PO linkages, and seven 3' terminal PS linkages. We then modified the two 3' terminal adenosines by either using MOE modifications (**ss-A33-MOE-2**), 2'-OMe modifications (**ss-A33-OMe**), or LNA modifications (**ss-A33-LNA**).

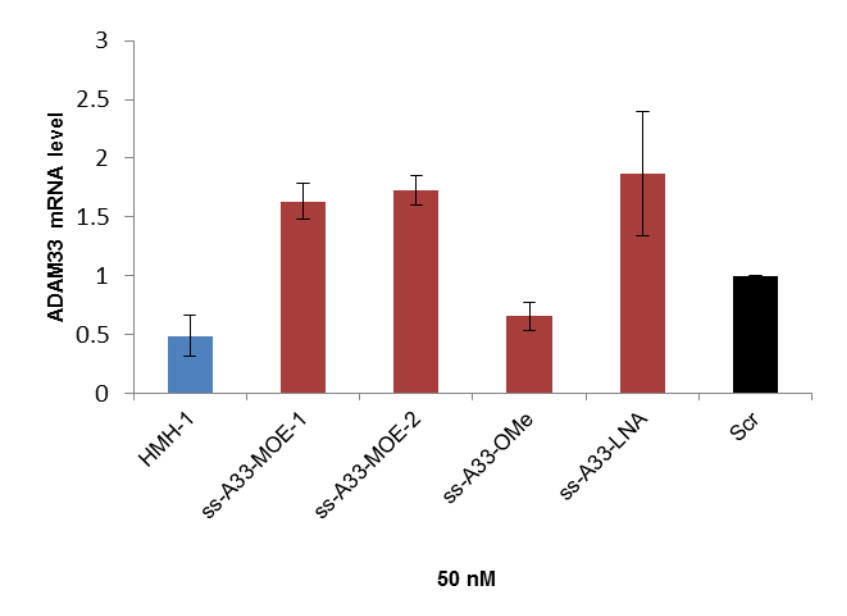


Figure 68. qRT-PCR results comparing potencies of different chemical modification schemes on ss-siRNA activity. All results are normalized to a scrambled siRNA duplex control. All oligonucleotides were transfected at 50nM. Error bars are standard deviation of two biological replicates.

Only the ss-siRNA with 2'-OMe modifications at the 3'-terminus was able to match the silencing activity of the duplex siRNA (Figure 68). As all of the current ss-siRNA literature uses oligonucleotides that are 2'-MOE modified at the 3' terminus (74, 235, 259, 260, 275), we were surprised to find that the ss-siRNA oligonucleotide with the commercially available 2'-OMe modification out-performed the 2'-MOE modified and the LNA modified ss-siRNA. Additionally, some of the inactive ss-siRNAs caused a small but reproducible activation of *ADAM33* expression relative to a scrambled control or untreated cells. We are not sure of the origin of this effect, but the effect is small and we decided not to follow up further as it would have distracted from the main focus of the project.

4.3 ss-siRNAs targeting progesterone receptor

Due to the unexpected results from our ss-siRNA *ADAM33* experiments, we began to test whether the 3'terminal modification had such a large effect on ss-siRNA potency across multiple sequences and cell lines. We first chose to target the progesterone receptor (PR) gene in MCF 7 cells as a potent inhibitory siRNA sequence had been previously published (*276-278*). The siRNA duplex and various non-targeting controls were tested, and results show a potent knockdown of *PR* gene with the PR-targeted siRNA, making the antisense strand of the duplex siRNA an appropriate template for our ss-siRNAs (Figure 69).

Α

siRNA	sequence	Tm (°C)
PR	5' AUG GAA GGG CAG CAC AAC U tt tt UAC CUU CCC GUC GUG UUG A 5'	72-73
ctrl 1	5' CAU GCA AUU UCC ACG GAC C tt tt GUA CGU UAA AGG UGC CUG G 5'	69

В

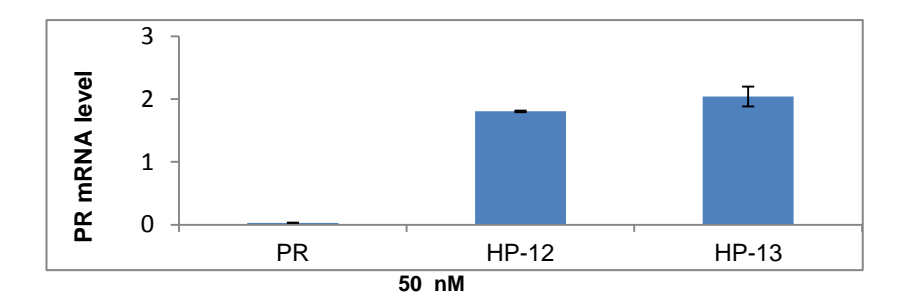


Figure 69. A) Duplex siRNA and control for inhibition of progesterone receptor. Sense strand is listed on top. Modification code: RNA, dna. (B) qRT-PCR results of PR mRNA levels when MCF 7 cells are treated with siRNAs at 50 nM concentration. Error bars represent standard deviation of three biological replicates.

We synthesized three ss-siRNA sequences based on the PR siRNA sequence using the chemical modification scheme from our *ADAM33* experiments (5' phosphate followed by alternating PS and PO linkages, and seven 3' terminal PS linkages). We then modified the two 3' terminal adenosines by either using MOE modifications (**PR-MOE**), 2'-OMe modifications (**PR-OMe**), or LNA modifications (**PR-LNA**) (Table 7) (Appendix D and E). As with the siRNAs, a forward transfection was performed and total cellular RNA was analyzed. The PR targeting duplex siRNA was used as a positive control in these transfections.

Table 7. Oligonucleotide sequences for *PR* inhibition. For duplex sequences, sense strand is listed on top. Modification code: RNA, dna, 2'-OMe, 2'-F, 2'- MOE, '+': LNA, 'S': phosphorothioate, P: 5' phosphate

siRNA	sequence	T _m (°C)
PR	5' AUG GAA GGG CAG CAC AAC U tt tt UAC CUU CCC GUC GUG UUG A 5'	72-73
ss- siRNA	Sequence (5' – 3')	
ss-PR- MOE	$\mathbf{P} - \underline{\mathbf{A}}_{\mathbf{S}} \mathbf{G}_{\mathbf{S}} \underline{\mathbf{U}} \mathbf{U}_{\mathbf{S}} \underline{\mathbf{G}} \mathbf{U}_{\mathbf{S}} \underline{\mathbf{G}} \mathbf{C}_{\mathbf{S}} \underline{\mathbf{U}} \mathbf{G}_{\mathbf{S}} \underline{\mathbf{C}}_{\mathbf{S}} \underline{\mathbf{C}}_{\mathbf{S}} \underline{\mathbf{C}}_{\mathbf{S}} \underline{\mathbf{C}}_{\mathbf{S}} \underline{\mathbf{C}}_{\mathbf{S}} \mathbf{C}_{\mathbf{S}} \underline{\mathbf{C}}_{\mathbf{S}} \underline{\mathbf{C}}_{\mathbf{S}$	80-81
ss-PR- OMe	$P-\underline{A}_{S} \underset{S}{G} \underset{UU}{UU}_{S} \underbrace{GU}_{S} \underbrace{GC}_{S} \underbrace{UG}_{S} \underbrace{CC}_{S} \underbrace{CU}_{S} \underbrace{U}_{S} \underbrace{C}_{S} \underbrace{A}_{S} \underbrace{U}_{S} \underbrace{A}_{S} \underbrace{A}_{S}$	78-80
ss-PR- LNA	P-A G UU GU GC SC	79-81
ss-scr	P-G G GC UG CG CC AC GA G G A C U A A	60

The results are consistent with the observation found with the *ADAM33* targeting ss-siRNAs, in that the oligonucleotide with the 2'-MOE modification at the 3' end failed to achieve the potency of the 2'-OMe modified oligonucleotide. In this case, the LNA-modified ss-siRNA was also highly active (Figure 70).

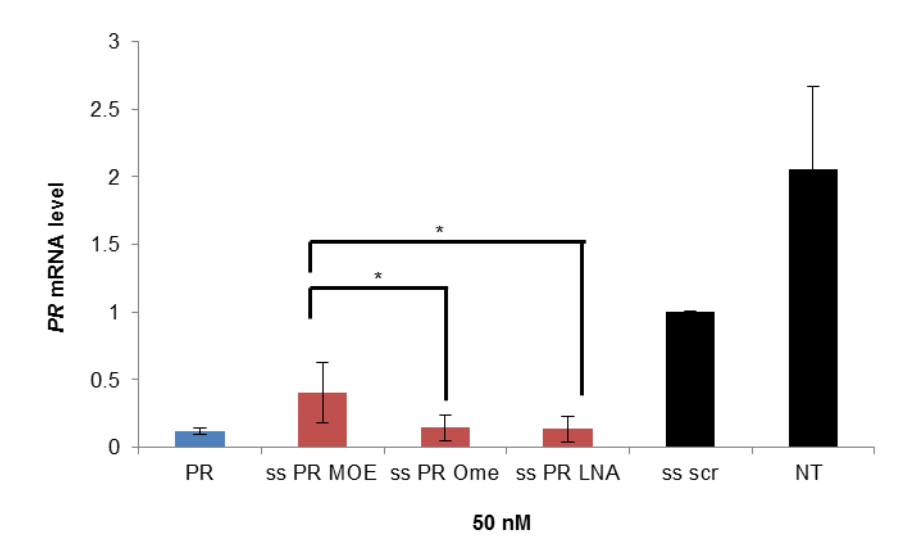


Figure 70. qRT-PCR results of PR mRNA levels when MCF 7 cells are treated with ss-siRNAs. Error bars represent standard deviation of six biological replicates. * = p<0.05.

A dose response analysis was done using the *PR* targeting duplex siRNA and the corresponding ss-siRNAs. The dose response shows that both LNA and 2'-OMe modification showed improved activity at moderate concentrations, and the sequence with 3' LNA modifications showed best potency among the ss-siRNAs tested at lower oligonucleotide concentrations (Figure 71). The

duplex siRNA was still slightly more potent than even our optimized ss-siRNAs, particularly at low concentrations.

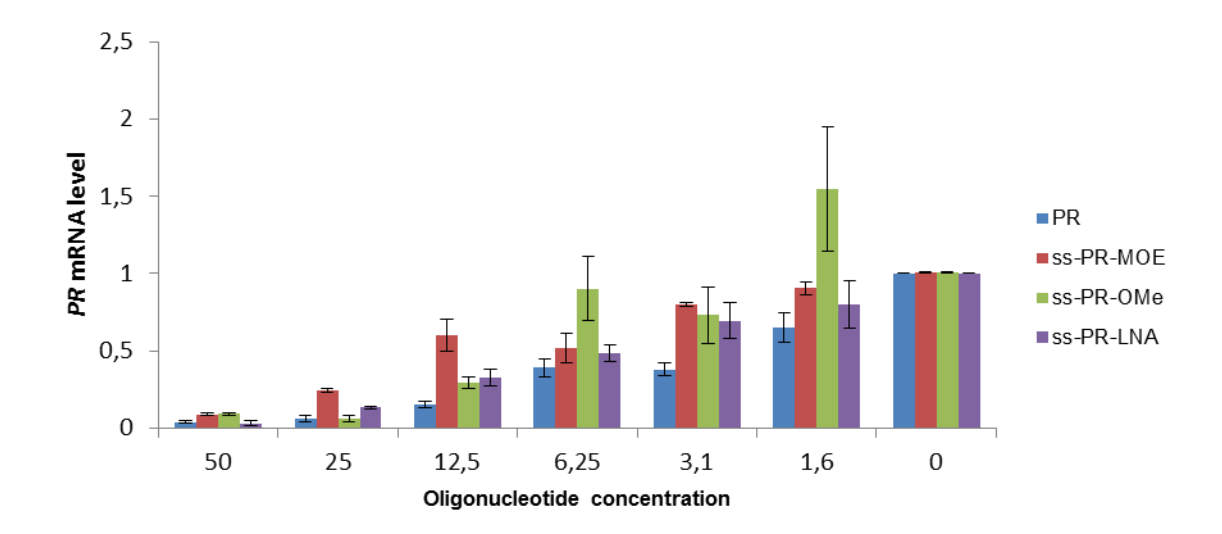


Figure 71. Dose response data of MCF 7 cells treated with *PR* targeting ss-siRNA oligonucleotides at various concentrations. Data is normalized to the 0 oligonucleotide concentration points. N=9 for the 50 nM dose and n=3 for the other concentrations.

4.4 Oligonucleotides targeting SIN3A

In order to further test the therapeutic potential of our ss-siRNAs, we chose to design sequences based on published reports of potent siRNA and miRNA duplexes in the treatment of cystic fibrosis (279). Ramachandran *et al.* found that the *SIN3A* gene interacts with mir-138 which helps regulate CFTR(279). A duplex siRNA that inhibits *SIN3A* was published and was used as our initial siRNA sequence. However, the published duplex was a dicer-substrate siRNA (disiRNA) and its antisense strand was a 27mer containing 2'-OMe modifications strategically placed in the sequence. We first designed a shorter siRNA duplex with 19 base pairs, shortening the published sequence so it would be more appropriate as a ss-siRNA template (Table 8) (Appendix D and E).

Table 8. Oligonucleotide sequences for *SIN3A* inhibition. For duplex sequences, sense strand is listed on top. Modification code: RNA, dna, <u>2'-OMe</u>, <u>2'-F</u>, <u>2'-MOE</u>, '+': LNA, 'S': phosphorothioate, P: 5' phosphate

siRNA	Sequence	T _m (°C)
disiRNA	P-GCG AUA CAU GAA UUC AGA UAC Uacc CUC GCU AUG UAC UUA AGU CUA UGA UGG-P	66-67
sin3A	5' AUA CAU GAA UUC AGA UAC U tt tt UAU GAU CUU AUG UCU AUG A 5'	55-57
scr	5' AGU CCU CGU GGC GCA GCC C tt tt UCA GGA GCA CCG CGU CGG G 5'	82-83
ss-siRNA	Sequence (5' – 3')	
sin3A-MOE	$\mathbf{P} - \underline{\mathbf{A}}_{\mathbf{S}} \mathbf{G}_{\mathbf{S}} \underline{\mathbf{U}} \mathbf{A}_{\mathbf{S}} \underline{\mathbf{U}} \mathbf{C}_{\mathbf{S}} \underline{\mathbf{U}} \mathbf{G}_{\mathbf{S}} \underline{\mathbf{A}}_{\mathbf{S}} \underline{\mathbf{U}} \mathbf{U}_{\mathbf{S}} \underline{\mathbf{C}} \mathbf{A}_{\mathbf{S}} \underline{\mathbf{U}}_{\mathbf{S}} \mathbf{G}_{\mathbf{S}} \underline{\mathbf{U}}_{\mathbf{S}} \mathbf{A}_{\mathbf{S}} \underline{\mathbf{U}}_{\mathbf{S}} \mathbf{A}_{\mathbf{S}} \underline{\mathbf{A}}_{\mathbf{S}} \mathbf{A}_{\mathbf{S}}$	62-63
sin3A-OMe	$\mathbf{P} - \underline{\mathbf{A}}_{\mathbf{S}} \underline{\mathbf{G}}_{\mathbf{S}} \underline{\mathbf{U}} \underline{\mathbf{A}}_{\mathbf{S}} \underline{\mathbf{U}} \underline{\mathbf{G}}_{\mathbf{S}} \underline{\mathbf{A}}_{\mathbf{A}} \underline{\mathbf{U}} \underline{\mathbf{U}}_{\mathbf{S}} \underline{\mathbf{C}} \underline{\mathbf{A}}_{\mathbf{S}} \underline{\mathbf{U}}_{\mathbf{S}} \underline{\mathbf{G}}_{\mathbf{S}} \underline{\mathbf{U}}_{\mathbf{S}} \underline{\mathbf{A}}_{\mathbf{S}} \underline{\mathbf{U}}_{\mathbf{S}} \underline{\mathbf{A}}_{\mathbf{S}} \underline{\mathbf{A}}_{\mathbf{S}}$	62-63
sin3A-LNA	P-ASGSUASUCSUGSAASUUSCASUSGSUSASUS+AS+A	62-63
ss-scr	$\mathbf{P} - \underline{\mathbf{G}}_{\mathbf{S}} \underline{\mathbf{G}}_{\mathbf{S}} \underline{\mathbf{U}} \underline{\mathbf{G}}_{\mathbf{S}} \underline{\mathbf{C}} \underline{\mathbf{G}}_{\mathbf{S}} \underline{\mathbf{C}}_{\mathbf{S}} \underline{\mathbf{A}} \underline{\mathbf{C}}_{\mathbf{S}} \underline{\mathbf{G}} \underline{\mathbf{A}}_{\mathbf{S}} \underline{\mathbf{G}}_{\mathbf{S}} \underline{\mathbf{G}}_{\mathbf{S}} \underline{\mathbf{A}}_{\mathbf{S}} \underline{\mathbf{C}}_{\mathbf{S}} \underline{\mathbf{U}}_{\mathbf{S}} \underline{\mathbf{A}}_{\mathbf{S}} \underline{\mathbf{A}}$	60

We transfected the published **disiRNA**, as well as our shortened version of the dicer substrate sequence, **SIN3A**, into HEK293 cells. Our shortened duplex siRNA sequence was as effective at *SIN3A* inhibition as the published sequence (Figure 72A), therefore the antisense strand was used as a template for ss-siRNA designs. The ss-siRNA architecture was the same as for the *ADAM33* and *PR*-targeting ss-siRNAs. Unfortunately, none of our *SIN3A*-targeting siRNAs were able to match the potency of the corresponding duplex siRNA. The 2'-OMe modified ss-siRNA gave a slight increase in silencing over the 2'-MOE and 2' LNA modified ss-siRNAs, but the difference was

not significant and its potency was nowhere near that of the duplex siRNAs (Figure 72B). These results could indicate that the ss-siRNA chemistry might be incompatible with the HEK293 cell line. Further studies would need to be performed to determine the cause of the poor ss-siRNA potency.

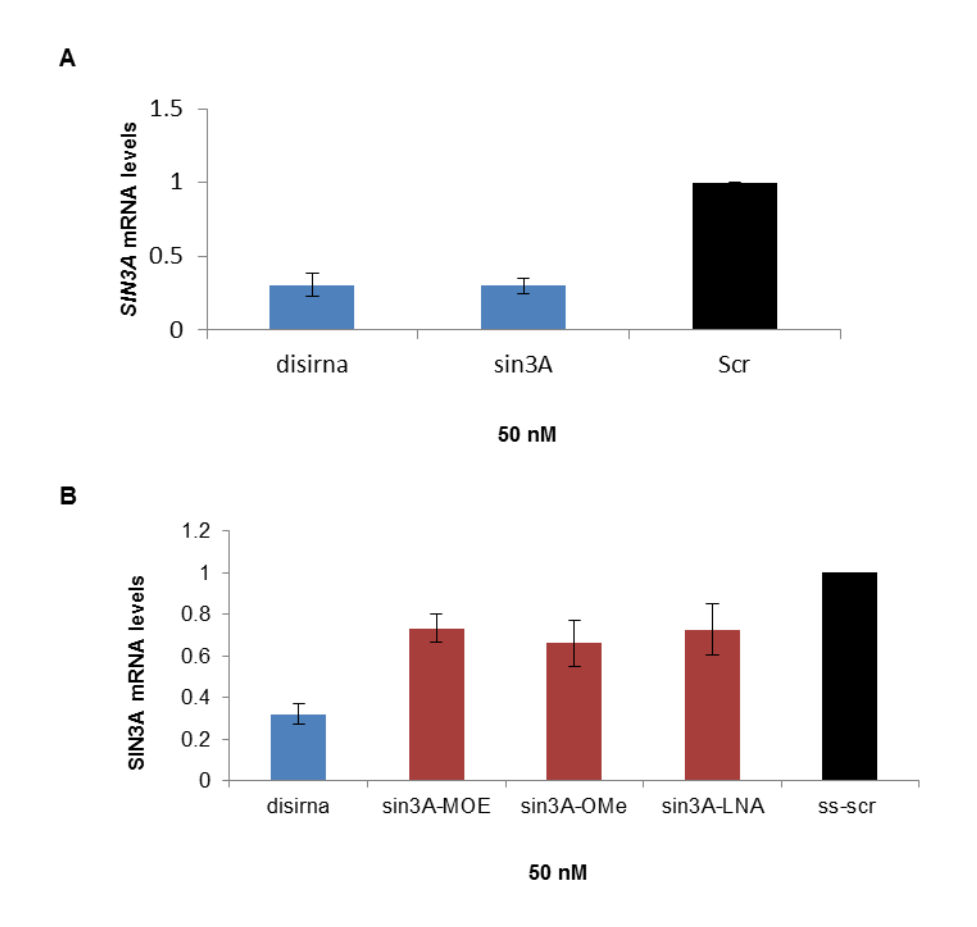


Figure 72. A) qRT-PCR results of SIN3A mRNA levels when treated with duplex siRNAs. HEK293 cells were reverse transfected with siRNAs. All siRNAs were transfected at 50nM concentration and normalized to a scrambled siRNA control. B) qRT-PCR results of SIN3A mRNA levels when HEK293 cells are treated with ss-siRNAs. Samples are normalized to a NT control and transfected at 50nM concentrations. In all cases, error bars are standard deviation of N=4.

4.5 EGFP-targeting oligonucleotides

We began to investigate whether the lower potency of the ss-siRNAs were sequence specific to the SIN3A mRNA target or if the HEK293 cells could be less receptive to the ss-siRNAs. To test this hypothesis, we designed oligonucleotides to target an EGFP gene sequence in a stable EGFP-expressing HEK293 cell line. As done previously, duplex siRNAs were first designed, synthesized, and tested for potency in order to determine if they would be a candidate sequence for our ss-siRNAs. We used a previously published (280) siRNA duplex (EGFP) as well as a novel siRNA duplex sequence (HP EGFP) for these experiments (Table 9) (Appendix D and E).

Table 9. Oligonucleotide sequences for SIN3A inhibition. For duplex sequences, sense strand is listed on top. Modification code: RNA, dna, 2'-OMe, 2'-F, 2'- MOE, '+': LNA, 'S': phosphorothioate, P: 5' phosphate

siRNA	sequence	T _m (°C)
EGFP	5' GAC GUA AAC GGC CAC AAG U tt tt CGC UGC AUU UGC CGG UGU UCA 5'	71
HP-EGFP	5' CAA CAG CCA CAA CGU CUA U tt tt GUU GUC GGU GUU GCA GAU A 5'	67
scr	5' AGU CCU CGU GGC GCA GCC C tt tt UCA GGA GCA CCG CGU CGG G 5'	82-83
HP-13	5' CAU GCA AUU UCC AGC GAC C tt tt GUA CGU UAA AGG UCG CUG G 5'	69-70
ss-siRNA	Sequence (5' – 3')	
egfp-MOE	P-A C UU GU GG CC GU UU A C G U C A A	75
egfp-OMe	$P-\underline{A}_s \overset{\textbf{C}}{\overset{\textbf{U}}}{\overset{\textbf{U}}{\overset{\textbf{U}}}{\overset{\textbf{U}}{\overset{\textbf{U}}}{\overset{\textbf{U}}{\overset{\textbf{U}}}{\overset{\textbf{U}}{\overset{\textbf{U}}{\overset{\textbf{U}}{\overset{\textbf{U}}}{\overset{\textbf{U}}{\overset{\textbf{U}}{\overset{\textbf{U}}{\overset{\textbf{U}}}{\overset{\textbf{U}}}{\overset{\textbf{U}}}{\overset{\textbf{U}}{\overset{\textbf{U}}}{\overset{\textbf{U}}}{\overset{\textbf{U}}}{\overset{\textbf{U}}}{\overset{\textbf{U}}}{\overset{\textbf{U}}}{\overset{\textbf{U}}{\overset{\textbf{U}}}{\overset{\textbf{U}}}{\overset{\textbf{U}}}{\overset{\textbf{U}}}{\overset{\textbf{U}}}{\overset{\textbf{U}}}{\overset{\textbf{U}}}{\overset{\textbf{U}}}{\overset{\textbf{U}}}{\overset{\textbf{U}}}{\overset{\textbf{U}}}}{\overset{\textbf{U}}}{\overset{\textbf{U}}}{\overset{\textbf{U}}}}{\overset{\textbf{U}}}{\overset{\textbf{U}}}{\overset{\textbf{U}}}{\overset{\textbf{U}}}{\overset{\textbf{U}}}{\overset{\textbf{U}}}}}{\overset{\textbf{U}}}{\overset{\textbf{U}}}{\overset{\textbf{U}}}{\overset{\textbf{U}}}{\overset{\textbf{U}}}}{\overset{\textbf{U}}}}{\overset{\textbf{U}}}{\overset{\textbf{U}}}{\overset{\textbf{U}}}{\overset{\textbf{U}}}}{\overset{\textbf{U}}}{\overset{\textbf{U}}}}{\overset{\textbf{U}}}{\overset{\textbf{U}}}{\overset{\textbf{U}}}}{\overset{\textbf{U}}}}{\overset{\textbf{U}}}}{\overset{\textbf{U}}}}{\overset{\textbf{U}}}{\overset{\textbf{U}}}}{\overset{\textbf{U}}}}{\overset{\textbf{U}}}}{\overset{\textbf{U}}}}{\overset{\textbf{U}}}}{\overset{\textbf{U}}}}{\overset{\textbf{U}}}}{\overset{\textbf{U}}}{\overset{\textbf{U}}}}{\overset{\textbf{U}}}}{\overset{\textbf{U}}}}{\overset{\textbf{U}}}}}{\overset{\textbf{U}}}}{\overset{\textbf{U}}}}{\overset{\textbf{U}}}}}{\overset{\textbf{U}}}}{\overset{\textbf{U}}}{\overset{U}}}{\overset{\textbf{U}}}}{\overset{U}}}{\overset{\textbf{U}}}}{\overset{U}}}{\overset{U}}}{\overset{U}}}{\overset{U}}}{\overset{U}}}{\overset{U}}}{\overset{U}}}{\overset{U}}}{\overset{U}}}{\overset{U}}}{\overset{U}}}{\overset{U}}}{\overset{U}}}{\overset{U}}}{\overset{U}}{\overset{U}}}{\overset{U}}}{\overset{U}}}{\overset{U}}}{\overset{U}}}{\overset{U}}}{\overset{U}}{\overset{U}}}{\overset{U}}}{\overset{U}}}{\overset{U}}}{\overset{U}}}{\overset{U}}}{\overset{U}}}{\overset{U}}}{\overset{U}}{\overset{U}}}{\overset{U}}}{\overset{U}}}{\overset{U}}{\overset{U}}}{\overset{U}}{\overset{U}}}{\overset{U}}}{\overset{U}}}{\overset{U}}}{\overset{U}}}{\overset{U}}{\overset{U}}}{\overset{U}}}{\overset{U}}}{\overset{U}}}{\overset{U}}}{\overset{U}}{\overset{U}}}{\overset{U}}}{\overset{U}}}{\overset{U}}{\overset{U}}{\overset{U}}}{\overset{U}}}$	76-79
egfp-LNA	$P-\underline{A}_s\overset{C}{_{S}}\underline{U}\overset{U}{_{S}}\underline{G}^{{_{S}}}\underline{G}^{{_{S}}}\underline{G}^{{_{S}}}\underline{G}^{{_{S}}}\underline{U}^{{_{S}}}\underline{G}^{{_{S}}}\underline{U}^{{_{S}}}\underline{G}^{{_{S}}}\underline{U}^{{_{S}}}\underline{G}^{{_{S}}}\underline{U}^{{_{S}}}\underline{G}^{{_{S}}}\underline{U}^{{_{S}}}\underline{G}^{{_{S}}}\underline{U}^{{_{S}}}\underline{G}^{{_{S}}}\underline{U}^{{_{S}}}\underline{G}^{{_{S}}}\underline{U}^{{_{S}}}\underline{G}^{{_{S}}}\underline{U}^{{_{S}}}\underline{G}^{{_{S}}}\underline{U}^{{_{S}}}\underline{G}^{{_{S}}}\underline{U}^{{_{S}}}\underline{G}^{{_{S}}}\underline{U}^{{_{S}}}\underline{G}^{{_{S}}}\underline{U}^{{_{S}}}\underline{G}^{{_{S}}}\underline{U}^{{_{S}}}\underline{G}^{{{_{S}}}\underline{G}^{{_{S}}}\underline{G}^{{_{S}}}\underline{G}^{{_{S}}}\underline{G}^{{_{S}}}\underline{G}^{{_{S}}}\underline{G}^{{_{S}}}\underline{G}^{{_{S}}}\underline{G}^{{_{S}}}\underline{G}^{{_{S}}}\underline{G}^{{_{S}}}\underline{G}^{{_{S}}}\underline{G}^{{_{S}}}\underline{G}^{{}}\underline{G}^{{}}\underline{G}}\underline{G}^{{}}\underline{G}}\underline{G}^{{}}\underline{G}^{{$	81
HP egfp-MOE	P-ASUSAGSACSUSUGSUGSCSUSUSUSUSUSUSUSUSUSUSUSUSUSUS	74-75
HP egfp-OMe	P-AUSAGSACSUUGSUGSCCSUSGSUSUSGASA	75
HP egfp-LNA	P-A U AG AC GU UG UG GC U G U U G +A +A	75-76
ss HP-13	$P-\underline{G}_s \underline{G}_s \underline{UC}_s \underline{CG}_s \underline{UG}_s \underline{GA}_s \underline{AA}_s \underline{UU}_s \underline{G}_s \underline{C}_s \underline{A}_s \underline{U}_s \underline{G}_s \underline{A}_s \underline{A}$	78.5

We were able to achieve potent knockdown of *EGFP* at both the RNA (Figure 73) and protein level (Figure 74) using our duplex siRNAs. We then used the antisense sequences from both duplex siRNAs, **EGFP** and **HP EGFP**, as template strands for our ss-siRNA sequences. However, upon transfection, the ss-siRNAs proved to be too toxic to our cultured EGFP-expressing HEK293 cells to have enough samples for RNA or protein analysis. We performed a dose response from 50nM to 3nM; at 3nM the toxicity was reduced but the ss-siRNAs showed no change in fluorescence as compared to the NT control. Interestingly, the negative control ss-siRNA (**ss-HP13**) was also significantly more toxic than the dsRNA control of the same sequence (**HP-13**). This toxicity was observed over all ss-siRNA sequences over multiple transfections with these sequences at both 50 and 25 nM.

As no toxicity was observed when the cells were transfected with the corresponding duplex siRNAs, we concluded that the ss-siRNA toxicity was independent of any targeting effect, and seems to be related to the way this cell line responds to the ss-siRNA chemistry itself. To validate this claim, we transfected three *SIN3A* targeting ss-siRNAs used previously in HEK293 cells with no

toxicity. All of the *SIN3A* targeting ss-siRNAs showed significant toxicity, comparable to the toxicity observed with the egfp-targeting ss-siRNAs. It is not clear why these stably EGFP-expressing cells respond with such toxicity to ss-siRNAs.

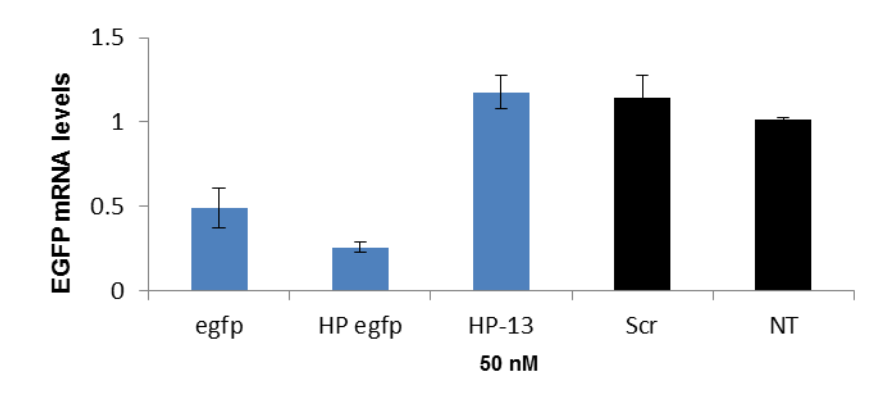


Figure 73. qRT-PCR results of EGFP mRNA levels when treated with duplex siRNAs. All siRNAs were transfected at 50nM concentration and normalized to a NT control. Error bars are standard deviation of n=4. (C)

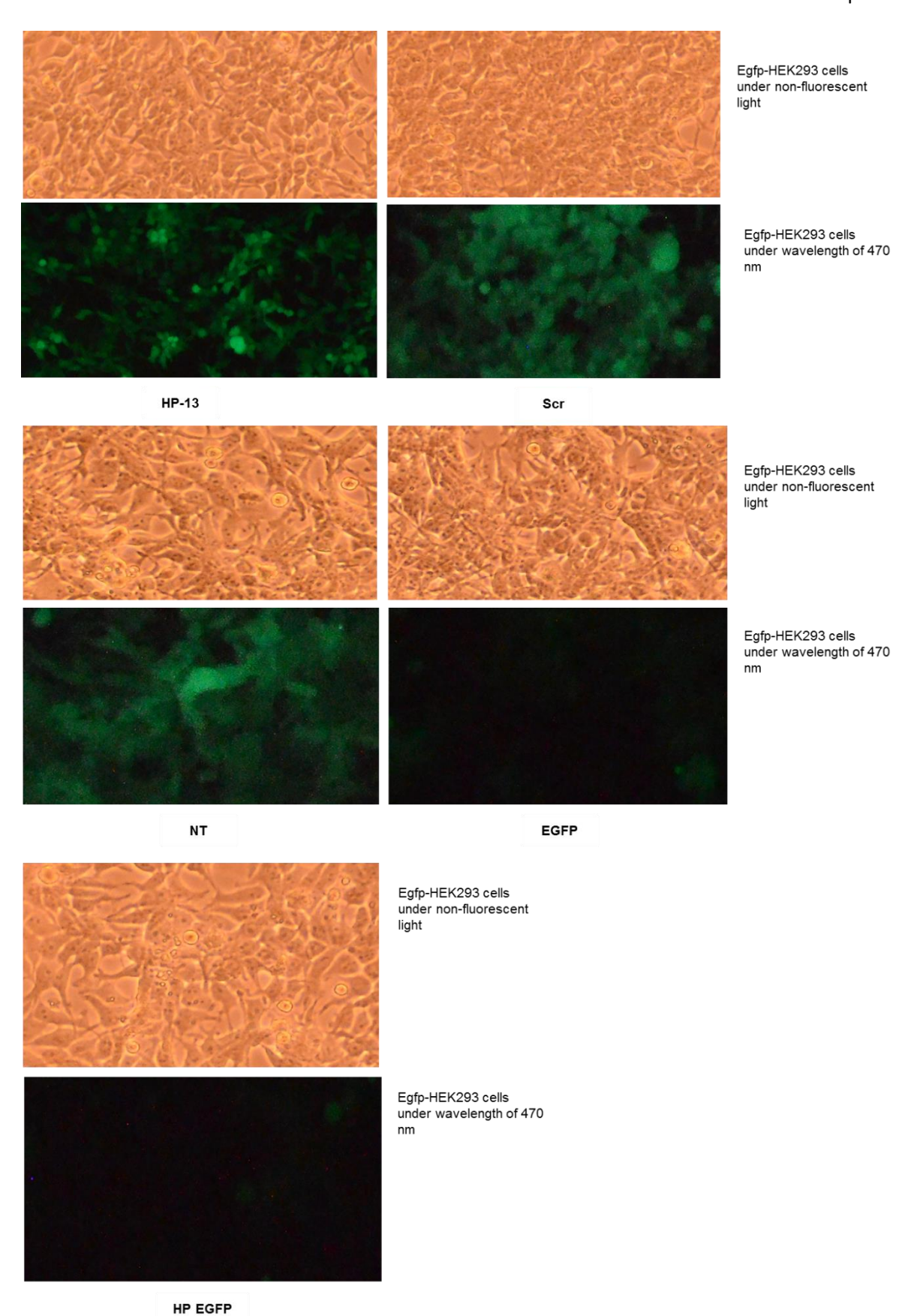


Figure 74. qRT-PCR results of EGFP mRNA levels when treated with duplex siRNAs. All siRNAs were transfected at 50nM concentration and normalized to a NT control. Error bars are standard deviation of n=4. (C) Fluorescent image of EGFP-expressing cells treated with duplex siRNAs showing potent knockdown of EGFP at the protein level relative to control oligomers or untreated controls.

4.6 Conclusions

Recently, it has been shown that ss-siRNA oligonucleotides may now engage gene silencing pathways that had previously been reserved for duplex RNAs (74, 236, 259). However, until now, the published reports using ss-siRNA technology have used 2'-MOE modifications at the 3' terminus which makes the synthesis oligonucleotides unattainable for many research groups. We have shown that the 3'-terminal chemistry of ss-siRNAs can have a significant impact on their activity. And more importantly, ss-siRNAs modified with 2'-OMe or LNA at the 3'-terminus showed greater silencing activity than those modified with MOE across two sequences. Since 2'OMe in particular is a readily available modification, this observation makes ss-siRNA technology widely accessible, at least for use in cultured cells.

We aimed to develop and optimize ss-siRNAs based on five active siRNA sequences, but three of the sequences failed to show any activity as ss-siRNAs, and in two of those cases the ss-siRNAs showed significantly increased toxicity relative to the parent duplexes. It appeared that some cell lines and sequences may be less receptive to the ss-siRNA technology as compared with duplex siRNA, exemplified by HEK293 cells in this study. We have concluded that both the nature of the RNA target and the cell type have a major impact of the efficacy of ss-siRNAs in gene silencing.

Chapter 5: Genome editing using the CRISPR/Cas type II system with chemically modified crRNAs

5.1 Introduction

Genome editing is a powerful tool for determining the function of a gene or protein within a cell. This technique allows DNA within a genome to be replaced, inserted, or removed using artificial nucleases that create double strand breaks in the target DNA sequence. Genome engineering has a tremendous range of applications including the exploration and modification of gene function in biological systems, the assembly and optimization of synthetic biological systems, and therapeutic purposes such as correction of genetic mutations and elimination of viral sequences.

As discussed in the introduction, several techniques have been developed in the field of genome engineering, including zinc finger nucleases and TALENS. However, the most promising recent genome engineering technique uses the RNA-guided Cas9 nuclease from the CRISPR/Cas type II system (most commonly the system from *Streptococcus pyogenes*). The type II CRISPR/Cas system uses only a single protein and two guide RNAs: Cas9 nuclease, a CRISPR RNA (crRNA) which is complementary to the 20-base DNA target, and a trans-activating crRNA (tracrRNA) whose sequence is constant. These three components make a large complex – Cas9 is a 159 kDa protein, crRNA is a 42mer RNA (ca. 14 kDa) and tracrRNA is a 75mer RNA (ca 25 kDa).

Since the discovery in 2012 (185) that the aforementioned components were sufficient to engineer site-specific cleavage of an arbitrary DNA sequence, thousands of studies have taken advantage of CRISPR technology for genome engineering (for key papers, see (185, 209-215)).

Chemically modified oligonucleotides can be designed to exhibit greater affinity and specificity to their target sequence and to be more stable in biological systems. We wanted to explore whether a chemically modified crRNA could improve the specificity or efficiency of cleavage of target DNA when compared to an unmodified crRNA. However, as no work has been published on chemically modified crRNAs, it was unknown whether the CRISPR/Cas system could tolerate chemical modifications and retain cleavage ability.

5.2 Gene silencing using the type II CRISPR/Cas system

5.2.1 Experimental Design

Although our final aim of this project is to determine the effects of chemically modified crRNAs on the efficacy of the type II CRISPR/Cas system, we initially needed to get efficient cleavage of a

target DNA sequence using unmodified RNAs. We decided, in keeping with common practice in the field at the time, to express both the guide RNAs and the Cas9 protein from a plasmid.

In 2013, Cong *et al.* published work on using CRISPR/Cas systems for multiplex genome engineering (*281*) (Figure 75). In order to take advantage of the CRISPR/Cas II system in mammalian cells, they designed a plasmid co-expressing the *S. pyogenes* Cas9 and the crRNA and tracrRNA which are required for DNA target cleavage. The two RNAs are expressed from U6 promoters. The plasmid can be digested in the crRNA sequence using a BbsI restriction enzyme creating a double strand break, which allows the insertion of an annealed DNA sequence to be cloned into the plasmid and become the DNA-binding domain of the crRNA sequence. (In fact, the plasmid contains a pair of inverted back-to-back BbsI recognition sites; since BbsI cleaves outside of its recognition site, BbsI digestion of this plasmid produces two noncomplementary sticky ends and no BbsI recognition sites.) The inserted DNA sequence is designed to be complementary to the target DNA sequence which must be adjacent to an NGG sequence (the *S. pyogenes* "Protospacer Adjacent Motif" or PAM). The plasmid already contains the tracrRNA binding sequence required for crRNA function, so all we needed to clone in was the DNA-binding portion of the crRNA.

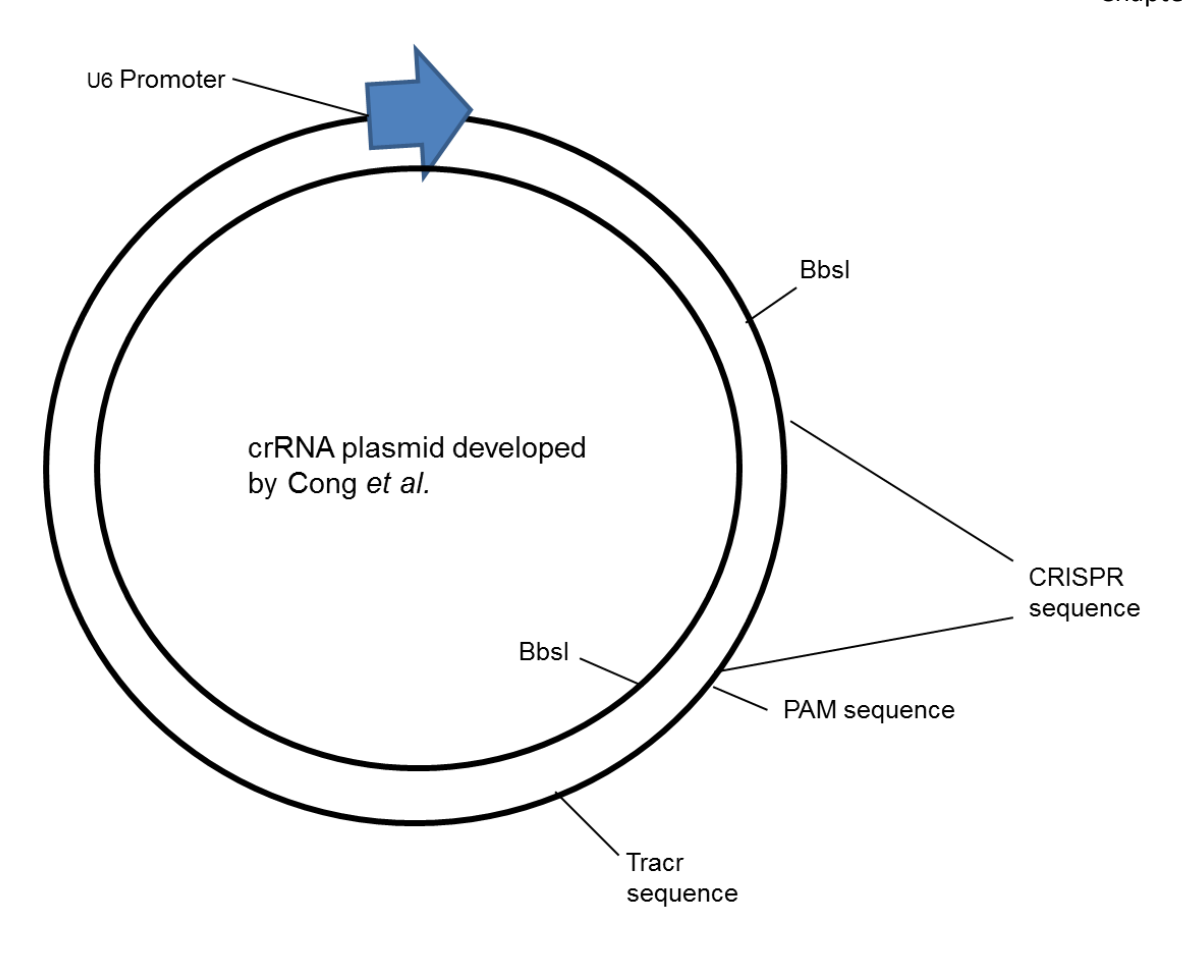


Figure 75. Simple schematic of the CRISPR plasmid developed by Cong et al.(281). The plasmid is transcribed starting at the U6 promoter. The plasmid is digested by BbsI restriction enzymes causing a double strand break where a new CRISPR insert can be ligated into the plasmid.

We chose to use this plasmid as our CRISPR/Cas array for targeting our chosen DNA target. As previous reports have experimentally validated genome engineering using mammalian human embryonic kidney (HEK293) cells (196, 204, 281-284), we chose to use an eGFP-HEK293 cell line for our *in vitro* assays.

We designed five oligonucleotide sequences to generate crRNAs that target eGFP. Our oligonucleotides were designed to have various lengths. This was due in part to a published report by Fu *et al.* stating that truncated crRNA sequences may improve CRISPR-Cas nuclease specificity (*285*). We designed two 20-mer (N1 20 and N2 20) and one 21-mer (HP 20) oligonucleotides which target three independent sites within the eGFP sequence (Table 10) (Appendix D and E). Additionally, we expanded two of the oligonucleotide sequences to 29 (N2 30) and 30 (HP 30) (Table 10) nucleotides as recommended by the protocol for our CRISPR/Cas plasmid (*281*). We sought to have the crRNA sequences begin with G, to optimize expression from the U6 promoter. The crRNAs encoded by the resulting plasmid sequences each encode target sequences directly adjacent to a NGG PAM. As the BbsI digestion of the plasmid gives products with noncomplementary sticky ends as noted above, each oligonucleotide was synthesized with the appropriate complementary sticky end.

Table 10. Insert sequences for ligation into a plasmid that would express crRNAs used to target eGFP in mammalian HEK293 cells. P represents 5'-phosphate required for ligation.

DNA	sequence
N1 20	5' P-AAAC GAGCTGGACGGCGACGTAAA
	CTCGACCTGCCGCTGCATTT AAAT-P 5'
N2 20	5' P-AAAC GTGAACCGCATCGAGCTGAA
	CACTTGGCGTAGCTCGACTT AAAT-P 5'
HP 20	5' P-AAAC GCTCGTGACCACCCTGACCAT
	CGAGCACTGGTGGGACTGGAT AAAT-P 5'
N2 30	5' P-AAAC GACACCCTGGTGAACCGCATCGAGCTGAA
	CTGTGGGACCACTTGGCGTAGCTCGACTT AAAT-P 5'
HP 30	5' P-AAAC GCTGGCCCACCCTCGTGACCACCCTGACCTA
	CGACCGGGTGGGACCTGGTGGGACTGGAT AAAT-P 5'
Ctrl	5' P-CAT ACGTAGTTAA GTAC
	TGCATCAATT 5'

5.2.2 Results

5.2.2.1 Ligation optimization

The CRISPR/Cas plasmid arrived as a bacterial stab and was cultured overnight followed by DNA extraction using a plasmid mini prep system. Our purified plasmid was digested with BbsI restriction enzyme in order to induce a double strand break in our plasmid DNA. For our oligonucleotide ligation conditions, we initially used a 1:50 and a 1:100 vector: insert ratio (V:I; i.e. digested plasmid: annealed oligonucleotides) to try and achieve successful ligation products. As the vector was over 10kb and the inserts were 20-30bp, we used such a large excess of insert for these reactions in an attempt to increase the success rate of our ligation. The ligation products were transformed into chemically competent DH5 alpha cells. None of our 1:50 V:I plates had colonies following transformation, but our 1:100 V:I plates had several colonies after transformation. A few colonies from each transformation plate were selected from each of the various insert plates for colony PCR. A 1% agarose gel of our colony PCR products indicated that we achieved a ligation product from each of our inserts. The plasmids were purified for sequencing analysis, but upon receiving the sequencing results, we discovered that none of our plasmids had the correct insert.

We re-digested our CRISPR/Cas plasmid with BbsI in order to obtain more material for our experiments. The digested plasmid was gel purified before ligation. Only annealed oligonucleotide N1 20 was used in order to optimize ligation conditions. We chose ligation conditions of 1:10, 1:25, and 1:50 V:I ratio. The ligation products were transformed into chemically competent DH5 α cells. Upon analysis, the positive transformation control plate produced several colonies, but none of our ligation reactions yielded any products.

As our ligations failed previously, we chose to troubleshoot several possible causes as to why our cloning was unsuccessful. We started by re-annealing our oligonucleotide inserts, leaving out the PBS buffer that was used previously. We tried this to avoid having too much phosphate in the ligation reactions.

We also chose to use a 1:200, 1:400, and 1:600 V:I ratio for our ligation reactions in order to have an even greater excess of our insert than previously used. The ligation conditions were attempted with and without PEG8000, as PEG has been shown to stimulate ligation activity (286). The ligated products were transformed. Following transformation, one colony from each plate was picked for colony PCR. The colony PCR was unsuccessful indicating that the ligation was still unsuccessful.

As we had exhausted several ligation options, we next chose to perform our ligations with vector: insert ratios of 1:200, 1:500, and 1:1000. We also compared our initial ligation protocol to one with additional ATP and buffer to the digestion mixture. Once again, only annealed oligo N1 20 was used for these troubleshooting experiments. The ligation products were transformed. Colonies grew under all conditions except 1:500 V:I ratio with the initial ligation mixture, and 1:200 V:I ratio with extra ATP and buffer. Three colonies were chosen from the following ligation conditions in addition one colony from the uncut plasmid positive control plate:

- 1) 1:200 V:I ratio with initial ligation conditions
- 2) 1:500 V:I ratio with additional buffer and ATP
- 3) 1:1000 V:I ratio with additional buffer and ATP

A mini prep was performed on each of the colonies selected from the ligation plates. An additional digestion was performed on the mini prepped plasmids as a way to test if the ligation was successful. Digesting this specific CRISPR/Cas plasmid with Ndel restriction enzyme will result in a 366 base pair fragment if there is no correct insert ligated, but a ~390 base pair fragment if the ligation was successful. This is due to the restriction sites flanking the insertion site. If the correct product is inserted, the DNA fragment will be larger than if the ligation was unsuccessful.

Base pairs	Ladder	Successful ligation	Unsuccessful ligation
500			
400			
300			
200			
100			

Figure 76. Schematic of a gel image following a Ndel restriction digest. The successfully ligated product will be ~390 base pair fragment and an unsuccessfully ligated product will be ~366 base pairs. Unfortunately the gel image was too faint for an image.

Upon digestion with Ndel restriction enzyme, the digestion products were run on a 1.5% agarose. Although faint, five of the nine samples showed a 390 base pair band. Samples from ligations from the 1:200 V:I ratio with initial ligation conditions and the 1:200 V:I ratio with the additional buffer and ATP ligation conditions were sent for sequencing. All of the ligations were correct as verified by our sequencing results.

Upon receiving positive results from our N1 20 insert, we repeated the successful conditions with the additional four oligonucleotide inserts. We digested the CRISPR/Cas plasmid with BbsI, and used a 1:200 V:I ratio for our ligations with additional ATP and buffer as with the successful N1 20 insert. The ligation products were transformed. A single colony was picked from each of the four insert plates, cultured, and mini prepped. The correct inserts were digested as before with Ndel restriction enzyme, and the successful inserts were sent for sequencing analysis. All of the inserts were successful as verified by sequencing.

In addition to the BbsI digests, we also attempted to clone a control plasmid which is entirely lacking the U6 promotor region and would thus not express any crRNA (Table 1). This plasmid was designed to be co-transfected with chemically modified crRNAs. Unfortunately our ligations were never successful. Although we used our optimized conditions, we were never able to obtain our negative control plasmid. One reason for this could be that our annealed oligonucleotide insert was only 10 base pairs, which is extremely challenging to clone into a 10kb plasmid.

5.2.2.2 Mammalian cell culture transfection

Although we did not have a negative control plasmid, we decided to transfect our eGFP targeting CRISPR/Cas plasmids into eGFP-HEK293 cells using a calcium chloride transfection method (287). All of the plasmid-treated cells showed what we initially thought were signs of contamination within 24 hours post-transfection (mostly this involved cellular toxicity and the formation of numerous small bodies, significantly smaller than the cells). We repeated the transfection four additional times using only sterile filtered reagents and new plasmid preps, but our treated cells never survived more than 48 hours post transfection. Our collaborator Noel Wortham (Biological Sciences, University of Southampton) also worked with this and related plasmids in a different cell culture facility with a different batch of cells, and observed the same results. Thus, the problem is not related to contamination, but we have not been able to identify the exact cause of the cell death, whether it is an inherently problematic plasmid or an incompatibly of the plasmid with our cells. We suspect that there may have been changes in the (very large) plasmid backbone, incorporated during our cloning experiments, that rendered it toxic in some way.

5.2.2.3 Alternative CRISPR/Cas experiments

Drs. William Skarnes and Mark Behlke presented independent recent findings showing that efficient target DNA cleavage may be obtained using a plasmid-free CRISPR system⁵(288). By combining in vitro the three components of the CRISPR/Cas system (Cas9 nuclease, tracrRNA, and crRNA), then transfecting them into cells as a ribonucleoprotein (RNP) complex, efficient cleavage of target DNA was achieved.

Besides circumventing the problems we had encountered with plasmid cloning, we immediately realised that this RNP approach was better-suited to applications involving chemically modified RNAs. We purchased *S. pyogenes* Cas9 nuclease (New England Biolabs) and tracrRNA (Dharmacon), and synthesized a series of native and chemically modified crRNAs. We chose to target the eGFP sequence as before, but a modified duplex DNA gBlock (linear double stranded DNA sequence) was ordered from IDT as opposed to using the plasmid-derived DNA sequence. Our eGFP DNA sequence needed to be altered as only two of our five oligonucleotide target sequences were flanked by a PAM sequence. Our gBlock design added PAM sequences 3' to our oligonucleotide targets. Three of our eGFP-targeting crRNA sequences (Fu 1, Fu 2, Fu 3) were published (*280, 285*), a fourth was based on a published siRNA sequence (*280*), and the fifth sequence (HP egfp) was based on the sequence of an siRNA we designed in-house.

_

⁵ CRISPR Oxford http://lpmhealthcare.com/crispr-2015

In order for target DNA cleavage by this method, a complex must be formed between the crRNA and the tracrRNA. We designed our crRNA sequences to contain a 5' stretch of 19-20 nucleotides complementary to the target eGFP DNA sequence followed by a 21 nucleotide sequence which is complementary to the tracrRNA (Table 11). A scrambled control sequence was designed as well, keeping the complementary tracrRNA unaltered but scrambling the DNA-binding region of the crRNA. The oligonucleotides were synthesized via solid phase synthesis, purified by PAGE, and verified correct by mass spectrometry.

Table 11. crRNA sequences used to target eGFP in plasmid-free CRISPR/Cas system. DNA binding domains (DBD) are shown in red, while tracrRNA binding domains (tracrBD, constant 3'-half) are shown in black.

crRNA	Sequence (5' to 3')	Ref
egfp	GACGUAAACGGCCACAAGU GUUUUAGAGCUAUGCUGUUUUG	(280)
HP egfp	CAACAGCCACAACGUCUAU GUUUUAGAGCUAUGCUGUUUUG	novel
Fu 1	GGGCACGGCAGCUUGCCGG GUUUUAGAGCUAUGCUGUUUUG	(285)
Fu 2	GAUGCCGUUCUUCUGCUUGU GUUUUAGAGCUAUGCUGUUUUG	(285)
Fu 3	GGUGGUGCAGAUGAACUUCA GUUUUAGAGCUAUGCUGUUUUG	(285)
Ctrl	GGUGGUGCAGAUGAACUUCA GUUUUAGAGCUAUGCUGUUUUG	novel

Once we had all of our experimental components in hand, we started optimizing the protocol for our eGFP DNA cleavage. We used protocols outlined in Jinek $et.\ al$ (185) as a guideline for our experimental design, using a 1:1 molar ratio of Cas9 nuclease to the tracrRNA:crRNA complex. We initially only used the Fu 2 crRNA in our optimization experiments. Several reaction conditions were tested, but we achieved our optimal target DNA cleavage using 100 nM Cas9 and tracrRNA:crRNA complex with 0.2 μg DNA (Figure 77).

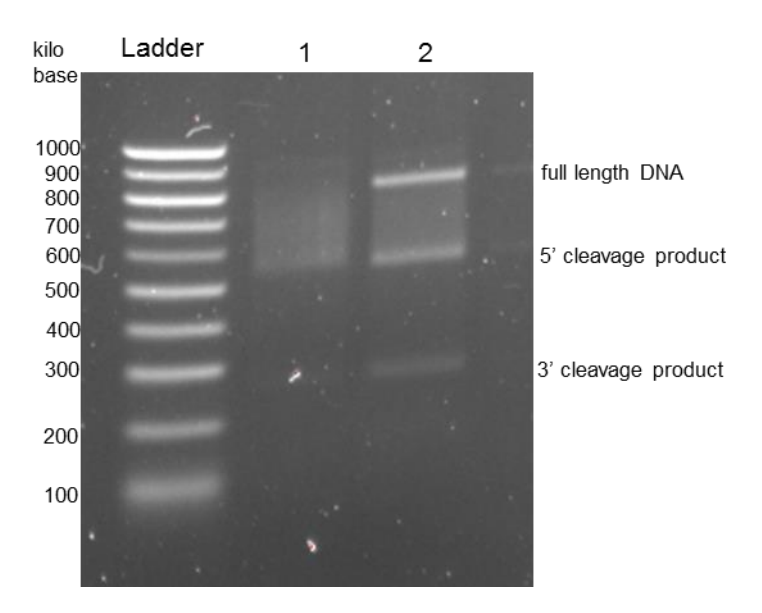


Figure 77. . Results of optimization experiment using crRNA Fu 2 targeting eGFP DNA. Either 50 nM Cas9 and tracrRNA:crRNA complex (Lane 1) or 100 nM Cas9 and tracrRNA:crRNA complex (Lane 2) was used in the presence of 0.1 μg (Lane 1) or 0.2 μg (Lane 2) target DNA. 1000 bp ladder was used as reference. 1% agarose gel stained with Nancy-520.

As we had optimized our protocol, we repeated the experiment using all of our crRNAs (Figure 78). As shown from the gel image, we were able to observe cleavage with all of our crRNAs, though **HP egfp** and **Fu2** showed the highest efficiency cleavage.

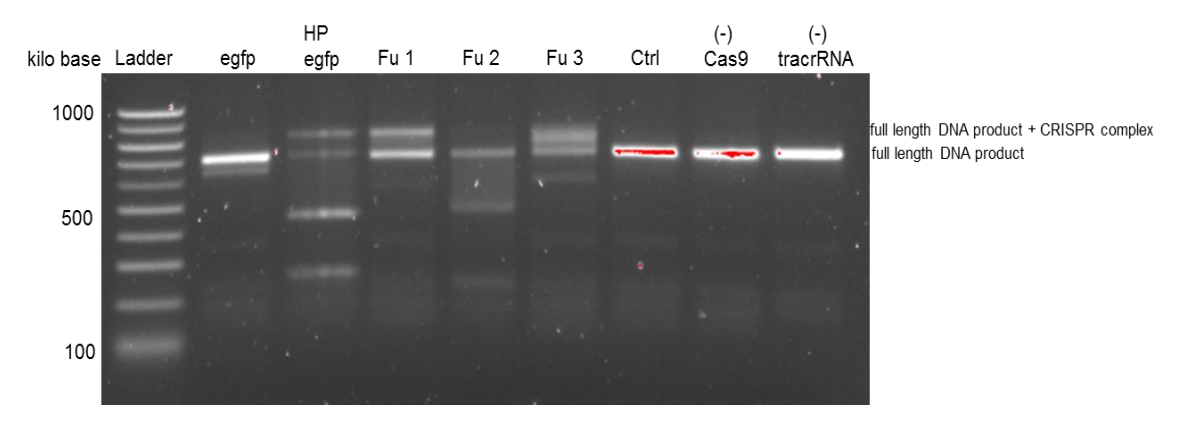


Figure 78. Results of 1% agarose gel showing the egfp cleavage by the Cas9: tracrRNA: CRISPR RNA complex with various CRISPR RNAs.

For several samples, we also observed bands of higher apparent molecular weight than the uncut DNA band (Figure 78). This could correspond to cut or uncut DNA fragments with the Cas9:tracRNA:CRISPR complex still attached. In order to test this theory, we added an SDS buffer solution in order to break up the potential complex, as other authors have also done (185). As shown in Figure 79, the DNA cleavage appears much more evident and the higher molecular weight complex disappears following the addition of SDS to the reaction mixture.

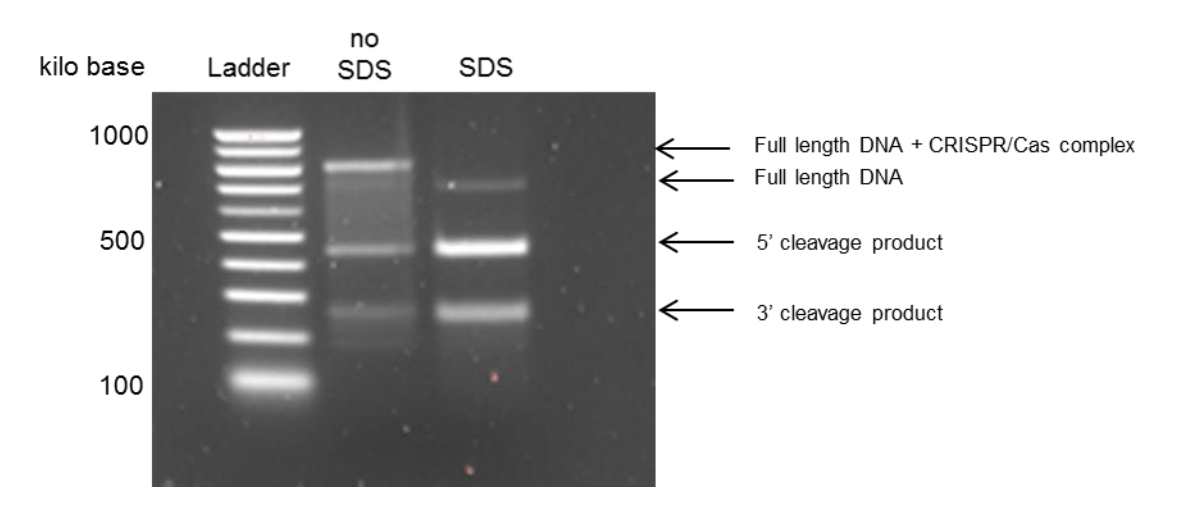


Figure 79. Results of 1% agarose gel showing the same sample, HP egfp, with and without SDS treatment.

5.2.3 Chemically modified crRNA

We chose to use the crRNA **HP egfp** as a template sequence for our chemically modified crRNA designs. As there are no current published reports on the effects of chemically modified crRNAs on DNA cleavage efficiency, we selected various regions of the oligonucleotide to incorporate chemical modifications. We chose to modify both the DNA binding domain (DBD) and the tracrRNA binding domain (tracrBD) of our oligonucleotides (Table 12).

Table 12. Chemically modified crRNAs used in this study. Modification code: RNA, dna, 2'-OMe, 2'-F, '+': LNA, 's': phosphorothioate.

_	
crRNA	Sequence (5' to 3')
HP egfp	CAACAGCCACAACGUCUAU GUUUUAGAGCUAUGCUGUUUUG
HP-PS-all	$C_{s}A_{s}G_{s$
HP-PS- DBD	$\mathbf{C_s}\mathbf{A_s}\mathbf{A_s}\mathbf{C_s}\mathbf{A_s}\mathbf{G_s}\mathbf{C_s}\mathbf{A_s}\mathbf{C_s}\mathbf{A_s}\mathbf{A_s}\mathbf{C_s}\mathbf{G_s}\mathbf{U_s}\mathbf{C_s}\mathbf{U_s}\mathbf{A_s}\mathbf{U_s}\mathbf{GUUUUAGAGCUAUGCUGUUUUG}$
HP-PS- tracrBD	$CAACAGCCACAACGUCUAU \; G_sU_sU_sU_sU_sA_sG_sA_sG_sC_sU_sA_sU_sG_sC_sU_sG_sU_sU_sU_sG$
HP-LD- DBD	+Caa+Cag+Cca+Caa+Cgt+Cta+T GUUUUAGAGCUAUGCUGUUUUG
HP-LR- DBD	+CAA+CAG+CCA+CAA+CGT+CTA+T GUUUUAGAGCUAUGCUGUUUUG
HP-LR- tracrBD	CAACAGCCACAACGUCUAU +GUU+TUA+GAG+CUA+TGC+TGU+TUUG
HP-LR-few	+CAA+CA+GCCACAACGUCUAU GUUUUAGAGCUAUGCUGUUUUG
HP-2OMe	CAACAGCCACAACGUCUAU GUUUUAGAGCUAUGCUGUUUUG
HP- Me/RNA	CAACAGCCACAACGUCUAU GUUUUAGAGCUAUGCUGUUUUG
HP-Me/F	CAACAGCCACAACGUCUAU GUUUUAGAGCUAUGCUGUUUUG

The rationale for trying the various modifications was as follows:

- As PS linkages are so useful in protecting synthetic oligomers from nuclease cleavage, we
 wanted to test wehther they are tolerated in either or both halves of the crRNA. (PS-all,
 PS-DBD, PS-tracrBD)
- As LNA shows improved binding affinity and specificity, we wanted to include it in various regions of the crRNA, particularly the DNA binding domain (we hoped that it might improve the specificity of DNA binding). (LD-DBD, LR-DBD, LR-tracrBD, LR-few). In most cases, we made strands as chimeras of LNA and RNA. However, in one case (LD-DBD) we made the DNA binding domain from a mixture of LNA and DNA. Our rationale for doing this was that the rigid LNA can induce an RNA-like conformation into neighbouring deoxynucleotides, and we wondered if this would be sufficient to yield an active crRNA)
- Finally, we wanted to include various 2'-modified sugars, including a fully modified 2'OMe-RNA and the alternating pattern of 2'OMe/2'F-RNA that has proven so useful in the context of siRNAs. (2OMe, Me/RNA, Me/F)

Using our optimized protocol, we performed the DNA cleavage experiment using our chemically modified oligonucleotides (Figure 80). Gratifyingly, we observed DNA cleavage from most of our chemically modified oligonucleotides. However, it is hard at this point to identify patterns that might predict or explain which crRNAs are active and inactive. For instance, the uniformly 2'-OMe modified crRNA (HP-OMe) was completely inactive, but the alternating 2'-OMe and 2'-F (HP-OMe\F) and 2'-OMe and RNA (HP-OMe\RNA) modified oligonucleotides retained cleavage activity. Even more surprisingly, the fully PS modified oligonucleotide(PS all) showed cleavage activity, but the oligonucleotide only PS modified in the tracrBD (HP-PS-transBD)was not active. Whether the inactivity of the few select oligonucleotides is due to conformational changes, binding affinity, or other factors is not clear at this time.

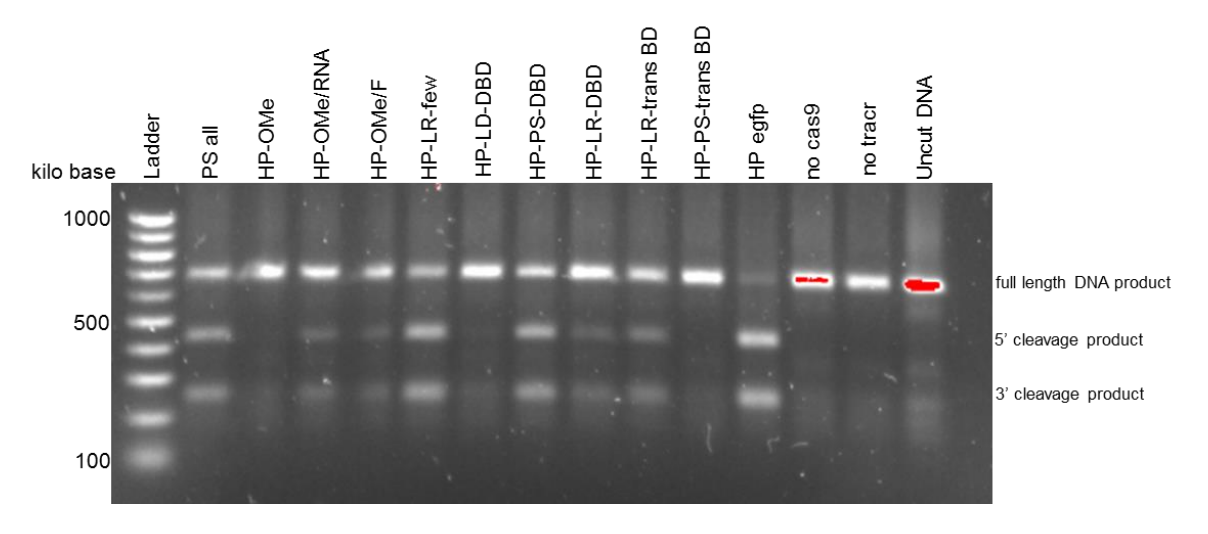


Figure 80. Results of 1% agarose gel showing the egfp cleavage by the Cas9: tracrRNA: CRISPR RNA complex with various chemically modified CRISPR RNAs. Gel is representative of three independent experiments.

5.3 Conclusions and Future Work

There have been several published reports on the efficient cleavage of target DNA by the CRISPR/Cas type II system. However, no published reports have investigated the effects of chemically modified crRNAs of the efficiency of the CRISPR/Cas system. From our initial results, we concluded that the CRISPR/Cas machinery is compatible with several chemical modifications. However, the chemically modified crRNAs were not as potent as the unmodified crRNA.

Our results are preliminary, and our future work will include testing the current chemical modification layouts on our other egfp targeting crRNAs. This will confirm that our results are not specific to the HP-egfp sequence and can be applied to other sequences and targets. We also need to design and synthesize several additional chemically modified sequences in order to observe a pattern of DNA cleavage.

Moreover, future work should include a study of what factors are contributing to the success and failure of these chemically modified crRNAs. Are they assembling correctly into the RNP complex but failing to bind DNA? Are they binding DNA but failing to cleave? Gel shift experiments and kinetic studies under single and multiple turnover conditions would constitute appropriate first steps to explore these questions.

Finally, it will be essential to return to the goals of this study using active modified sequences. Can we improve the potency and specificity of CRISPR/Cas9-based genome engineering using chemically modified RNA? This remains an open question, but our results are encouraging that there will be a role for oligonucleotide chemistry in advancing this exciting field.

Chapter 6: Concluding remarks

In this thesis work, we were able to successfully design and synthesize oligonucleotides of varying chemistries and lengths via solid phase synthesis. The successful synthesis methods were a result of modifying and optimizing several synthesis steps, deprotection methods, and purification techniques.

Using the oligonucleotides we made via solid phase synthesis, we were able to successfully inhibit the asthma susceptibility gene, *ADAM33*. The inhibition of *ADAM33* is a crucial step in the development of a therapeutic approach to correct airway remodelling. We compared the potencies of several classes of oligonucleotides, LNA gapmers, siRNAs, ss-siRNAs, and conjugates on the silencing of *ADAM33*. From this comparison, we concluded that our ASO oligonucleotides were more potent than RISC engaging oligonucleotides. A major contributing factor to this result could be that *ADAM33* mRNA is 95% localised in the nucleus.

While designing ss-siRNAs to silence *ADAM33*, we observed that minor modifications to the 3' terminus of our ss-siRNA greatly reduced or enhanced the potency. Specifically, the widely available modification 2'-OMe-RNA was the optimal modification for the 3'-terminus of the ss-siRNAs. Using ss-siRNAs with either 2'-OMe, MOE, or LNA modifications at the 3'-end, we targeted several genes in multiple cell lines. Our results were similar to the *ADAM33* results when targeting progesterone receptor in MCF7 cells. meaning that the ss-siRNA technology could now be more widely available to academic labs. However, when we treated two HEK293 cell lines with various ss-siRNAs, we either observed significant toxicity or no ss-siRNA activity.

Finally, using the CRISPR/Cas9 type II system, we were successfully able to use chemically modified guide RNAs to induce double strand breaks in a target DNA sequence. We have shown that the CRISPR/Cas machinery could tolerate chemically modified oligonucleotides. Although we were able to achieve target DNA cleavage, it was not as efficient as DNA cleavage using unmodified guide RNAs.

Chapter 7: Experimental

7.1 Oligonucleotide synthesis

All oligonucleotides synthesized in-house were at a $1.0\mu M$ scale on an Applied Biosystems 394 DNA/RNA synthesizer with standard acid-catalyzed detritylation, coupling, capping, and either oxidation or sulfurization.

7.1.1 RNA

The siRNAs (**HMH-1**, **HMH-2**, **HP-1** thru **HP-4**) were purchased and purified by IDT. All other oligonucleotides were synthesized in-house.

RNA phosphoramidite monomers (ChemGenes) were 2'protected with tert-butyldimethylsilyl (TBS) and base protected with n-benzoyl (A), n-isobutyl (G), or n-actetyl (C). All monomers were dissolved to a concentration of 0.15M in anhydrous acetonitrile immediately prior to use. A 0.3M solution of 5-Benzylthio-1H-Tetrazole was used as the coupling agent and all coupling times were 10 minutes. Either a Unylinker (ChemGenes) support column was used at $1.0\mu M$ or $1.0\mu M$ of CPG with 3' terminal G (ChemGenes) was used.

Unmodified RNA was deprotected using a 3:1 ratio of NH₄OH/ EtOH for 48 hours at room temperature unless otherwise stated. RNA 2'OH TBS protecting group was removed with a 4:1 DMSO/ TEA·3HF solution at 65°C for 3 hours, inverting the tube every 30 minutes to ensure product is dissolved. The reaction was cooled to room temperature then precipitated with 1:5 ratio of 3M NaOAc: BuOH. The mixture was centrifuged at 4°C for 5 minutes at 8000 rpm, washed with 70% EtOH, air dried, and the pellet was resuspended in RNase-free water.

 $20\mu\text{M}$ working stocks of siRNAs were prepared by annealing the sense and antisense strands in a final 2.5x PBS buffer. The solutions were heated at 95°C for 10 minutes and then cooled to room temperature at a rate of 1°C per minute.

7.1.2 ss-siRNA synthesis

The modified 2'F and 2'OMe RNA phosphoramidites (ChemGenes) were dissolved in anhydrous acetonitrile at a 0.15M concentration. A 1.0 μ M Unylinker support column was used per sequence. The first set of ss-siRNAs were synthesized using five separate steps: 1) the 2'-MOE was attached to the Unylinker support using the 1.0 μ M RNA synthesis cycle (Appendix A) with 0.02 M I₂ in H2O/Pyridine as oxidant 2) The phosphorothioated section was synthesized using

TETD as the sulfurizing reagent under the $1\mu M$ Sulfr+ cycle (Appendix B) 3) the phosphodiester section was synthesized using the $1.0~\mu M$ RNA cycle 4) The 5' phosphorothioated section was synthesized using TETD as the sulfurizing reagent under the $1\mu M$ Sulfr+ cycle 5) the 5' phosphate was added using the $1.0~\mu M$ RNA cycle followed by the end CE cycle (Appendix B).

Subsequent synthetic work followed the above cycle with two changes; an alternating pattern of PS and PO linkages in the 5'-half of the duplex, requiring multiple cycle changes, and the use of 3-Ethoxy-1,2,3-dithiazoline-5-one (EDITH, 0.05M in ACN, Link Technologies) as sulphurizing agent with sulphurizing time of 120 seconds total unless otherwise stated.

2' modified RNA and DNA was deprotected with pure NH₄OH at 55°C overnight. The oligonucleotide was evaporated to dryness by rotary evaporation then resuspended in 1mL RNase- free water until ready for further analysis.

7.1.3 LNA gapmers

The LNA and DNA amidites were dissolved in acetonitrile at a 0.1M or 0.15M concentration. A 1.0μM of Unylinker support column was used per sequence.

A modified 1μ M Sulfr+ cycle (Appendix C) was used for this synthesis: 1) BTT was used instead of tetrazole as a coupling reagent 2) 0.05M EDITH solution was used as a sulfurizing reagent instead of TETD.

7.1.4 1-*O*-hexadecylpropanediol

1-*O*-hexadecylpropanediol phosphoramidite was synthesized in two steps by lab member Alexandre Debacker and former member Liisa Niitso. Treatment of propanediol in DMF with NaH followed by addition of hexadecyl bromide and catalytic potassium iodide gave 1-O-hexadecyl-1,3,-propanediol in a single step as previously observed (*245*); recrystallisation with hexane yielded white crystals of excellent purity. The phosphoramidite was synthesized under standard conditions (*231*) using 2-cyanoethyloxy(*N*,*N*-diisopropylamino)phosphonamidic chloride.).) Rf in EtOAc =0.28. MS (ESI): found 501 (M+H); mass expected for (C28H57N2O3P + H = 501.4). 1H NMR (400 MHz, CDCl3) δ 0.89 (t, J=6.85 Hz, 3H, CH3CH2) 1.19 (dd, J=6.72, 3.42 Hz, 12H, 2 (CH3)2CHN) 1.26 (s, 26 H, 13 (CH2)n) 1.56 (quin, J=6.94 Hz, 2H, OCH2CH2CH2) 1.88 (quin, J=6.30 Hz, 2H, POCH2CH2CH2O) 2.64 (t, J=6.60 Hz, 2H, CH2CN) 3.40 (t, J=6.66 Hz, 2H, OCH2CH2CH2O) 3.50 (t, J=6.30 Hz, 2H, POCH2CH2CH2O) 3.54 - 3.65 (m, 2H, 2 CH) 3.65 - 3.79 (m, 2H, POCH2CH2CH2O) 3.79 - 3.93 ppm (m, 2H, POCH2CH2CN). 13C NMR (101 MHz, CDCl3) δ 14.1 (s, 1C, CH3CH2) 20.3 (d, J=6.60 Hz, 1C, CH2CN) 22.7 (s, 1C, CH2CH2CH3) 24.5 and 24.63 (2 d, J=7.70 Hz, 2x2C,

(CH3)2CHN) 26.2 (s, 1C, OCH2CH2CH2) 29.3 (s, 1CH2n) 29.5 (s, 1CH2n) 29.6 (s, 2CH2n) 29.6 (s, 1CH2n) 29.7 (s, 5CH2n) 29.8 (s, 1CH2n) 31.5 (d, J=7.34 Hz, 1C, POCH2CH2CH2O) 31.9 (s, 1CH2n) 43.0 (d, J=11.74 Hz, 2C, 2 CH) 58.3 (d, J=19.07 Hz, 1C, POCH2CH2CN) 60.7 (d, J=17.61 Hz, 1C, POCH2CH2CH2O) 67.3 (s, 1C, POCH2CH2CH2O) 71.1 (s, 1C, OCH2CH2CH2), 117.6 ppm (s, 1C, CN). 31P NMR (162 MHz, CDCl3, 1H-decoupled) δ 147.56 ppm (s).

7.1.5 Bio cleavable hexadecyloxypropyl conjugates

This synthesis was done by Mike Moazami. This synthesis was completed in stages by Mike Moazami as follows. 6-chlorohexanol was refluxed with potassium iodide and thiourea in EtOH overnight, the following morning a solution of NaOH was added and all left to stir at room temperature overnight. The mix was bought to reflux for 3 hours, then cooled to room temperature and acidified with 1M HCl(aq) to pH= 3. The mixture was extracted with Et_2O and the organics removed *in vacuo* to give 6-mercaptohexanol as a clear oil in a quantitative yield.

To a solution of 6-mercaptohexanol in MeOH was added Et₃N and iodine. The reaction was allowed to stir at room temperature before being concentrated in vacuo. The residue was taken into water and extracted (DCM), the organic phase dried and concentrated in vacuo to give a residue that was purified by column chromatography to provide 6,6'-Disulfanediylbis(hexan-1-ol) as an off white solid in 79% yield.

6,6'-Disulfanediylbis(hexan-1-ol) was dissolved in pyridine and DMT-Cl added. The reaction was stirred overnight, then concentrated in vacuo and purified by column chromatography to give 6-((6-(Bis(4- methoxyphenyl)(phenyl)methoxy)hexyl) disulfanyl)hexan-1-ol as a clear yellow oil in a 79% yield. This compound was phosphitylated using 2-cyanoethyl *N,N*-diisopropylchlorophosphoramidite in THF to give the final linker phosphoramidite as a clear yellow oil in 92 % yield.

Mercaptohexanol: ¹H NMR (400 MHz, CDCl₃) δ 3.63 (2H, s, H-1), 2.53 (1H, dt, J = 7.2 Hz, H-6), 1.49 - 1.68 (4H, m, H-2, 5), 1.30 - 1.47 (4H, m, H-4, 3) ¹³C NMR (100 MHz, CDCl₃) δ 62.8 (C-1), 33.9 (C-6), 32.6 (C-2), 28.1 (C-5), 25.21 (C-3), 24.5 (C-4) 6,6′-Disulfanediylbis(hexan-1-ol) ¹H NMR (400 MHz, CDCl₃) δ 3.65 (4H, br t, J = 6.2 Hz, H-9, 1), 2.69 (4H, t, J = 7.3 Hz, H-14, 6), 1.67 - 1.74 (4H, m, H-13, 5), 1.58 (4H, quin, J = 6.8 Hz, H-10, 2), 1.47 - 1.51 (2H, m, M06), 1.33 - 1.46 (8H, m, H-11, 3, 12, 4) ¹³C NMR (100 MHz, CDCl₃) δ 62.8 (C-9, 1), 39.0 (C-14, 6), 32.6 (C-10, 2), 29.1 (C-13, 5), 28.2 (C-12, 4), 25.4 (C-11, 3)6-((6-DMT)disulfanyl)hexan-1-ol ¹H NMR (400 MHz, CDCl₃) δ 7.41 - 7.48 (2H, m), 7.28 - 7.36 (6H, m), 7.17 - 7.23 (1H, m), 6.76 - 6.89 (4H, m), 3.80 (6H, s, O-Me), 3.64 (2H, br td, J = 6.5 Hz, J = 5.3 Hz CH2OH), 3.00 - 3.11 (2H, m, OCH2), 2.62 - 2.75 (4H, m), 1.52 - 1.76 (9H, m), 1.31 - 1.49 (9H, m) ¹³C NMR (100 MHz, CDCl₃) δ 158.3, 145.4, 136.7,

130.0, 128.2, 127.7, 126.6, 113.0, 85.7 (C-9), 63.3 (C-11), 62.9 (C-24), 55.2 (C-8, 39), 39.0, 32.6, 29.2, 28.4, 26.0 6-((6-(DMT)hexyl)disulfanyl)hexyl(2- cyanoethyl)diisopropylphosphoramidite ^{31}P NMR(135 MHz, CD₃CN) δ 148.37

7.2 Oligonucleotide quantitation and validation

The oligonucleotide was evaporated to dryness by rotary evaporation then resuspended in 1mL RNase- free water. The oligonucleotide concentration was calculated by UV absorbance on a Cary 300 bio UV-Visible spectrophotometer using Beer-Lambert law Absorbance=(concentration)(molar extinction coefficient)(path length).

Oligonucleotides were diluted to a $20\mu M$ concentration and characterized on a Bruker MicrOTOF Ultimate 3000 spectrometer with electrospray and time of flight in negative ionization mode. The data was analysed using Compas DataAnalysis software.

Buffer A: 100mM hexafluoroisopropanol with 10mM triethylammonium acetate; Buffer B: 20mM triethylammonium acetate and acetonitrile.

7.3 Oligonucleotide purification and electrophoresis

Approximately 20 ODUs (denaturing gel) or 0.1 ODUs (analytical gel) was loaded into a 16 or 20% polyacrylamide gel (420g urea, 100 10x TBE, 500mL 19:1 acrylamide:bis acrylamide solution (Sigma), 100mL water) and was run at 400V for ~3 hours. For denaturing gel: the highest molecular weight band was cut out of the gel and soaked in RNase-free water overnight. The aqueous solution was the evaporated to dryness and resuspended in RNase-free water. A Nap-25 column (GE Healthcare) was run to desalt the oligonucleotide. The oligonucleotide was evaporated to dryness again and resuspended in a small volume of RNase-free water. For analytical gel: the gel was soaked overnight in Stains-all (Sigma) and an image was taken after 24 hours.

7.4 Mammalian cell culture and transfection

7.4.1 MRC-5 fibroblast cells

MRC-5 embryonic fibroblasts were maintained in DMEM supplemented with 10% FBS, 2% L-Glutamine, 1% NEAA, and 1% sodium pyruvate (all from Sigma). Cells were plated in 6-well plates

at 150k cells/well (MRC-5) for lipofection transfections or 65k cell/well for gymnotic experiments 24 hours prior to transfection (forward transfection) or day of transfection (reverse transfection), unless otherwise stated. Oligonucleotides were transfected at 50nM concentration for single dose or decreasing doses for dose responses. Cells were transfected using RNAiMAX (Life Technologies) using 0.75µL lipid per 1µL of oligonucleotide in OptiMEM (Life Technologies). Cells were harvested for RNA analysis 3 days after transfection. Gymnotic transfections were transfected 24 hours post seeding with media change and additional oligonucleotide add day 5 post transfection. Cells were harvested for RNA 7-8 days post transfection.

7.4.2 MCF-7 cells

MCF-7 cells were maintained in MEM supplemented with 10% FBS, 10mM HEPES, 1mM sodium pyruvate, 0.5x NEAA, and 0.4 units ml⁻¹ bovine insulin. Cells were seeded 250k cells/well 24 hours prior to transfection (forward transfection) or day of transfection (reverse transfection), unless otherwise stated. Oligonucleotides were transfected at 50nM concentration for single dose or decreasing doses for dose responses. Cells were transfected using RNAiMAX (Life Technologies) using 0.75μL lipid per 1μL of oligonucleotide in OptiMEM (Life Technologies). Cells were harvested for RNA analysis 3 days after transfection.

For gymnotic delivery, 24 h post-seeding, cells were treated with fresh media containing 1-3 μ M oligonucleotide. Media were changed and the oligonucleotide replenished on day 5 post transfection. Cells were harvested for RNA 7-8 days after transfection.

7.4.3 HEK293 and eGFP-HEK293 cells

HEK293 and EGFP-expressing HEK293 cells were maintained in DMEM supplemented with 10% FBS, 1x Pen/Strep, and 20 moles L-glutamine. Additionally, the EGFP-expressing HEK293 cells were supplemented with hygromycin. All cells were maintained at 37°C and 5% CO_2 . Cells were seeded either 250k cells/ well (HEK293) or 300k cells/well (eGFP-HEK293) 24 hours prior to transfection (forward transfection) or day of transfection (reverse transfection), unless otherwise stated. Oligonucleotides were transfected at 50nM concentration for single dose or decreasing doses for dose responses. Cells were transfected using RNAiMAX (Life Technologies) using 0.75 μ L lipid per 1 μ L of oligonucleotide in OptiMEM (Life Technologies). Cells were harvested for RNA analysis 3 days after transfection.

7.4.4 RNA harvest and quantitative real-time PCR (qRT-PCR)

Total RNA from cells was harvested 3 days post transfection unless otherwise stated. After washing each well with 1mL PBS, 1mL of RiboZol (Amresco) was added to each well, incubated for 2 min at room temperature and transferred to 1.5-mL microcentrifuge tube. Chloroform (200µL) was added to each tube and the mixture was shaken vigorously for 1 minute then incubated at room temperature for 10 minutes. The mixture was centrifuged at 13,000 rpm for 20 min then the clear aqueous layer was transferred to a new 1.5-mL tube, avoiding any cloudy interphase. 600µL of 2-propanol was added to the aqueous layer followed by a 1 minute vigorous shake then a 20 minute incubation at -20°C followed by a 15 minute centrifugation at 14k rpm. The resulting pellet was washed with ice cold 70% ethanol, re-centrifuged at 8000 rpm for 10 minutes, and then briefly allowed to air dry. The pellet was resuspended in RNase-free water, heated to 55°C for 5 min, then was quantitated by UV spectroscopy.

1 μ g of RNA (MRC-5) or 2 μ g (MCF-7, HEK293, EGFP-HEK293) was treated with 2 units of DNase I (Worthington Biochemical Corporation) for 10 min at 37°C followed by 10 min at 75°C. RNA was reverse transcribed using a High Capacity cDNA Reverse Transcription Kit (Life Technologies) per manufacturer's protocol.

qRT-PCR was performed using iTaq Supermix (BioRad) on a BioRad CFX96 real time system. Data were normalized relative to levels of GAPDH mRNA. **ADAM33**: forward primer, 5'-GGCCTCTGCAAACAACATAATT-3'; reverse primer, 5'-GGGCTCAGGAACCACCTAGG-3'; probe, 5'-CTTCCTGTTTCTTCCCACCCTGTCTTCTCT-3'. **PR**: forward primer, 5'-CTTACCTGTGGGAGCTGTA-3'; reverse primer, 5'-GCACTTTCTAAGGCGACATG-3'; **SIN3A**: forward primer, 5'-GCACAGAAACCAGTATTTCTCCC-3'; reverse primer, 5'-GGTCTTCTTGCTGTTTCCTTCC-3'; **egfp**: forward primer: 5'-GAGCGCACCATCTTCTTCAA-3'; reverse primer, 5'-TCCTTGAAGTCGATGCCCTT-3'; **GAPDH** primer/probe assay (IDT); forward primer, 5'-TGGTCCAGGGGTCTTACT; reverse primer, 5'-CCTCAACGACCACCTTTGT; probe, 5'-CTCATTTCCTGGTATGACAACGAATTTGGC-3'.

Experiments were performed in duplicate technical replicates, and error is reported as standard deviation of biological replicates unless otherwise stated. The qRT-PCR cycle is as follows: **ADAM33**: 95°C for 7 minutes; (95°C for 15 seconds; 60°C for 30 seconds) x 40 cycles. **EGFP, SIN3A, PR**: 50°C for 2 minutes; 95°C for 7 minutes; (95°C for 15 seconds, 50°C for 30 seconds, 72°C for 45 seconds) x 40 cycles.

7.4.5 Thermal denaturation by UV Melt analysis

Thermal denaturation analysis of duplex siRNAs or ss-siRNA:RNA duplexes was carried out using a CARY 100 UV–Vis spectrophotometer. Absorbance was monitored at 260 nm in a 1 cm quartz cuvette. siRNA (1 μ M) or ss-siRNA annealed to complementary RNA (1 μ M) in 10 mM Tris-HCl (Sigma) and 40 mM NaCl (Sigma) was annealed and melted three times from 15 to 95°C at a ramp rate of 1 °C/min. The T_m values were calculated using the integrated Cary software as the first derivative of the melt curve.

7.4.6 Fluorescence microscopy for detection of GFP

Detection of EGFP was carried out using a Nikon eclipse T_i-S compound microscope equipped with a Nikon D5100 digital camera. Images were captured at 40x magnification using Cool LED pE excitation system at a 470 nm wavelength filter.

7.5 Cloning experiments

7.5.1 Luria broth media

6.25 g LB broth powder (Fisher) was dissolved in 250 mL diH $_2$ O and autoclaved for 20 minutes at 121°C.

7.5.2 LB Agar plates

10 g of LB agar powder (Fisher) was dissolved in 250 mL diH₂O and autoclaved for 20 minutes at 121°C. 20 mg/mL Ampicillin was added when solution was cooled to 50°C. The mixture was poured into sterilized petri dishes and allowed to dry at 37°C prior to use.

7.5.3 SOC media

50 mL of LB media supplemented with 500 μ L of 2 M MgSO₄, 20% (w/v) glucose solution, and 500 μ L of 1M MgCl₂. Solution was mixed by inversion, sterile filtered, and aliquoted before storage at 4°C.

7.5.4 Plasmid purification

Single colonies were selected from agar plates and shaken overnight at 37°C in 10 mL of LB agar with Ampicillin. The culture was centrifuged at 3500 RPM for 5 minutes at 4°C. Plasmids were purified using Gene Jet mini-prep kit (Fisher) as per manufacturer's instructions.

7.5.5 Transformation

Plasmid px42229 (Addgene) was transformed into DH5 alpha cells. 100 μ L cell aliquots were defrosted on ice for 15 min. 5 μ L of purified plasmid and ligation mix was added to cell aliquots. Cells were gently mixed and left on ice for 30 minutes. Cells were heat shocked at 42°C for 40s before an ice recovery for 2 min. Cells were added to 895 μ L warm SOC (37°C) media and incubated with agitation for 1 hr. 10-100% of each SOC recovery mixture was plated on antibiotic agar plates and incubated overnight at 37°C.

7.5.6 Colony PCR

 $6.25~\mu L$ of molecular biology H₂O (ABI), 2 μL Go Taq polymerase buffer 5x (Promega), 1 μL dNTPs from 10 mM stock(Promega), 0.25 μL each forward (5' ACA TGT GAG GGC CTA TTT CC) and reverse primer (5' CTT CTC GAA GAC CCG TTT TG) (IDT) from 10 nM stock, 0.05 μL GoTaq DNA polymerase, 5 unit/ μL (Promega) was added to each single bacterial colony. PCR cycle: 6 min 95°C, 94°C for 60s, 55°C for 60s, 72°C for 30 sec (repeat from step 2 34x), 72°C for 10 min, 4°C forever.

7.5.7 Agarose gel

Agarose gels of 0.8%-1% (w/v) in 1x TAE buffer (unless otherwise stated) were prepared containing 4 μ L of Nancy-520 (Sigma). Electrophoresis was carried out in 1x TAE buffer at 100V for 30-90 minutes and visualized under UV light.

7.5.8 DNA sequencing

Sequencing was performed by MWG Eurofins (Germany) as per kit instructions using primers listed in section 7.5.6.

7.6 CRISPR/Cas experiments

7.6.1 DNA amplification

1 μL gBlock DNA at 10 ng/ μL stock (IDT) was mixed with 1 μL of 10 mM dNTPs, 2.5 μL of 10 μM forward (5' GAG GAG CTG TTC ACC GGG)and reverse primers (5' CGT CCA TGC CGA GAG TGA T), Q5 5x reaction buffer (NEB), Q5 polymerase 0.05 μL (NEB), and 32.5 μL RNase-free H_2).

PCR cycle was 98°C for 30s, 98°C for 10s, 52°C for 10s, 72°C for 20 sec, repeat to step 2 29x, 72°C for 2 min, 4°C forever.

7.6.2 PCR cleanup

A PCR GeneJet purification kit (Fisher) was used as per manufacturer's instructions. DNA was quantified on a NanoDrop spectrophotometer.

7.6.3 DNA cleavage assay

0.1 μ M crRNAs (made in house),0.1 μ M trRNA (Dharmacon), 100 nM Cas9 nuclease (NEB), 2 μ L 10x Cas9 nuclease buffer (NEB were made up to 20 μ L total volume with RNase-free water. The mixture was incubated at 37°C for 1 hour before 0.2 μ g of DNA was added. The complete mixture was incubated a further 2 hrs at 37°C. A 5x SDS solution of 30% glycerol, 1.2% SDS, and 250 mM EDTA was added to the mixture unless otherwise stated. A 1.0% agarose gel was run as described in 7.5.7.

References

- 1. Dahm, R. (2008) Discovering DNA: Friedrich Miescher and the early years of nucleic acid research, *Hum. Genet.* 122, 565-581.
- 2. Watson, J. D., and Crick, F. H. C. (1953) Molecular Structure of Nucleic Acids: A Structure for Deoxyribonucleic Acids, *Nature 171*, 737-738.
- 3. Kirk, J. T. O. (1967) Determination of the base composition of deoxyribonucleic acid by measurement of the adenine/guanine ratio, *Biochem. J.* 105, 673-677.
- 4. Yakovchuk, P., Protozanova, E., and Frank-Kamenetskii, M. D. (2006) Base-stacking and base-pairing contributions into thermal stability of the DNA double helix, *Nucleic Acids Res.* 34, 564-574.
- 5. Yang, X., Molimau, S., Doherty, G. P., Johnston, E. B., Marles-Wright, J., Rothnagel, R., Hankamer, B., Lewis, R. J., and Lewis, P. J. (2009) The structure of bacterial RNA polymerase in complex with the essential transcription elongation factor NusA, *Embo Reports* 10, 997-1002.
- 6. Cook, D., and Slater, R. (1993) Eukaryotic Nuclear RNA Polymerases (EC 2.7.7.6), in *Enzymes of Molecular Biology* (Burrell, M., Ed.), pp 59-72, Humana Press.
- 7. Kornberg, R. D. (1999) Eukaryotic transcriptional control, *Trends Biochem. Sci. 24*, M46-M49.
- 8. Cramer, P., Armache, K. J., Baumli, S., Benkert, S., Brueckner, E., Buchen, C., Damsma, G. E., Dengl, S., Geiger, S. R., Jaslak, A. J., Jawhari, A., Jennebach, S., Kamenski, T., Kettenberger, H., Kuhn, C. D., Lehmann, E., Leike, K., Sydow, J. E., and Vannini, A. (2008) Structure of eukaryotic RNA polymerases, in *Annual Review of Biophysics*, pp 337-352.
- 9. Buratowski, S., Hahn, S., Guarente, L., and Sharp, P. A. (1989) Five intermediate complexes in transcription initiation by RNA polymerase II, *Cell* 56, 549-561.
- 10. Weil, P. A., Luse, D. S., Segall, J., and Roeder, R. G. (1979) Selective and accurate initiation of transcription at the Ad2 major late promotor in a soluble system dependent on purified RNA polymerase II and DNA, *Cell* 18, 469-484.
- 11. Hurwitz, J., Furth, J. J., Anders, M., Ortiz, P. J., and August, J. T. (1961) The enzymatic incorporation of ribonucleotides into RNA and the role of DNA, *Cold Spring Harb. Symp. Quant. Biol.* 26, 91-100.
- 12. Dieci, G., Fiorino, G., Castelnuovo, M., Teichmann, M., and Pagano, A. (2007) The expanding RNA polymerase III transcriptome, *Trends Genet. 23*, 614-622.
- 13. Wahl, M. C., Will, C. L., and Luehrmann, R. (2009) The Spliceosome: Design Principles of a Dynamic RNP Machine, *Cell* 136, 701-718.
- 14. Cho, E. J., Takagi, T., Moore, C. R., and Buratowski, S. (1997) mRNA capping enzyme is recruited to the transcription complex by phosphorylation of the RNA polymerase II carboxy-terminal domain, *Genes Dev.* 11, 3319-3326.
- 15. Fabrega, C., Shen, V., Shuman, S., and Lima, C. D. (2003) Structure of an mRNA capping enzyme bound to the phosphorylated carboxy-terminal domain of RNA polymerase II, *Mol. Cell* 11, 1549-1561.

References

- 16. Ho, C. K., Lehman, K., and Shuman, S. (1999) An essential surface motif (WAQKW) of yeast RNA triphosphatase mediates formation of the mRNA capping enzyme complex with RNA guanylyltransferase, *Nucleic Acids Res. 27*, 4671-4678.
- 17. Shatkin, A. J. (1976) Capping of eukaryotic messenger-RNAs *Cell 9*, 645-653.
- 18. Edmonds, M., Vaughan, M. H., and Nakazato, H. (1971) Polyadenylic acid sequences in heterogeneous nuclear RNA and rapidly-labeled polyribosomal RNA of Hela cells-possible evidence for a precursor relationship (messenger RNA/poly(dT) cellulose, *Proc. Natl. Acad. Sci. U. S. A. 68*, 1336-&.
- 19. Sarkar, N. (1997) Polyadenylation of mRNA in prokaryotes, in *Annu. Rev. Biochem.* (Richardson, C. C., Ed.), pp 173-197.
- 20. Guhaniyogi, J., and Brewer, G. (2001) Regulation of mRNA stability in mammalian cells, *Gene 265*, 11-23.
- 21. Merkel, C. G., Wood, T. G., and Lingrel, J. B. (1976) Shortening of the poly(A) region of mouse globin messenger RNA, *J. Biol. Chem. 251*, 5512-5515.
- 22. Grabowski, P. J., and Black, D. L. (2001) Alternative RNA splicing in the nervous system, *Prog. Neurobiol. 65*, 289-308.
- 23. Fica, S. M., Tuttle, N., Novak, T., Li, N.-S., Lu, J., Koodathingal, P., Dai, Q., Staley, J. P., and Piccirilli, J. A. (2013) RNA catalyses nuclear pre-mRNA splicing, *Nature 503*, 229-234.
- 24. Tennyson, C. N., Klamut, H. J., and Worton, R. G. (1995) The human dystrophin gene requires 16 hours to be transcribed and is cotranscriptionally spliced, *Nat. Genet. 9*, 184-190.
- 25. Gilbert, W. (1978) Why genes in pieces, *Nature 271*, 501-501.
- 26. Black, D. L. (2003) Mechanisms of alternative pre-messenger RNA splicing, in *Annual Review of Biochemistry. Volume 72* (Richardson, C. C., Ed.), pp 291-336.
- 27. Graveley, B. R. (2001) Alternative splicing: increasing diversity in the proteomic world, *Trends Genet. 17*, 100-107.
- 28. Black, D. L. (2000) Protein diversity from alternative splicing: A challenge for bioinformatics and post-genome biology, *Cell 103*, 367-370.
- 29. Modrek, B., and Lee, C. (2002) A genomic view of alternative splicing, *Nat. Genet. 30*, 13-19.
- 30. Early, P., Rogers, J., Davis, M., Calame, K., Bond, M., Wall, R., and Hood, L. (1980) 2 messenger-RNAs can be produced from a single immonoglobulin-mu gene by alternative RNA processing pathways, *Cell* 20, 313-319.
- 31. Lopez-Bigas, N., Audit, B., Ouzounis, C., Parra, G., and Guigo, R. (2005) Are splicing mutations the most frequent cause of hereditary disease?, *FEBS Lett.* 579, 1900-1903.
- 32. Lim, K. H., Ferraris, L., Filloux, M. E., Raphael, B. J., and Fairbrother, W. G. (2011) Using positional distribution to identify splicing elements and predict pre-mRNA processing defects in human genes, *Proc. Natl. Acad. Sci. U. S. A. 108*, 11093-11098.
- 33. Ward, A. J., and Cooper, T. A. (2010) The pathobiology of splicing, J. Pathol. 220, 152-163.

- 34. Skotheim, R. I., and Nees, M. (2007) Alternative splicing in cancer: Noise, functional, or systematic?, *Int. J. Biochem. Cell Biol.* 39, 1432-1449.
- 35. Kohler, A., and Hurt, E. (2007) Exporting RNA from the nucleus to the cytoplasm, *Nat. Rev. Mol. Cell Biol. 8*, 761-773.
- 36. Mattick, J. S., Dinger, M. E., Mercer, T. R., and Mehler, M. F. (2009) RNA regulation of epigenetic processes, *BioEssays 31*, 51-59.
- 37. Bennett, F. C. (2002) Efficiency of Antisense Oligonucleotide Drug Discovery, *Antisense Nucleic Acid Drug Dev.* 12, 215–224.
- 38. Myers, S., and Baker, A. (2001) Drug discovery--an operating model for a new era, *Nat. Biotechnol.* 19, 727-730.
- 39. Janowski, B. A., Younger, S. T., Hardy, D. B., Ram, R., Huffman, K. E., and Corey, D. R. (2007) Activating gene expression in mammalian cells with promoter-targeted duplex RNAs, *Nat. Chem. Biol.* 3, 166-173.
- 40. Li, L.-C., Okino, S. T., Zhao, H., Pookot, D., Place, R. F., Urakami, S., Enokida, H., and Dahiya, R. (2006) Small dsRNAs induce transcriptional activation in human cells, *Proc. Natl. Acad. Sci. U. S. A.* 103, 17337-17342.
- 41. Matsui, M., Sakurai, F., Elbashir, S., Foster, D. J., Manoharan, M., and Corey, D. R. (2010) Activation of LDL Receptor Expression by Small RNAs Complementary to a Noncoding Transcript that Overlaps the LDLR Promoter, *Chem. Biol.* 17, 1344-1355.
- 42. Zamecnik, P. C., and Stephenson, M. L. (1978) Inhibition of Rous-sarcoma virus-Replication and cell transformation by a specific oligodeoxynucleotide, *Proc. Natl. Acad. Sci. U. S. A. 75*, 280-284.
- 43. Mulamba, G. B., Hu, André, Azad, Raana F., Anderson, Kevin P., Coen, Donald M. (1998) Human Cytomegalovirus Mutant with Sequence-Dependent Resistance to the Phosphorothioate Oligonucleotide Romivirsen (ISIS 2922), *Antimicrob Agents Chemother* 42, 971-973.
- 44. Merki, E., Graham, M. J., Mullick, A. E., Miller, E. R., Crooke, R. M., Pitas, R. E., Witztum, J. L., and Tsimikas, S. (2008) Antisense Oligonucleotide Directed to Human Apolipoprotein B-100 Reduces Lipoprotein(a) Levels and Oxidized Phospholipids on Human Apolipoprotein B-100 Particles in Lipoprotein(a) Transgenic Mice, Circulation 18, 743-753.
- 45. Sharma, V. K., Sharma, R. K., and Singh, S. K. (2014) Antisense oligonucleotides: modifications and clinical trials, *Medchemcomm 5*, 1454-1471.
- 46. Watts, J. K., and Corey, D. R. (2012) Silencing disease genes in the laboratory and the clinic, *J. Pathol. 226*, 365-379.
- 47. Phillips, M. I. (1996) Methods in Molecular Medicine: Antisense therapeutics.
- Venter, J. C., Adams, M. D., Myers, E. W., Li, P. W., Mural, R. J., Sutton, G. G., Smith, H. O., Yandell, M., Evans, C. A., Holt, R. A., Gocayne, J. D., Amanatides, P., Ballew, R. M., Huson, D. H., Wortman, J. R., Zhang, Q., Kodira, C. D., Zheng, X. H., Chen, L., Skupski, M., Subramanian, G., Thomas, P. D., Zhang, J., Gabor Miklos, G. L., Nelson, C., Broder, S., Clark, A. G., Nadeau, J., McKusick, V. A., Zinder, N., Levine, A. J., Roberts, R. J., Simon, M., Slayman, C., Hunkapiller, M., Bolanos, R., Delcher, A., Dew, I., Fasulo, D., Flanigan, M., Florea, L., Halpern, A., Hannenhalli, S., Kravitz, S., Levy, S., Mobarry, C., Reinert, K., Remington, K., Abu-Threideh, J., Beasley, E., Biddick, K., Bonazzi, V., Brandon, R., Cargill,

M., Chandramouliswaran, I., Charlab, R., Chaturvedi, K., Deng, Z., Di Francesco, V., Dunn, P., Eilbeck, K., Evangelista, C., Gabrielian, A. E., Gan, W., Ge, W., Gong, F., Gu, Z., Guan, P., Heiman, T. J., Higgins, M. E., Ji, R. R., Ke, Z., Ketchum, K. A., Lai, Z., Lei, Y., Li, Z., Li, J., Liang, Y., Lin, X., Lu, F., Merkulov, G. V., Milshina, N., Moore, H. M., Naik, A. K., Narayan, V. A., Neelam, B., Nusskern, D., Rusch, D. B., Salzberg, S., Shao, W., Shue, B., Sun, J., Wang, Z., Wang, A., Wang, X., Wang, J., Wei, M., Wides, R., Xiao, C., Yan, C., Yao, A., Ye, J., Zhan, M., Zhang, W., Zhang, H., Zhao, Q., Zheng, L., Zhong, F., Zhong, W., Zhu, S., Zhao, S., Gilbert, D., Baumhueter, S., Spier, G., Carter, C., Cravchik, A., Woodage, T., Ali, F., An, H., Awe, A., Baldwin, D., Baden, H., Barnstead, M., Barrow, I., Beeson, K., Busam, D., Carver, A., Center, A., Cheng, M. L., Curry, L., Danaher, S., Davenport, L., Desilets, R., Dietz, S., Dodson, K., Doup, L., Ferriera, S., Garg, N., Gluecksmann, A., Hart, B., Haynes, J., Haynes, C., Heiner, C., Hladun, S., Hostin, D., Houck, J., Howland, T., Ibegwam, C., Johnson, J., Kalush, F., Kline, L., Koduru, S., Love, A., Mann, F., May, D., McCawley, S., McIntosh, T., McMullen, I., Moy, M., Moy, L., Murphy, B., Nelson, K., Pfannkoch, C., Pratts, E., Puri, V., Qureshi, H., Reardon, M., Rodriguez, R., Rogers, Y. H., Romblad, D., Ruhfel, B., Scott, R., Sitter, C., Smallwood, M., Stewart, E., Strong, R., Suh, E., Thomas, R., Tint, N. N., Tse, S., Vech, C., Wang, G., Wetter, J., Williams, S., Williams, M., Windsor, S., Winn-Deen, E., Wolfe, K., Zaveri, J., Zaveri, K., Abril, J. F., Guigo, R., Campbell, M. J., Sjolander, K. V., Karlak, B., Kejariwal, A., Mi, H., Lazareva, B., Hatton, T., Narechania, A., Diemer, K., Muruganujan, A., Guo, N., Sato, S., Bafna, V., Istrail, S., Lippert, R., Schwartz, R., Walenz, B., Yooseph, S., Allen, D., Basu, A., Baxendale, J., Blick, L., Caminha, M., Carnes-Stine, J., Caulk, P., Chiang, Y. H., Coyne, M., Dahlke, C., Mays, A., Dombroski, M., Donnelly, M., Ely, D., Esparham, S., Fosler, C., Gire, H., Glanowski, S., Glasser, K., Glodek, A., Gorokhov, M., Graham, K., Gropman, B., Harris, M., Heil, J., Henderson, S., Hoover, J., Jennings, D., Jordan, C., Jordan, J., Kasha, J., Kagan, L., Kraft, C., Levitsky, A., Lewis, M., Liu, X., Lopez, J., Ma, D., Majoros, W., McDaniel, J., Murphy, S., Newman, M., Nguyen, T., Nguyen, N., Nodell, M., Pan, S., Peck, J., Peterson, M., Rowe, W., Sanders, R., Scott, J., Simpson, M., Smith, T., Sprague, A., Stockwell, T., Turner, R., Venter, E., Wang, M., Wen, M., Wu, D., Wu, M., Xia, A., Zandieh, A., and Zhu, X. (2001) The sequence of the human genome, Science 291, 1304-1351.

- 49. Dias, N., and Stein, C. A. (2002) Antisense oligonucleotides: Basic concepts and mechanisms, *Mol. Cancer Ther.* 1, 347-355.
- 50. Krutzfeldt, J., Rajewsky, N., Braich, R., Rajeev, K. G., Tuschl, T., Manoharan, M., and Stoffel, M. (2005) Silencing of microRNAs in vivo with 'antagomirs', *Nature 438*, 685-689.
- 51. Hutvágner, G., Simard, M. J., Mello, C. C., and Zamore, P. D. (2004) Sequence-Specific Inhibition of Small RNA Function, *PLoS Biol. 2*, e98.
- 52. Davis, S., Lollo, B., Freier, S., and Esau, C. (2006) Improved targeting of miRNA with antisense oligonucleotides, *Nucleic Acids Res.* 34, 2294-2304.
- 53. Esau, C., Davis, S., Murray, S. F., Yu, X. X., Pandey, S. K., Pear, M., Watts, L., Booten, S. L., Graham, M., McKay, R., Subramaniam, A., Propp, S., Lollo, B. A., Freier, S., Bennett, C. F., Bhanot, S., and Monia, B. P. (2006) miR-122 regulation of lipid metabolism revealed by in vivo antisense targeting, *Cell Metab. 3*, 87-98.
- 54. Elmen, J., Lindow, M., Schutz, S., Lawrence, M., Petri, A., Obad, S., Lindholm, M., Hedtjarn, M., Hansen, H. F., Berger, U., Gullans, S., Kearney, P., Sarnow, P., Straarup, E. M., and Kauppinen, S. (2008) LNA-mediated microRNA silencing in non-human primates, *Nature* 452, 896-899.

- 55. Khoo, B., Roca, X., Chew, S. L., and Krainer, A. R. (2007) Antisense oligonucleotide-induced alternative splicing of the APOB mRNA generates a novel isoform of APOB, *BMC Mol. Biol.* 8.
- 56. Peacey, E., Rodriguez, L., Liu, Y., and Wolfe, M. S. (2012) Targeting a pre-mRNA structure with bipartite antisense molecules modulates tau alternative splicing, *Nucleic Acids Res.*
- 57. Walder, R. Y., and Walder, J. A. (1988) Role of RNase-H in hybrid-arrested translation by antisense oligonucleotides, *Proc. Natl. Acad. Sci. U. S. A. 85*, 5011-5015.
- 58. Stein, H., and Hausen, P. (1969) Enzyme from calf thymus degrading the RNA moiety of DNA RNA hybrids effect on DNA dependent RNA polymerase, *Science (Washington D C)* 166, 393-395.
- 59. Wu, H. J., Lima, W. F., Zhang, H., Fan, A., Sun, H., and Crooke, S. T. (2004) Determination of the role of the human RNase H1 in the pharmacology of DNA-like antisense drugs, *J. Biol. Chem. 279*, 17181-17189.
- 60. Behlke, M. (2014) oral presentation at the 10th Annual Meeting of the Oligonucleotide Therapeutics Society, San Diego, USA, October 2014.
- 61. Poongavanam, V., Narayana Moorthy, N. S. H., and Kongsted, J. (2014) Dual mechanism of HIV-1 integrase and RNase H inhibition by diketo derivatives a computational study, *RSC Advances 4*, 38672-38681.
- 62. Fire, A., Xu, S., Montgomery, M. K., Kostas, S. A., Driver, S. E., and Mello, C. C. (1998) Potent and specific genetic interference by double-stranded RNA in Caenorhabditis elegans, *Nature 391*, 806-811.
- 63. Corey, D. R. (2007) Chemical modification: the key to clinical application of RNA interference? , *J Clin Invest 17*, 3615-3622.
- 64. Wilson, R. C., and Doudna, J. A. (2013) Molecular Mechanisms of RNA Interference *Annu. Rev. Biophys.* 42, 217-239.
- 65. Meister, G., and Tuschl, T. (2004) Mechanisms of gene silencing by double-stranded RNA, *Nature 431*, 343-349.
- 66. Cenik, E. S., and Zamore, P. D. (2011) Argonaute proteins, Curr. Biol. 21, R446-R449.
- 67. Hu, J. X., Liu, J., and Corey, D. R. (2010) Allele-Selective Inhibition of Huntingtin Expression by Switching to an miRNA-like RNAi Mechanism, *Chem. Biol.* 17, 1183-1188.
- 68. Filipowicz, W. (2005) RNAi: The Nuts and Bolts, *Cell* 122, 17-20.
- 69. Kretschmer-Kazemi Far, R., and Sczakiel, G. (2003) The activity of siRNA in mammalian cells is related to structural target accessibility: a comparison with antisense oligonucleotides, *Nucleic Acids Res.* 31, 4417-4424.
- 70. Kini, H. K., and Walton, S. P. (2007) In vitro binding of single-stranded RNA by human Dicer., *FEBS Lett.* 581, 5611-5616.
- 71. Holen, T., Amarzguioui, M., Babaie, E., and Prydz, H. (2003) Similar behaviour of single-strand and double-strand siRNAs suggests they act through a common RNAi pathway, *Nucleic Acids Res.* 31, 2401-2407.
- 72. Martinez, J., Patkaniowska, A., Urlaub, H., Luhrmann, R., and Tuschl, T. (2002) Single-stranded antisense siRNAs guide target RNA cleavage in RNAi, *Cell* 110, 563-574.

- 73. Yu, D., Pendergraff, H., Liu, J., Kordasiewicz, H., Cleveland, D., Swayze, E., Lima, W., Crooke, S., Prakash, T., and Corey, D. (2012) Single-standed RNAs use RNAi to potently and allele-selectively inhibit mutant huntingtin expression, *Cell* 150, 895-908.
- 74. Lima, W. F., Prakash, T. P., Murray, H. M., Kinberger, G. A., Li, W. Y., Chappell, A. E., Li, C. S., Murray, S. F., Gaus, H., Seth, P. P., Swayze, E. E., and Crooke, S. T. (2012) Single-Stranded siRNAs Activate RNAi in Animals, *Cell* 150, 883-894.
- 75. Elbashir, S. M., Harborth, J., Lendeckel, W., Yalcin, A., Weber, K., and Tuschl, T. (2001) Duplexes of 21-nucleotide RNAs mediate RNA interference in cultured mammalian cells., *Nature 411*, 494-498.
- 76. Allerson, C. R., Sioufi, N., Jarres, R., Prakash, T. P., [...], and Bhat, B. (2005) Fully 2'-modified oligonucleotide duplexes with improved in vitro potency and stability compared to unmodified small interfering RNA., *J. Med. Chem.* 48, 901-904.
- 77. Eckstein, F. (2000) Phosphorothioate oligodeoxynucleotides: What is their origin and what is unique about them?, *Antisense Nucleic Acid Drug Dev. 10*, 117-121.
- 78. Eckstein, F. (1966) Nucleoside Phosphorothioates J. Am. Chem. Soc. 88, 4292-4294.
- 79. Eckstein, F., and Sternbach, H. (1967) Nucleoside 5'-O-phosphorothioates as inhibitors for phosphatases, *Biochim. Biophys. Acta* 146, 618-619.
- 80. Geary, R. S., Yu, R. Z., and Levin, A. A. (2001) Pharmacokinetics of phosphorothioate antisense oligodeoxynucleotides, *Curr opin Investig Drugs 2*, 562-573.
- 81. Vickers, T. A., Koo, S., Bennett, C. F., Crooke, S. T., Dean, N. M., and Baker, B. F. (2003) Efficient reduction of target RNAs by small interfering RNA and RNase H-dependent antisense agents A comparative analysis, *J. Biol. Chem. 278*, 7108-7118.
- 82. Stein, C. A., Subasinghe, C., Shinozuka, K., and Cohen, J. S. (1988) Physiochemical properties of phosphorothioate oligodeoxynucleotides, *Nucleic Acids Res.* 16, 3209-3221.
- 83. Prakash, T. P. (2011) An Overview of Sugar-Modified Oligonucleotides for Antisense Therapeutics, *Chem. Biodivers.* 8, 1616-1641.
- 84. Freier, S. M., and Altmann, K. H. (1997) The ups and downs of nucleic acid duplex stability: structure-stability studies on chemically-modified DNA:RNA duplexes, *Nucleic Acids Res.* 25, 4429-4443.
- 85. Majlessi, M., Nelson, N. C., and Becker, M. M. (1998) Advantages of 2 '-O-methyl oligoribonucleotide probes for detecting RNA targets, *Nucleic Acids Res. 26*, 2224-2229.
- 86. Robbins, M., Judge, A., Liang, L., McClintock, K., Yaworski, E., and MacLachlan, I. (2007) 2[prime]-O-methyl-modified RNAs Act as TLR7 Antagonists, *Mol. Ther.* 15, 1663-1669.
- 87. Teplova, M., Minasov, G., Tereshko, V., Inamati, G. B., Cook, P. D., Manoharan, M., and Egli, M. (1999) Crystal structure and improved antisense properties of 2 '-O-(2-methoxyethyl)-RNA, *Nat. Struct. Mol. Biol. 6*, 535-539.
- 88. Singh, S. K., Nielsen, P., Koshkina, A. A., and Wengel, J. (1998) LNA (locked nucleic acids): synthesis and high-affinity nucleic acid recognition, *Chem. Commun*, 455-456.
- 89. Obika, S., Nanbu, D., Hari, Y., Morio, M.-i., In, Y., Ishida, T., and Imanishi, T. (1997) Synthesis of 2'O, 4'-C-Methyleneuridine and- cytidine. Novel Bicyclic Nucleosides Having a Fixed C3- endo Sugar Puckering, *Tetrahedron Lett. 38*, 8735-8738.

- 90. Kauppinene, S., Vester, B., and Wengel, J. (2005) Locked nucleic acid (LNA): High affinity targeting of RNA for diagnostics and therapeutics., *Drug Discov Today: Technologies 2*, 287-290.
- 91. Vester, B., and Wengel, J. (2004) LNA (Locked nucleic acid): High-affinity targeting of complementary RNA and DNA, *Biochemistry 43*, 13233-13241.
- 92. Seth, P. P., Siwkowski, A., Allerson, C. R., Vasquez, G., Lee, S., Prakash, T. P., Kinberger, G., Migawa, M. T., Gaus, H., Bhat, B., and Swayze, E. E. (2008) Design, synthesis and evaluation of constrained methoxyethyl (cMOE) and constrained ethyl (cEt) nucleoside analogs, *Nucleic acids symposium series* (2004), 553-554.
- 93. Kurreck, J., Wyszko, E., Gillen, C., and Erdmann, V. A. (2002) Design of antisense oligonucleotides stabilized by locked nucleic acids, *Nucleic Acids Res. 30*, 1911-1918.
- 94. Seitz, O. (1999) Chemically Modified Antisense Oligonucleotides-Recent Improvements of RNA Binding and Ribonuclease H Recruitment, *Angew. Chem. Int. Ed 38*, 3466-3469.
- 95. Monia, B. P., Lesnik, E. A., Gonzalez, C., Lima, W. F., McGee, D., Guinosso, C. J., Kawasaki, A. M., Cook, P. D., and Freier, S. M. (1993) Evaluation of 2'-modified oligonucleotides containing 2'-deoxy gaps as antisense inhibitors of gene expression, *J. Biol. Chem. 268*, 14514-14522.
- 96. Madani, F., Lindberg, S., Langel, Ü., Futaki, S., and Gräslund, A. (2011) Mechanisms of Cellular Uptake of Cell-Penetrating Peptides, *Journal of Biophysics 2011 (2011)*, 1-10.
- 97. Akhtar, S., Basu, S., Wickstrom, E., and Juliano, R. L. (1991) Interactions of Antisense DNA Oligonucleotide Analogs with Phospholipid-Membranes (Liposomes), *Nucleic Acids Res.* 19, 5551-5559.
- 98. Nakai, D., Seita, T., Terasaki, T., Iwasa, S., Shoji, Y., Mizushima, Y., and Sugiyama, Y. (1996) Cellular uptake mechanism for oligonucleotides: Involvement of endocytosis in the uptake of phosphodiester oligonucleotides by a human colorectal adenocarcinoma cell line, HCT-15, J. Pharmacol. Exp. Ther. 278, 1362-1372.
- 99. Macklon, A. E., and Higinbotham, N. (1970) Active and passive transport of potassium in cells of excised pea epicotyls, *Plant Physiol.* 45, 133-138.
- 100. Kell, D. B., Dobson, P. D., Bilsland, E., and Oliver, S. G. (2013) The promiscuous binding of pharmaceutical drugs and their transporter-mediated uptake into cells: what we (need to) know and how we can do so, *Drug Discov. Today 18*, 218-239.
- 101. Xiao, G., and Gan, L.-S. (2013) Receptor-Mediated Endocytosis and Brain Delivery of Therapeutic Biologics, *Int. J. Cell Biol. 2013*, 14.
- 102. Pavelka, M., and Roth, J. (2010) Fluid-Phase Endocytosis and Phagocytosis, in *Functional Ultrastructure*, pp 104-105, Springer Vienna.
- 103. Juliano, R. L., Ming, X., and Nakagawa, O. (2012) Cellular Uptake and Intracellular Trafficking of Antisense and siRNA Oligonucleotides, *Bioconj. Chem. 23*, 147-157.
- 104. Beltinger, C., Saragovi, H. U., Smith, R. M., LeSauteur, L., Shah, N., DeDionisio, L., Christensen, L., Raible, A., Jarett, L., and Gewirtz, A. M. (1995) Binding, uptake, and intracellular trafficking of phosphorothioate-modified oligodeoxynucleotides, *J Clin Invest* 95, 1814-1823.

- 105. Khalil, I. A., Kogure, K., Akita, H., and Harashima, H. (2006) Uptake pathways and subsequent intracellular trafficking in nonviral gene delivery, *Pharmacol. Rev.* 58, 32-45.
- 106. Stein, C. A., Hansen, J. B., Lai, J., Wu, S., Voskresenskiy, A., Hog, A., Worm, J., Hedtjarn, M., Souleimanian, N., Miller, P., Soifer, H. S., Castanotto, D., Benimetskaya, L., Orum, H., and Koch, T. (2010) Efficient gene silencing by delivery of locked nucleic acid antisense oligonucleotides, unassisted by transfection reagents, *Nucleic Acids Res. 38*.
- 107. Stein, C. A. (1997) Controversies in the cellular pharmacology of oligodeoxynucleotides, *Ciba Found. Symp. 209*, 79-89; discussion 89-93.
- 108. Castanotto, D., Lin, M., Kowolik, C., Wang, L., Ren, X. Q., Soifer, H. S., Koch, T., Hansen, B. R., Oerum, H., Armstrong, B., Wang, Z., Bauer, P., Rossi, J., and Stein, C. A. (2015) A cytoplasmic pathway for gapmer antisense oligonucleotide-mediated gene silencing in mammalian cells, *Nucleic Acids Res.* 43, 9350-9361.
- 109. Zhang, Y., Qu, Z., Kim, S., Shi, V., Liao, B., Kraft, P., Bandaru, R., Wu, Y., Greenberger, L. M., and Horak, I. D. (2011) Down-modulation of cancer targets using locked nucleic acid (LNA)-based antisense oligonucleotides without transfection, *Gene Ther.* 18, 326-333.
- 110. Nakamori, M., Gourdon, G., and Thornton, C. A. (2011) Stabilization of expanded (CTG)*(CAG) repeats by antisense oligonucleotides, *Mol. Ther.* 19, 2222-2227.
- Morrison, D. J., Hogan, L. E., Condos, G., Bhatla, T., Germino, N., Moskowitz, N. P., Lee, L., Bhojwani, D., Horton, T. M., Belitskaya-Levy, I., Greenberger, L. M., Horak, I. D., Grupp, S. A., Teachey, D. T., Raetz, E. A., and Carroll, W. L. (2012) Endogenous knockdown of survivin improves chemotherapeutic response in ALL models, *Leukemia 26*, 10.1038/leu.2011.1199.
- 112. Gagnon, K. T., Watts, J. K., Pendergraff, H. M., Montaillier, C., Thai, D., Potier, P., and Corey, D. R. (2011) Antisense and Antigene Inhibition of Gene Expression by Cell-Permeable Oligonucleotide-Oligospermine Conjugates, *J. Am. Chem. Soc.* 133, 8404-8407.
- 113. Souleimanian, N., Deleavey, G. F., Soifer, H., Wang, S., Tiemann, K., Damha, M. J., and Stein, C. A. (2012) Antisense 2 '-Deoxy, 2 '-Fluoroarabino Nucleic Acid (2 ' F-ANA) Oligonucleotides: In Vitro Gymnotic Silencers of Gene Expression Whose Potency Is Enhanced by Fatty Acids, *Mol Ther Nucleic Acids* 1, 1-9.
- 114. Wolfrum, C., Shi, S., Jayaprakash, K. N., Jayaraman, M., Wang, G., Pandey, R. K., Rajeev, K. G., Nakayama, T., Charrise, K., Ndungo, E. M., Zimmermann, T., Koteliansky, V., Manoharan, M., and Stoffel, M. (2007) Mechanisms and optimization of in vivo delivery of lipophilic siRNAs, *Nat. Biotechnol. 25*, 1149-1157.
- 115. Hostetler, K. Y., Rybak, R. J., Beadle, J. R., Gardner, M. F., Aldern, K. A., Wright, K. N., and Kern, E. R. (2001) In vitro and in vivo activity of 1-O-hexadecylpropane-diol-3-phosphoganciclovir and 1-O-hexadecylpropane-diol-3-phospho-penciclovir in cytomegalovirus and herpes simplex virus infections, *Antiviral Chem. Chemother.* 12, 61-70.
- 116. Prakash, T. P., Graham, M. J., Yu, J., Carty, R., Low, A., Chappell, A., Schmidt, K., Zhao, C., Aghajan, M., Murray, H. F., Riney, S., Booten, S. L., Murray, S. F., Gaus, H., Crosby, J., Lima, W. F., Guo, S., Monia, B. P., Swayze, E. E., and Seth, P. P. (2014) Targeted delivery of antisense oligonucleotides to hepatocytes using triantennary N-acetyl galactosamine improves potency 10-fold in mice, *Nucleic Acids Res. 42*, 8796-8807.
- 117. Singh, Y., Murat, P., and Defrancq, E. (2010) Recent developments in oligonucleotide conjugation, *Chem. Soc. Rev. 39*, 2054-2070.

- 118. Zhou, J., Shum, K.-T., Burnett, J. C., and Rossi, J. J. (2013) Nanoparticle-Based Delivery of RNAi Therapeutics: Progress and Challenges, *Pharmaceuticals (Basel) 6*, 85-107.
- 119. Soutschek, J., Akinc, A., Bramlage, B., Charisse, K., Constien, R., Donoghue, M., Elbashir, S., Geick, A., Hadwiger, P., Harborth, J., John, M., Kesavan, V., Lavine, G., Pandey, R. K., Racie, T., Rajeev, K. G., Rohl, I., Toudjarska, I., Wang, G., Wuschko, S., Bumcrot, D., Koteliansky, V., Limmer, S., Manoharan, M., and Vornlocher, H. P. (2004) Therapeutic silencing of an endogenous gene by systemic administration of modified siRNAs, *Nature 432*, 173-178.
- 120. Akinc, A., Querbes, W., De, S., Qin, J., Frank-Kamenetsky, M., Jayaprakash, K. N., Jayaraman, M., Rajeev, K. G., Cantley, W. L., Dorkin, J. R., Butler, J. S., Qin, L., Racie, T., Sprague, A., Fava, E., Zeigerer, A., Hope, M. J., Zerial, M., Sah, D. W. Y., Fitzgerald, K., Tracy, M. A., Manoharan, M., Koteliansky, V., de Fougerolles, A., and Maier, M. A. (2010) Targeted Delivery of RNAi Therapeutics With Endogenous and Exogenous Ligand-Based Mechanisms, *Mol. Ther.* 18, 1357-1364.
- 121. Winkler, J. (2013) Oligonucleotide conjugates for therapeutic applications, *Ther. Deliv. 4*, 791-809.
- 122. Kjems, J., and Howard, K. A. (2012) Oligonucleotide Delvery to the Lung: Waiting to Inhale, *Mol Ther Nucleic Acids*.
- 123. Bitko, V., Musiyenko, A., Shulyayeva, O., and Barik, S. (2005) Inhibition of respiratory viruses by nasally administered siRNA, *Nat. Med.* 11, 50-55.
- 124. DeVincenzo, J., Lambkin-Williams, R., [...], and Vaishnaw, A. (2010) A randomized, double-blind, placebo-controlled study of an RNAi-based therapy directed against respiratory syncytial virus, *Proc Natl Acad Sci 107*, 8800-8805.
- 125. Koppelman, G. H., and Sayers, I. (2011) Evidence of a genetic contribution to lung function decline in asthma, *J. Allergy Clin. Immunol.* 128, 479-484.
- 126. Tang, M. L. K., Wilson, J. W., Stewart, A. G., and Royce, S. G. (2006) Airway remodelling in asthma: Current understanding and implications for future therapies, *Pharmacol. Ther.* 112, 474-488.
- 127. No author listed. (2007) Global surveillance, prevention and control of chronic respiratory disease: a comprehensive approach., *World Health Organization*.
- 128. Holgate, S. T., and Polosa, R. (2006) The mechanisms, diagnosis, and management of severe asthma in adults, *Lancet 368*, 780-793.
- 129. Woodcock, A., Lowe, L.A., Murray, C.S., Simpson, B.M., Pipis, S.D., Kissen, P., Simpson, A., Custovic, A. . (2004) Early Life Environmental Conrol: Effect on Symptoms, Sensitization, and Lung Function at Age 3 Years., *Am J Respir Crit Care Med. 170*, 433-439.
- 130. Ober, C., and Yao, T.-C. (2011) The genetics of asthma and allergic disease: a 21st century perspective, *Immunol. Rev.* 242, 10-30.
- 131. Van Eerdewegh, P., Little, R. D., Dupuis, J., Del Mastro, R. G., Falls, K., Simon, J., Torrey, D., Pandit, S., McKenny, J., Braunschweiger, K., Walsh, A., Liu, Z., Hayward, B., Folz, C., Manning, S. P., Bawa, A., Saracino, L., Thackston, M., Benchekroun, Y., Capparell, N., Wang, M., Adair, R., Feng, Y., Dubois, J., FitzGerald, M. G., Huang, H., Gibson, R., Allen, K. M., Pedan, A., Danzig, M. R., Umland, S. P., Egan, R. W., Cuss, F. M., Rorke, S., Clough, J. B., Holloway, J. W., Holgate, S. T., and Keith, T. P. (2002) Association of the ADAM33 gene with asthma and bronchial hyperresponsiveness, *Nature 418*, 426-430.

- 132. Primakoff, P., and Myles, D. G. (2000) The ADAM gene family surface proteins with adhesion and protease activity, *Trends Genet. 16*, 83-87.
- 133. Black, R. A., Rauch, C. T., Kozlosky, C. J., Peschon, J. J., Slack, J. L., Wolfson, M. F., Castner, B. J., Stocking, K. L., Reddy, P., Srinivasan, S., Nelson, N., Boiani, N., Schooley, K. A., Gerhart, M., Davis, R., Fitzner, J. N., Johnson, R. S., Paxton, R. J., March, C. J., and Cerretti, D. P. (1997) A metalloproteinase disintegrin that releases tumour-necrosis factor-alpha from cells, *Nature 385*, 729-733.
- 134. McGinn, O. J., English, W. R., Roberts, S., Ager, A., Newham, P., and Murphy, G. (2011) Modulation of integrin alpha 4 beta 1 by ADAM28 promotes lymphocyte adhesion and transendothelial migration, *Cell Biol. Int.* 35, 1043-1053.
- 135. Kveiborg, M., Instrell, R., Rowlands, C., Howell, M., and Parker, P. J. (2011) PKC alpha and PKC delta Regulate ADAM17-Mediated Ectodomain Shedding of Heparin Binding-EGF through Separate Pathways, *PLoS One 6*.
- 136. Chen, H., Pyluck, A. L., Janik, M., and Sampson, N. S. (1998) Peptides corresponding to the epidermal growth factor-like domain of mouse fertilin: Synthesis and biological activity, *Biopolymers 47*, 299-307.
- 137. Zou, J., Zhang, R. M., Zhu, F., Liu, J. J., Madison, V., and Umland, S. P. (2005) ADAM33 enzyme properties and substrate specificity, *Biochemistry 44*, 4247-4256.
- 138. Umland, S. P., Garlisi, C. G., Shah, H., Wan, Y. T., Zou, J., Devito, K. E., Huang, W. M., Gustafson, E. L., and Ralston, R. (2003) Human ADAM33 messenger RNA expression profile and post-transcriptional regulation, *Am. J. Respir. Crit. Care Med 29*, 571-582.
- 139. Yang, Y., Haitchi, H. M., Cakebread, J., Sammut, D., Harvey, A., Powell, R. M., Holloway, J. W., Howarth, P., Holgate, S. T., and Davies, D. E. (2008) Epigenetic mechanisms silence a disintegrin and metalloprotease 33 expression in bronchial epithelial cells, *J. Allergy Clin. Immunol.* 121, 1393-1399.
- 140. Simpson, A., Maniatis, N. Jury, F., Cakebreak, J., Lowe, L.A., Holgate, S.T., Woodcock, A., Ollier, W.E.R., Collins, A., Custovic, A., Holloway, J.W., John, S.L. (2005) Polymorphisms in a disintegrin and metalloprotesase 33 (ADAM33) predict impaired early-life lung function, *Am. J. Pespir. Crit. Care Med 172*, 55-60.
- 141. Holgate, S. T., Davies, D. E., Powell, R. M., and Holloway, J. W. (2006) ADAM33: a newly identified protease involved in airway remodelling, *Pulm. Pharmacol. Ther.* 19, 3-11.
- 142. Holgate, S. T., Davies, D. E., Rorke, S., Cakebread, J., Murphy, G., Powell, R. M., and Holloway, J. W. (2004) ADAM 33 and its association with airway remodeling and hyperresponsiveness in asthma, *Clin. Rev. Allergy Immunol.* 27, 23-34.
- 143. Michelson, A. M., and Todd, A. R. (1955) Nucleotides part XXXII. Synthesis of a dithymidine dinucleotide containing a 3[prime or minute]: 5[prime or minute]-internucleotidic linkage, *Journal of the Chemical Society (Resumed)*, 2632-2638.
- 144. Hall, R. H., Todd, A., and Webb, R. F. (1957) 644. Nucleotides. Part XLI. Mixed anhydrides as intermediates in the synthesis of dinucleoside phosphates, *J. Chem. Soc. (Resumed)*, 3291-3296.
- 145. Gilham, P. T., and Khorana, H. G. (1958) Studies on Polynucleotides. I. A New and General Method for the Chemical Synthesis of the C5"-C3" Internucleotidic Linkage. Syntheses of Deoxyribo-dinucleotides1, *J. Am. Chem. Soc. 80*, 6212-6222.

- 146. Letsinger, R. L., Ogilvie, K. K., and Miller, P. S. (1969) Nucleotide chemistry. XV. Developments in syntheses of oligodeoxyribonucleotides and their organic derivatives, *Journal of the American Chemical Society 91*, 3360-3365.
- 147. Letsinger, R. L., Finnan, J. L., Heavner, G. A., and Lunsford, W. B. (1975) Nucleotide chemistry. XX. Phosphite coupling procedure for generating internucleotide links, *J. Am. Chem. Soc.* 97, 3278-3279.
- 148. Letsinger, R. L., and Mahadevan, V. (1965) Oligonucleotide synthesis on a polymer support, *J. Am. Chem. Soc. 87*, 3526-3527.
- 149. Beaucage, S. L., and Caruthers, M. H. (1981) Deoxynucleoside phosphoroamidites- A new class of key intermediates for deoxypolynucleotide synthesis, *Tetrahedron Lett. 22*.
- 150. McBride, L. J., and Caruthers, M. H. (1983) An investigation of several deoxynucleoside phosphoramidites useful for synthesizing deoxyoligonucleotides, *Tetrahedron Lett. 24*, 245-248.
- 151. Chiang, P. W., Song, W. J., Wu, K. Y., Korenberg, J. R., Fogel, E. J., Van Keuren, M. L., Lashkari, D., and Kurnit, D. M. (1996) Use of a fluorescent-PCR reaction to detect genomic sequence copy number and transcriptional abundance, *Genome Res. 6*, 1013-1026.
- 152. Heid, C. A., Stevens, J., Livak, K. J., and Williams, P. M. (1996) Real time quantitative PCR, *Genome Res.* 6, 986-994.
- 153. Riedy, M. C., Timm, E. A., Jr., and Stewart, C. C. (1995) Quantitative RT-PCR for measuring gene expression, *BioTechniques* 18, 70-74, 76.
- 154. VanGuilder, H. D., Vrana, K. E., and Freeman, W. M. (2008) Twenty-five years of quantitative PCR for gene expression analysis, *BioTechniques* 44, 619-626.
- 155. Boch, J., Scholze, H., Schornack, S., Landgraf, A., Hahn, S., Kay, S., Lahaye, T., Nickstadt, A., and Bonas, U. (2009) Breaking the Code of DNA Binding Specificity of TAL-Type III Effectors, *Science 326*, 1509-1512.
- 156. Gibson, U. E., Heid, C. A., and Williams, P. M. (1996) A novel method for real time quantitative RT-PCR, *Genome Res.* 6, 995-1001.
- 157. Holland, P. M., Abramson, R. D., Watson, R., and Gelfand, D. H. (1991) Detection of specific polymerase chain reaction product by utilizing the 5'----3' exonuclease activity of Thermus aquaticus DNA polymerase, *Proc. Natl. Acad. Sci. U. S. A. 88*, 7276-7280.
- 158. Ririe, K. M., Rasmussen, R. P., and Wittwer, C. T. (1997) Product differentiation by analysis of DNA melting curves during the polymerase chain reaction, *Anal. Biochem. 245*, 154-160.
- 159. Schneeberger, C., Speiser, P., Kury, F., and Zeillinger, R. (1995) Quantitative detection of reverse transcriptase-PCR products by means of a novel and sensitive DNA stain, *PCR Methods Appl.* 4, 234-238.
- 160. Wittwer, C. T., Herrmann, M. G., Moss, A. A., and Rasmussen, R. P. (1997) Continuous fluorescence monitoring of rapid cycle DNA amplification, *BioTechniques 22*, 130-131, 134-138.
- 161. Dheda, K., Huggett, J. F., Bustin, S. A., Johnson, M. A., Rook, G., and Zumla, A. (2004) Validation of housekeeping genes for normalizing RNA expression in real-time PCR, *BioTechniques 37*, 112-114, 116, 118-119.

- 162. Livak, K. J., and Schmittgen, T. D. (2001) Analysis of Relative Gene Expression Data Using Real-Time Quantitative PCR and the $2-\Delta\Delta$ CT Method, *Methods* 25, 402-408.
- 163. Winer, J., Jung, C. K. S., Shackel, I., and Williams, P. M. (1999) Development and Validation of Real-Time Quantitative Reverse Transcriptase–Polymerase Chain Reaction for Monitoring Gene Expression in Cardiac Myocytesin Vitro, *Anal. Biochem. 270*, 41-49.
- 164. Schmittgen, T. D., Zakrajsek, B. A., Mills, A. G., Gorn, V., Singer, M. J., and Reed, M. W. (2000) Quantitative Reverse Transcription—Polymerase Chain Reaction to Study mRNA Decay: Comparison of Endpoint and Real-Time Methods, *Anal. Biochem. 285*, 194-204.
- 165. Luu-The, V., Paquet, N., Calvo, E., and Cumps, J. (2005) Improved real-time RT-PCR method for high-throughput measurements using second derivative calculation and double correction, *BioTechniques 38*, 287-293.
- 166. Wang, T., and Brown, M. J. (1999) mRNA quantification by real time TaqMan polymerase chain reaction: validation and comparison with RNase protection, *Anal. Biochem. 269*, 198-201.
- 167. Yuan, J. S., Reed, A., Chen, F., and Stewart, C. N. (2006) Statistical analysis of real-time PCR data, *BMC Bioinformatics 7*, 85-85.
- 168. Laity, J. H., Lee, B. M., and Wright, P. E. (2001) Zinc finger proteins: new insights into structural and functional diversity, *Curr. Opin. Struct. Biol.* 11, 39-46.
- 169. Urnov, F. D., Rebar, E. J., Holmes, M. C., Zhang, H. S., and Gregory, P. D. (2010) Genome editing with engineered zinc finger nucleases, *Nat. Rev. Genet.* 11, 636-646.
- 170. Beumer, K., Bhattacharyya, G., Bibikova, M., Trautman, J. K., and Carroll, D. (2006) Efficient gene targeting in Drosophila with zinc-finger nucleases, *Genetics* 172, 2391-2403.
- 171. Doyon, Y., McCammon, J. M., Miller, J. C., Faraji, F., Ngo, C., Katibah, G. E., Amora, R., Hocking, T. D., Zhang, L., Rebar, E. J., Gregory, P. D., Urnov, F. D., and Amacher, S. L. (2008) Heritable targeted gene disruption in zebrafish using designed zinc-finger nucleases, *Nat Biotech 26*, 702-708.
- 172. Meng, X., Noyes, M. B., Zhu, L. J., Lawson, N. D., and Wolfe, S. A. (2008) Targeted gene inactivation in zebrafish using engineered zinc-finger nucleases, *Nat. Biotechnol.* 26, 695-701.
- 173. Foley, J. E., Yeh, J.-R. J., Maeder, M. L., Reyon, D., Sander, J. D., Peterson, R. T., and Joung, J. K. (2009) Rapid Mutation of Endogenous Zebrafish Genes Using Zinc Finger Nucleases Made by Oligomerized Pool Engineering (OPEN), *PLoS One 4*, e4348.
- 174. Townsend, J. A., Wright, D. A., Winfrey, R. J., Fu, F., Maeder, M. L., Joung, J. K., and Voytas, D. F. (2009) High-frequency modification of plant genes using engineered zinc-finger nucleases, *Nature* 459, 442-445.
- 175. Lombardo, A., Genovese, P., Beausejour, C. M., Colleoni, S., Lee, Y. L., Kim, K. A., Ando, D., Urnov, F. D., Galli, C., Gregory, P. D., Holmes, M. C., and Naldini, L. (2007) Gene editing in human stem cells using zinc finger nucleases and integrase-defective lentiviral vector delivery, *Nat. Biotechnol. 25*, 1298-1306.
- 176. Bot, A. (2010) The landmark approval of Provenge, what it means to immunology and "in this issue": the complex relation between vaccines and autoimmunity, *Int. Rev. Immunol.* 29, 235-238.

- 177. Carlson, D. F., Tan, W., Lillico, S. G., Stverakova, D., Proudfoot, C., Christian, M., Voytas, D. F., Long, C. R., Whitelaw, C. B. A., and Fahrenkrug, S. C. (2012) Efficient TALEN-mediated gene knockout in livestock, *Proc. Natl. Acad. Sci. 109*, 17382-17387.
- 178. Sung, Y. H., Baek, I.-J., Kim, D. H., Jeon, J., Lee, J., Lee, K., Jeong, D., Kim, J.-S., and Lee, H.-W. (2013) Knockout mice created by TALEN-mediated gene targeting, *Nat Biotech 31*, 23-24.
- 179. Cermak, T., Doyle, E. L., Christian, M., Wang, L., Zhang, Y., Schmidt, C., Baller, J. A., Somia, N. V., Bogdanove, A. J., and Voytas, D. F. (2011) Efficient design and assembly of custom TALEN and other TAL effector-based constructs for DNA targeting, *Nucleic Acids Res. 39*, e82.
- 180. Hockemeyer, D., Wang, H., Kiani, S., Lai, C. S., Gao, Q., Cassady, J. P., Cost, G. J., Zhang, L., Santiago, Y., Miller, J. C., Zeitler, B., Cherone, J. M., Meng, X., Hinkley, S. J., Rebar, E. J., Gregory, P. D., Urnov, F. D., and Jaenisch, R. (2011) Genetic engineering of human pluripotent cells using TALE nucleases, *Nat Biotech 29*, 731-734.
- 181. Reyon, D., Khayter, C., Regan, M. R., Joung, J. K., and Sander, J. D. (2012) Engineering designer transcription activator-like effector nucleases (TALENs) by REAL or REAL-Fast assembly, *Curr. Protoc. Mol. Biol. Chapter 12*, Unit 12 15.
- 182. Miller, J. C., Tan, S., Qiao, G., Barlow, K. A., Wang, J., Xia, D. F., Meng, X., Paschon, D. E., Leung, E., Hinkley, S. J., Dulay, G. P., Hua, K. L., Ankoudinova, I., Cost, G. J., Urnov, F. D., Zhang, H. S., Holmes, M. C., Zhang, L., Gregory, P. D., and Rebar, E. J. (2011) A TALE nuclease architecture for efficient genome editing, *Nat Biotech 29*, 143-148.
- 183. Sun, N., and Zhao, H. (2013) Transcription activator-like effector nucleases (TALENs): a highly efficient and versatile tool for genome editing, *Biotechnol. Bioeng.* 110, 1811-1821.
- 184. Weidenheft, B., van Duijin, E., Bultema, J. B., Waghmaree, S. P., Zhoua, K., Barendregtc, A., Westphalb, W., Heckc, A. J. R., Boekemad, E. J., Dickmane, M. J., and Doudna, J. A. (2011) RNA-guided complex from a bacterial immune system enhances target recognition through seed sequence interactions, *Proc. Natl. Acad. Sci. 108*, 10092-10097.
- 185. Jinek, M., Chylinski, K., Fonfara, I., Hauer, M., Doudna, J. A., and Charpentier, E. (2012) A Programmable Dual-RNA–Guided DNA Endonuclease in Adaptive Bacterial Immunity, *Science 337*, 816-821.
- 186. Grissa, I., Vergnaud, G., and Pourcel, C. (2007) The CRISPRdb database and tools to display CRISPRs and to generate dictionaries of spacers and repeats, *BMC Bioinformatics 8*.
- 187. Ishino, Y., Shinagawa, H., Makino, K., Amemura, M., and Nakata, A. (1987) Nucleotide sequence of the iap gene, responsible for alkaline phosphatase isozyme conversion in Escherichia coli, and identification of the gene product, *J. Bacteriol.* 169, 5429-5433.
- 188. Mojica, F. J., Diez-Villasenor, C., Soria, E., and Juez, G. (2000) Biological significance of a family of regularly spaced repeats in the genomes of Archaea, Bacteria and mitochondria, *Mol. Microbiol.* 36, 244-246.
- 189. Bolotin, A., Quinquis, B., Sorokin, A., and Ehrlich, S. D. (2005) Clustered regularly interspaced short palindrome repeats (CRISPRs) have spacers of extrachromosomal origin, *Microbiology* 151, 2551-2561.
- 190. Mojica, F. M., Díez-Villaseñor, C. s., García-Martínez, J., and Soria, E. (2005) Intervening Sequences of Regularly Spaced Prokaryotic Repeats Derive from Foreign Genetic Elements, J. Mol. Evol. 60, 174-182.

- 191. Pourcel, C., Salvignol, G., and Vergnaud, G. (2005) CRISPR elements in Yersinia pestis acquire new repeats by preferential uptake of bacteriophage DNA, and provide additional tools for evolutionary studies, *Microbiology* 151, 653-663.
- 192. Barrangou, R., Fremaux, C., Deveau, H., Richards, M., Boyaval, P., Moineau, S., Romero, D. A., and Horvath, P. (2007) CRISPR Provides Acquired Resistance Against Viruses in Prokaryotes, *Science 315*, 1709-1712.
- 193. Makarova, K. S., Aravind, L., Wolf, Y. I., and Koonin, E. V. (2011) Unification of Cas protein families and a simple scenario for the origin and evolution of CRISPR-Cas systems, *Biol. Direct* 6, 38-38.
- 194. Yosef, I., Goren, M. G., and Qimron, U. (2012) Proteins and DNA elements essential for the CRISPR adaptation process in Escherichia coli, *Nucleic Acids Res.* 40, 5569-5576.
- 195. Sander, J. D., and Joung, J. K. (2014) CRISPR-Cas systems for editing, regulating and targeting genomes, *Nat. Biotechnol*.
- 196. Hsu, P. D., Scott, D. A., Weinstein, J. A., Ran, F. A., Konermann, S., Agarwala, V., Li, Y., Fine, E. J., Wu, X., Shalem, O., Cradick, T. J., Marraffini, L. A., Bao, G., and Zhang, F. (2013) DNA targeting specificity of RNA-guided Cas9 nucleases, *Nat Biotech 31*, 827-832.
- 197. Hsu, P. D., Lander, E. S., and Zhang, F. (2014) Development and applications of CRISPR-Cas9 for genome engineering, *Cell* 157, 1262-1278.
- 198. Zhang, F., Wen, Y., and Guo, X. (2014) CRISPR/Cas9 for genome editing: progress, implications and challenges, *Hum. Mol. Genet.* 23, R40-46.
- 199. Karvelis, T., Gasiunas, G., Miksys, A., Barrangou, R., Horvath, P., and Siksnys, V. (2013) crRNA and tracrRNA guide Cas9-mediated DNA interference in Streptococcus thermophilus, *RNA Biol.* 10, 841-851.
- 200. Karvelis, T., Gasiunas, G., and Siksnys, V. (2013) Programmable DNA cleavage in vitro by Cas9, *Biochem. Soc. Trans. 41*, 1401-1406.
- 201. Deltcheva, E., Chylinski, K., Sharma, C. M., Gonzales, K., Chao, Y., Pirzada, Z. A., Eckert, M. R., Vogel, J., and Charpentier, E. (2011) CRISPR RNA maturation by trans-encoded small RNA and host factor RNase III, *Nature 471*, 602-+.
- 202. Nishimasu, H., Ran, F. A., Hsu, Patrick D., Konermann, S., Shehata, Soraya I., Dohmae, N., Ishitani, R., Zhang, F., and Nureki, O. Crystal Structure of Cas9 in Complex with Guide RNA and Target DNA, *Cell* 156, 935-949.
- 203. Jiang, F., Zhou, K., Ma, L., Gressel, S., and Doudna, J. A. (2015) A Cas9–guide RNA complex preorganized for target DNA recognition, *Science 348*, 1477-1481.
- 204. Ran, F. A., Hsu, P. D., Wright, J., Agarwala, V., Scott, D. A., and Zhang, F. (2013) Genome engineering using the CRISPR-Cas9 system, *Nat. Protocols 8*, 2281-2308.
- 205. Jore, M. M., Brouns, S. J. J., and van der Oost, J. (2012) RNA in Defense: CRISPRs Protect Prokaryotes against Mobile Genetic Elements, *Cold Spring Harb. Perspect. Biol. 4*, a003657.
- 206. Sternberg, S. H., Redding, S., Jinek, M., Greene, E. C., and Doudna, J. A. (2014) DNA interrogation by the CRISPR RNA-guided endonuclease Cas9, *Nature 507*, 62-67.
- 207. Li, M., Wang, R., and Xiang, H. (2014) Haloarcula hispanica CRISPR authenticates PAM of a target sequence to prime discriminative adaptation, *Nucleic Acids Res*.

- 208. Mojica, F. J., Diez-Villasenor, C., Garcia-Martinez, J., and Almendros, C. (2009) Short motif sequences determine the targets of the prokaryotic CRISPR defence system, *Microbiology* 155, 733-740.
- 209. Mali, P., Yang, L., Esvelt, K. M., Aach, J., Guell, M., DiCarlo, J. E., Norville, J. E., and Church, G. M. (2013) RNA-guided human genome engineering via Cas9, *Science 339*, 823-826.
- 210. Liang, P., Xu, Y., Zhang, X., Ding, C., Huang, R., Zhang, Z., Lv, J., Xie, X., Chen, Y., Li, Y., Sun, Y., Bai, Y., Songyang, Z., Ma, W., Zhou, C., and Huang, J. (2015) CRISPR/Cas9-mediated gene editing in human tripronuclear zygotes, *Protein Cell* 6, 363-372.
- 211. Cho, S. W., Kim, S., Kim, J. M., and Kim, J. S. (2013) Targeted genome engineering in human cells with the Cas9 RNA-guided endonuclease, *Nat. Biotechnol.* 31, 230-232.
- 212. Niu, Y., Shen, B., Cui, Y., Chen, Y., Wang, J., Wang, L., Kang, Y., Zhao, X., Si, W., Li, W., Xiang, A. P., Zhou, J., Guo, X., Bi, Y., Si, C., Hu, B., Dong, G., Wang, H., Zhou, Z., Li, T., Tan, T., Pu, X., Wang, F., Ji, S., Zhou, Q., Huang, X., Ji, W., and Sha, J. (2014) Generation of genemodified cynomolgus monkey via Cas9/RNA-mediated gene targeting in one-cell embryos, *Cell* 156, 836-843.
- 213. Ma, Y., Zhang, X., Shen, B., Lu, Y., Chen, W., Ma, J., Bai, L., Huang, X., and Zhang, L. (2014) Generating rats with conditional alleles using CRISPR/Cas9, *Cell Res. 24*, 122-125.
- 214. Yasue, A., Mitsui, S. N., Watanabe, T., Sakuma, T., Oyadomari, S., Yamamoto, T., Noji, S., Mito, T., and Tanaka, E. (2014) Highly efficient targeted mutagenesis in one-cell mouse embryos mediated by the TALEN and CRISPR/Cas systems, *Sci. Rep. 4*, 5705.
- 215. Hai, T., Teng, F., Guo, R., Li, W., and Zhou, Q. (2014) One-step generation of knockout pigs by zygote injection of CRISPR/Cas system, *Cell Res. 24*, 372-375.
- 216. Schaller, H., Weimann, G., Lerch, B., and Khorana, H. G. (1963) Studies on Polynucleotides. XXIV.1 The Stepwise Synthesis of Specific Deoxyribopolynucleotides (4).2 Protected Derivatives of Deoxyribonucleosides and New Syntheses of Deoxyribonucleoside-3" Phosphates3, J. Am. Chem. Soc. 85, 3821-3827.
- 217. Xu, Q., Musier-Forsyth, K., Hammer, R. P., and Barany, G. (1996) Use of 1,2,4-dithiazolidine-3,5-dione (DtsNH) and 3-ethoxy-1,2,4-dithiazoline-5-one (EDITH) for synthesis of phosphorothioate-containing oligodeoxyribonucleotides., *Nucleic Acids Res.* 24, 1602-1607.
- 218. Gerster, M., Maier, M., Clausen, N., Schewitz, J., and Bayer, E. (1997) Optimized Large Scale Synthesis of Phosphorothioate Oligonucleotides on PS-PEG Supports, in *Zeitschrift für Naturforschung B*, p 110.
- 219. Haitchi, H. M., Bassett, D. J., Bucchieri, F., Gao, X., Powell, R. M., Hanley, N. A., Wilson, D. I., Holgate, S. T., and Davies, D. E. (2009) Induction of a disintegrin and metalloprotease 33 during embryonic lung development and the influence of IL-13 or maternal allergy., *J Allergy Clin Immunol.* 124, 590-597.
- 220. Haitchi, H. M. (2008) The expression and function of the asthma susceptibility gene, A Disintegrin and Metalloprotease (ADAM) 33, in airways of normal and asthmatic subjects and in developing lungs, in *Faculty of Medicine, Health and Life Sciences*, University of Southampton.
- 221. Ui-Tei, K., Naito, Y., Takahashi, F., Haraguchi, T., Ohki-Hamazaki, H., Juni, A., Ueda, R., and Saigo, K. (2004) Guidelines for the selection of highly effective siRNA sequences for mammalian and chick RNA interference, *Nucleic Acids Res. 32*, 936-948.

- 222. Naito, Y., Yamada, T., Ui-Tei, K., Morishita, S., and Saigo, K. (2004) siDirect: highly effective, target-specific siRNA design software for mammalian RNA interference, *Nucleic Acids Res.* 32, W124-W129.
- 223. Zuker, M. (2003) Mfold web server for nucleic acid folding and hybridization prediction, *Nucleic Acids Res. 31*, 3406-3415.
- 224. Altschul, S. F., Gish, W., Miller, W., Myers, E. W., and Lipman, D. J. (1990) Basic local alignment search tool, *J. Mol. Biol. 215*, 403–410.
- 225. Haitchi, H. M., Davies, D. E., and Holgate, S. T. (2008) PhD thesis, University of Southampton.
- 226. Sano, M., Sierant, M., Miyagishi, M., Nakanishi, M., Takagi, Y., and Sutou, S. (2008) Effect of asymmetric terminal structures of short RNA duplexes on the RNA interference activity and strand selection, *Nucleic Acids Res.* 36, 5812-5821.
- 227. Garlisi, C. G., Zou, J., Devito, K. E., Tian, F., Zhu, F. X., Liu, J., Shah, H., Wan, Y., Motasim Billah, M., Egan, R. W., and Umland, S. P. (2003) Human ADAM33: protein maturation and localization, *Biochem. Biophys. Res. Commun. 301*, 35-43.
- 228. Chesnoy, S., and Huang, L. (2000) Structure and function of lipid-DNA complexes for gene delivery, *Annu. Rev. Biophys. Biomol. Struct. 29*, 27-47.
- 229. Marshall, J., Nietupski, J. B., Lee, E. R., Siegel, C. S., Rafter, P. W., Rudginsky, S. A., Chang, C. D., Eastman, S. J., Harris, D. J., Scheule, R. K., and Cheng, S. H. (2000) Cationic lipid structure and formulation considerations for optimal gene transfection of the lung, *J. Drug Targeting 7*, 453-469.
- 230. Behr, J.-P. (1994) Gene Transfer with Synthetic Cationic Amphiphiles: Prospects for Gene Therapy, *Bioconj. Chem. 5*, 382-389.
- 231. Chillemi, R., Greco, V., Nicoletti, V. G., and Sciuto, S. (2013) Oligonucleotides Conjugated to Natural Lipids: Synthesis of Phosphatidyl-Anchored Antisense Oligonucleotides, *Bioconj. Chem.* 24, 648-657.
- 232. Haringsma, H. J., Li, J. J., Soriano, F., Kenski, D. M., Flanagan, W. M., and Willingham, A. T. (2012) mRNA knockdown by single strand RNA is improved by chemical modifications, *Nucleic Acids Res.* 40, 4125-4136.
- 233. Xu, Y. H., Linde, A., Larsson, A., Thormeyer, D., Elmen, J., Wahlestedt, C., and Liang, Z. C. (2004) Functional comparison of single- and double-stranded siRNAs in mammalian cells, *Biochem. Biophys. Res. Commun.* 316, 680-687.
- 234. Hall, A. H. S., Wan, J., Spesock, A., Sergueeva, Z., Shaw, B. R., and Alexander, K. A. (2006) High potency silencing by single-stranded boranophosphate siRNA, *Nucleic Acids Res. 34*, 2773-2781.
- 235. Matsui, M., Prakash, T. P., and Corey, D. R. (2013) Transcriptional Silencing by Single-Stranded RNAs Targeting a Noncoding RNA That Overlaps a Gene Promoter, *ACS Chem. Biol. 8*, 122-126.
- 236. Liu, J., Yu, D., Aiba, Y., Pendergraff, H., Swayze, E. E., Lima, W. F., Hu, J., Prakash, T. P., and Corey, D. R. (2013) ss-siRNAs allele selectively inhibit ataxin-3 expression: multiple mechanisms for an alternative gene silencing strategy, *Nucleic Acids Res.* 41, 9570-9583.

- 237. Hu, J. X., Liu, J., Yu, D. B., Aiba, Y., Lee, S., Pendergraff, H., Boubaker, J., Artates, J. W., Lagier-Tourenne, C., Lima, W. F., Swayze, E. E., Prakash, T. P., and Corey, D. R. (2014) Exploring the Effect of Sequence Length and Composition on Allele-Selective Inhibition of Human Huntingtin Expression by Single-Stranded Silencing RNAs, *Nucl. Acid Ther.* 24, 199-209.
- 238. Lu, X., Sun, C., Valentine, W. J., Shuyu, E., Liu, J., Tigyi, G., and Bittmani, R. (2009) Chiral Vinylphosphonate and Phosphonate Analogues of the Immunosuppressive Agent FTY720, *J. Org. Chem. 74*, 3192-3195.
- Kumar, R., Singh, S. K., Koshkin, A. A., Rajwanshi, V. K., Meldgaard, M., and Wengel, J. (1998) The first analogues of LNA (Locked Nucleic Acids): Phosphorothioate-LNA and 2 'thio-LNA, *Bioorg. Med. Chem. Lett* 8, 2219-2222.
- 240. Wahlestedt, C., Salmi, P., Good, L., Kela, J., Johnsson, T., Hokfelt, T., Broberger, C., Porreca, F., Lai, J., Ren, K. K., Ossipov, M., Koshkin, A., Jakobsen, N., Skouv, J., Oerum, H., Jacobsen, M. H., and Wengel, J. (2000) Potent and nontoxic antisense oligonucleotides containing locked nucleic acids, *Proc. Natl. Acad. Sci. USA 97*, 5633-5638.
- 241. Straarup, E. M., Fisker, N., Hedtjarn, M., Lindholm, M. W., Rosenbohm, C., Aarup, V., Hansen, H. F., Orum, H., Hansen, J. B. R., and Koch, T. (2010) Short locked nucleic acid antisense oligonucleotides potently reduce apolipoprotein B mRNA and serum cholesterol in mice and non-human primates, *Nucleic Acids Res. 38*, 7100-7111.
- 242. Cheng, Y., and Prusoff, W. H. (1973) Relationship between inhibition constant (K1) and concentration of inhibitor which causes 50 per cent inhibition (I50) of an enzymatic-reaction, *Biochem. Pharmacol.* 22, 3099-3108.
- 243. Aldern, K. A., Ciesla, S. L., Winegarden, K. L., and Hostetler, K. Y. (2003) Increased antiviral activity of 1-O-hexadecyloxypropyl- 2-C-14 cidofovir in MRC-5 human lung fibroblasts is explained by unique cellular uptake and metabolism, *Mol. Pharmacol.* 63, 678-681.
- 244. Hostetler, K. Y. (2009) Alkoxyalkyl prodrugs of acyclic nucleoside phosphonates enhance oral antiviral activity and reduce toxicity: Current state of the art, *Antiviral Res. 82*, A84-A98.
- 245. Yamano, Y., Tsuboi, K., Hozaki, Y., Takahashi, K., Jin, X.-H., Ueda, N., and Wada, A. (2012) Lipophilic amines as potent inhibitors of N-acylethanolamine-hydrolyzing acid amidase, *Biorg. Med. Chem.* 20, 3658-3665.
- 246. Niculescu-Duvaz, I. (2000) Technology evaluation: gemtuzumab ozogamicin, Celltech Group, *Curr. Opin. Mol. Ther. 2*, 691-696.
- 247. Garnett, M. C. (2001) Targeted drug conjugates: principles and progress, *Adv. Drug Del. Rev. 53*, 171-216.
- 248. Oupicky, D., Carlisle, R. C., and Seymour, L. W. (2001) Triggered intracellular activation of disulfide crosslinked polyelectrolyte gene delivery complexes with extended systemic circulation in vivo, *Gene Ther. 8*, 713-724.
- 249. Gosselin, M. A., Guo, W., and Lee, R. J. (2001) Efficient Gene Transfer Using Reversibly Cross-Linked Low Molecular Weight Polyethylenimine, *Bioconj. Chem.* 12, 989-994.
- 250. Ishida, T., Kirchmeier, M. J., Moase, E. H., Zalipsky, S., and Allen, T. M. (2001) Targeted delivery and triggered release of liposomal doxorubicin enhances cytotoxicity against human B lymphoma cells, *Biochim. Biophys. Acta* 1515, 144-158.

- 251. Holmgren, A., and Bjornstedt, M. (1995) [21] Thioredoxin and thioredoxin reductase, in *Methods Enzymol*. (Lester, P., Ed.), pp 199-208, Academic Press.
- 252. Darby, N. J., Freedman, R. B., and Creighton, T. E. (1994) Dissecting the Mechanism of Protein Disulfide Isomerase: Catalysis of Disulfide Bond Formation in a Model Peptide, *Biochemistry* 33, 7937-7947.
- 253. Meister, A., and Anderson, M. E. (1983) Glutathione, Annu. Rev. Biochem. 52, 711-760.
- Ezzat, K., Aoki, Y., Koo, T., McClorey, G., Benner, L., Coenen-Stass, A., O'Donovan, L., Lehto, T., Garcia-Guerra, A., Nordin, J., Saleh, A. F., Behlke, M., Morris, J., Goyenvalle, A., Dugovic, B., Leumann, C., Gordon, S., Gait, M. J., El-Andaloussi, S., and Wood, M. J. (2015) Self-Assembly into Nanoparticles Is Essential for Receptor Mediated Uptake of Therapeutic Antisense Oligonucleotides, *Nano Lett.* 15, 4364-4373.
- 255. Edwardson, T. G., Carneiro, K. M., Serpell, C. J., and Sleiman, H. F. (2014) An efficient and modular route to sequence-defined polymers appended to DNA, *Angew. Chem. Int. Ed. Engl.* 53, 4567-4571.
- 256. Banga, R. J., Chernyak, N., Narayan, S. P., Nguyen, S. T., and Mirkin, C. A. (2014) Liposomal Spherical Nucleic Acids, *J. Am. Chem. Soc. 136*, 9866-9869.
- 257. Powell, R. M., Wicks, J., Holloway, J. W., Holgate, S. T., and Davies, D. E. (2004) The splicing and fate of ADAM33 transcripts in primary human airways fibroblasts, *Am. J. Respir. Cell Mol. Biol.* 31, 13-21.
- 258. Gagnon, K. T., Watts, J. K., and Oligonucleotide Therapeutics, S. (2014) 10th Annual Meeting of the Oligonucleotide Therapeutics Society San Diego, California October 12-15, 2014 Session Summaries, *Nucl. Acid Ther. 24*, 428-434.
- 259. Yu, D., Pendergraff, H., Liu, J., Kordasiewicz, H. B., Cleveland, Don W., Swayze, Eric E., Lima, Walt F., Crooke, Stanley T., Prakash, Thazha P., and Corey, David R. (2012) Single-Stranded RNAs Use RNAi to Potently and Allele-Selectively Inhibit Mutant Huntingtin Expression, *Cell* 150, 895-908.
- 260. Hu, J. X., Liu, J., Narayanannair, K. J., Lackey, J. G., Kuchimanchi, S., Rajeev, K. G., Manoharan, M., Swayze, E. E., Lima, W. F., Prakash, T. P., Xiang, Q., Martinez, C., and Corey, D. R. (2014) Allele-Selective Inhibition of Mutant Atrophin-1 Expression by Duplex and Single-Stranded RNAs, *Biochemistry 53*, 4510-4518.
- 261. (2005) Rapid amplification of 5[prime] complementary DNA ends (5[prime] RACE), *Nat Meth 2*, 629-630.
- 262. Matranga, C., Tomari, Y., Shin, C., Bartel, D. P., and Zamore, P. D. (2005) Passenger-Strand Cleavage Facilitates Assembly of siRNA into Ago2-Containing RNAi Enzyme Complexes, *Cell* 123, 607-620.
- 263. Meister, G., Landthaler, M., Patkaniowska, A., Dorsett, Y., Teng, G., and Tuschl, T. (2004) Human Argonaute2 Mediates RNA Cleavage Targeted by miRNAs and siRNAs, *Mol. Cell* 15, 185-197.
- 264. Rivas, F. V., Tolia, N. H., Song, J.-J., Aragon, J. P., Liu, J., Hannon, G. J., and Joshua-Tor, L. (2005) Purified Argonaute2 and an siRNA form recombinant human RISC, *Nat. Struct. Mol. Biol.* 12, 340-349.
- 265. MacDonald, M. E., Ambrose, C. M., Duyao, M. P., Myers, R. H., Lin, C., Srinidhi, L., Barnes, G., Taylor, S. A., James, M., Groot, N., MacFarlane, H., Jenkins, B., Anderson, M. A.,

- Wexler, N. S., Gusella, J. F., Bates, G. P., Baxendale, S., Hummerich, H., Kirby, S., North, M., Youngman, S., Mott, R., Zehetner, G., Sedlacek, Z., Poustka, A., Frischauf, A.-M., Lehrach, H., Buckler, A. J., Church, D., Doucette-Stamm, L., O'Donovan, M. C., Riba-Ramirez, L., Shah, M., Stanton, V. P., Strobel, S. A., Draths, K. M., Wales, J. L., Dervan, P., Housman, D. E., Altherr, M., Shiang, R., Thompson, L., Fielder, T., Wasmuth, J. J., Tagle, D., Valdes, J., Elmer, L., Allard, M., Castilla, L., Swaroop, M., Blanchard, K., Collins, F. S., Snell, R., Holloway, T., Gillespie, K., Datson, N., Shaw, D., and Harper, P. S. (1993) A novel gene containing a trinucleotide repeat that is expanded and unstable on Huntington's disease chromosomes, *Cell 72*, 971-983.
- 266. Nasir, J., Floresco, S. B., O'Kusky, J. R., Diewert, V. M., Richman, J. M., Zeisler, J., Borowski, A., Marth, J. D., Phillips, A. G., and Hayden, M. R. (1995) Targeted disruption of the Huntington's disease gene results in embryonic lethality and behavioral and morphological changes in heterozygotes, *Cell* 81, 811-823.
- 267. Hu, J., Liu, J., and Corey, D. (2010) Allele-selective inhibition of huntingtin expression by switching to an miRNA-like RNAi mechanism, *Chem Biol 17*, 1183-1188.
- 268. Hu, J., Matsui, M., and Corey, D. R. (2009) Allele-Selective Inhibition of Mutant Huntingtin by Peptide Nucleic Acid (PNA)-Peptide Conjugates, Locked Nucleic Acid (LNA), and siRNA, *Ann. N. Y. Acad. Sci.* 1175, 24-31.
- 269. Hu, J., Matsui, M., Gagnon, K. T., Schwartz, J. C., Gabillet, S., Arar, K., Wu, J., Bezprozvanny, I., and Corey, D. R. (2009) Allele-specific silencing of mutant huntingtin and ataxin-3 genes by targeting expanded CAG repeats in mRNAs, *Nat. Biotechnol.* 27, 478-484.
- 270. Gagnon, K. T. (2010) HD Therapeutics- CHDI Fifth Annual Conference, iDrugs 13, 219-223.
- 271. Liu, J., Hu, J., Hicks, J. A., Prakash, T. P., and Corey, D. R. (2015) Modulation of Splicing by Single-Stranded Silencing RNAs, *Nucl. Acid Ther.* 25, 113-120.
- 272. Prakash, T. P., Lima, W. F., Murray, H. M., Li, W., Kinberger, G. A., Chappell, A. E., Gaus, H., Seth, P. P., Bhat, B., Crooke, S. T., and Swayze, E. E. (2015) Identification of metabolically stable 5 '- phosphate analogs that support single-stranded siRNA activity, *Nucleic Acids Res. 43*, 2993-3011.
- 273. Zhao, T., Wu, Z., Wang, S., and Chen, L. (2014) Expression and function of natural antisense transcripts in mouse embryonic stem cells, *Sci. China Life Sci.* 57, 1183-1190.
- 274. Hu, J., Liu, J., Narayanannair, K. J., Lackey, J. G., Kuchimanchi, S., Rajeev, K. G., Manoharan, M., Swayze, E. E., Lima, W. F., Prakash, T. P., Xiang, Q., Martinez, C., and Corey, D. R. (2014) Allele-selective inhibition of mutant atrophin-1 expression by duplex and single-stranded RNAs, *Biochemistry 53*, 4510-4518.
- 275. Liu, J., Yu, D. B., Aiba, Y., Pendergraff, H., Swayze, E. E., Lima, W. F., Hu, J. X., Prakash, T. P., and Corey, D. R. (2013) ss-siRNAs allele selectively inhibit ataxin-3 expression: multiple mechanisms for an alternative gene silencing strategy, *Nucleic Acids Res.* 41, 9570-9583.
- 276. Janowski, B. A., and Corey, D. R. (2010) Minireview: Switching on Progesterone Receptor Expression with Duplex RNA, *Mol. Endocrinol.* 24, 2243-2252.
- 277. Janowski, B. A., Huffman, K. E., Schwartz, J. C., Ram, R., Nordsell, R., Shames, D. S., Minna, J. D., and Corey, D. R. (2006) Involvement of AGO1 and AGO2 in mammalian transcriptional silencing, *Nat. Struct. Mol. Biol.* 13, 787-792.

- 278. Younger, S. T., and Corey, D. R. (2011) Transcriptional gene silencing in mammalian cells by miRNA mimics that target gene promoters, *Nucleic Acids Res.* 39, 5682-5691.
- 279. Ramachandran, S., Karp, P. H., Jiang, P., Ostedgaard, L. S., Walz, A. E., Fisher, J. T., Keshavjee, S., Lennox, K. A., Jacobi, A. M., Rose, S. D., Behlke, M. A., Welsh, M. J., Xing, Y., and McCray, P. B. (2012) A microRNA network regulates expression and biosynthesis of wild-type and ΔF508 mutant cystic fibrosis transmembrane conductance regulator, *Proc Natl Acad Sci. 109*, 13362-13367.
- 280. Yoshinari, K., Miyagishi, M., and Taira, K. (2004) Effects on RNAi of the tight structure, sequence and position of the targeted region, *Nucleic Acids Res. 32*, 691-699.
- 281. Cong, L., Ran, F. A., Cox, D., [...], and Zhang, F. (2013) Multiplex Genome Engineering Using CRISPR/Cas Systems, *Science 339*, 819-823.
- 282. Ran, F. A., Hsu, Patrick D., Lin, C.-Y., Gootenberg, Jonathan S., Konermann, S., Trevino, A. E., Scott, David A., Inoue, A., Matoba, S., Zhang, Y., and Zhang, F. (2013) Double Nicking by RNA-Guided CRISPR Cas9 for Enhanced Genome Editing Specificity, *Cell* 154, 1380-1389.
- 283. Munoz, I. M., Szyniarowski, P., Toth, R., Rouse, J., and Lachaud, C. (2014) Improved Genome Editing in Human Cell Lines Using the CRISPR Method, *PLoS One 9*, e109752.
- 284. Zhu, Z., Verma, N., González, F., Shi, Z.-D., and Huangfu, D. A CRISPR/Cas-Mediated Selection-free Knockin Strategy in Human Embryonic Stem Cells, *Stem Cell Reports 4*, 1103-1111.
- 285. Fu, Y., Sander, J. D., Reyon, D., Cascio, V. M., and Joung, J. K. (2014) Improving CRISPR-Cas nuclease specificity using truncated guide RNAs, *Nat Biotech 32*, 279-284.
- 286. Harrison, B., and Zimmerman, S. B. (1984) Polymer-stimulated ligation: enhanced ligation of oligo- and polynucleotides by T4 RNA ligase in polymer solutions, *Nucleic Acids Res. 12*, 8235-8251.
- 287. Kingston, R. E., Chen, C. A., and Okayama, H. (2001) Calcium Phosphate Transfection, in *Curr. Protoc. Neurosci.*, John Wiley & Sons, Inc.
- 288. Aida, T., Chiyo, K., Usami, T., Ishikubo, H., Imahashi, R., Wada, Y., Tanaka, K. F., Sakuma, T., Yamamoto, T., and Tanaka, K. (2015) Cloning-free CRISPR/Cas system facilitates functional cassette knock-in in mice, *Genome Biol.* 16, 87.

Appendix A Solid phase synthesis cycle for $\underline{1\mu M}$ RNA

Legend: 9- tetrazole; 10- Ammonia; 11- acetic anhydride; 12- 1-methylimidazole/tetrahydrofuran; 14- TCA deblock; 15- 0.02M lodine/water/pyridine/THF; 18- acetonitrile; 19- dichloromethane

<u>Step</u>	Time (s)
Begin	
18 to waste	3.0
18 to column	30.0
Reverse flush	10.0
Block flush	4.0
Phos prep	3.0
Column 1 on	
Block vent	2.0
Tet to waste	1.7
B+Tet to column	2.5
Tet to column	1.0
B+Tet to column	3.5
Push to column	
Column 1 off	
Column 2 on	
18 to waste	4.0
Block flush	3.0
Block vent	2.0
Tet to waste	1.7
B+Tet to column	2.5
Tet to column	1.0

Appendix A	
B+Tet to column	3.5
Push to column	
Column 2 off	
Column 3 on	
18 to waste	4.0
Block flush	3.0
Block vent	2.0
Tet to waste	1.7
B+Tet to column	2.5
Tet to column	1.0
B+Tet to column	3.5
Push to column	
Column 3 off	
Column 4 on	
18 to waste	4.0
Block flush	3.0
Block vent	2.0
Tet to waste	1.7
B+Tet to column	2.5
Tet to column	1.0
B+Tet to column	3.5
Push to column	

Column 4 off

Wait

Cap prep

18 to waste

600.0

3.0

8.0

Reverse flush	7.0
Block flush	3.0
Cap to column	10.0
Wait	5.0
18 to waste	4.0
Reverse flush	7.0
Block flush	3.0
15 to column	8.0
18 to waste	4.0
Block flush	3.0
Wait	15.0
18 to column	10.0
Flush to waste	6.0
18 to column	10.0
Reverse flush	7.0
Block flush	3.0
If not monitoring	
14 to column	6.0
Trityl flush	5.0
14 to column	6.0
Wait	5.0
Trityl flush	5.0
14 to column	5.0
Wait	5.0
Trityl flush	5.0
18 to column	10.0

Appendix A

Trityl flush 8.0

End monitoring

18 to column 8.0

Reverse flush 5.0

Block flush 4.0

End

Appendix B Solid phase synthesis cycle for 1 µM Sulfr+

Legend: 9- tetrazole/BTT; 10- Ammonia; 11- acetic anhydride; 12- 1-methylimidazole/tetrahyfrofuran; 14- TCA deblock; 15- TETD or EDITH; 18- acetonitrile; 19-dichloromethane

Step	Time (s)
Begin	
18 to waste	3.0
18 to column	10.0
Reverse flush	10.0
Block flush	4.0
Phos prep	3.0
Column 1 on	
Block vent	2.0
Tet to waste	1.7
B+Tet to column	2.5
Tet to column	1.0
B+Tet to column	2.5
Push to column	
Column 1 off	
Column 2 on	
18 to waste	4.0
Block flush	3.0
Block vent	2.0
Tet to waste	1.7
B+Tet to column	2.5
Tet to column	1.0

Appendix C B+Tet to column Push to column Column 2 off

2.5

Column 3 on

18 to waste 4.0

Block flush 3.0

Block vent 2.0

Tet to waste 1.7

B+Tet to column 2.5

Tet to column 1.0

B+Tet to column 2.5

Push to column

Column 3 off

Column 4 on

4.0 18 to waste

Block flush 3.0

Block vent 2.0

Tet to waste 1.7

2.5 B+Tet to column

Tet to column 1.0

B+Tet to column 2.5

Push to column

Column 4 off

Wait 600.0

Cap prep 3.0

Reverse flush 7.0

15 to column	8.0
18 to waste	4.0
Wait	900.0
18 to column	10.0
Flush to waste	6.0
18 to column	10.0
Reverse flush	7.0
18 to column	10.0
Reverse flush	1.0
18 to column	10.0
Reverse flush	1.0
Block flush	3.0
Cap to column	10.0
Wait	5.0
Wait 18 to waste	5.0
18 to waste	4.0
18 to waste Reverse flush	4.0 7.0
18 to waste Reverse flush 18 to column	4.0 7.0 10.0
18 to waste Reverse flush 18 to column Reverse flush	4.0 7.0 10.0 7.0
18 to waste Reverse flush 18 to column Reverse flush 18 to column	4.0 7.0 10.0 7.0 10.0
18 to waste Reverse flush 18 to column Reverse flush 18 to column Reverse flush	4.0 7.0 10.0 7.0 10.0 7.0
18 to waste Reverse flush 18 to column Reverse flush 18 to column Reverse flush Block flush	4.0 7.0 10.0 7.0 10.0 7.0 3.0
18 to waste Reverse flush 18 to column Reverse flush 18 to column Reverse flush Block flush 18 to column	4.0 7.0 10.0 7.0 10.0 7.0 3.0 10.0
18 to waste Reverse flush 18 to column Reverse flush 18 to column Reverse flush Block flush 18 to column Flush to waste	4.0 7.0 10.0 7.0 10.0 7.0 3.0 10.0 4.0

Flush to waste	4.0
Reverse flush	7.0
Block flush	3.0
If not monitoring	
14 to column	6.0
Wait	5.0
Trityl flush	5.0
14 to column	5.0
Wait	5.0
Trityl flush	5.0
14 to column	5.0
Wait	5.0
Trityl flush	8.0
18 to column	10.0
Trityl flush	8.0
End monitoring	
18 to column	8.0
Reverse flush	5.0
Block flush	4.0
End	

Appendix C Solid phase synthesis cycle for modified 1μM Sulfr+

Legend: 9- tetrazole/BTT; 10- Ammonia; 11- acetic anhydride; 12- 1-methylimidazole/tetrahyfrofuran; 14- TCA deblock; 15- TETD or EDITH; 18- acetonitrile; 19-dichloromethane

<u>Step</u>	Time (s)
Begin	
18 to waste	3.0
18 to column	10.0
Reverse flush	10.0
Block flush	4.0
Phos prep	3.0
Column 1 on	
Block vent	2.0
Tet to waste	1.7
B+Tet to column	2.5
Tet to column	1.0
B+Tet to column	2.5
Push to column	
Column 1 off	
Column 2 on	
18 to waste	4.0
Block flush	3.0
Block vent	2.0
Tet to waste	1.7
B+Tet to column	2.5

Appendix C Tet to colur B+Tet to co

Tet to column 1.0

B+Tet to column 2.5

Push to column

Column 2 off

Column 3 on

18 to waste 4.0

Block flush 3.0

Block vent 2.0

Tet to waste 1.7

B+Tet to column 2.5

Tet to column 1.0

B+Tet to column 2.5

Push to column

Column 3 off

Column 4 on

18 to waste 4.0

Block flush 3.0

Block vent 2.0

Tet to waste 1.7

B+Tet to column 2.5

Tet to column 1.0

B+Tet to column 2.5

Push to column

Column 4 off

Wait 600.0

Cap prep 3.0

Reverse flush	7.0
15 to column	8.0
18 to waste	4.0
Wait	60.0
15 to column	6.0
18 to waste	4.0
Wait	60.0
18 to column	10.0
Flush to waste	6.0
18 to column	10.0
Reverse flush	7.0
18 to column	10.0
Reverse flush	1.0
18 to column	10.0
Reverse flush	1.0
Block flush	3.0
Cap to column	10.0
Wait	5.0
18 to waste	4.0
Reverse flush	7.0
18 to column	10.0
Reverse flush	7.0
18 to column	10.0
Reverse flush	7.0
Block flush	3.0
18 to column	10.0

Flush to waste	4.0
18 to column	10.0
Reverse flush	7.0
18 to column	10.0
Flush to waste	4.0
Reverse flush	7.0
Block flush	3.0
If not monitoring	
14 to column	6.0
Wait	5.0
Trityl flush	5.0
14 to column	5.0
Wait	5.0
Trityl flush	5.0
14 to column	5.0
Wait	5.0
Trityl flush	8.0
18 to column	10.0
Trityl flush	8.0
End monitoring	
18 to column	8.0
Reverse flush	5.0
Block flush	4.0
End	

Appendix DMass spectrometry values

<u>Oligonucleotide</u>	Expected Mass (g/mol)	Actual Mass (g/mol)
HMH-1 sense	6124.7	6123.8
HMH-1 antisense	6567.0	6565.8
HMH-2 sense	6140.7	6139.8
HMH-2 antisense	6566.0	6567.4
HP-1 sense	6109.7	6108.7
HP-1 antisense	6552.0	6550.8
HP-2 sense	6163.8	6162.7
HP-2 antisense	6543.0	6542.7
HP-3 sense	6164.8	6163.7
HP-3 antisense	6527.0	6525.7
HP-4 sense	6156.7	6155.7
HP-4 antisense	6565.0	6564.8
HP-5 sense	6572.1	6570.9
HP-5 antisense	6743.1	6742.9
HP-6 sense	6701.1	6701.0
HP-6 antisense	6644.1	6643.0
HP-7 sense	6652.1	6652.0
HP-7 antisense	6663.0	6662.9
HP-8 sense	6606.0	6605.9
HP-8 antisense	6709.1	6708.0
HP-9 sense	6739.1	6739.0
HP-9 antisense	6636.1	6636.0
HP-10 sense	6676.1	6675.0

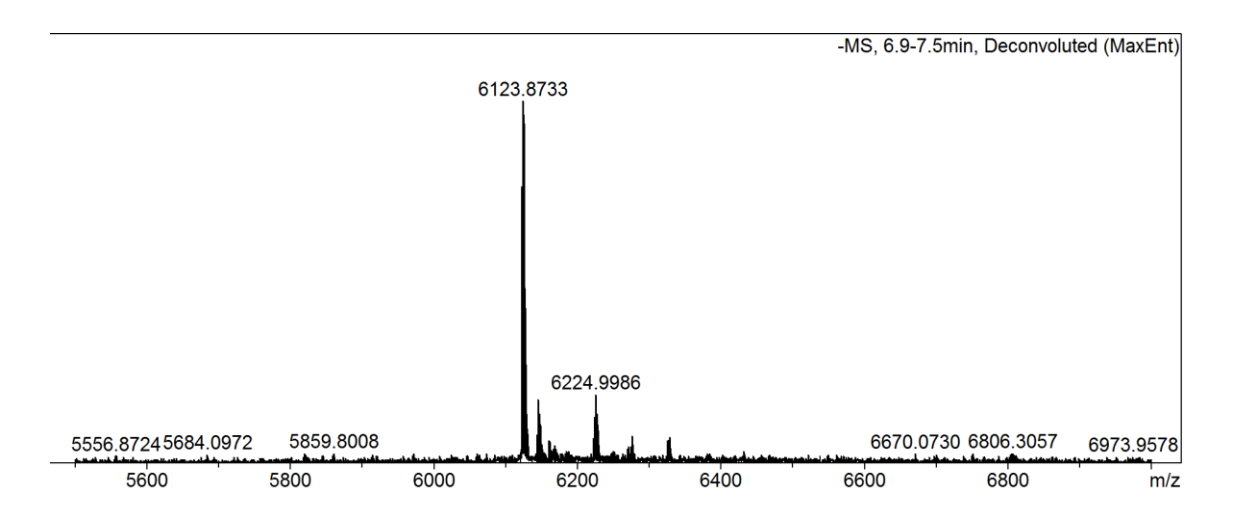
HP-10 antisense	6624.0	6623.8
HP-11 sense	6596.1	6594.9
HP-11 antisense	6704.0	6703.9
HP-12 sense	6661.1	6660.8
HP-12 antisense	6609.0	6607.2
HP-13 sense	6589.0	6587.8
HP-13 antisense	6726.1	6725.7
HP-14 sense	6597.1	6595.7
HP-14 antisense	6688.0	6686.7
HP-15 sense	6725.1	6724.8
HP-15 antisense	6605.0	6603.8
Scr sense	6636.1	6636.0
Scr antisense	6739.1	6739.0
ss-A33-MOE-1	7131.0	7131.6
ss-HP-A33-2	7407.0	7106.6
ss-HP-A33-3	7091.0	7090.6
ss-A33-MOE-2	7196.0	7195.7
ss-A33-OMe	7108.1	7107.7
ss-A33-LNA	7104.1	7103.6
33-G	5023.0	5022.1
33-Н	5007.0	5006.1
33-1	5016.0	5015.1
33-J	5015.0	5014.0
33-K	5079.0	5078.1
33-L	4996.0	4995.0
33-M	5012.0	5011.1

33-N	5022.0	5021.0
33-0	5003.0	5002.1
33-P	4994.0	4993.1
33-Q	5006.0	5005.0
33-R	5027.0	5026.1
Lna ctrl	4949.0	4948.4
PR sense	6755.2	6765.4
PR antisense	6559.9	6558.2
ss-PR-MOE	7189.1	7186.4
ss-PR-OMe	7101.0	7099.5
ss-PR-LNA	7097.0	7095.4
Disirna sense	7997.7	7995.2
Disirna antisense	8750.2	8749.2
Sin3A sense	6623.1	6620.7
Sin3A antisense	6617.0	6615.8
Sin3A-MOE	7246.2	7245.6
Sin3A-OMe	7158.1	7156.6
Sin3A-LNA	7154.1	7153.6
ss-scr	7280.2	7278.6
EGFP sense	6106.8	6105.9
EGFP antisense	6642.0	6640.8
HP-EGFP sense	5987.7	5986.9
HP-EGFP antisense	6704.0	6702.8
Egfp-MOE	7229.2	7255.4
Egfp-OMe	7141.1	7138.4
Egfp-LNA	7137.0	7134.4

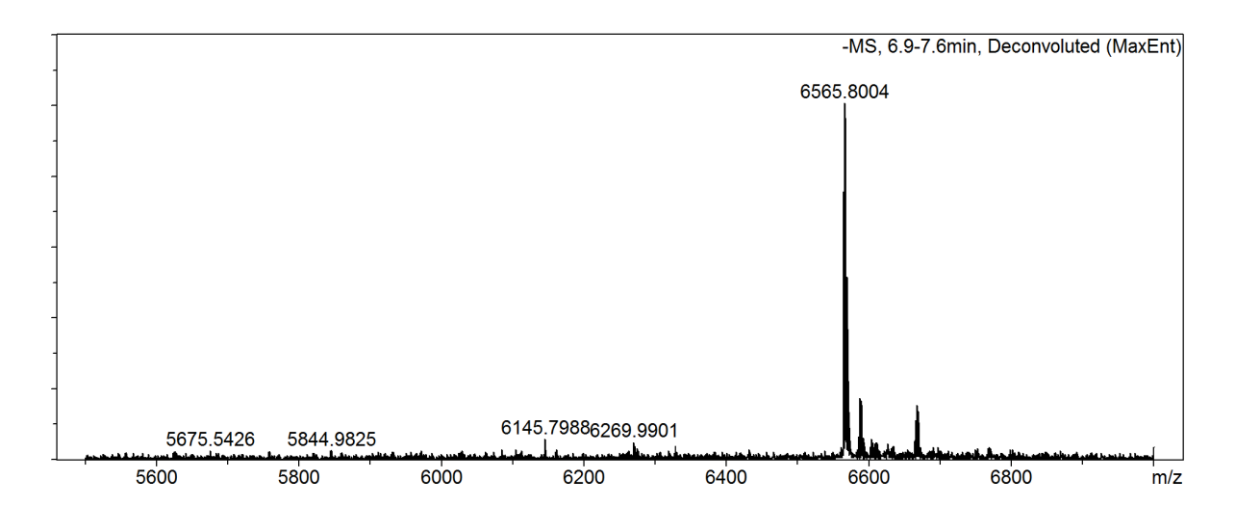
HP egfp-MOE	7333.2	7330.5
HP-egfp-OMe	7245.1	7242.4
HP-egfp-LNA	7241.1	7238.4
ss-HP-13	7267.2	7253.5
HP-2OMe	13599.9	13600.8
HP-Me/F	13359.1	13358.0
HP-Me/RNA	13319.3	13318.6
HP-PS-all	13667.2	ND
HP-PS-DBD	13329.9	ND
HP-PS-tracrBD	13362.1	13358.0
HP-LD-DBD	13042.1	13042.2
HP-LR-DBD	13207.0	13211.1
HP-LR-tracrBD	13178.0	13192.7
HP-LR-few1	13088.9	ND

Appendix E Mass Spectra

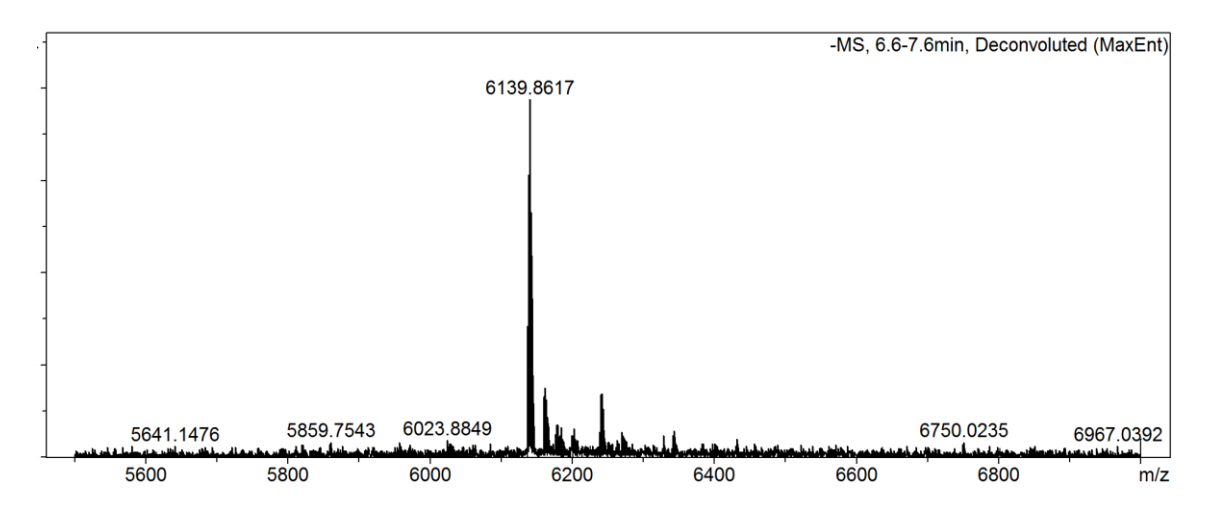
HMH-A33-1 sense strand



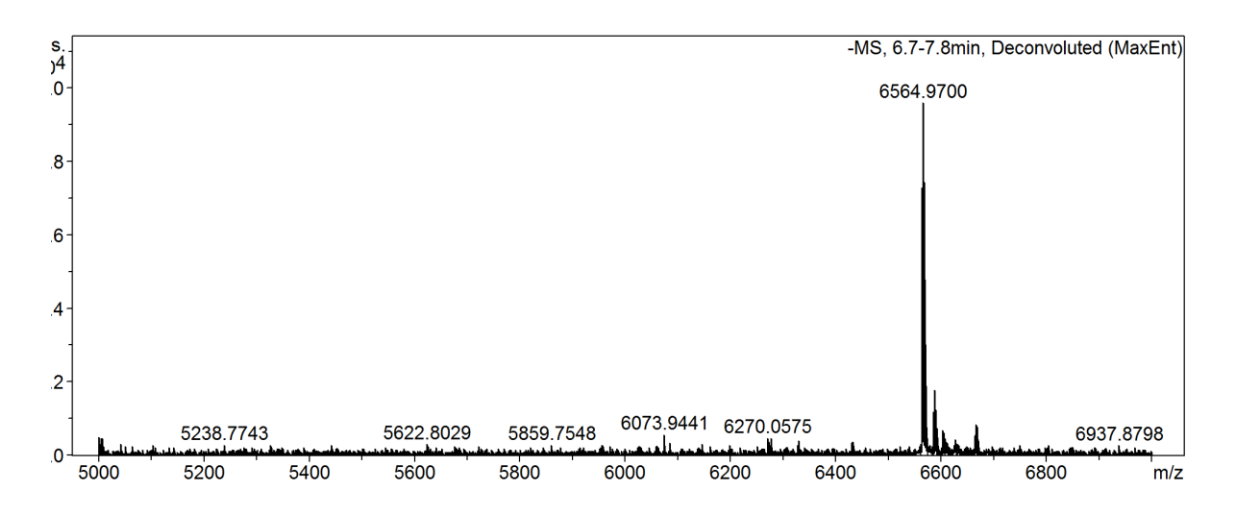
HMH-A33-1 antisense strand



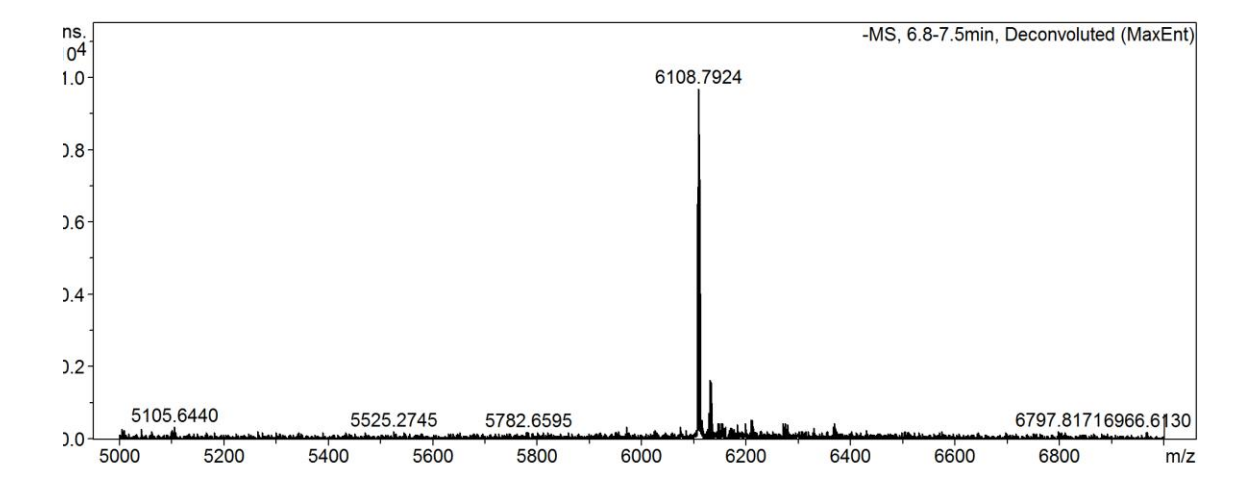
HMH-A33-2 sense strand



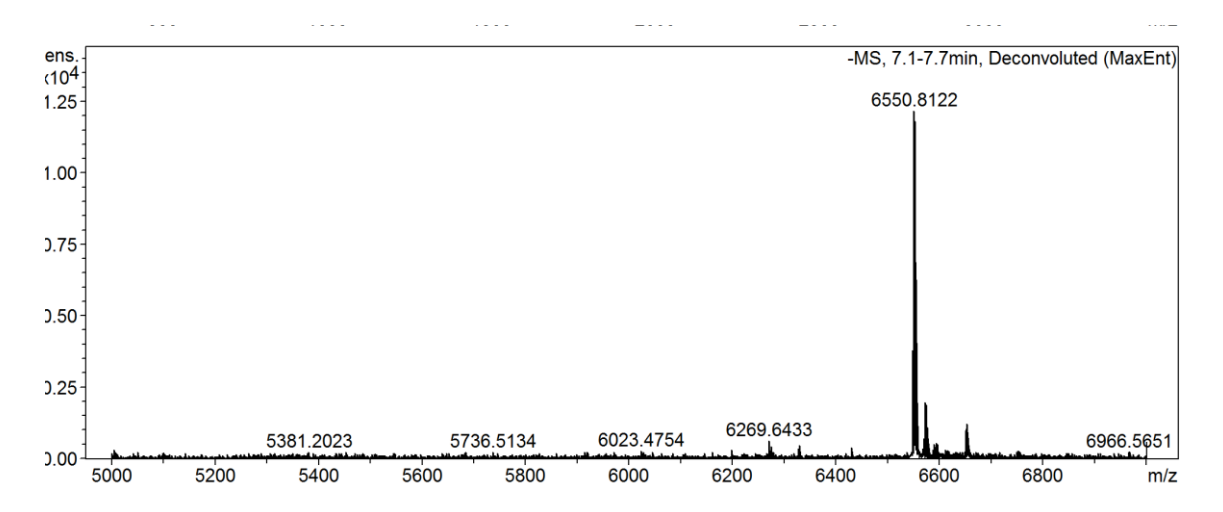
HMH-A33-2 antisense strand



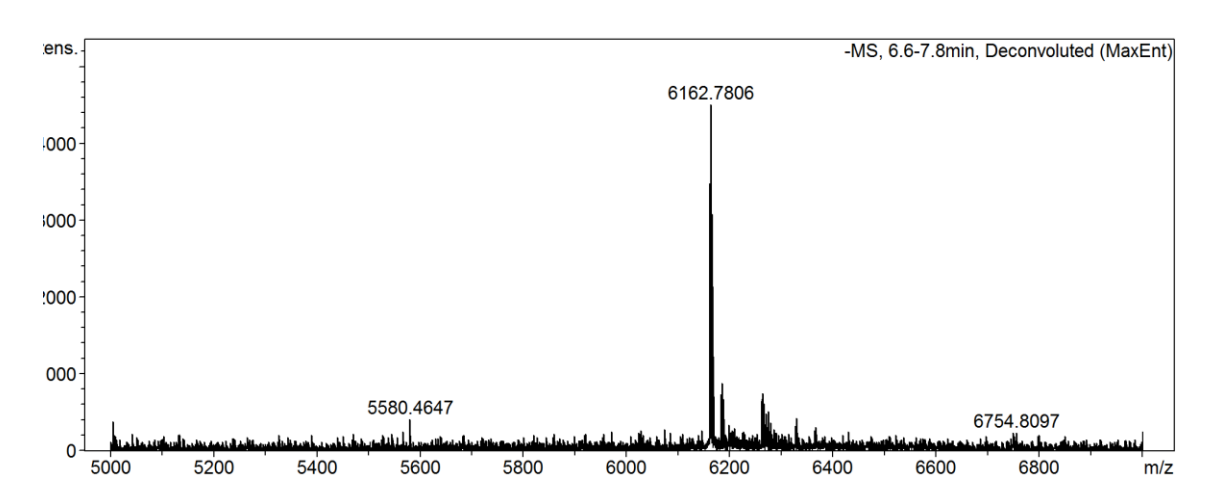
HP-A33-1 sense strand



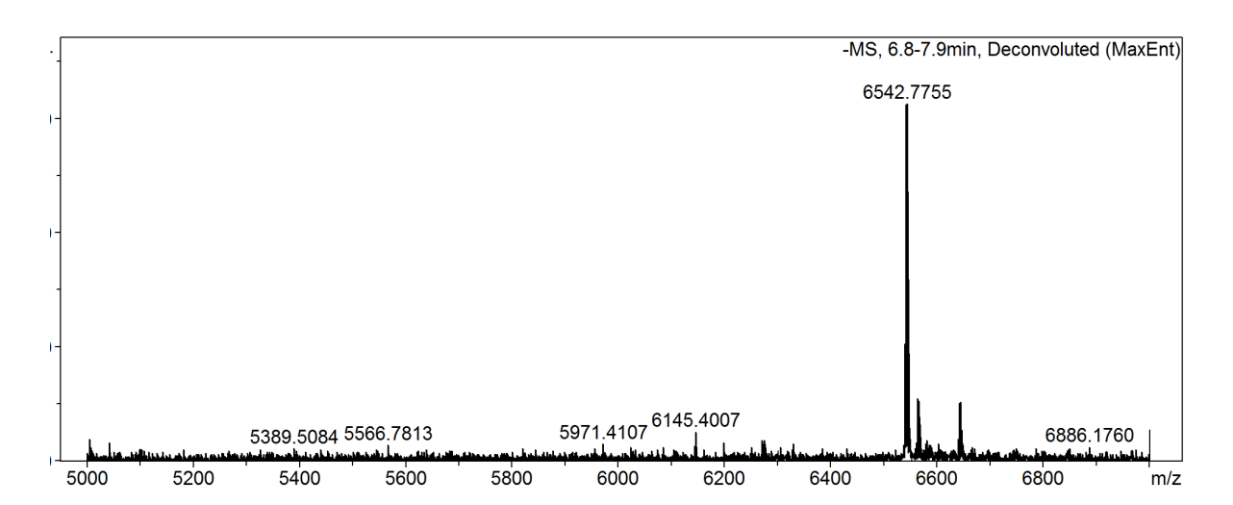
HP-A33-1 antisense strand



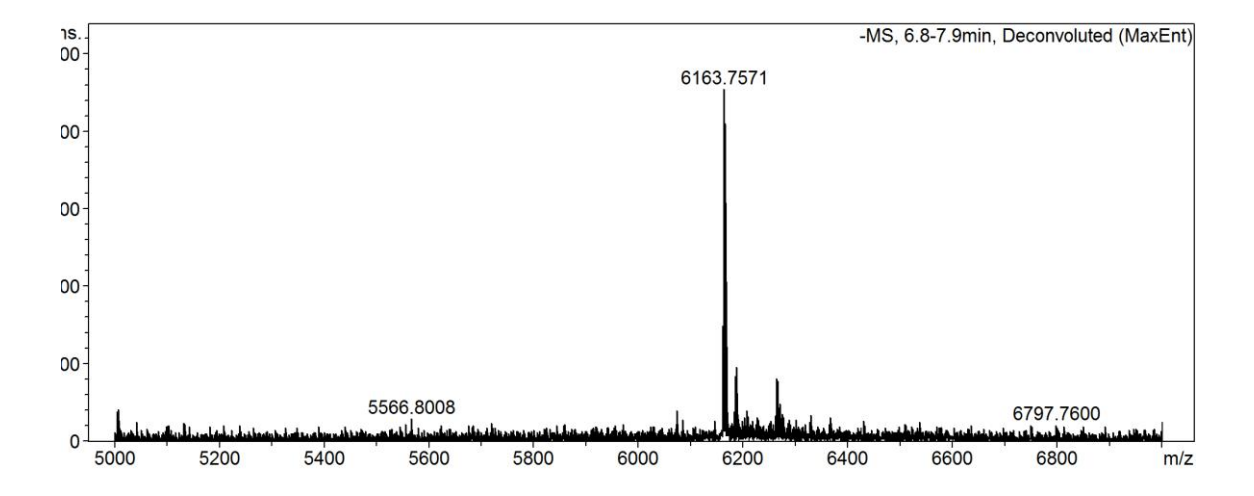
HP-A33-2 sense strand



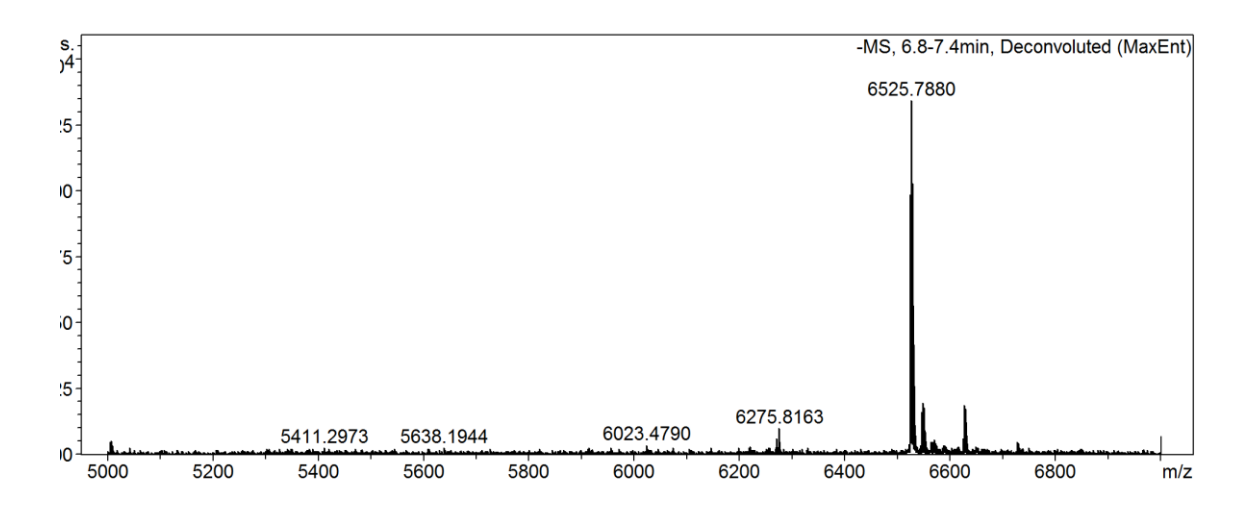
HP-A33-2 antisense strand



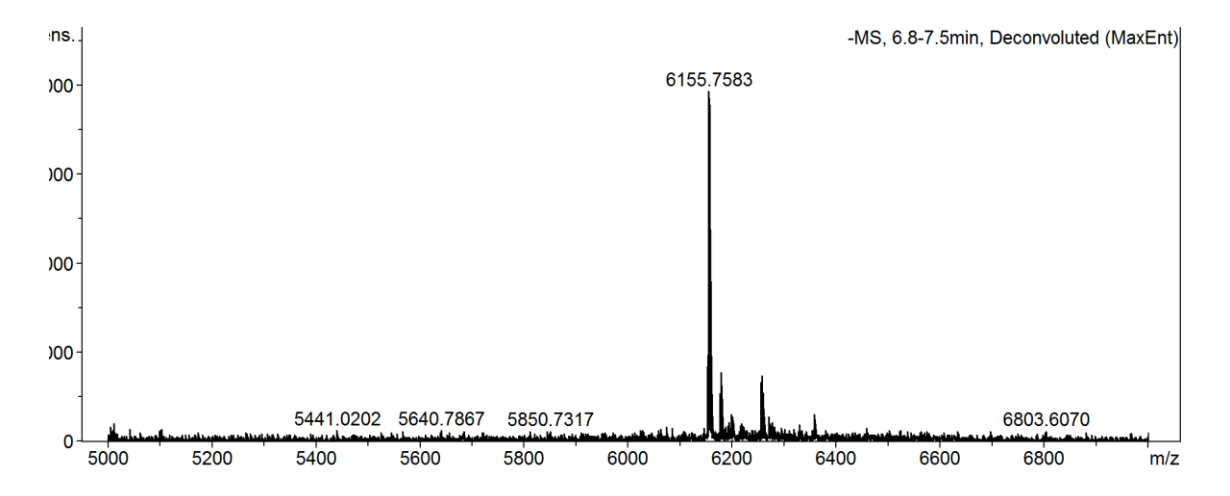
HP-A33-3 sense strand



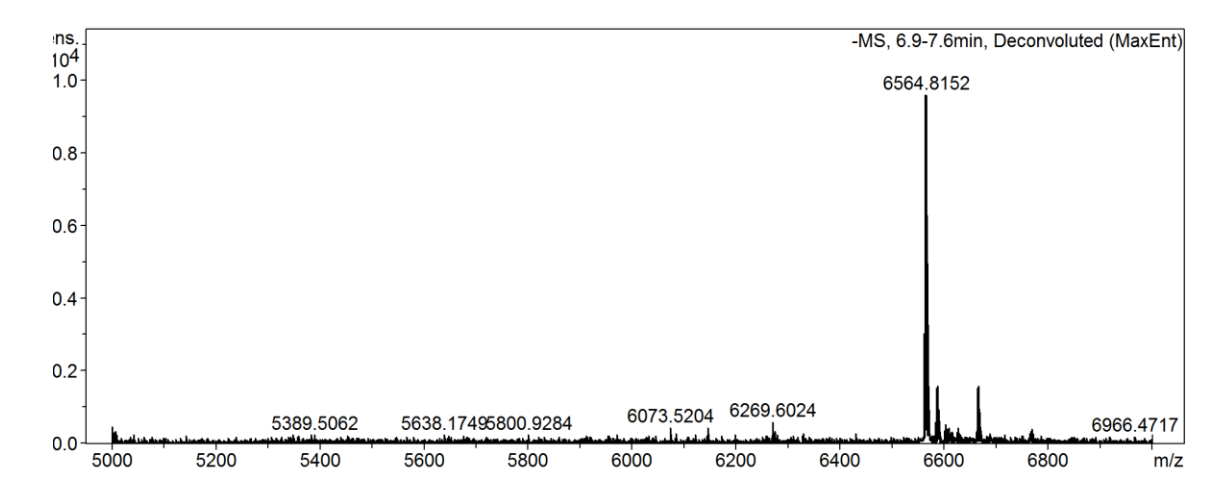
HP-A33-3 antisense strand



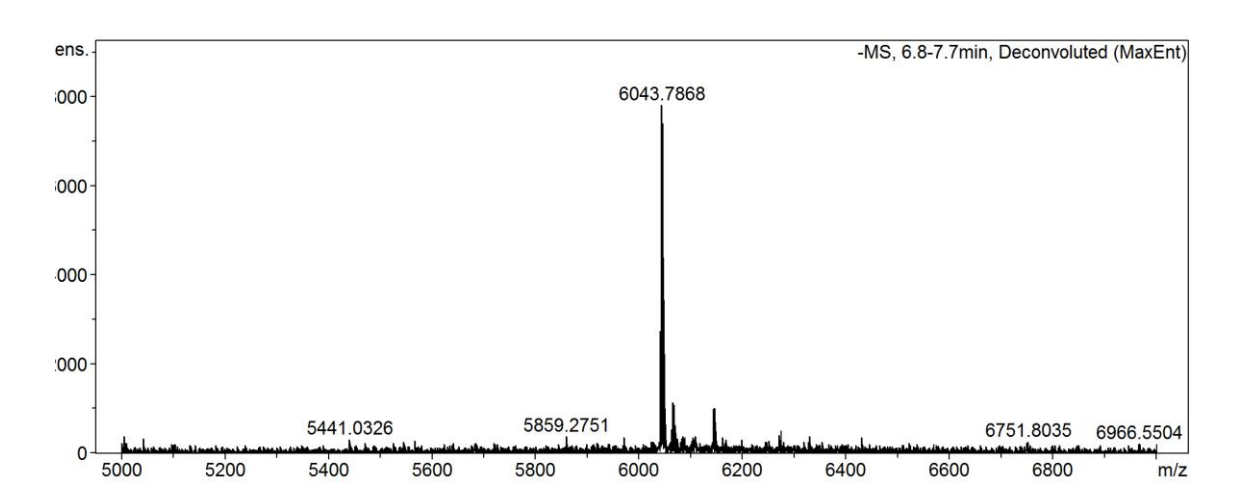
HP-A33-4 sense strand



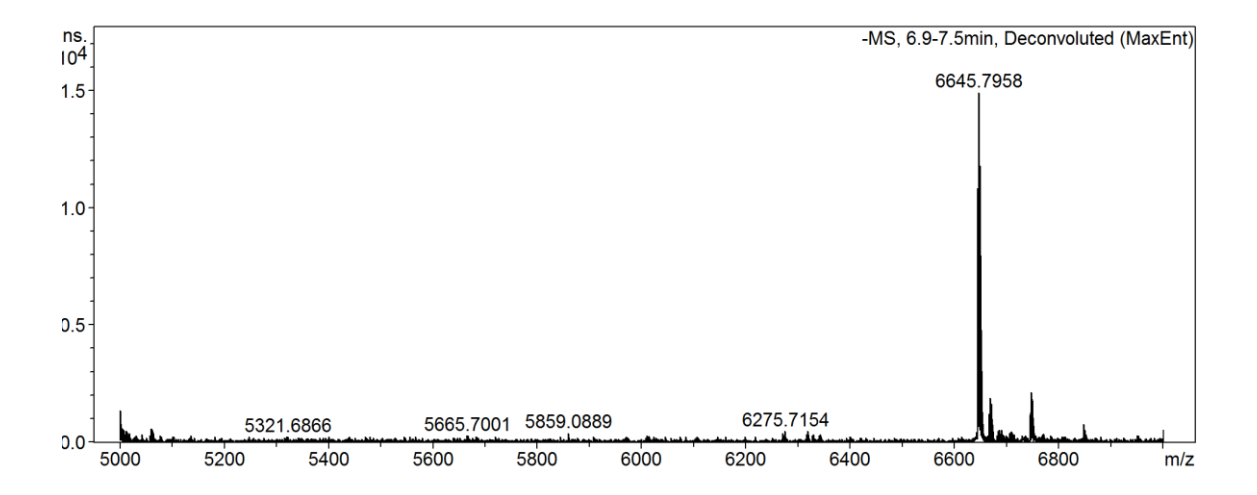
HP-A33-4 antisense strand



HP-atxn-1 sense strand

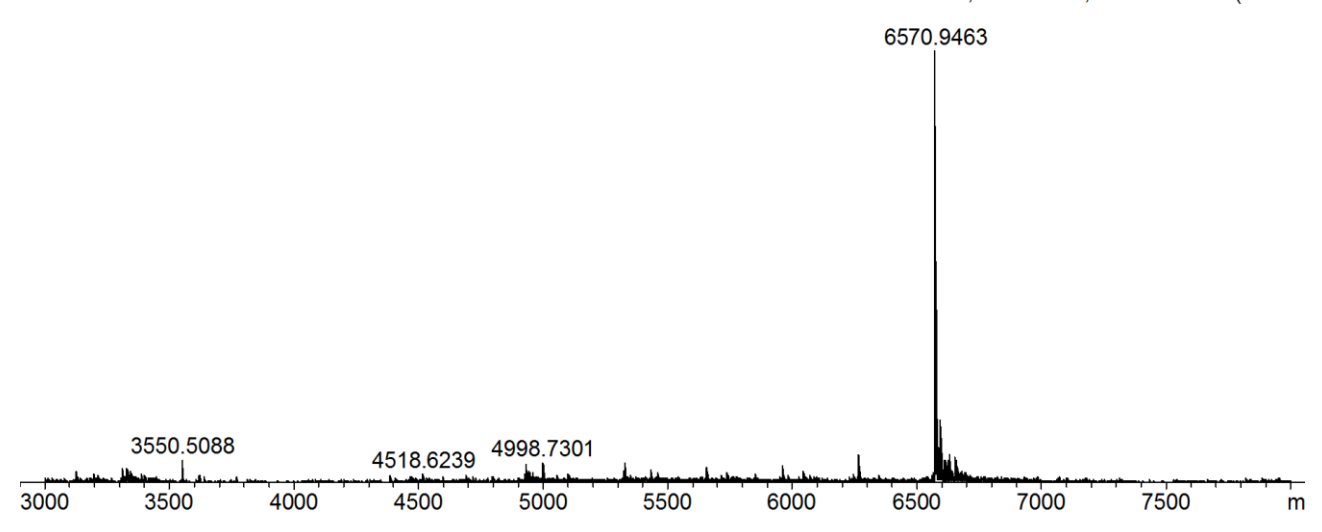


HP-atxn-1 antisense strand

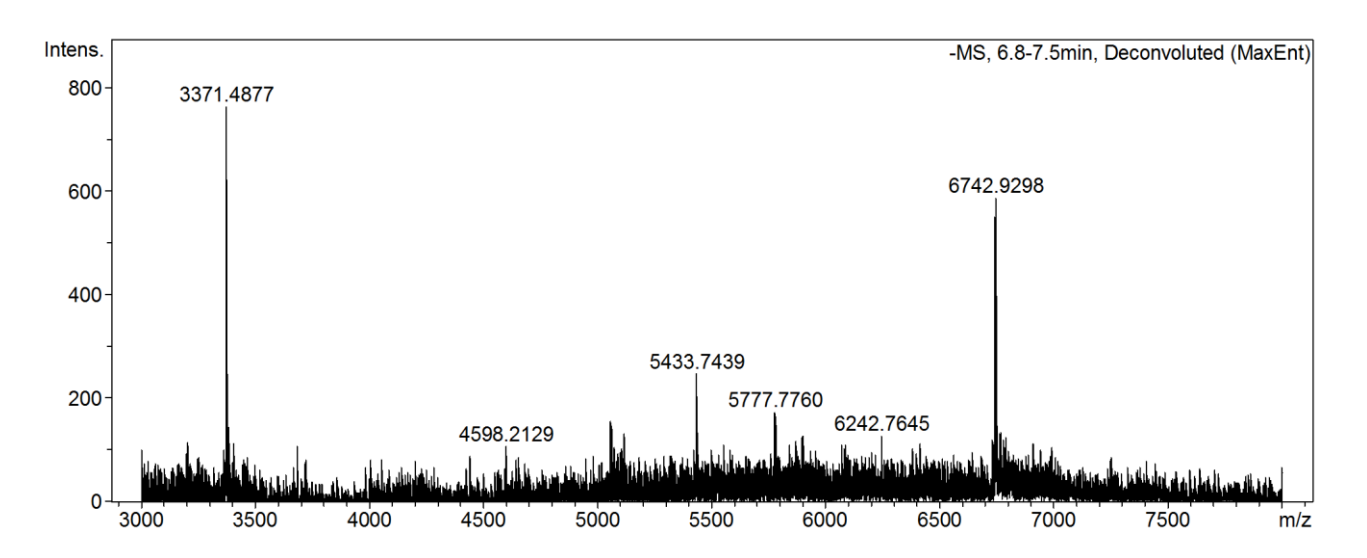


HP-A33-5sense strand

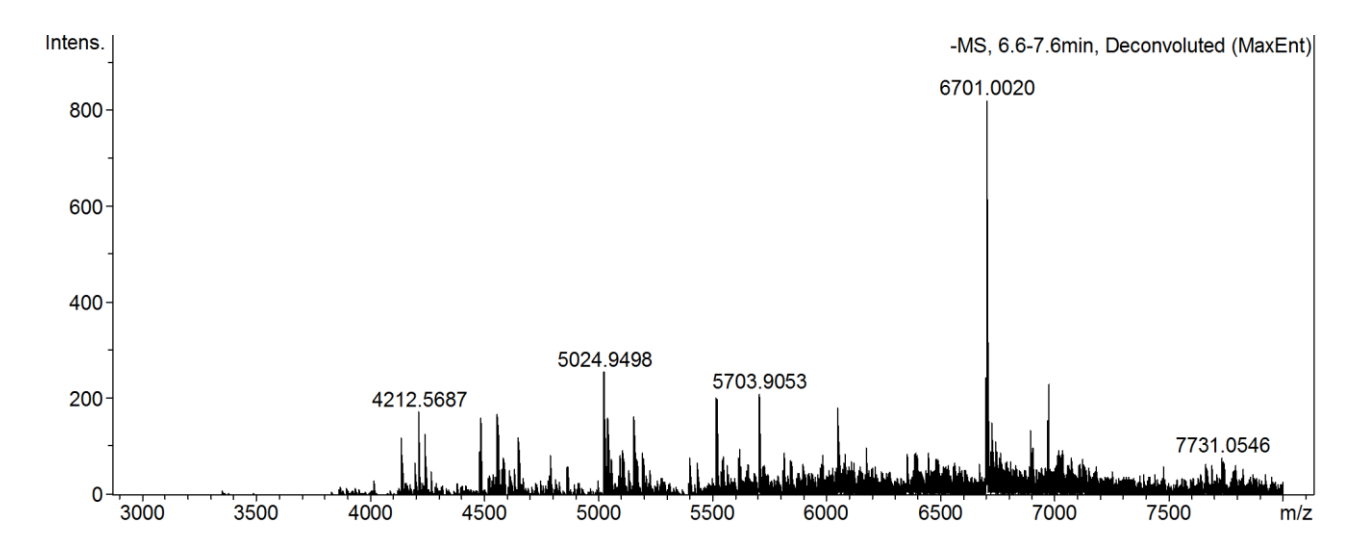
-MS, 6.8-7.4min, Deconvoluted (MaxEn



HP-A33-5 antisense strand

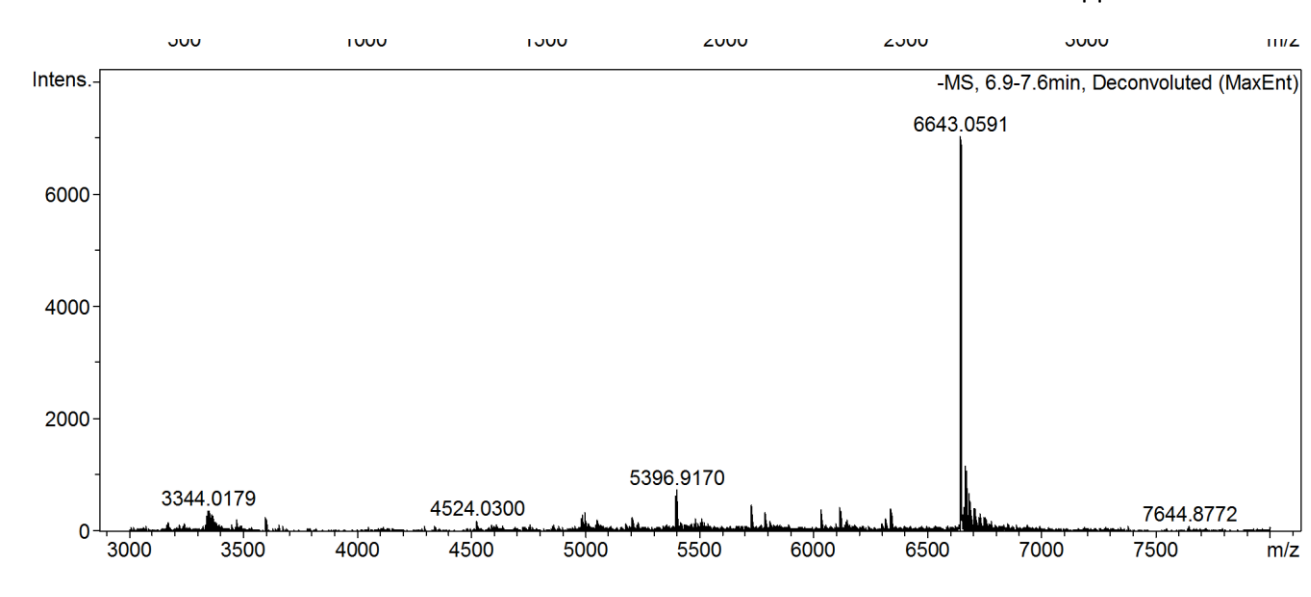


HP-A33-6 sense strand

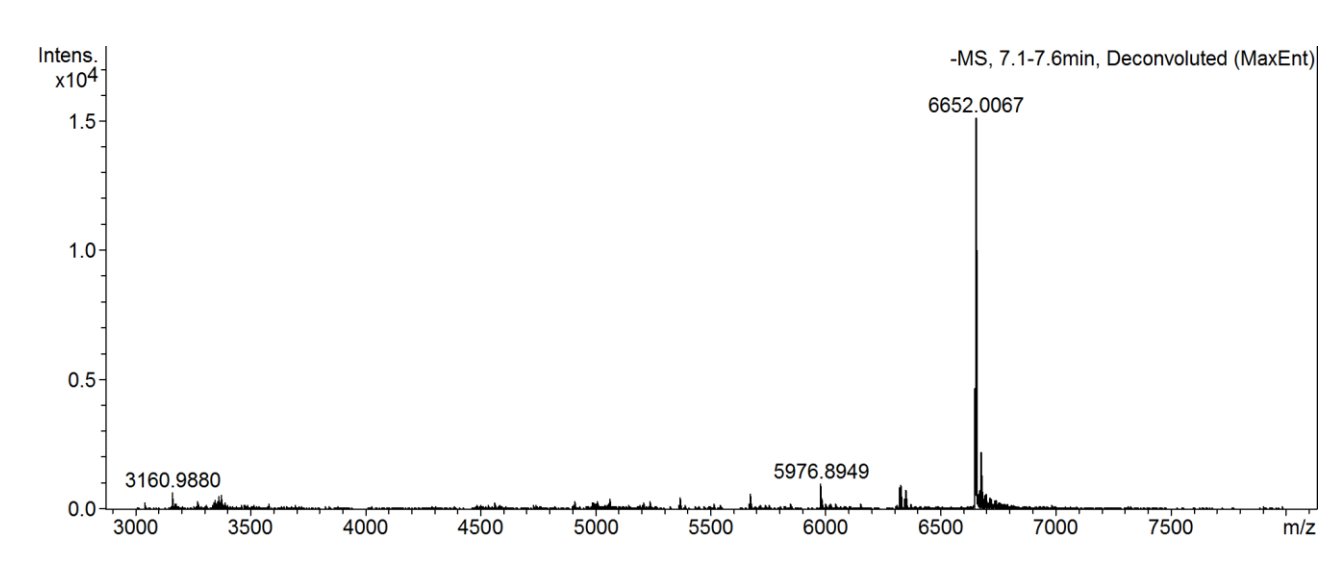


HP-A33-6 antisense strand

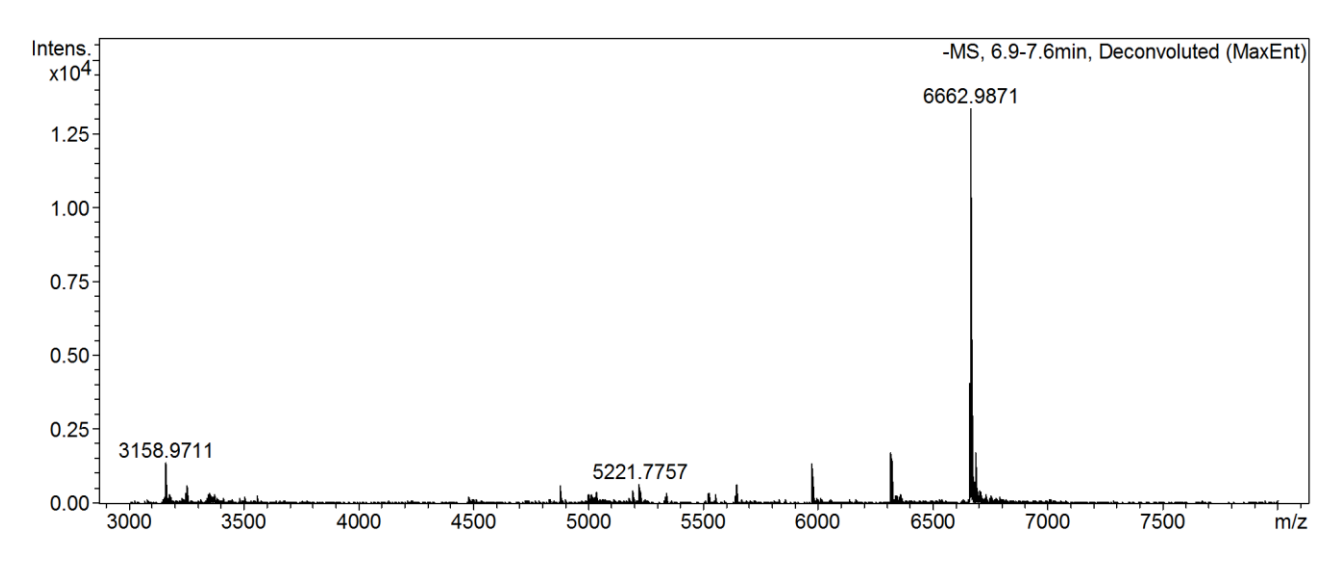
Appendix E



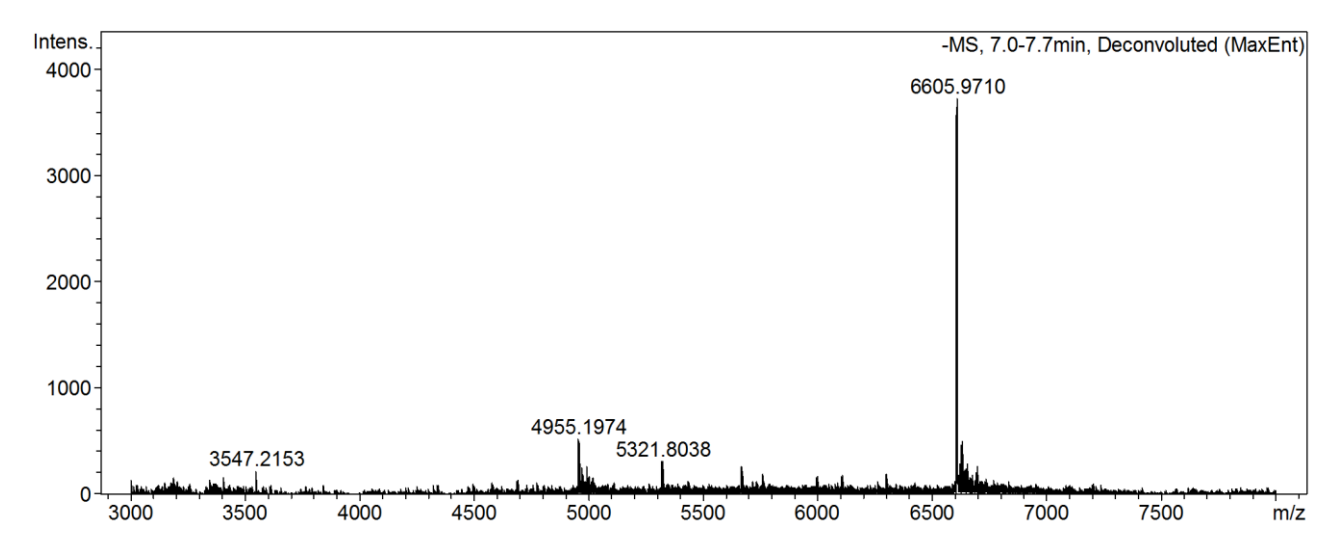
HP-A33-7 sense strand



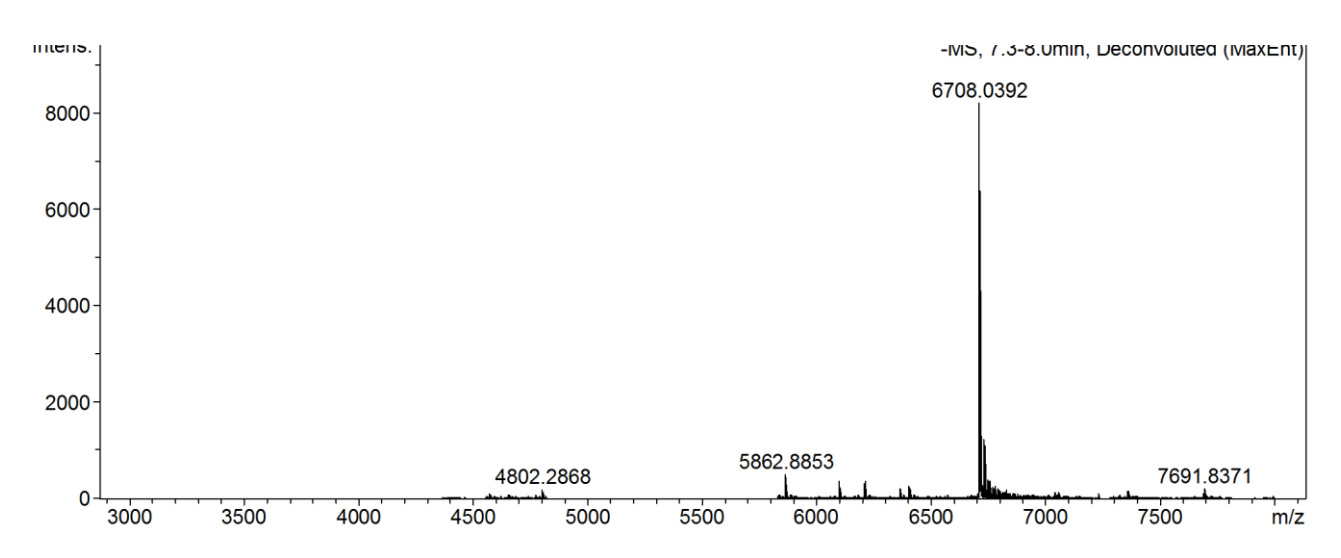
HP-A33-7 antisense strand



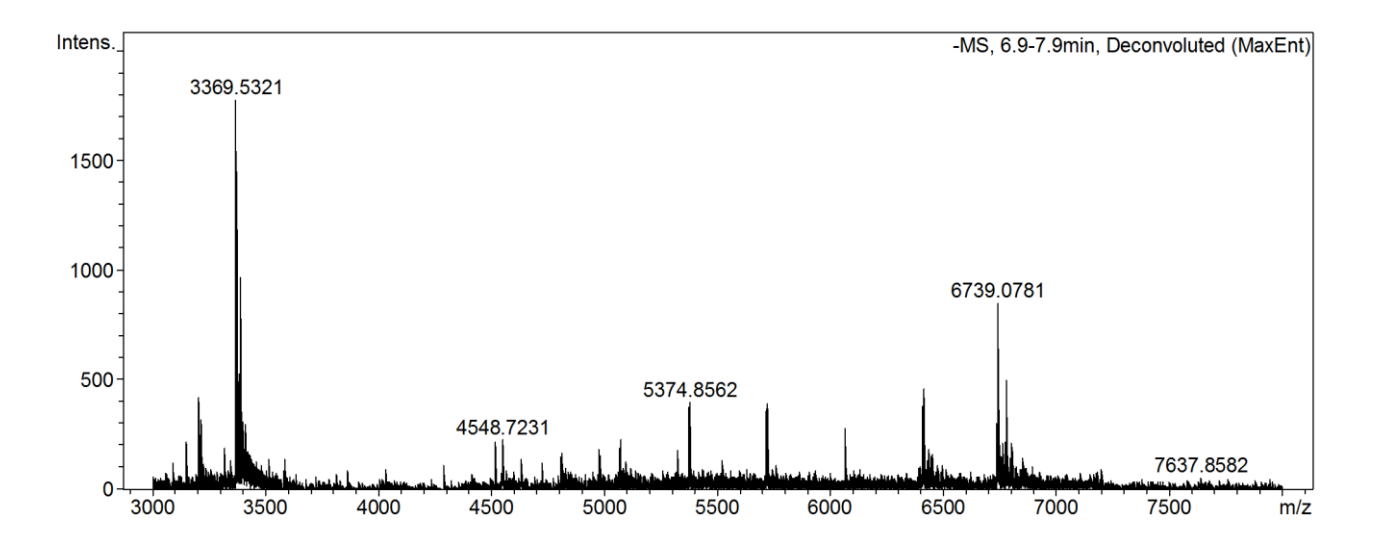
HP-A33-8 sense strand



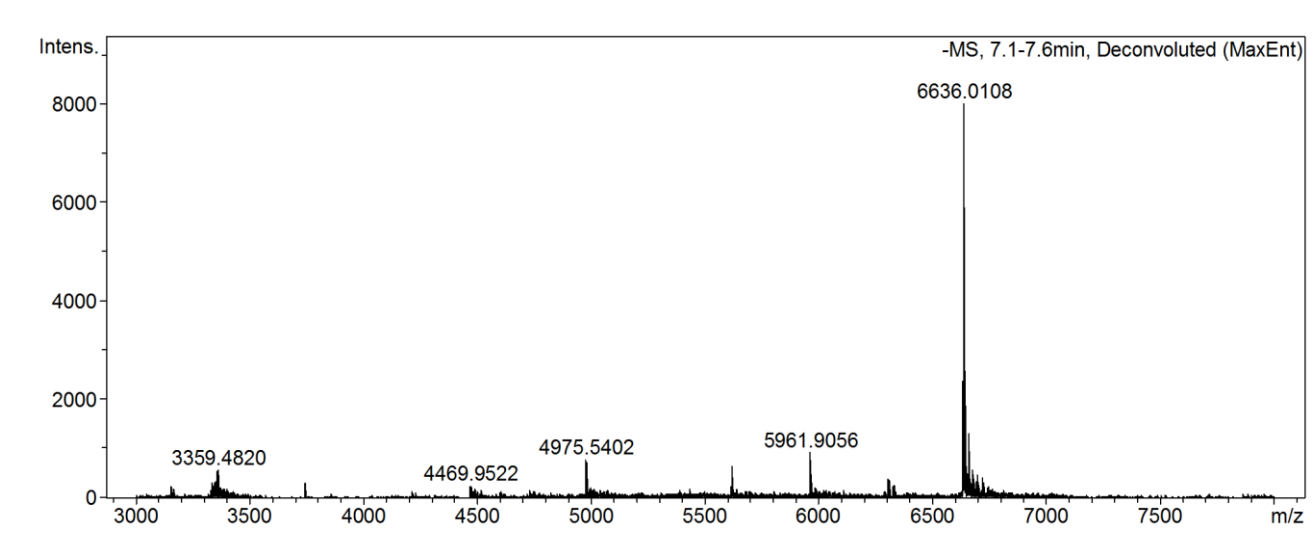
HP-A33-8 antisense strand



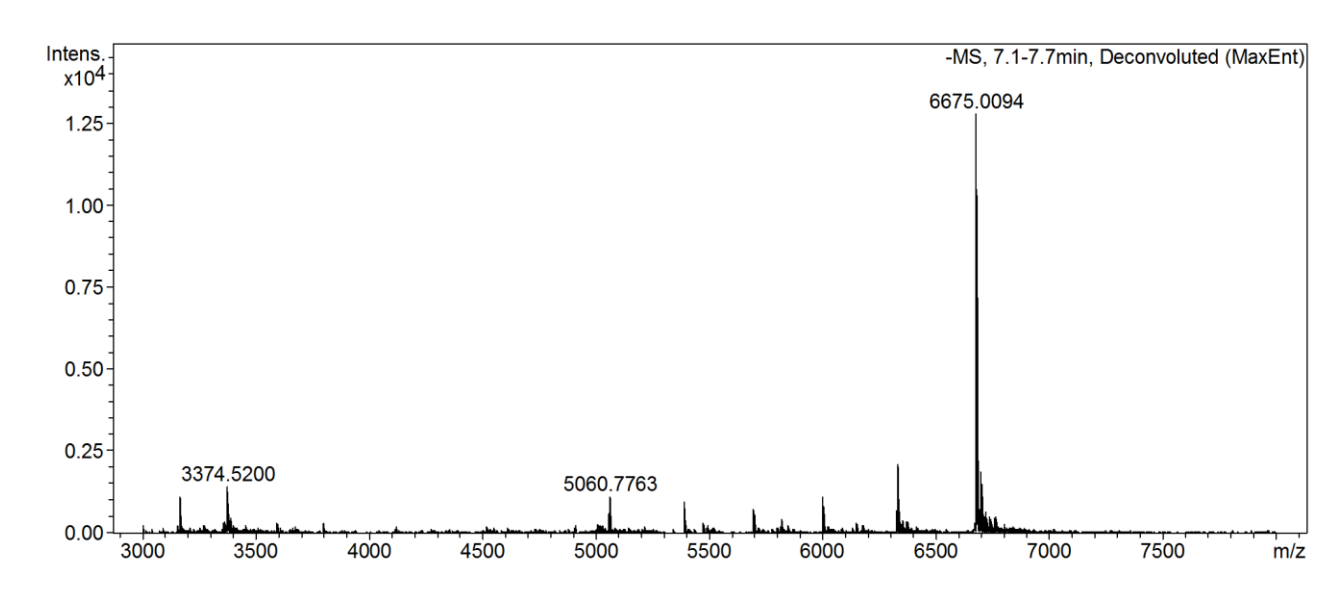
HP-A33-9 sense strand



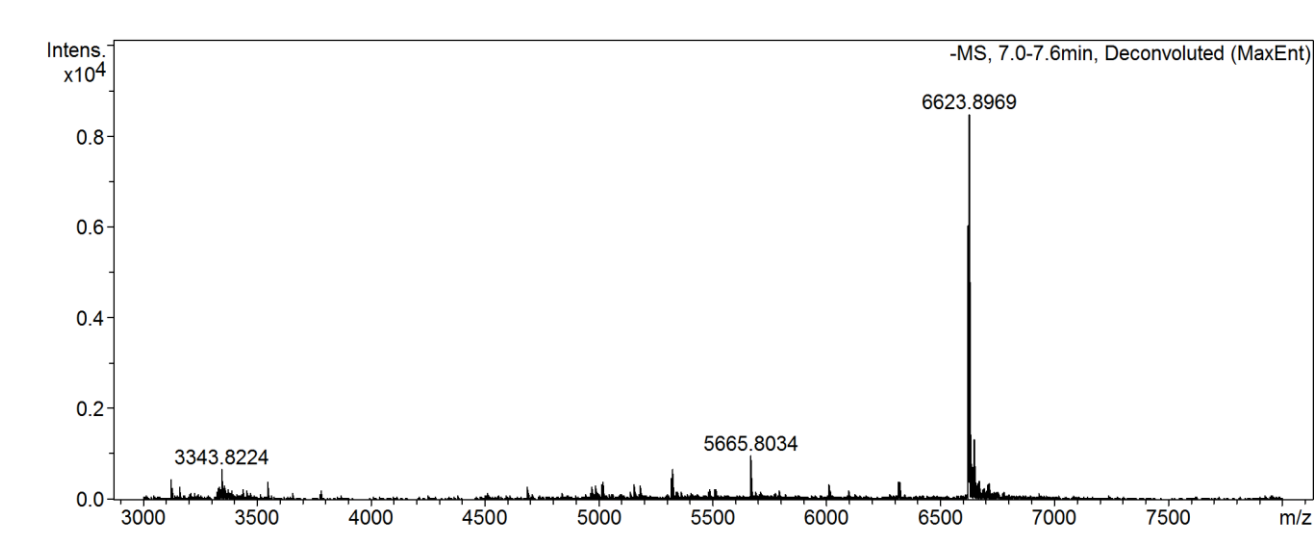
HP-A33-9 antisense strand



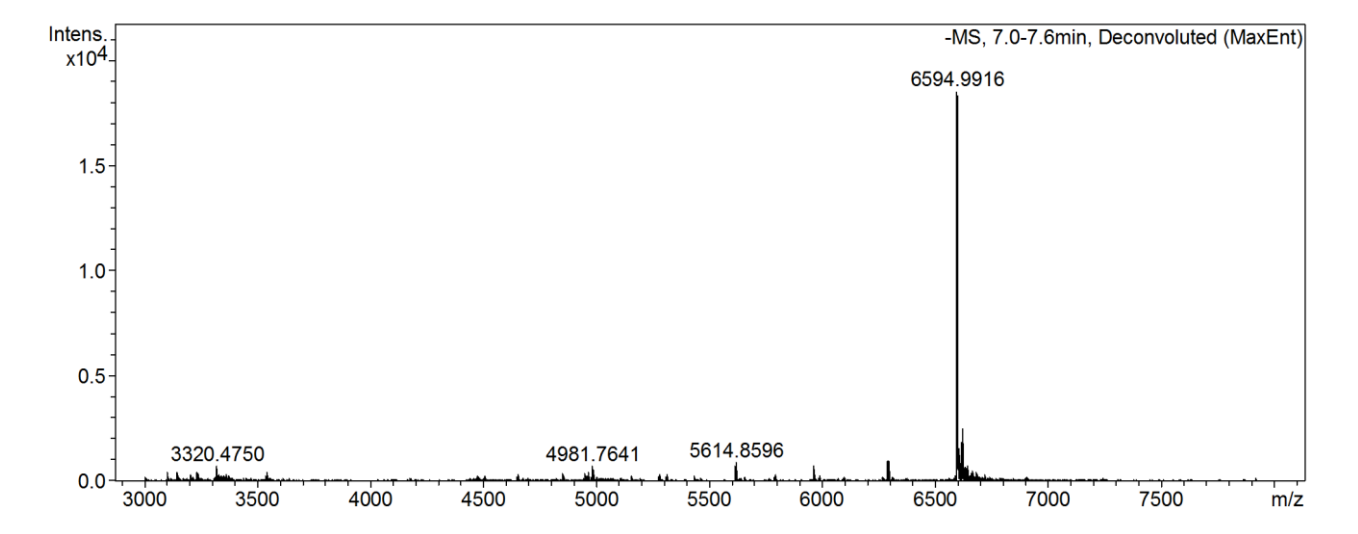
HP-A33-10 sense strand



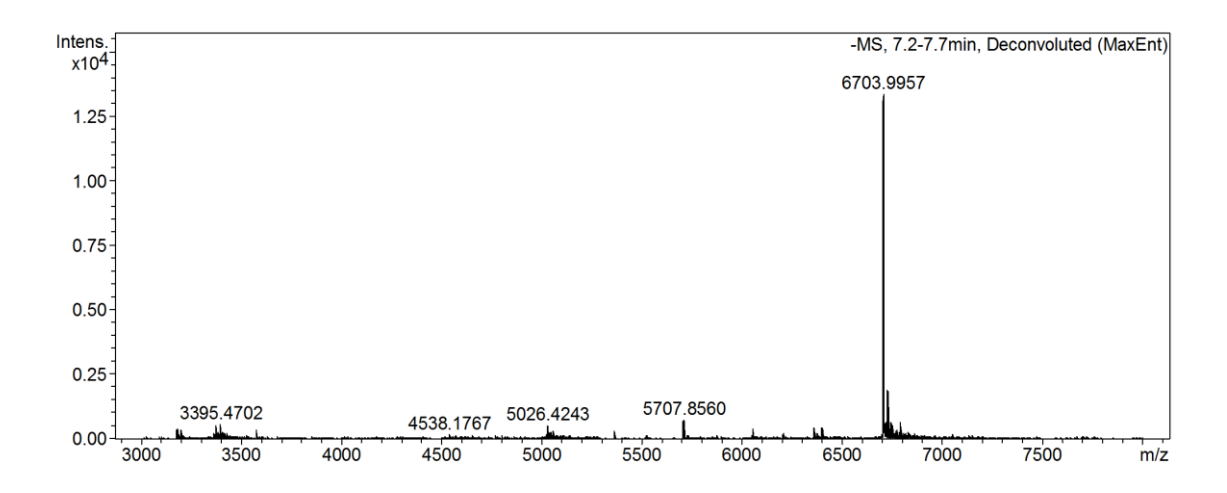
HP-A33-10 antisense strand



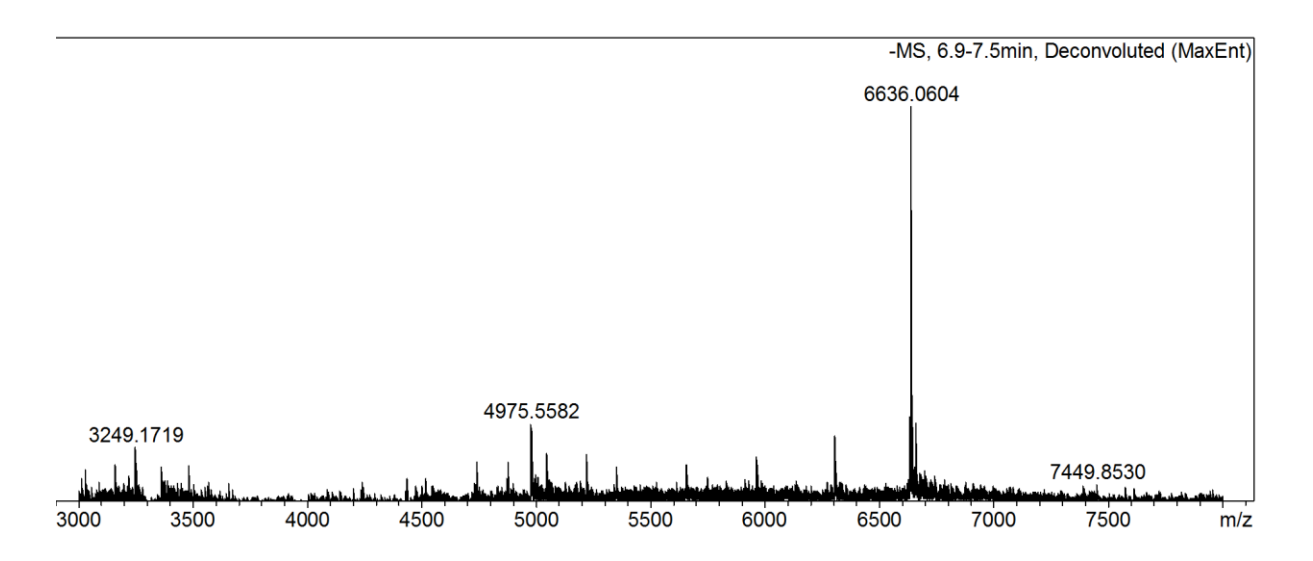
HP-A33-11sense strand



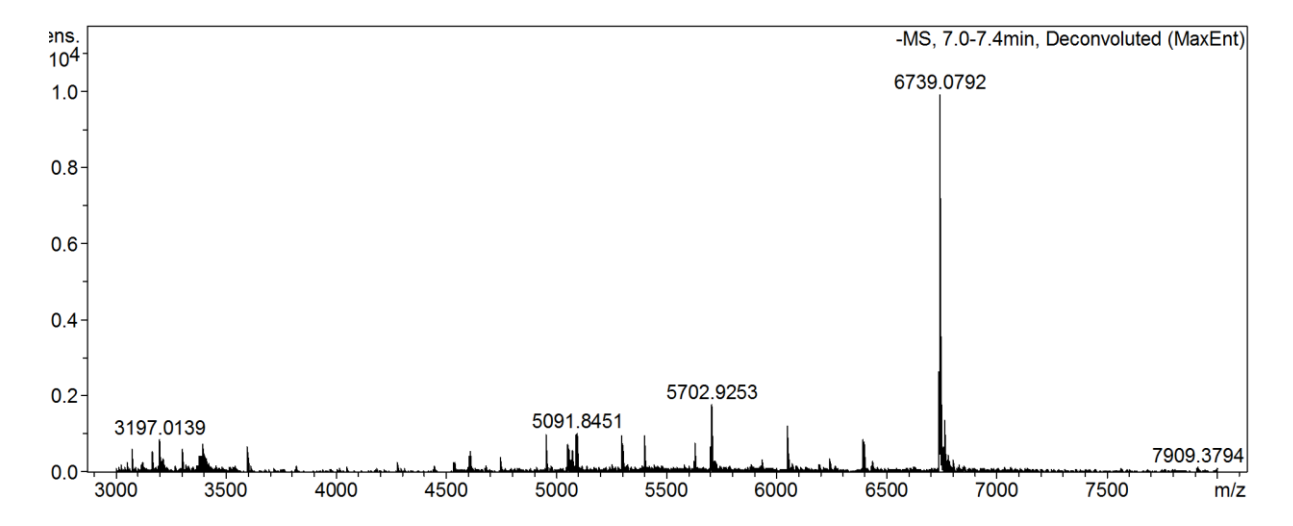
HP-A33-11 antisense strand



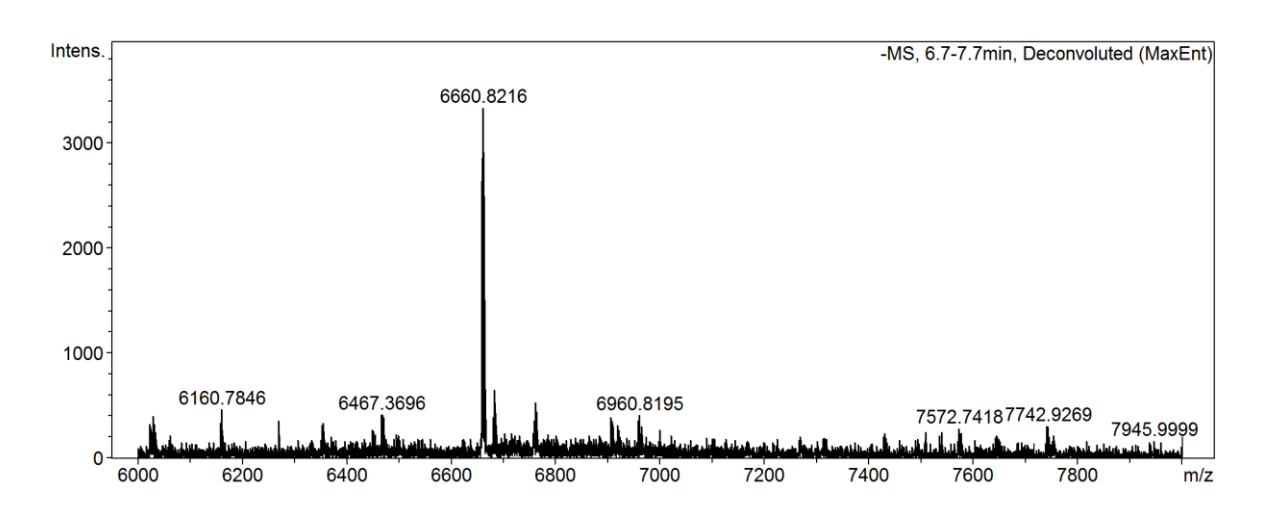
Scr sense strand



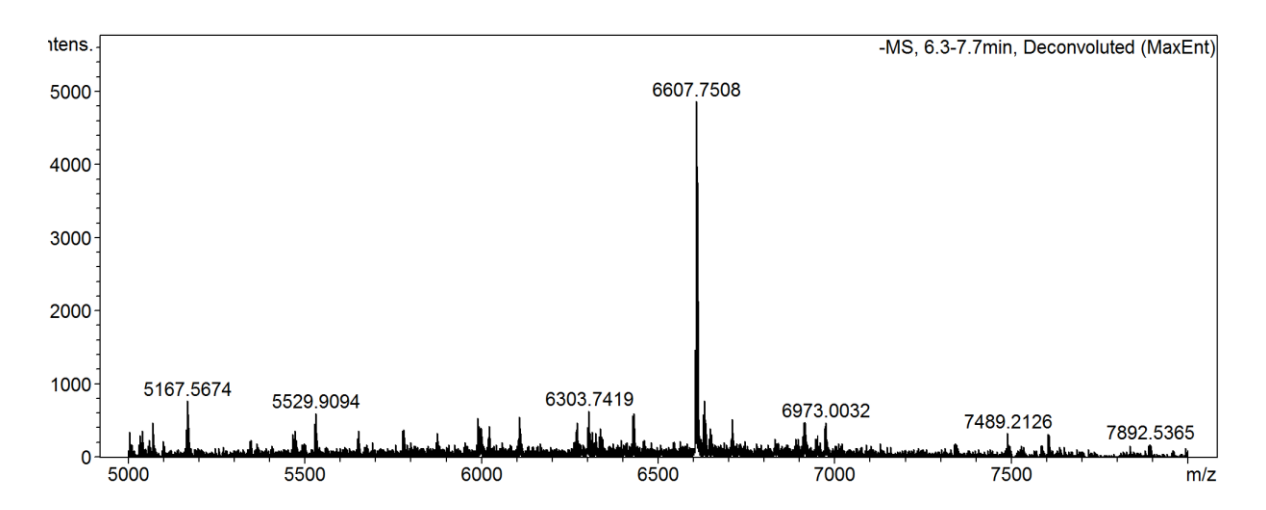
Scr antisense strand



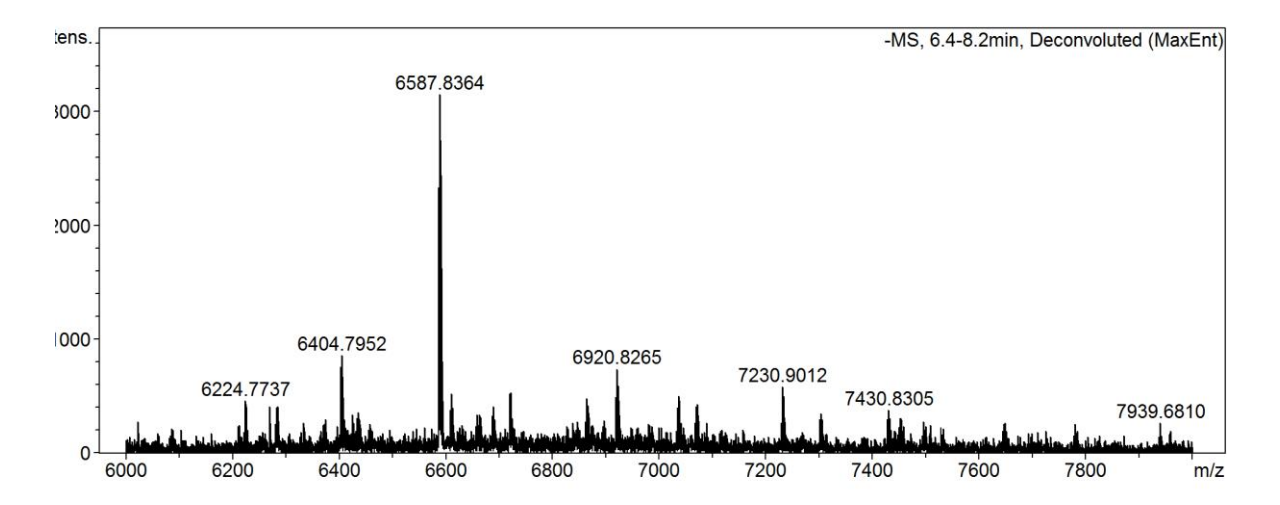
HP-12 sense



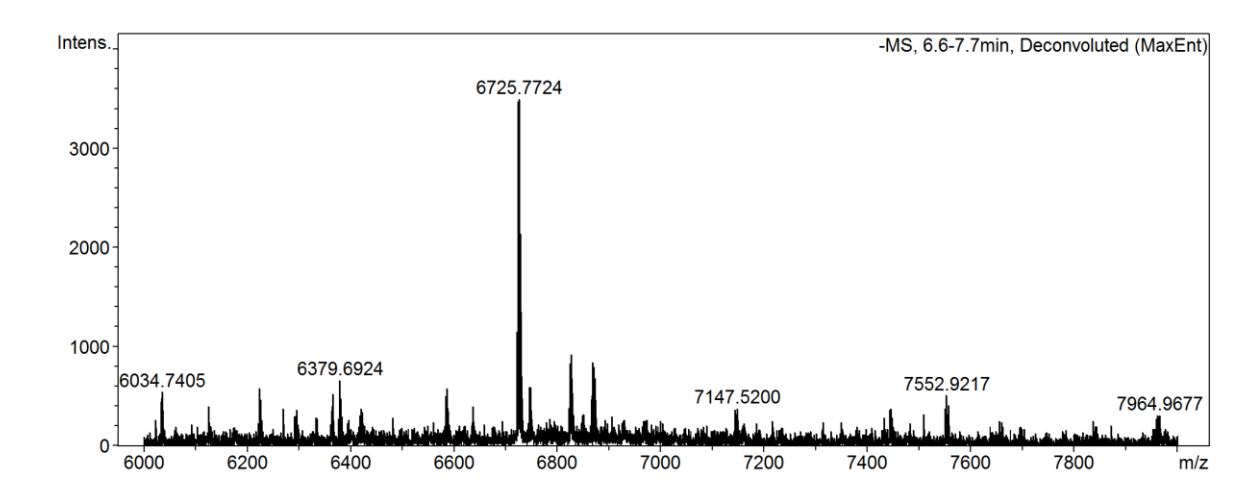
HP-12 antisense



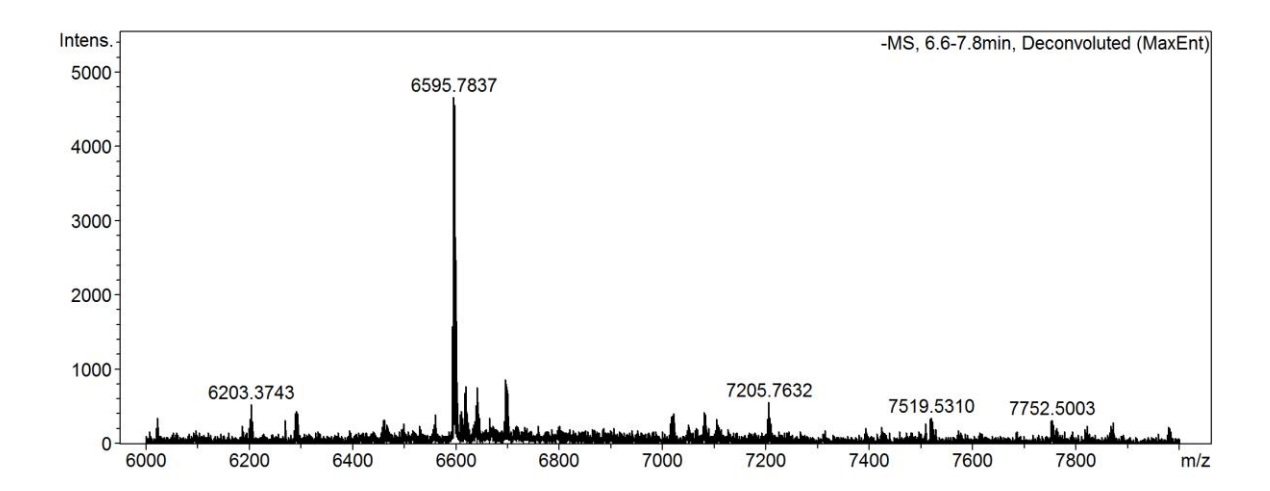
HP-13 sense



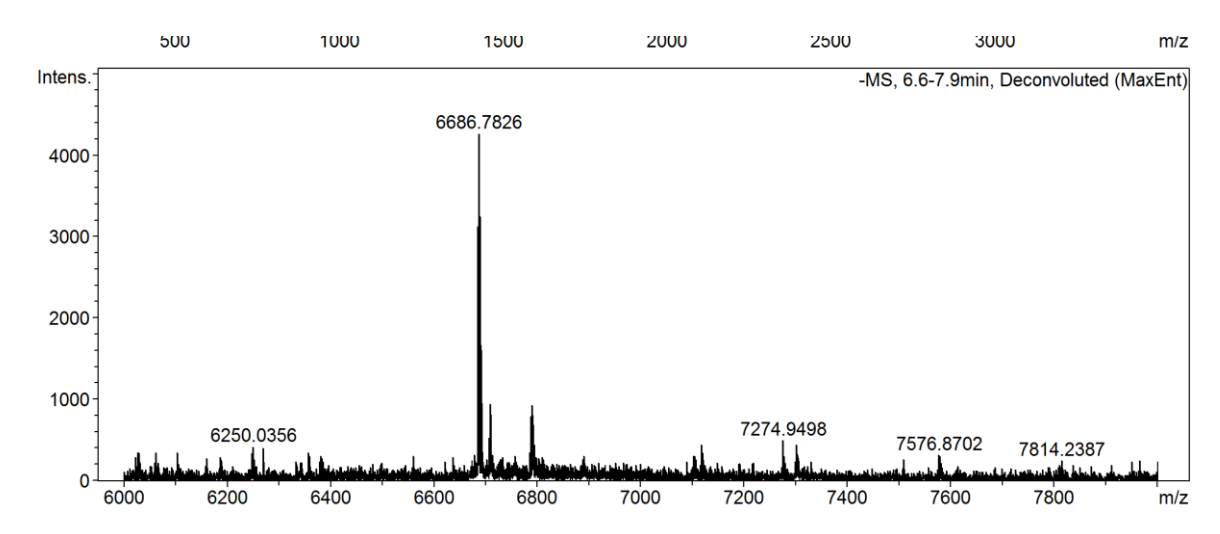
HP-13 antisense



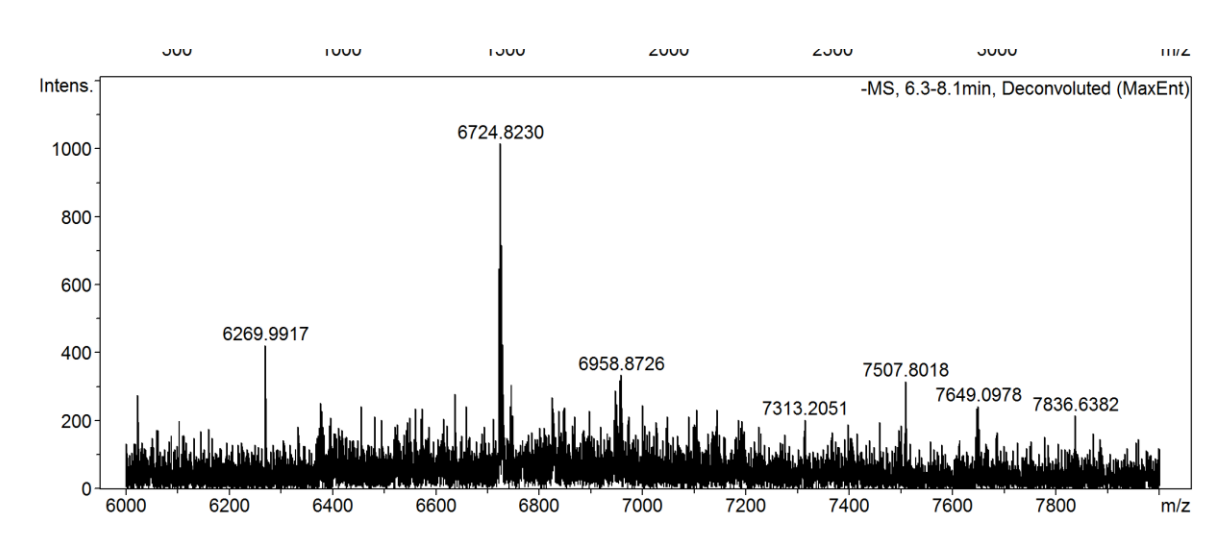
HP-14 sense



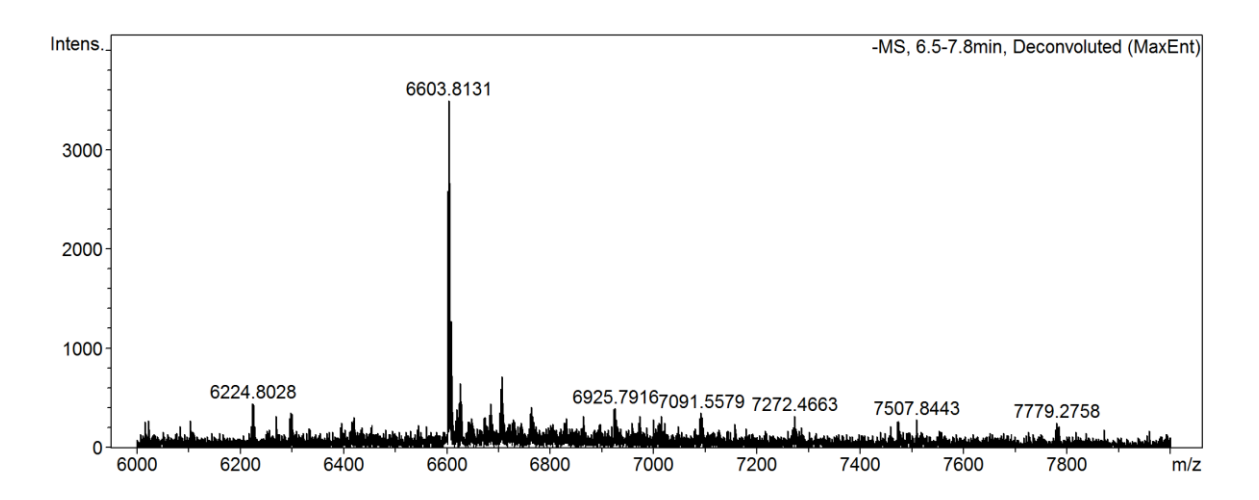
HP-14 antisense



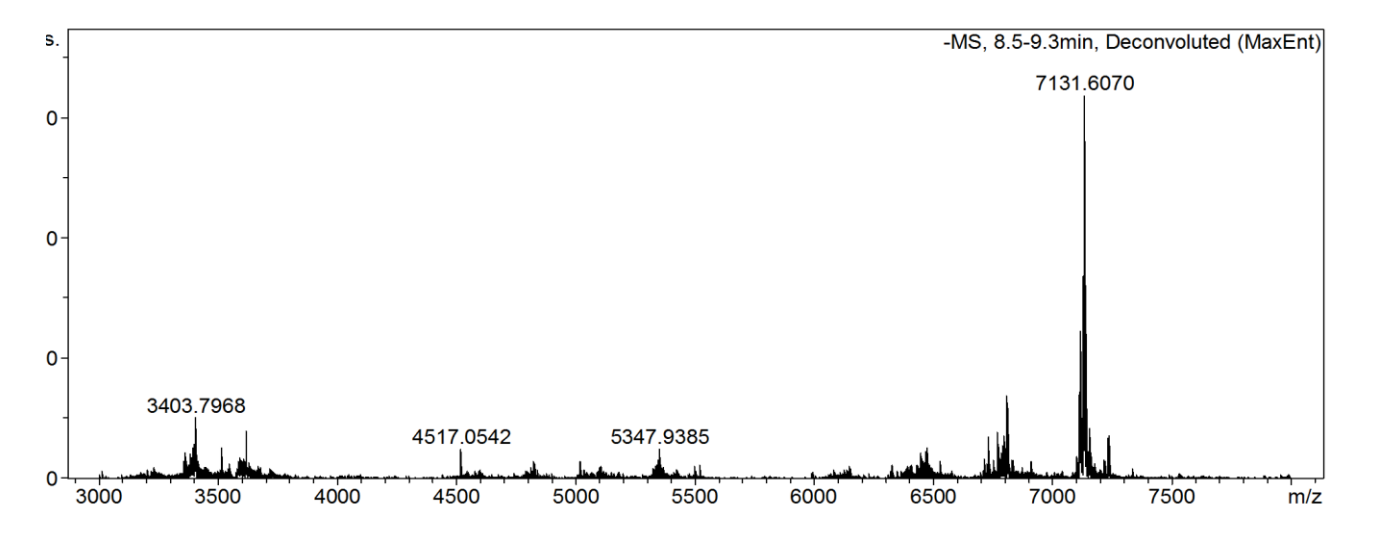
HP-15 sense



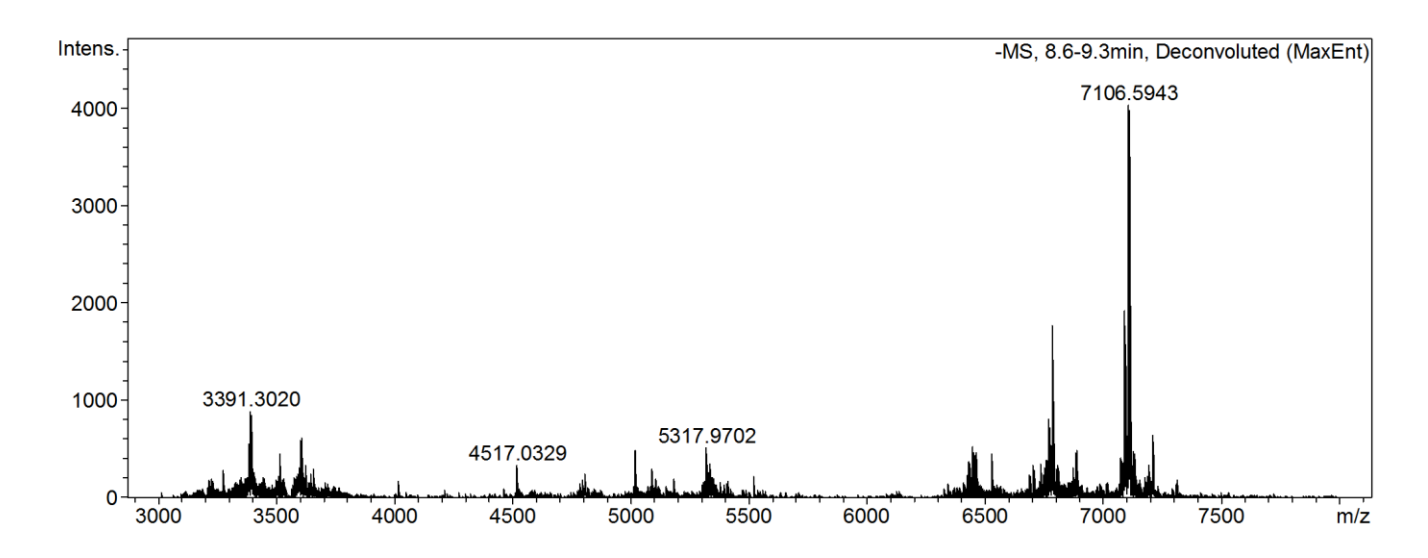
HP-15 antisense



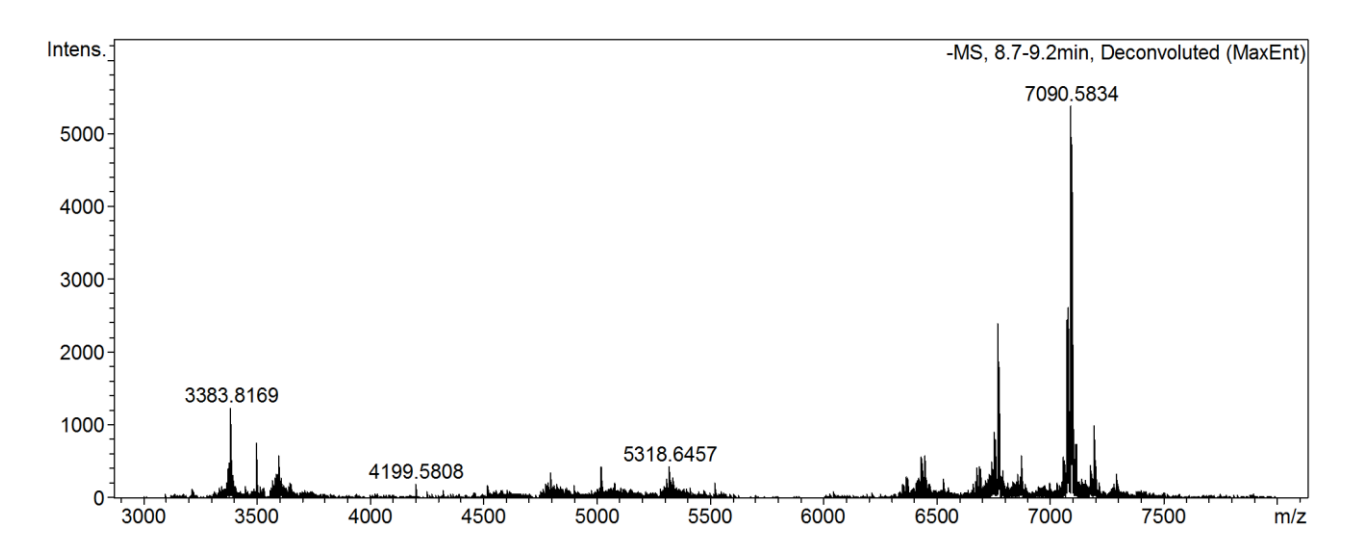
ss-A33-MOE-1



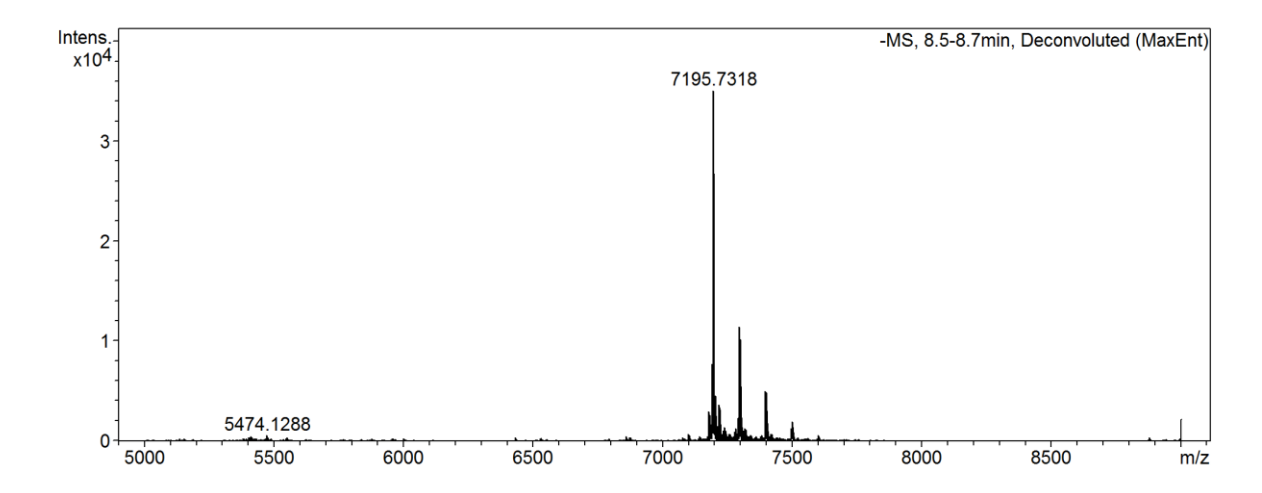
ss-HP -A33-2



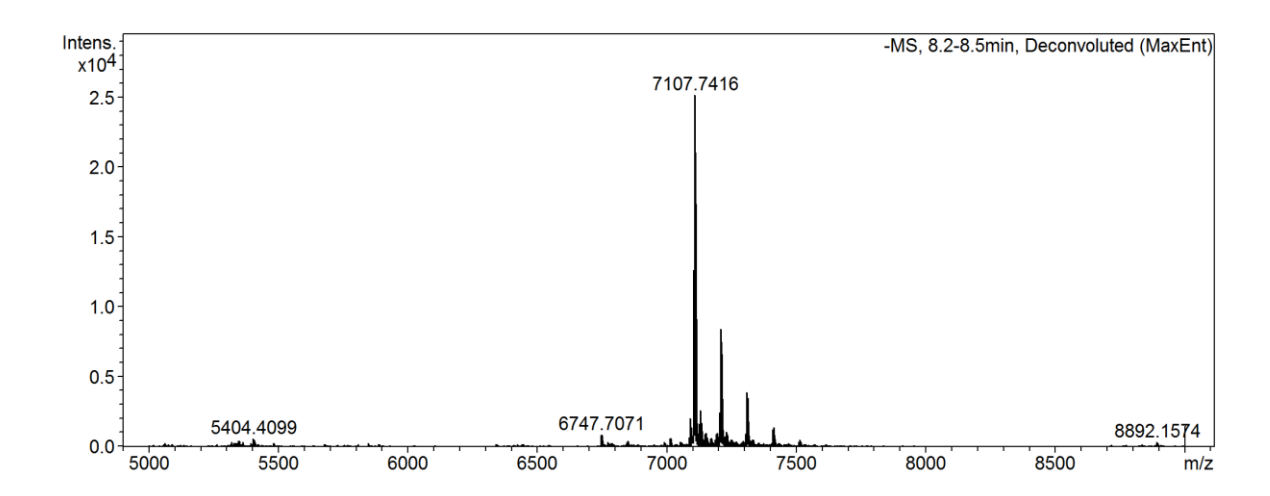
ss-HP-A33-3



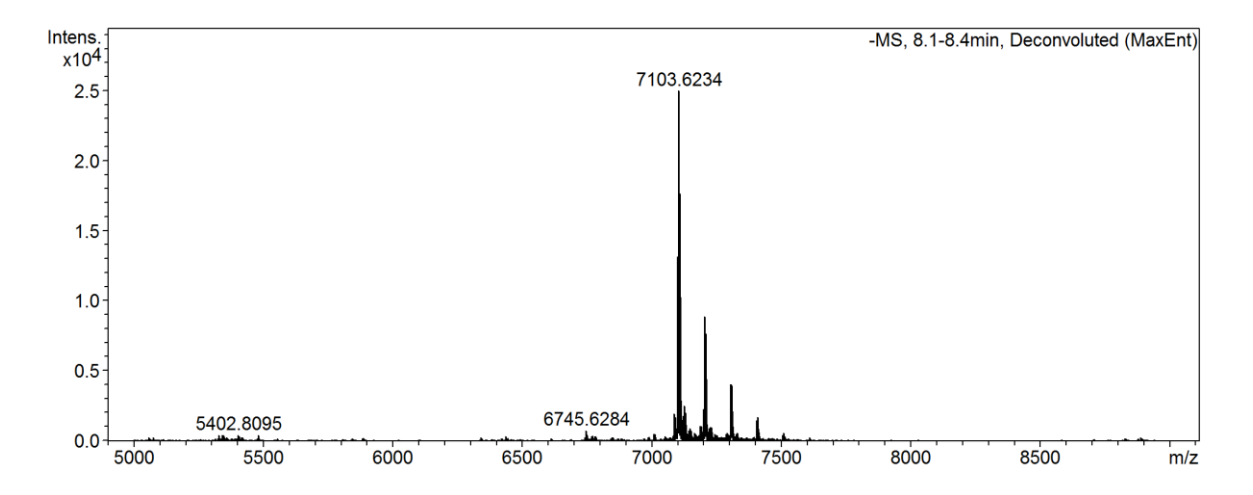
ss-A33-MOE-2



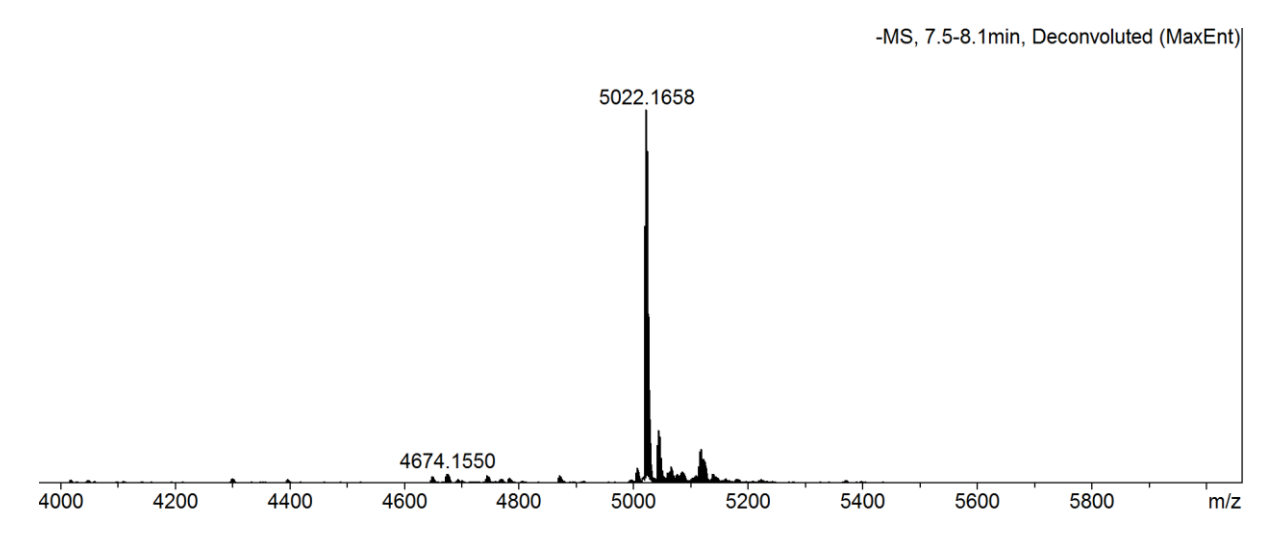
ss-A33-OMe



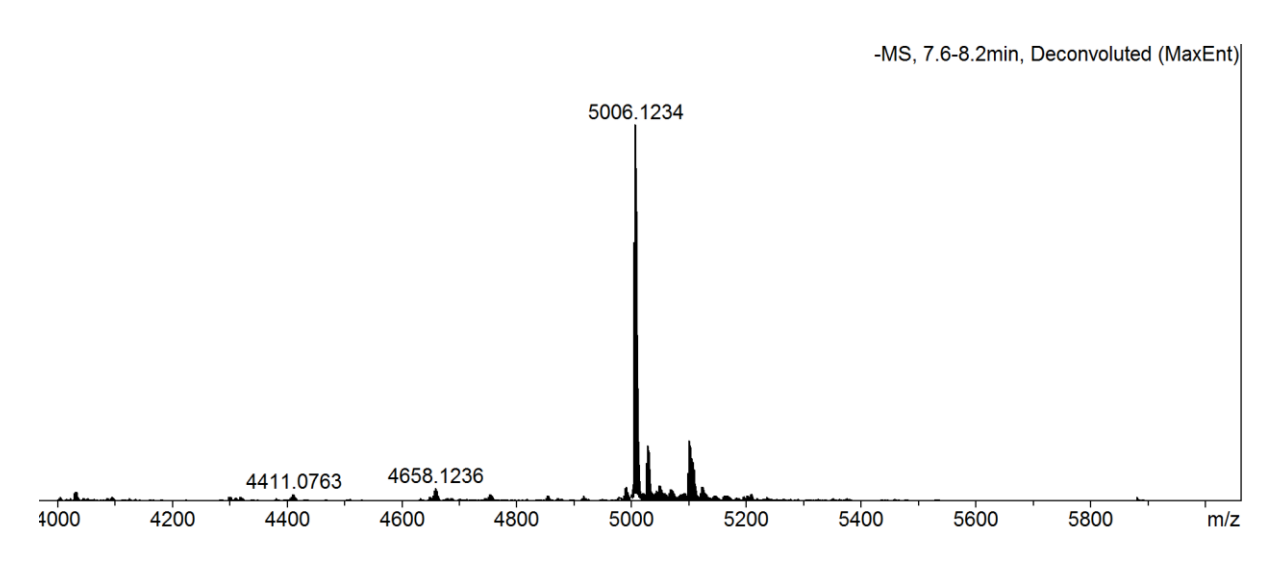
ss-A33-LNA



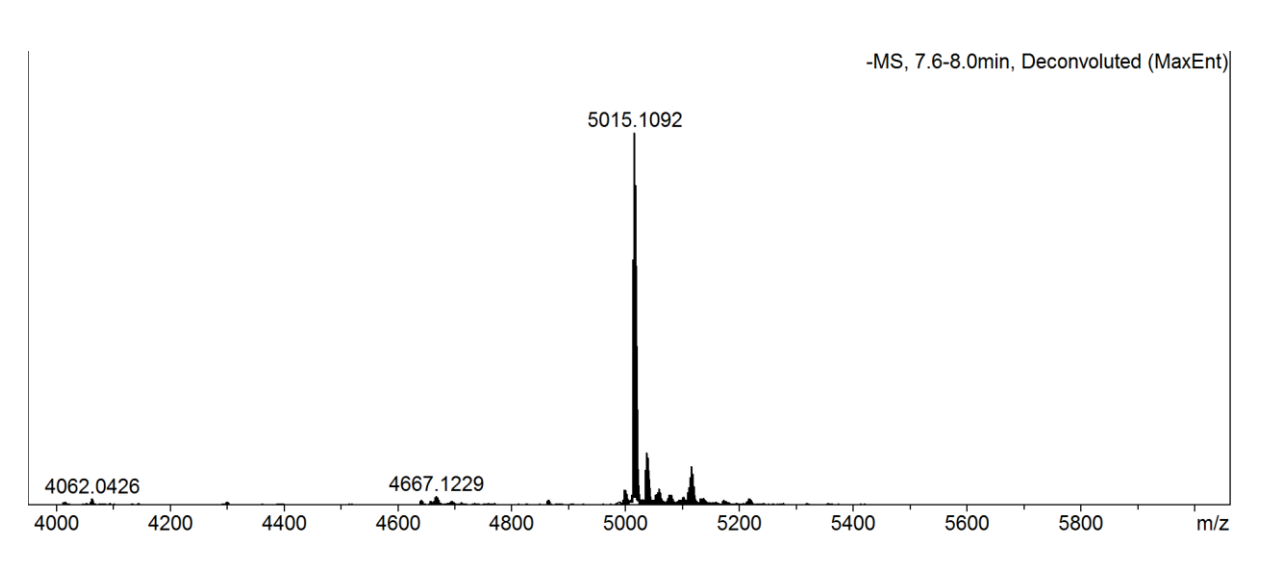
33-g with EDITH



33-h with EDITH

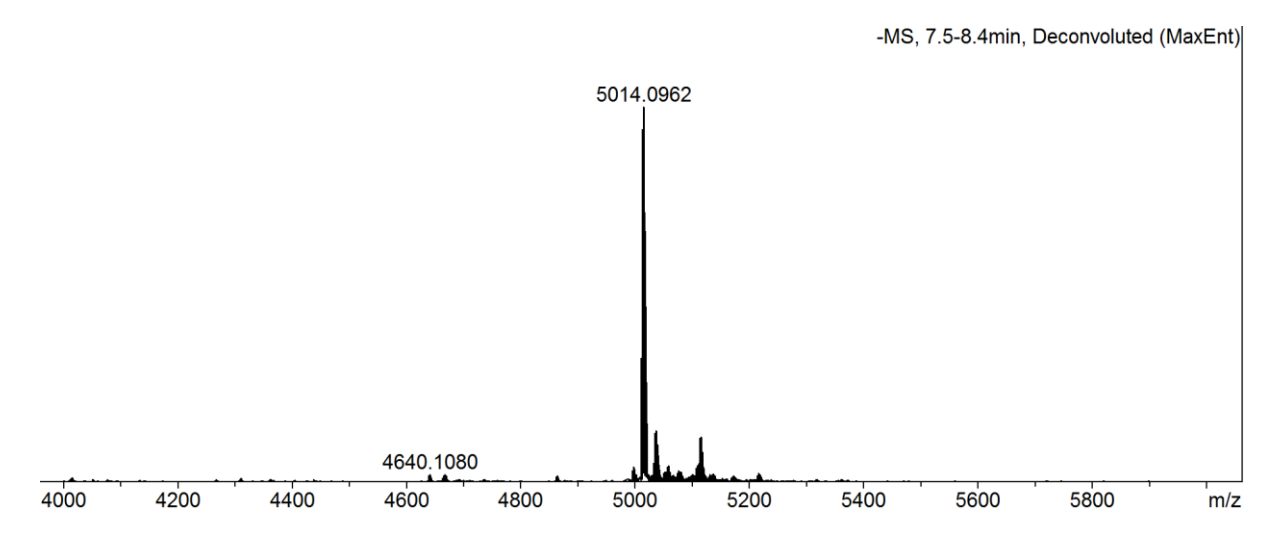


33-i with EDITH

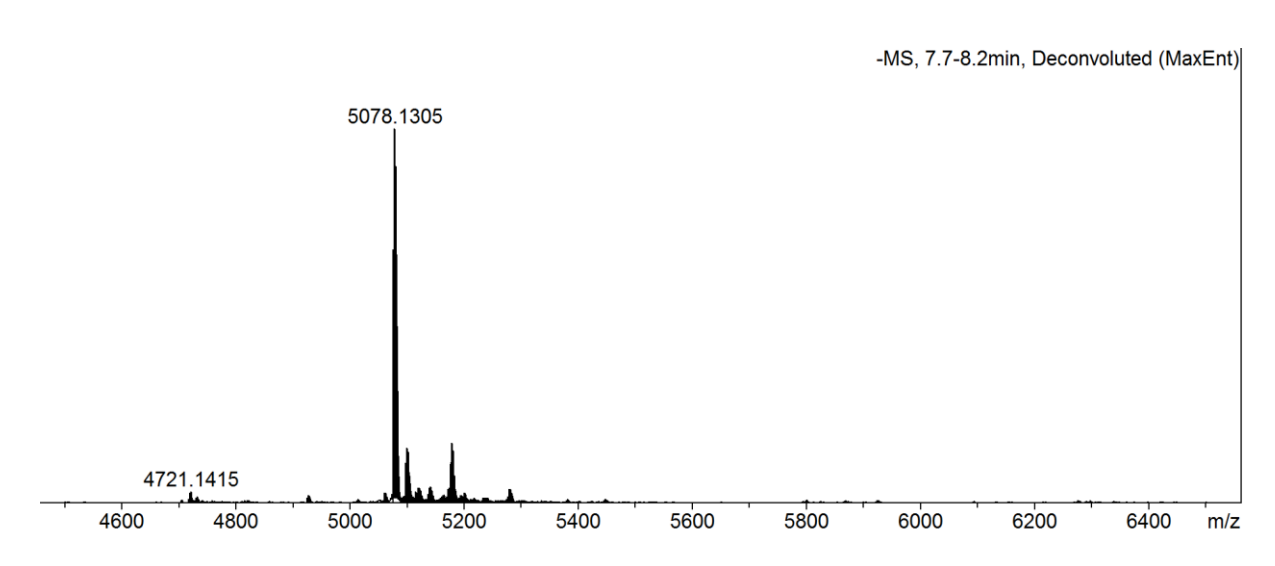


33-j with EDITH

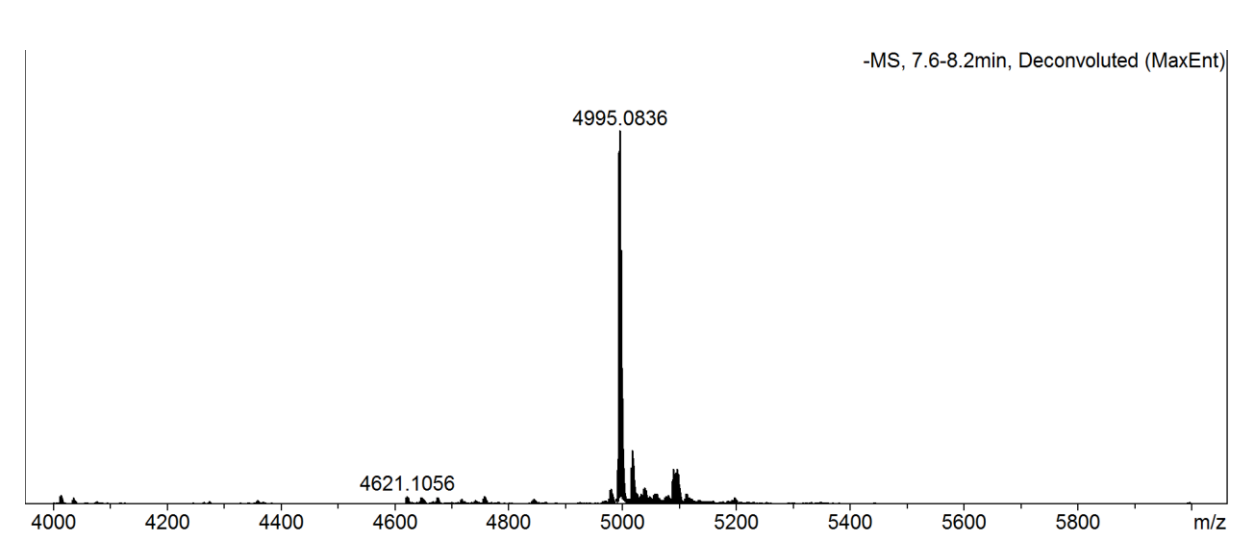
Appendix E



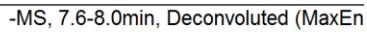
33-k with EDITH

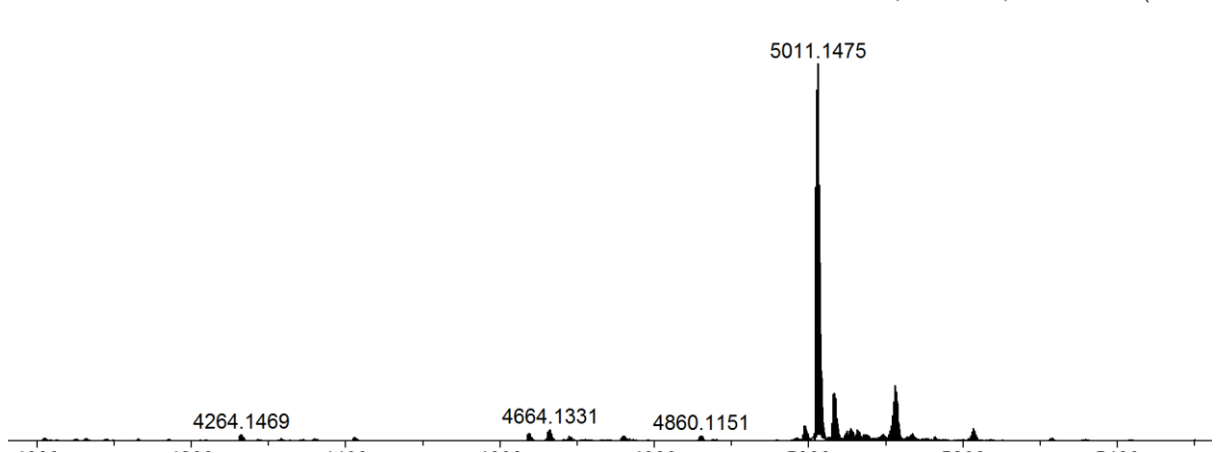


33-I with EDITH

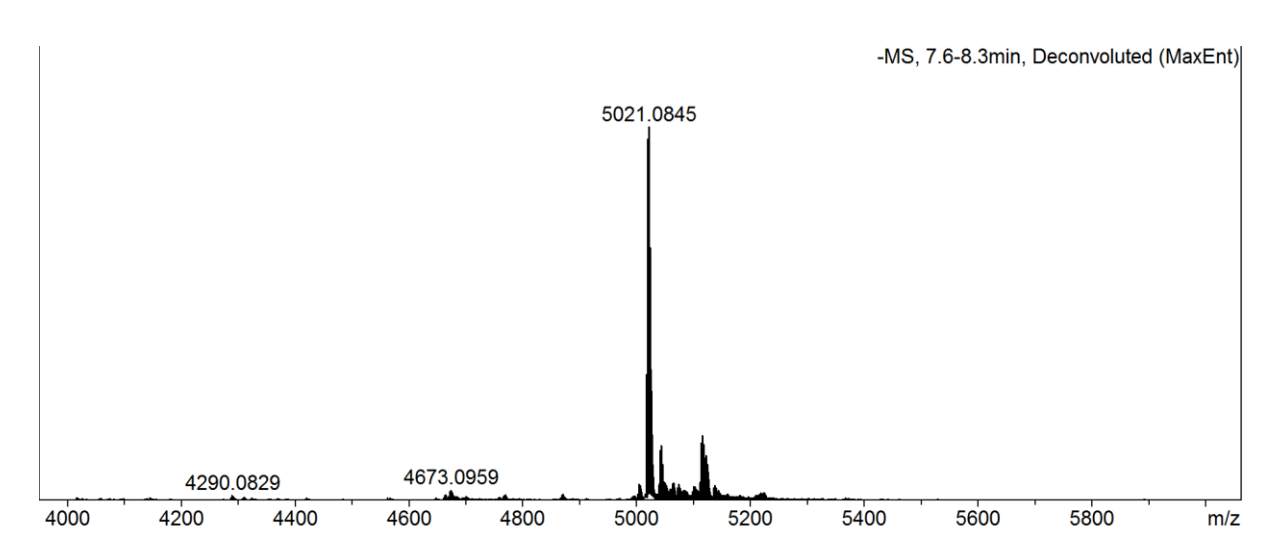


33-m with EDITH

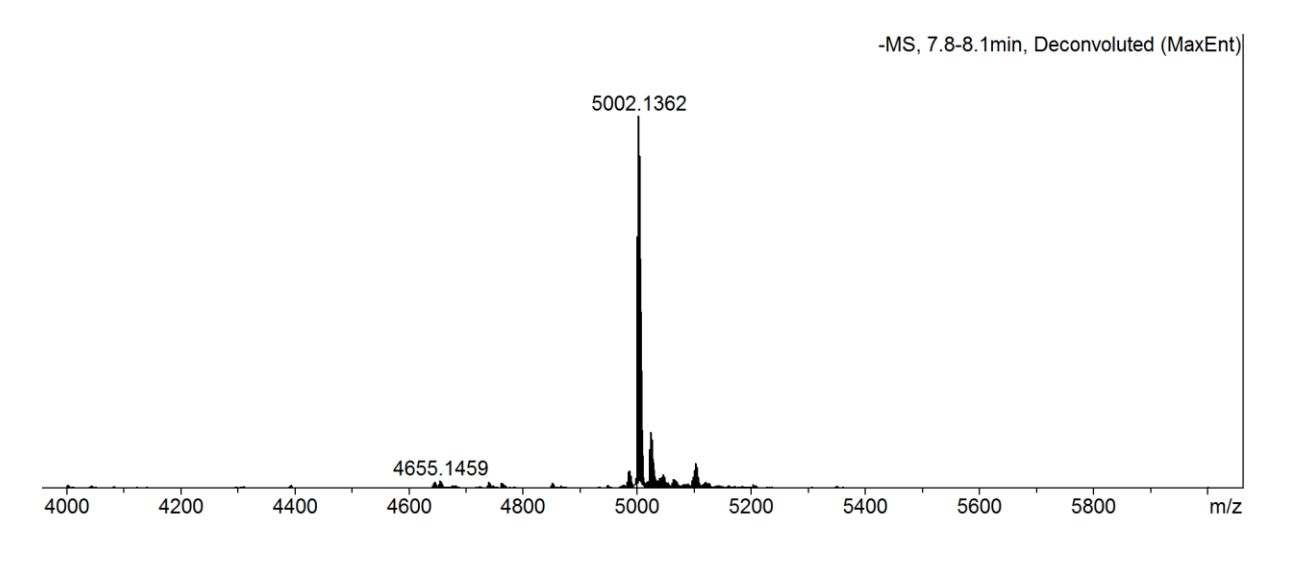




33-n with EDITH

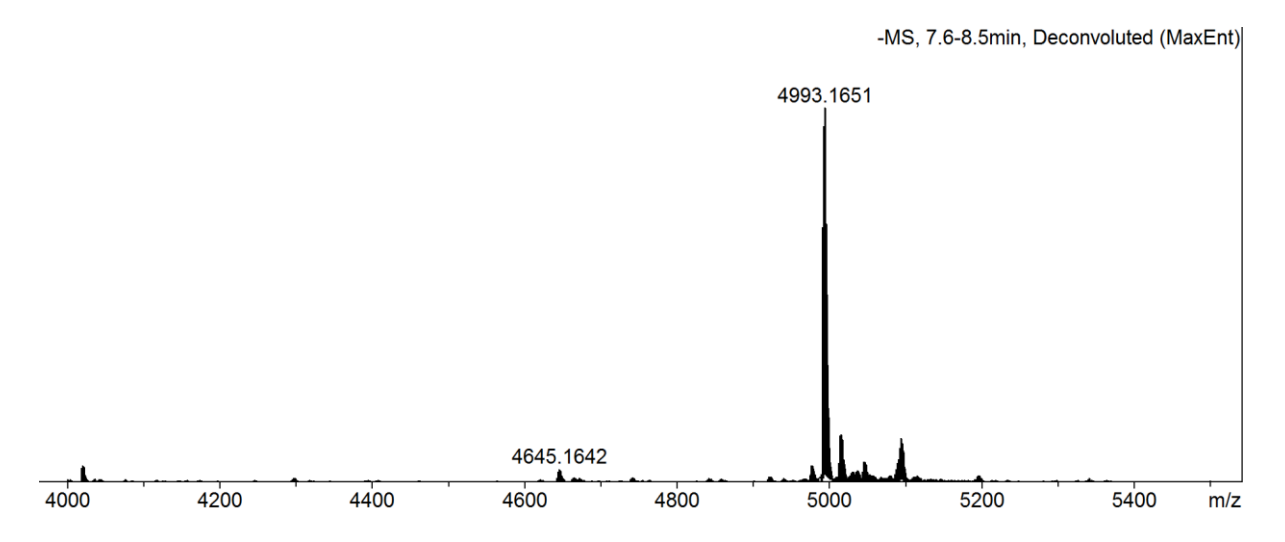


33-o with EDITH

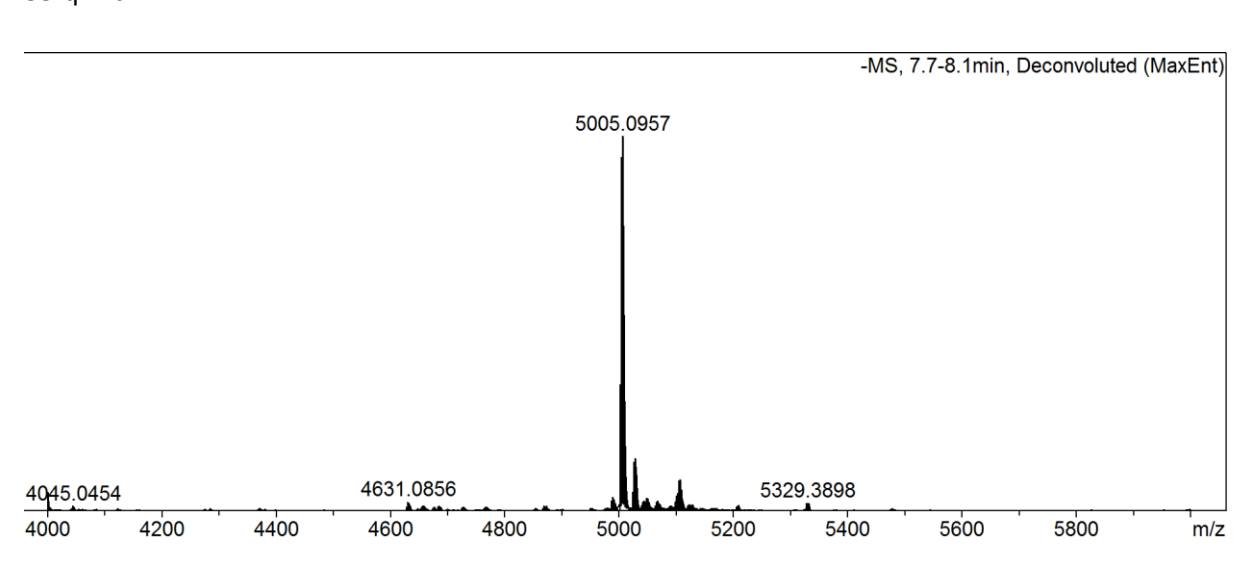


33-p with EDITH

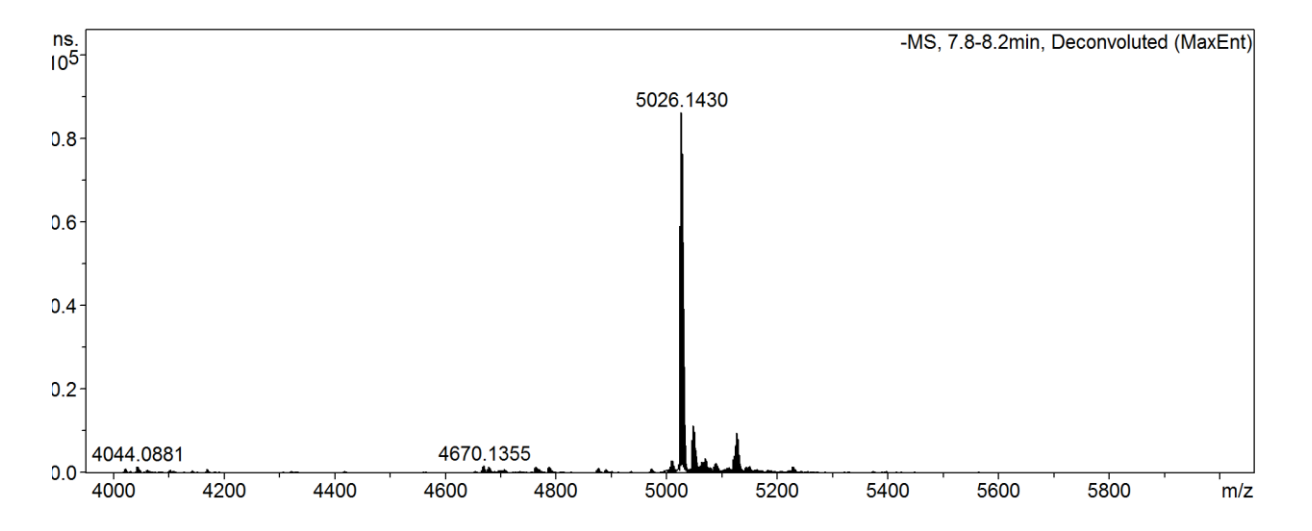
Appendix E



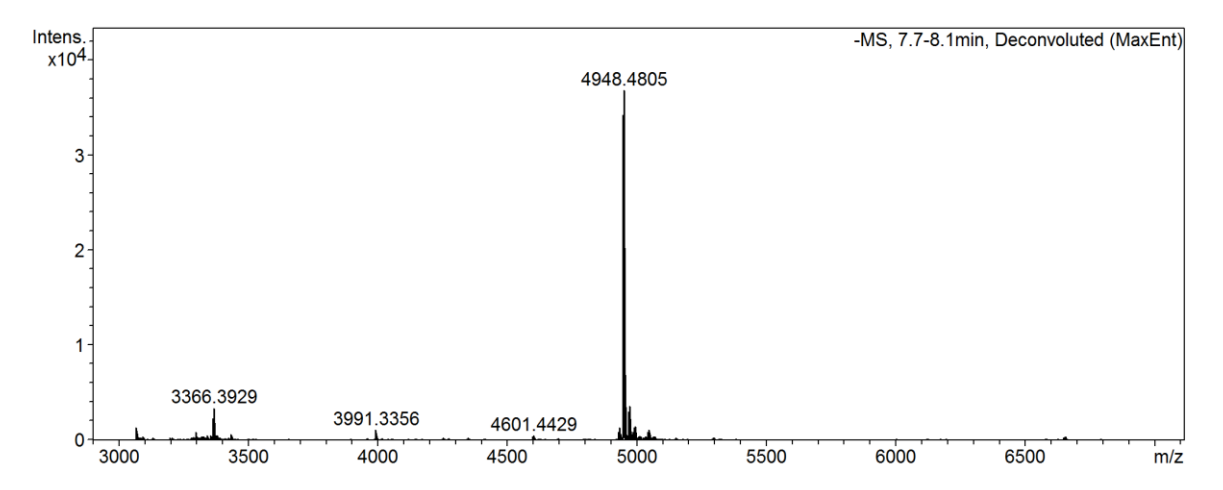
33-q with EDITH



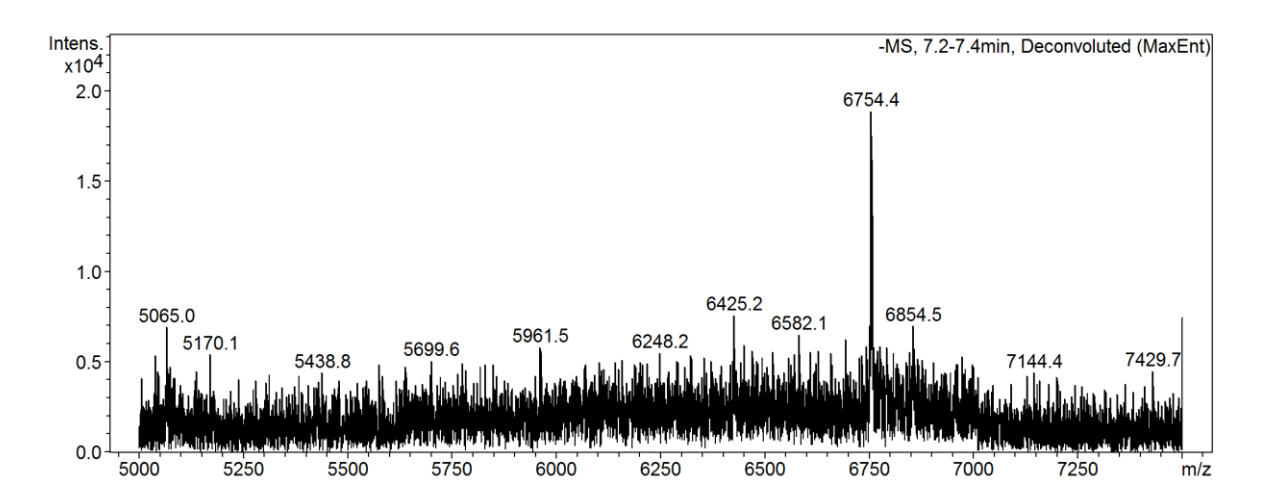
33-r with EDITH



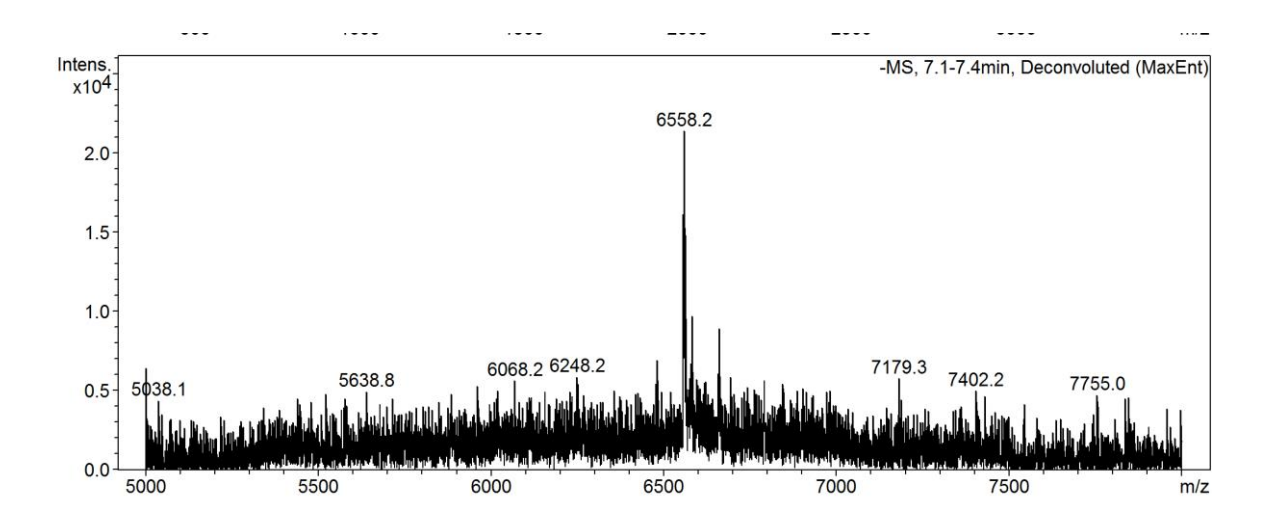
Lna ctrl



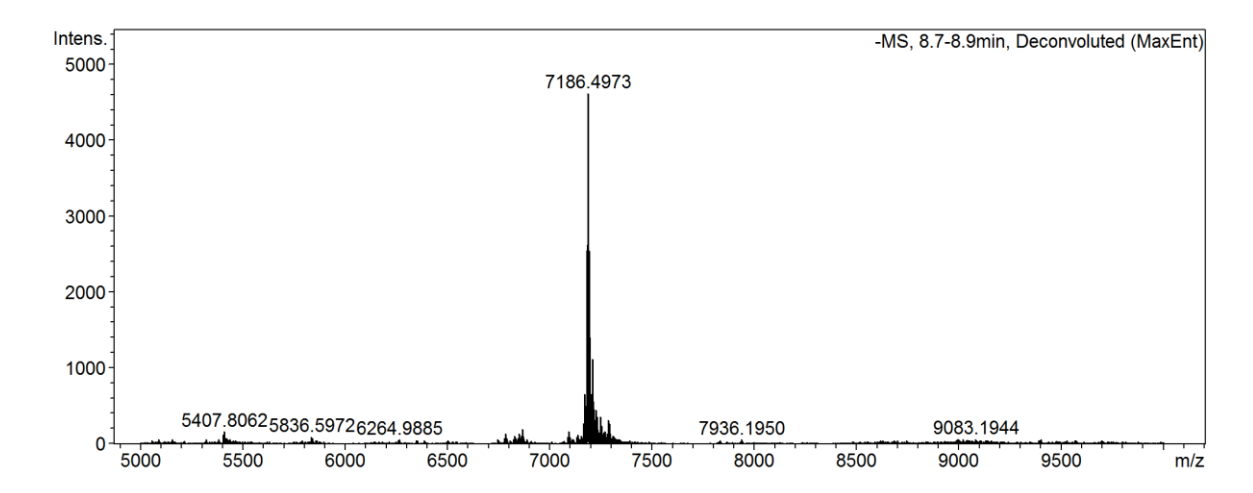
PR sense



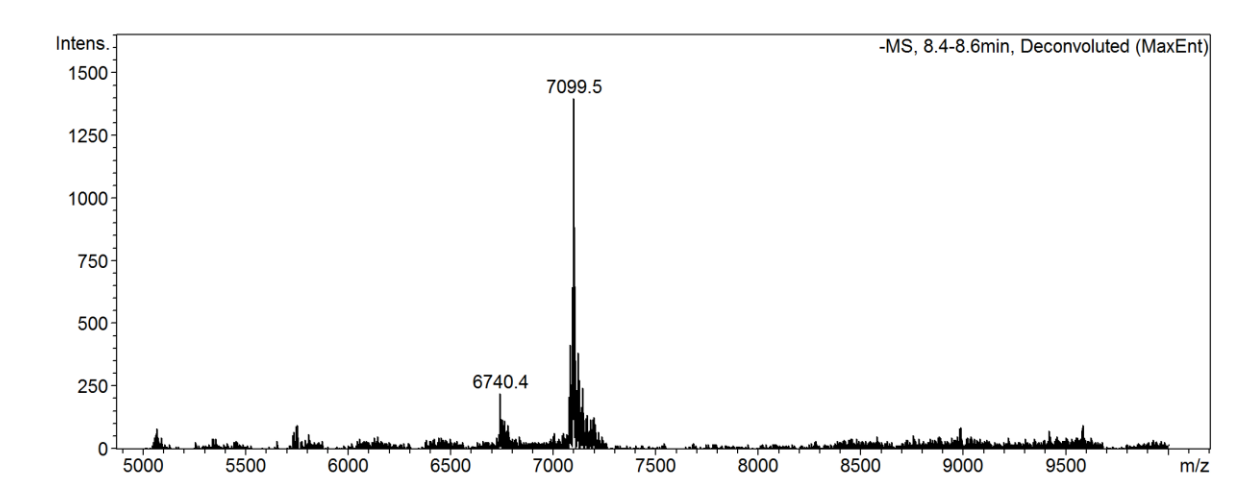
PR antisense



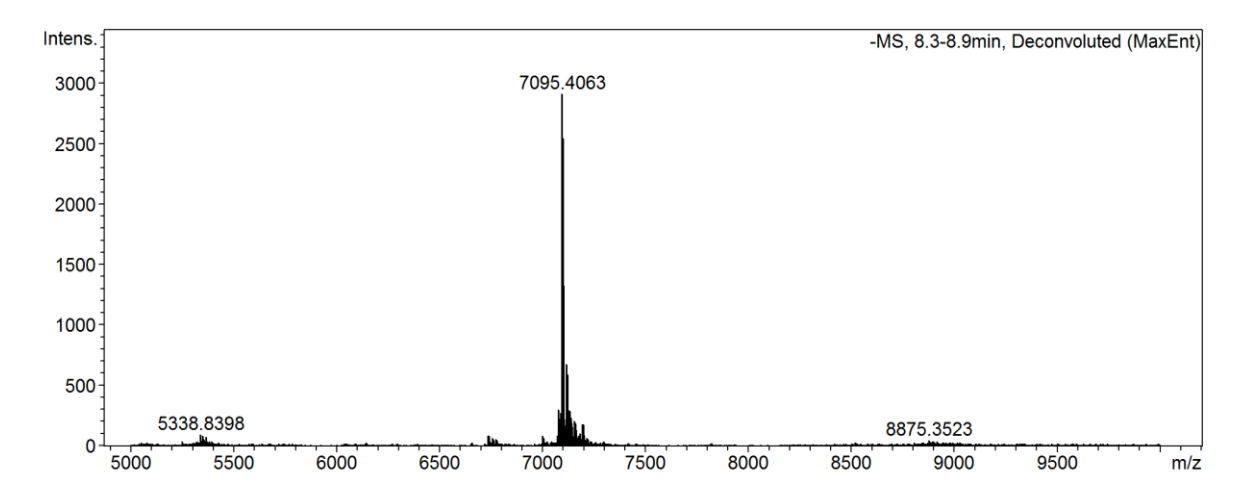
ss-PR-MOE



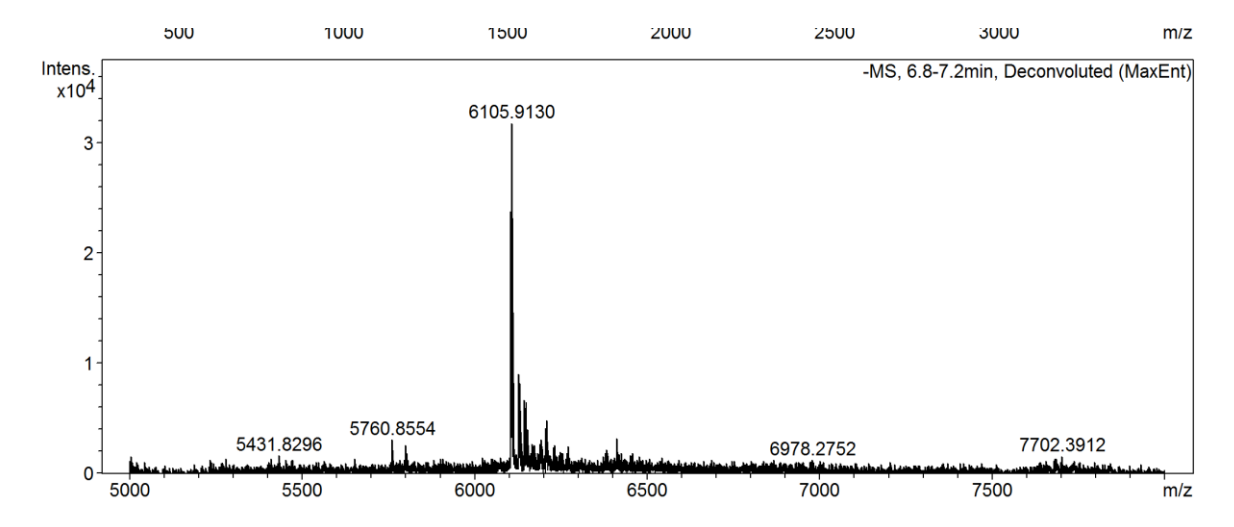
ss-PR-OMe



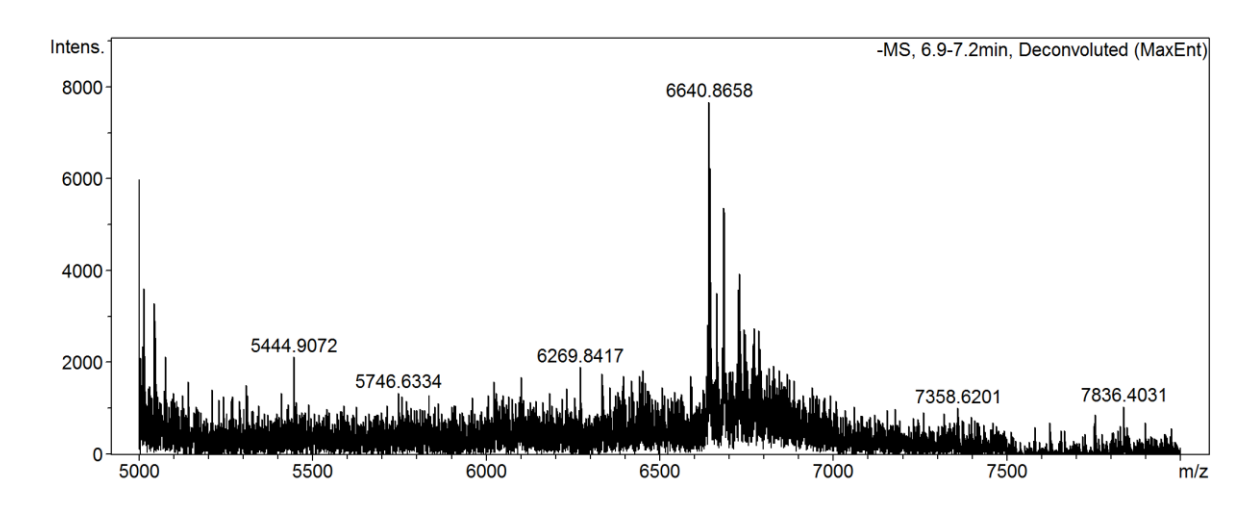
ss-PR-LNA



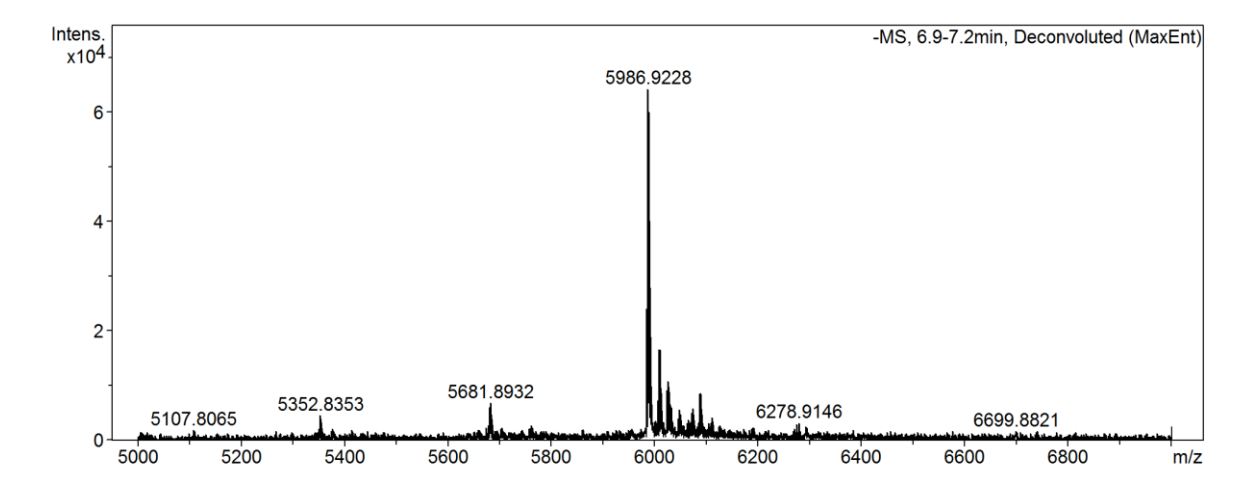
EGFP sense



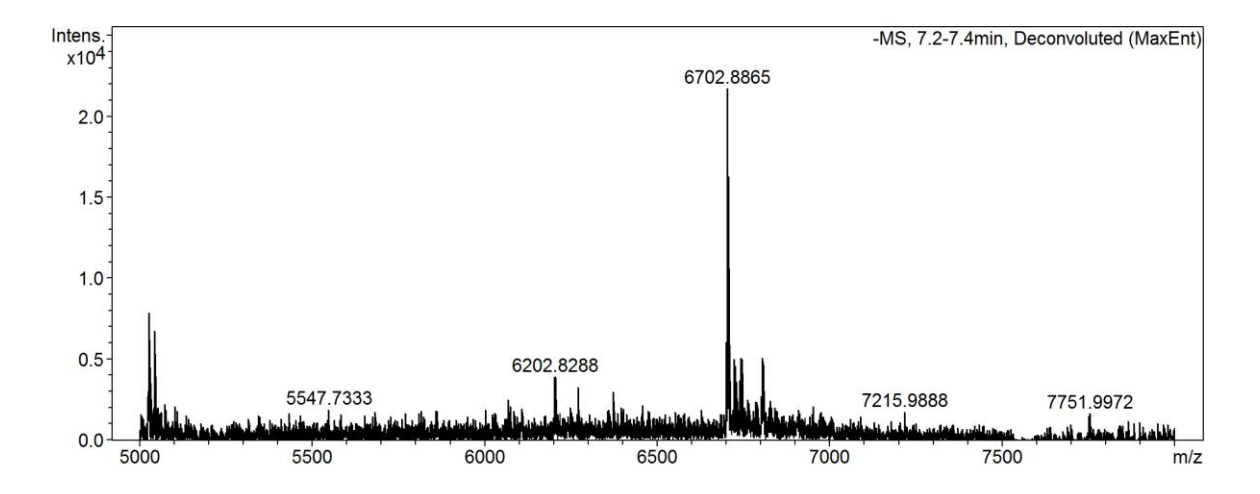
EGFP antisense



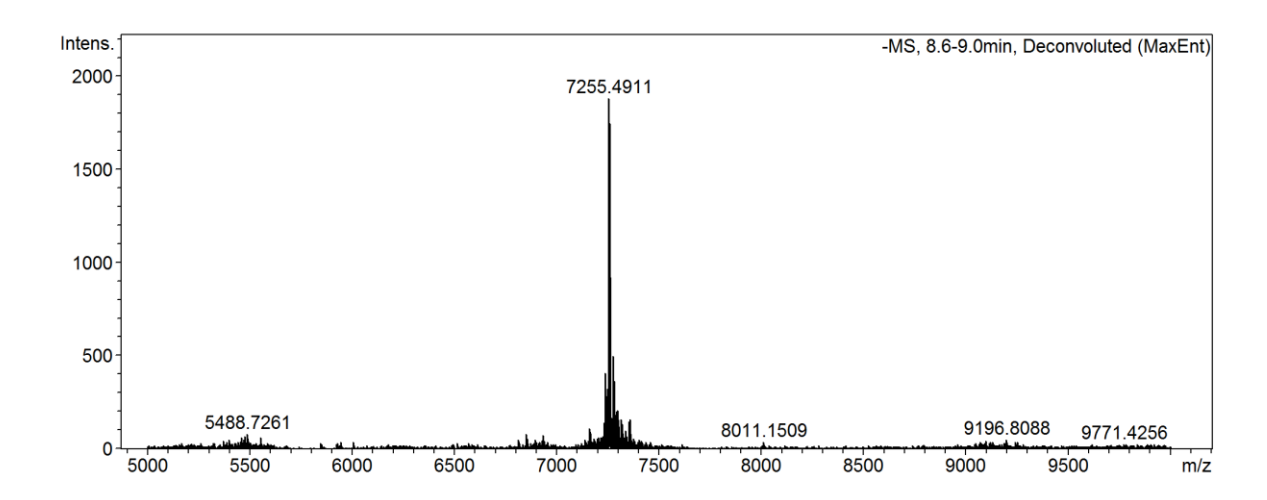
HP-EGFP sense



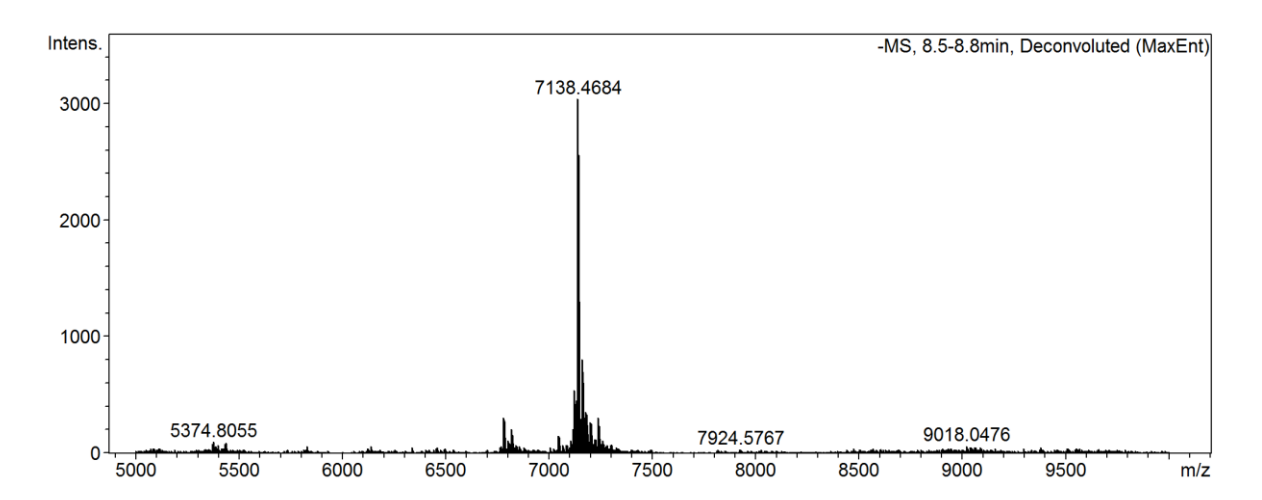
HP-EGFP antisense



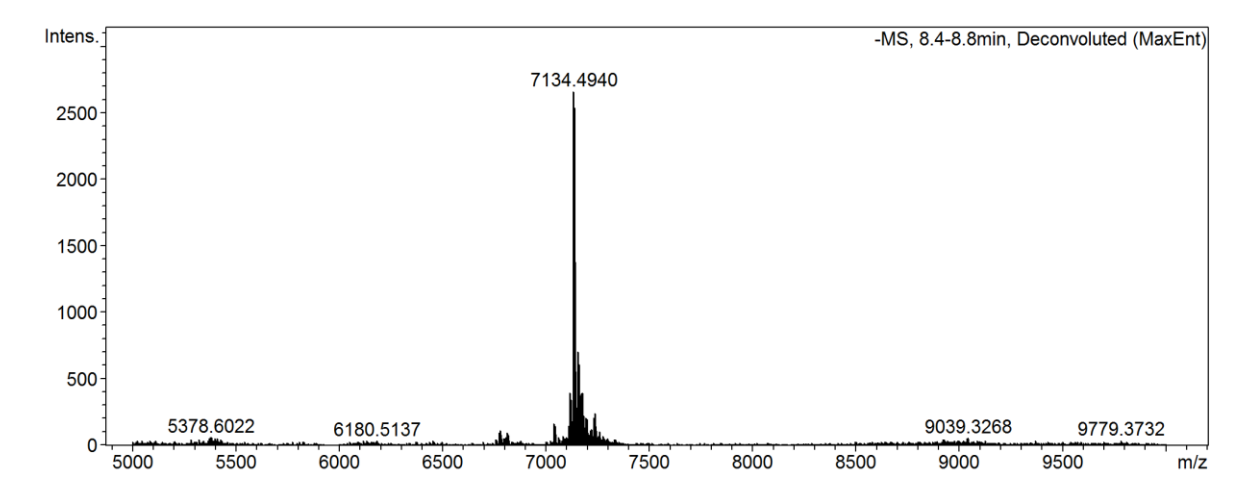
EGFP-MOE



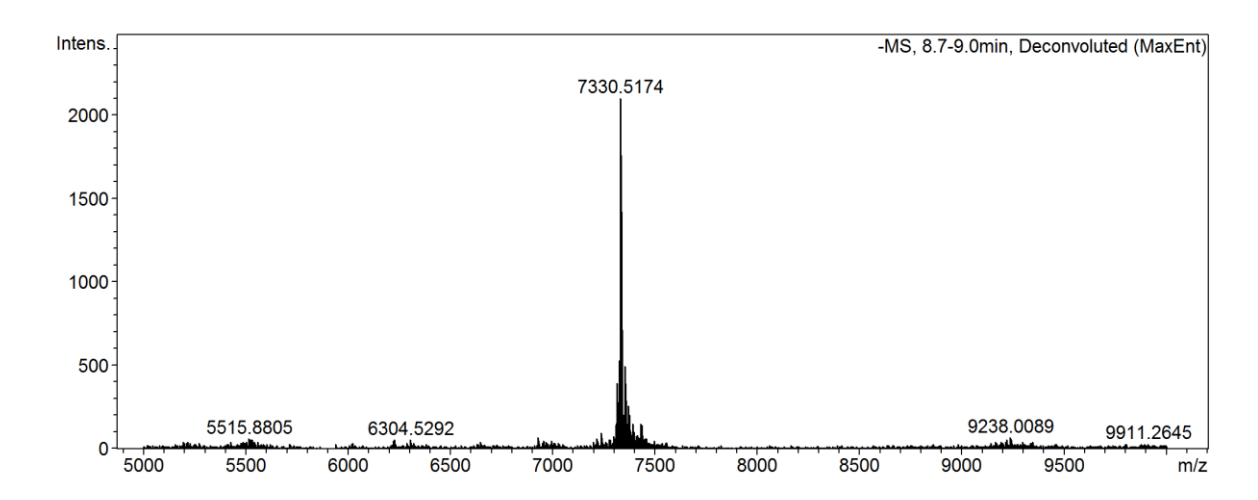
EGFP-OMe



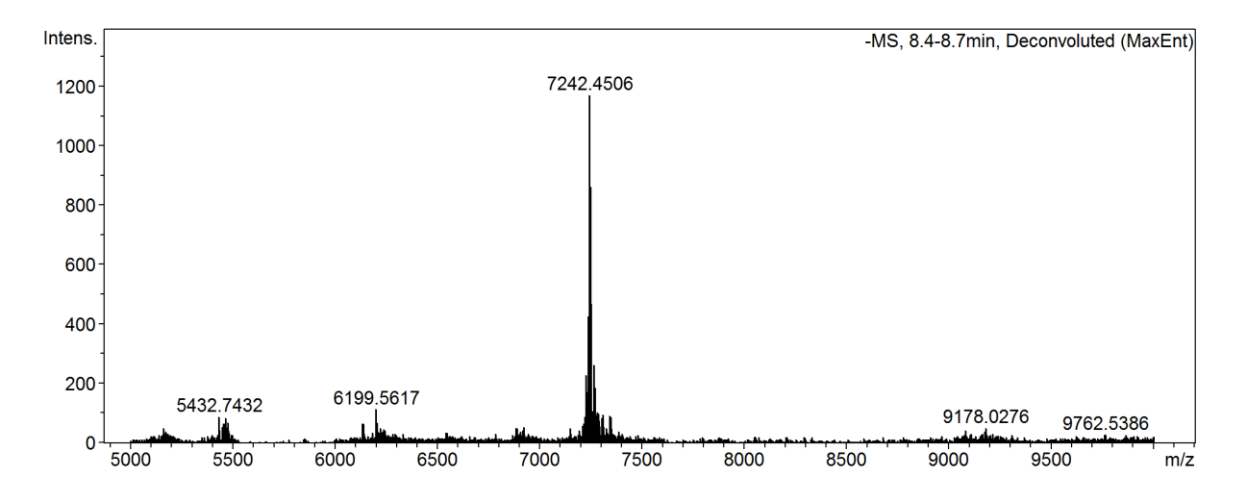
EGFP-LNA



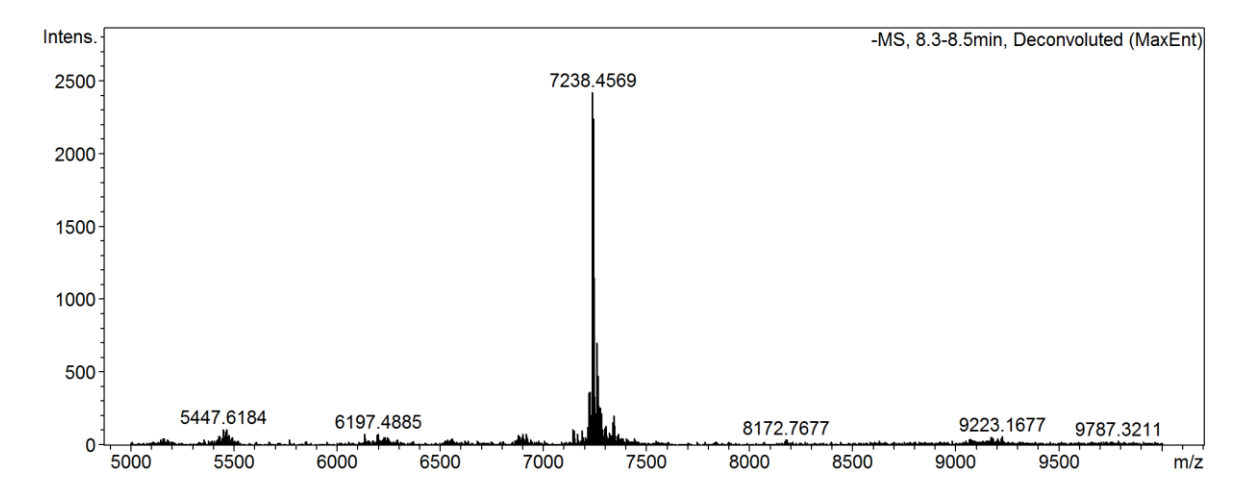
HP-EGFP MOE



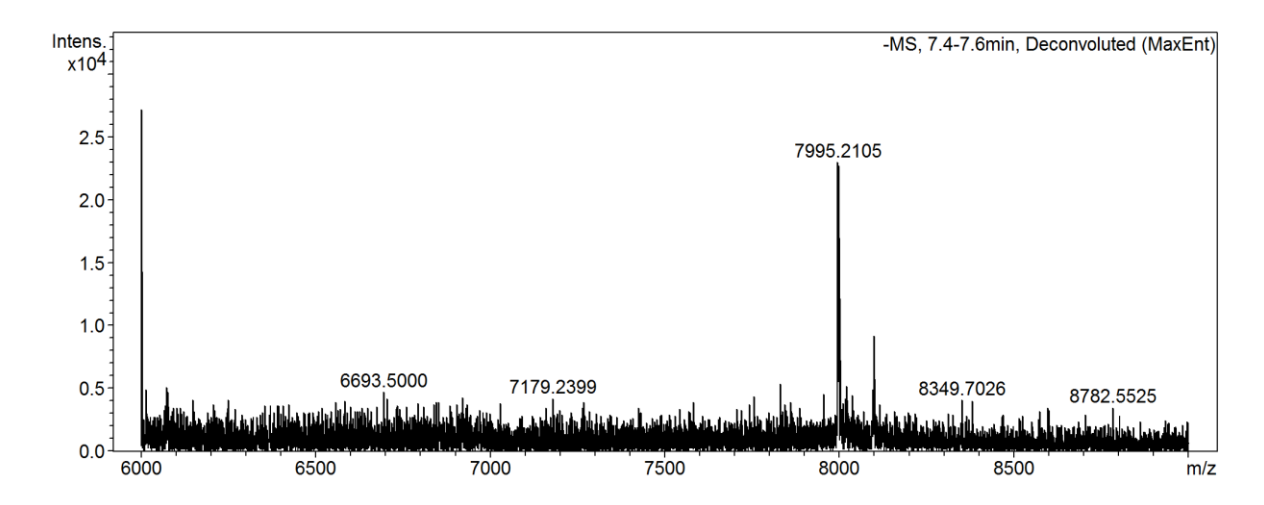
HP-EGFP-OMe



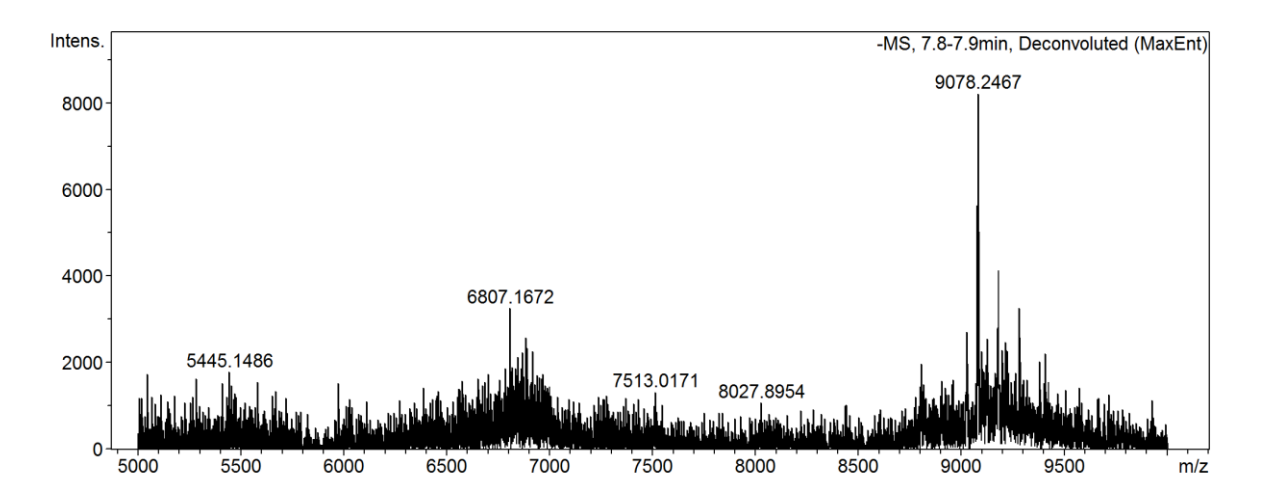
HP-EGFP-LNA



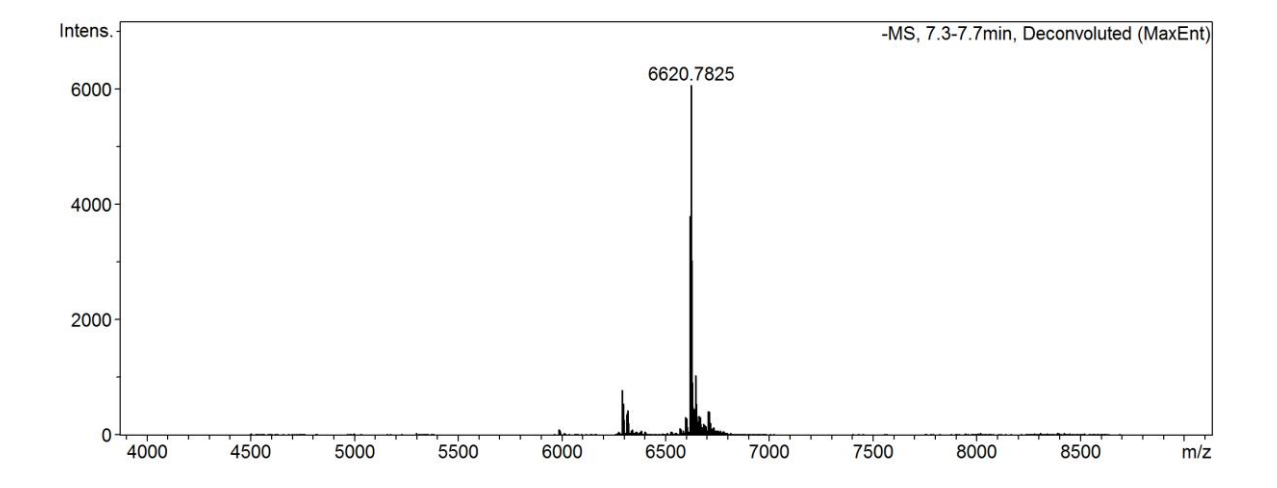
Disirna sense



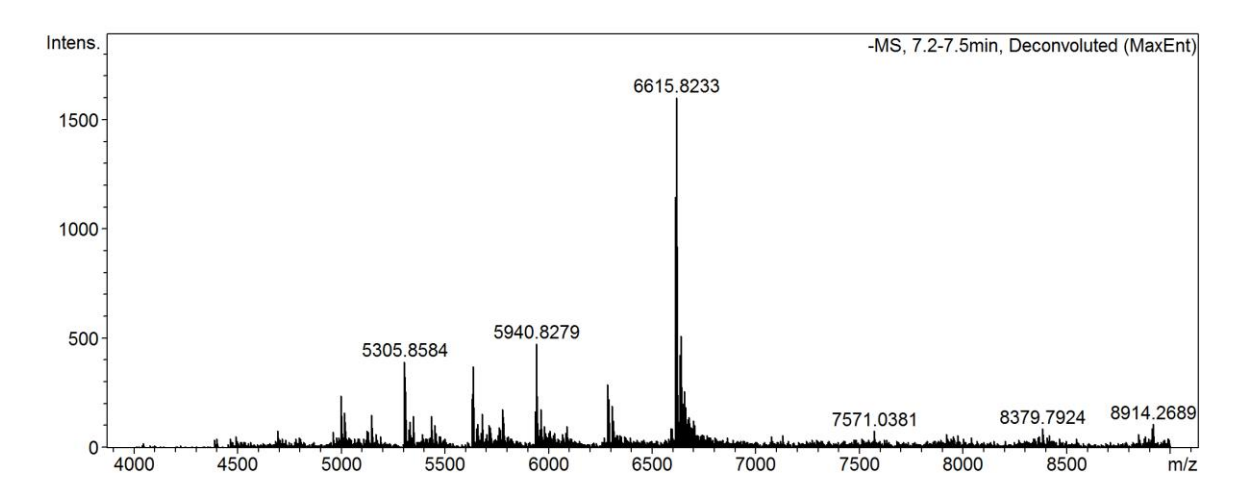
Disirna antisense



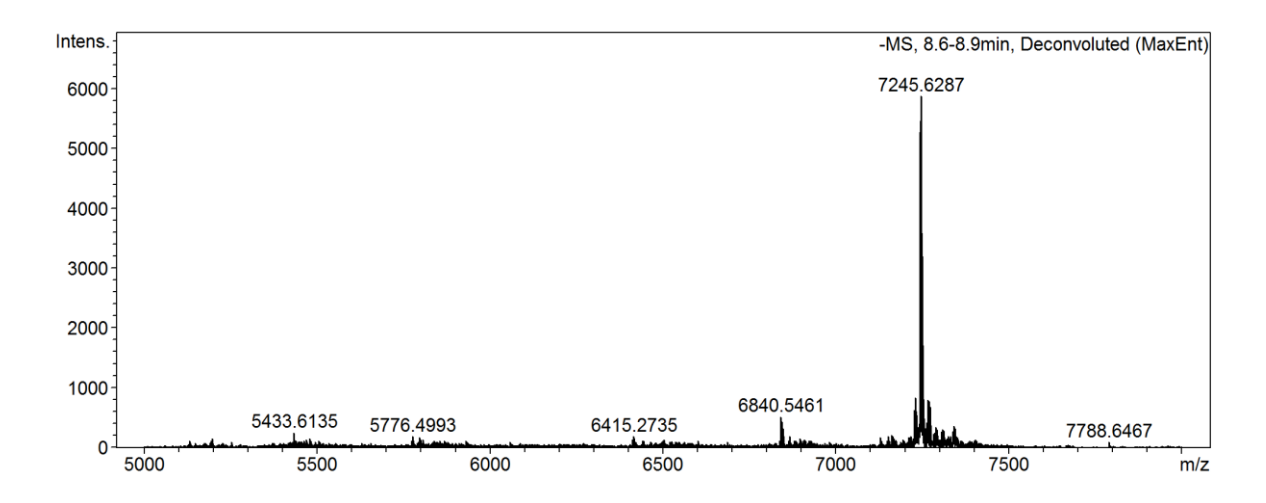
Sin3A sense



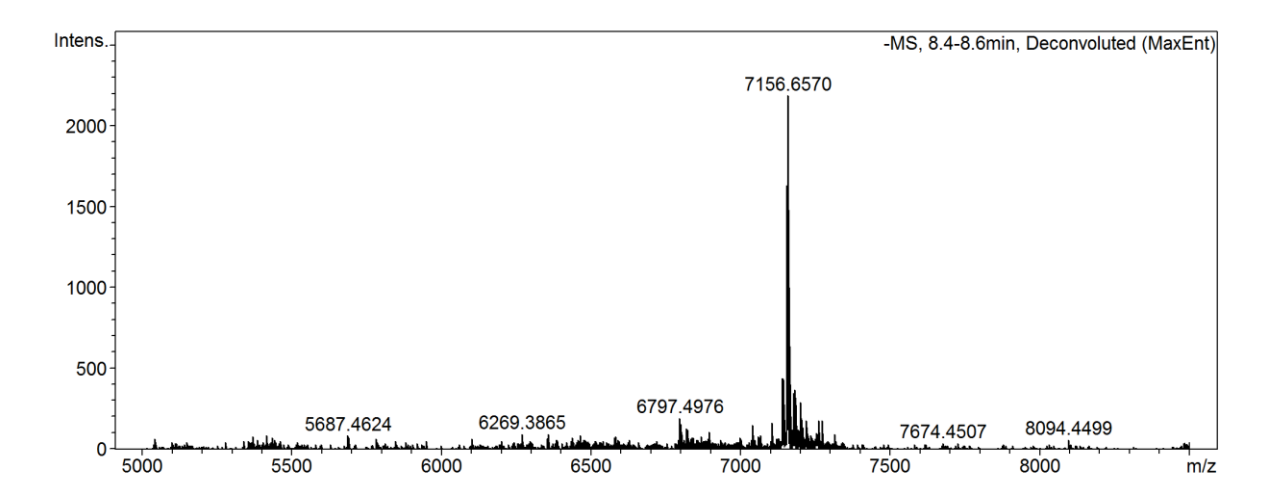
Sin3A antisense



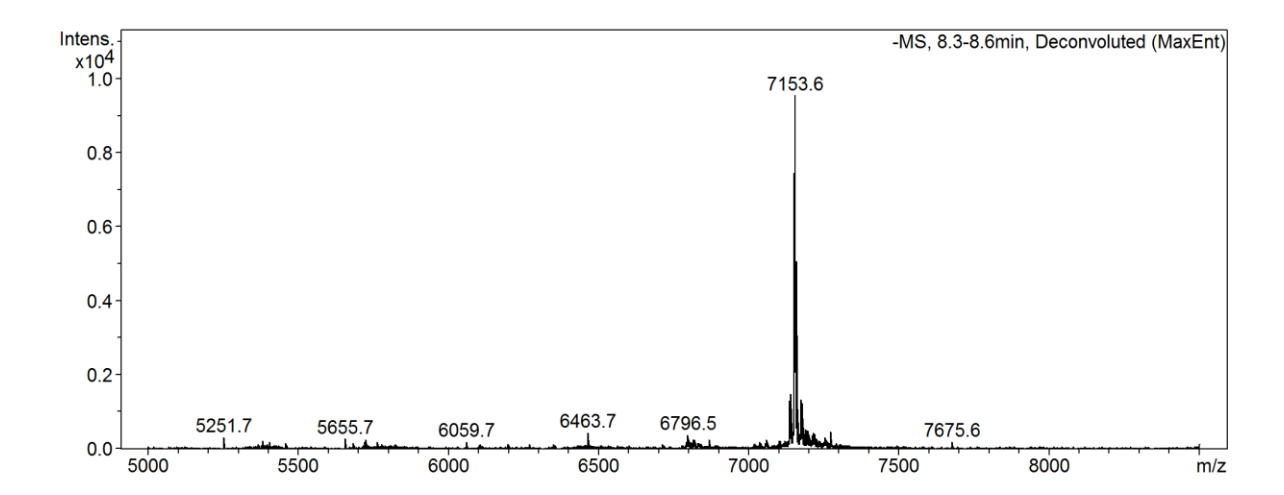
Sin3A-Moe



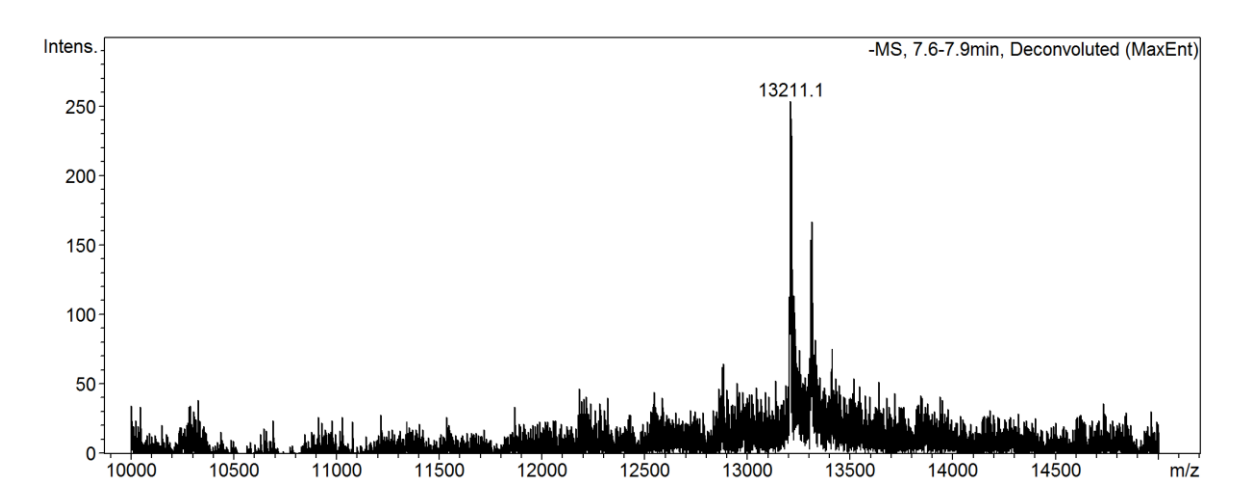
Sin3A-OMe



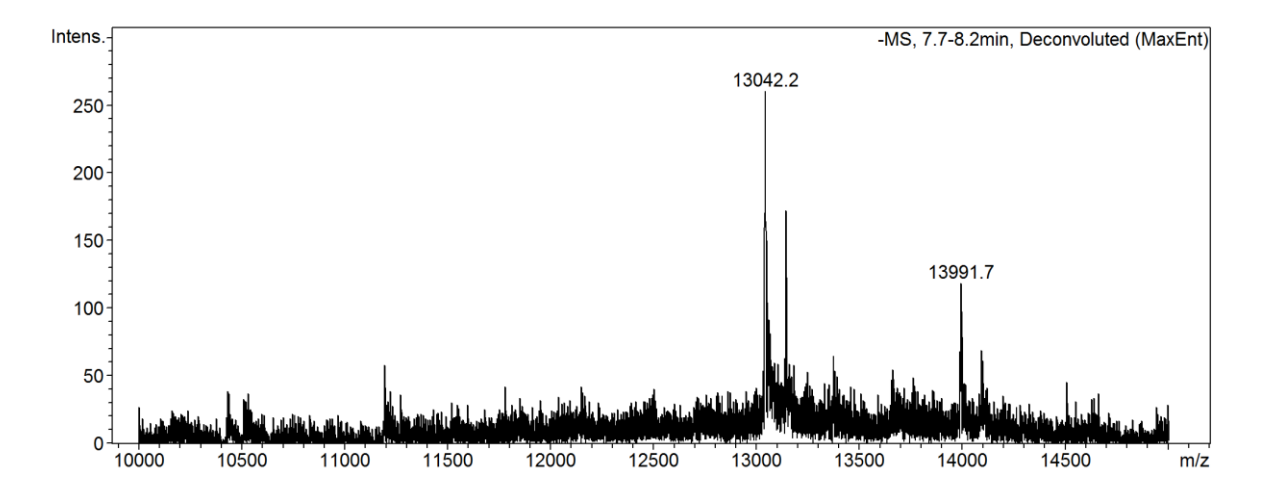
Sin3A-LNA



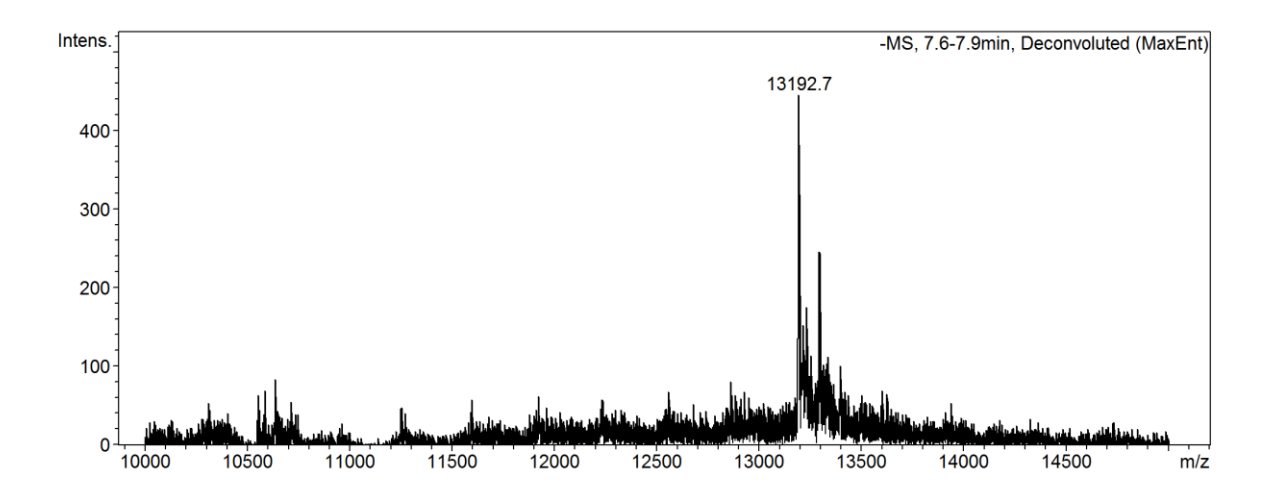
LR-DBD



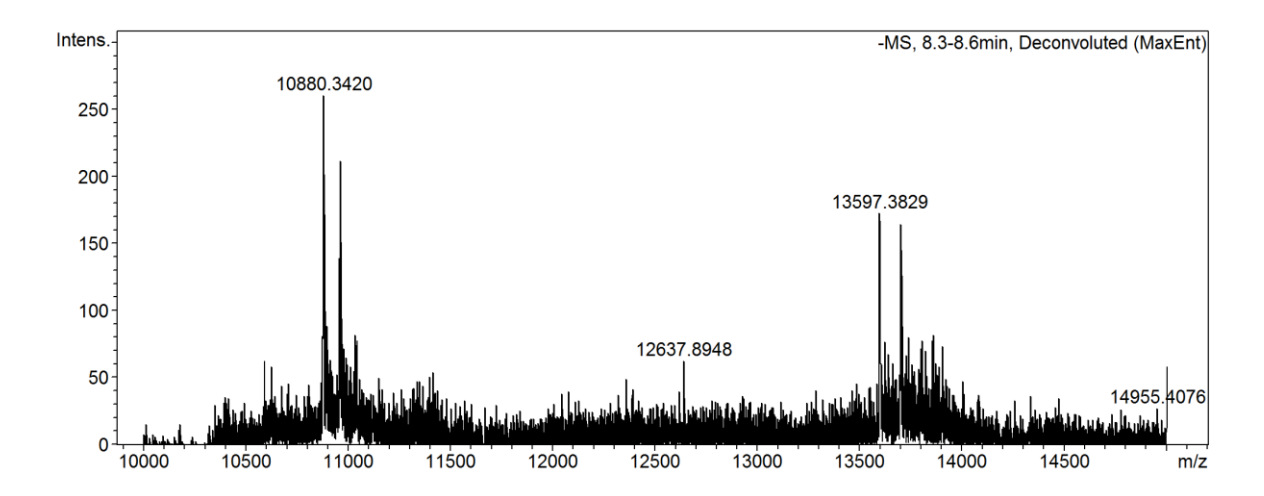
LD-DBD



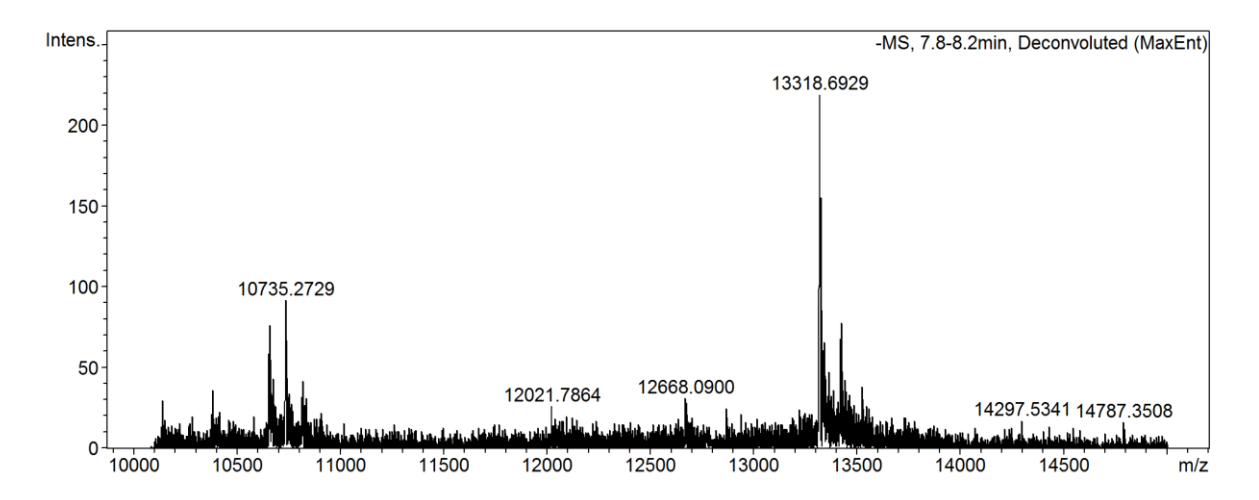
LR-tracrBD



HP-OMe



HP-OMe/RNA



PS-tracrBD

